NASA Contractor Report 181916, Volume II

INVESTIGATION OF DIFFICULT COMPONENT EFFECTS ON FINITE ELEMENT MODEL VIBRATION PREDICTION FOR THE BELL AH-1G HELICOPTER

Volume II - Correlation Results

R. V. Dompka

Bell Helicopter TEXTRON
A Subsidiary of Textron Inc

Ft. Worth, TX 76101

Contract NAS1-17496
October 1989

National Aeronautics and Space Administration

Langley Research Center
Hampton, Virginia 23665-5225

FOREWORD

Bell Helicopter Textron Inc. (BHTI) has been conducting a study of finite element modeling of helicopter airframes to predict vibration. This work is being performed under U.S. Government Contract NAS1-17496. The contract is monitored by the NASA Langley Research Center, Structures Directorate.

This report summarizes analytical studies conducted using a finite element vibration model of the AH-1G helicopter airframe to quantify the effects of various components on overall airframe vibratory response. Key NASA and BHTI personnel are listed below:

NASA Langley

Panice H. Clark, Contracting Officer

Joseph W. Ownes, Contract Specialist

John H. Cline, Technical Representative

Raymond G. Kvaternik, Leader, Rotorcraft Structural Dynamics Group

Bell Helicopter Textron

Warren Young, Manager, Research

James D. Cronkhite, Group Engineer, Structural Dynamics

Robert V. Dompka, Senior Research Engineer, Structures

Table of Contents

1. INTRODUCTION

INTRODUCTION - DIFFICULT COMPONENTS INVESTIGATIONS

The NASA Langley Research Center is sponsoring a rotorcraft structural dynamics program with the overall objective of establishing, in the United States, a superior capability in the utilization of finite element analysis models to support the industrial design of helicopter airframe structures. Viewed as a whole, the program plan includes efforts by NASA, several universities, and the U.S. helicopter industry. In the initial phase of the program, teams from the major U.S. manufacturers of helicopter airframes will use extant finite element analysis methods to calculate static internal loads and vibrations of both metal and composite airframes, conduct laboratory measurements of the structural behavior of these airframes, and perform correlations between analytical and measured data to establish a base upon which to evaluate the results of applications. To maintain the necessary scientific observation and control, emphasis throughout these activities will be on advanced planning, documentation of methods and procedures, and a thorough discussion of results and experiences, all with industry-wide critique to allow maximum technology transfer between companies. The finite element models formed during this phase will then serve as the basis for the development, application, and evaluation of both improved modeling techniques and advanced analytical and computational techniques, all aimed at strengthening and enhancing the technology basis that supports industrial design of helicopter airframe structures. Here again, procedures for mutual critique have been established, and these procedures call for a thorough discussion among the program participants of each method prior to application and of the results and experiences after application. The aforementioned rotorcraft structural dynamics program has been given the acronym DAMVIBS (Design Analysis Methods for VIBrationS).

Based on previous correlations of a NASTRAN finite element model (FEM) of the AH-1G helicopter airframe (Ref. 1), vibration response predictions in the 20-30 Hz frequency range encompassing 4p were identified as needing further investigation. The purpose of this task is to evaluate the effects of difficult components (e.g., transmission, engine, secondary structure) on airframe vibration response and on the aforementioned correlations. Under this task, Bell Helicopter Textron, Inc. (BHTI) performed the following: (a) conducted ground vibration tests on an AH-1G helicopter airframe and selected components to evaluate the effect of difficult components on the vibration response of the airframe; (b) performed correlations using an extant NASTRAN FEM of the AH-1G airframe; and (c) reformulated the FEM as necessary and, based on the results of the correlations, made recommendations for further R&T work to improve vibration modeling and prediction methodology.

Volume II of this report addresses items (b) and (c), i.e., it summarizes the analytical studies conducted by BHTI to quantify the effects of various components on the overall vibratory response of the Bell AH-1G helicopter airframe.

INTRODUCTION -
DIFFICULT COMPONENTS INVESTIGATIONS

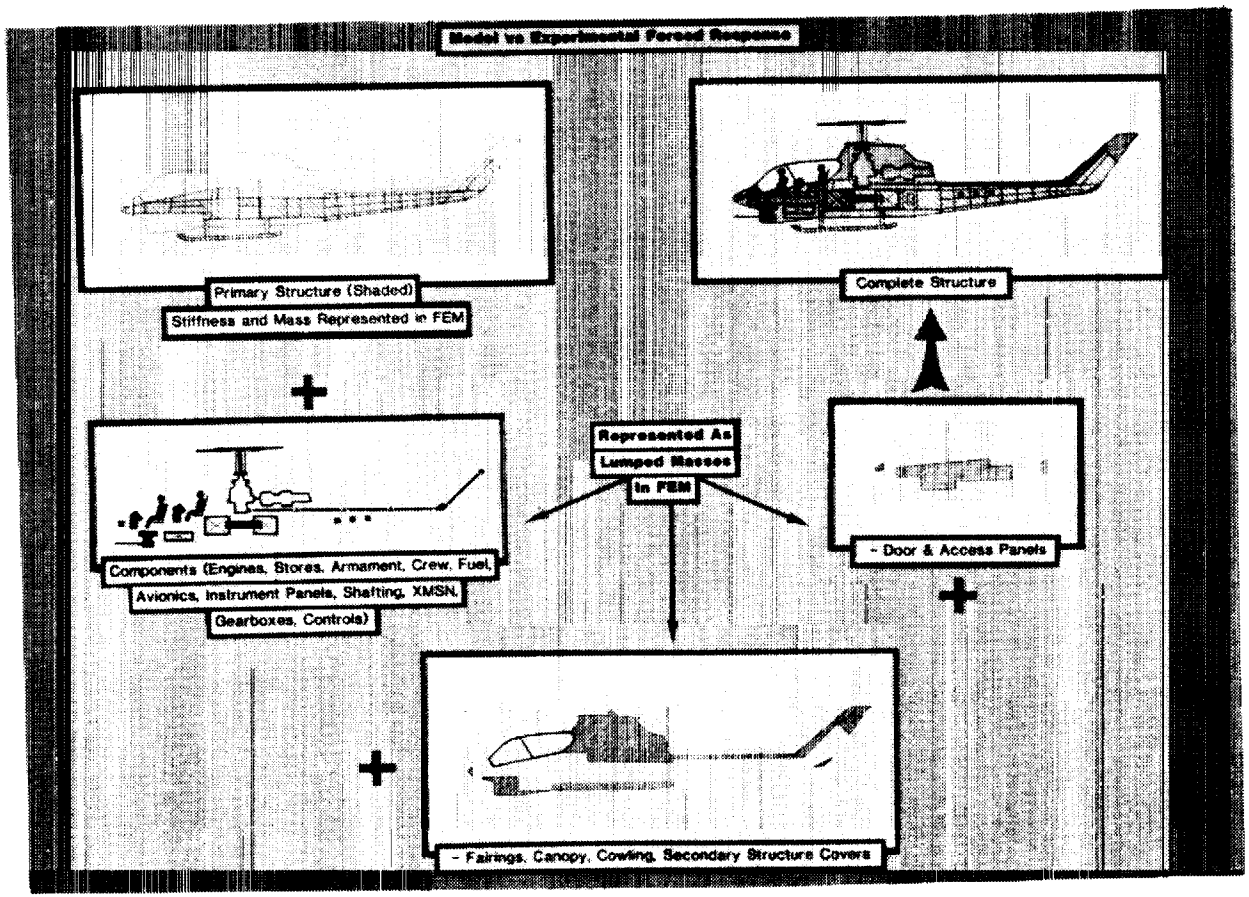

ORIGINAL PAGE
BLACK AND WHITE PHOTOGRAPH

2. AH-1G HELICOPTER DESCRIPTION AND CORRELATION BACKGROUND

AH-1G HELICOPTER

BHTI began development of the AH-1G (Model 209) in March 1965 as a company-funded development of the UH-1B/C Iroquois intended specifically for armed helicopter missions. The original design combined the basic rotor system, transmission, and powerplant of the UH-1C with a new, streamlined fuselage designed for increased speed, armament load, and crew efficiency. Tandem seating is provided for the crew of two with the copilot/gunner forward and the pilot aft.

The Model 209 prototype made its first flight on 7 September 1965, and the U.S. Army's intention to order the aircraft was announced on 11 March 1966, the initial model being known as the AH-1G Huey Cobra. Total orders to date for all versions of the Huey Cobra/Sea Cobra exceed 1800.

The original version for the U.S. Army was powered by a single 1400-shp Avco Lycoming T53-L-13 turboshaft engine derated to 1100 shp for takeoff and maximum continuous rating. The AH-1G uses a Model 540 two-bladed, wide-chord, 'door hinge,' 44-ft-diameter main rotor system similar to that of the UH-1C. The interchangeable blades are built up of extruded aluminum spars and laminates. The two-bladed tail rotor is an all-metal, flex-beam, tractor design located on the starboard side and is of honeycomb construction. The main rotor speed is 294 to 324 rpm. The 44.5-ft-long AH-1G fuselage is a conventional all-metal semimonocoque structure with a low silhouette and narrow profile. The small mid-mounted stub wings carry armament and off-load the rotor in flight. The landing gear is a nonretractable tubular skid-type gear.

The AH-1G maximum takeoff and landing weight is 9500 lb. The never-exceed speed is 190 knots (kn), while the maximum level speed at sea level is 149 kn.

AH-1G HELICOPTER

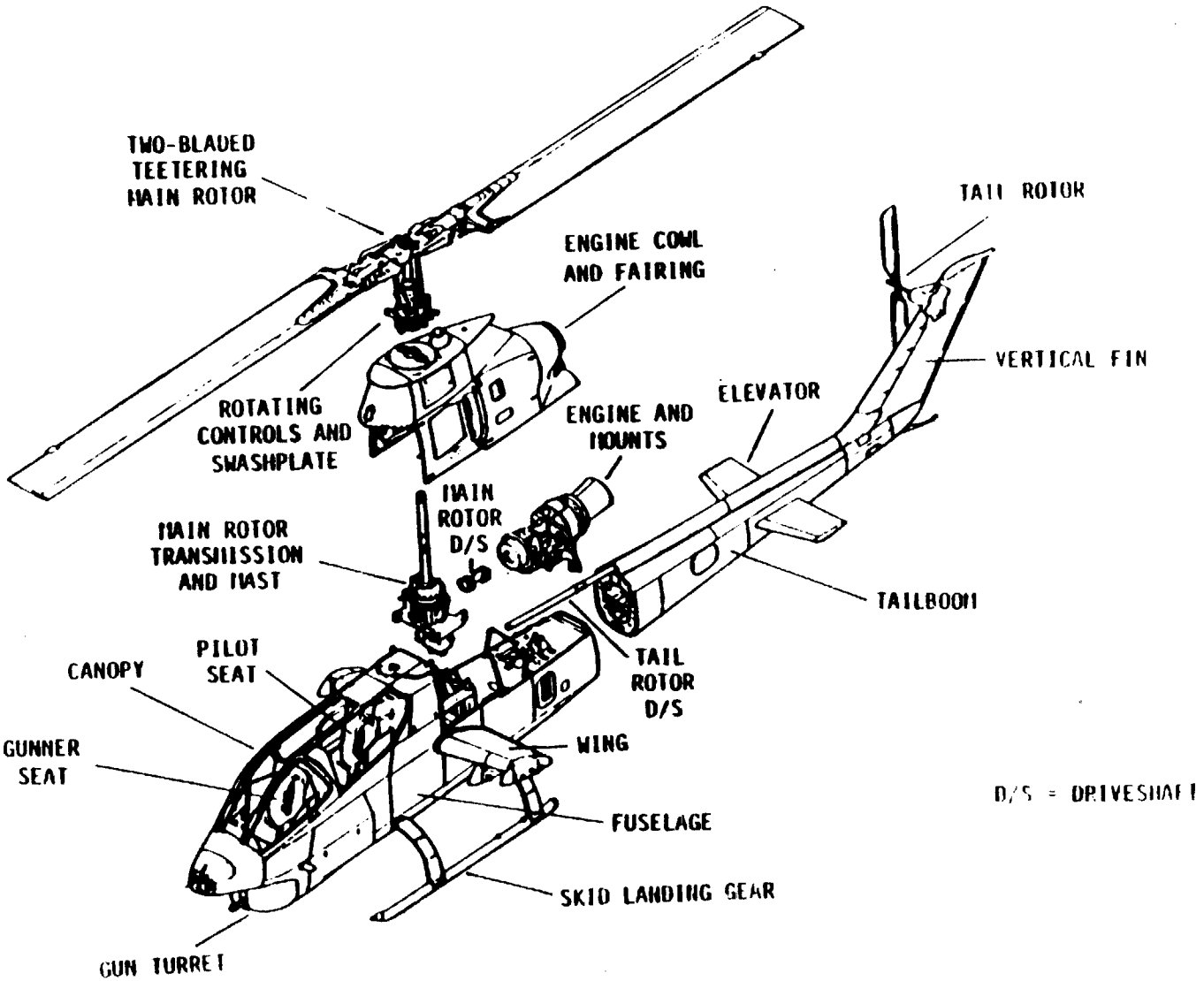

D/S = DRIVESHAFT

AIRFRAME STRUCTURE DESCRIPTION

A brief structural description of three major divisions of the AH-1G is presented: the fuselage structure, the main rotor pylon, and the tailboom and vertical fin structures with panels removed. These are illustrated below.

The fuselage structure is built around the two main beams running the length of the fuselage (FS 61 to FS 300). The main beams provide the primary vertical bending stiffness in the fuselage structure, while differential bending of the main beams provides torsional stiffness in the open sections of the forward fuselage. The main beams are tied together by the lower horizontal floors to give the fuselage lateral stiffness. The cross-sectional areas in the figure detail the fuselage structure.

The main rotor pylon located at FS 200 above WL 65 provides the structural tie between the main rotor and the fuselage. It is attached to the fuselage through five elastomeric mounts and a lift link. This lift link is the primary vertical load path and is pinned to the center wing carry-through beam or "lift beam." The elastomeric mounts are designed to produce low pylon rocking frequencies to isolate the main rotor in-plane vibratory loads from the fuselage and to react the main rotor torque. The carry-through consists of three beams that are attached to the spars by pinned connections at the fuselage contour.

The tailboom is of semimonocoque construction having aluminum skins, stringers, and longerons. The longerons and stringers are supported by bulkhead frames spaced down the length of the boom. The tailboom is bolted to the fuselage at FS 299 by means of four attachment fittings located at the four main longeron locations.

AIRFRAME STRUCTURE DESCRIPTION

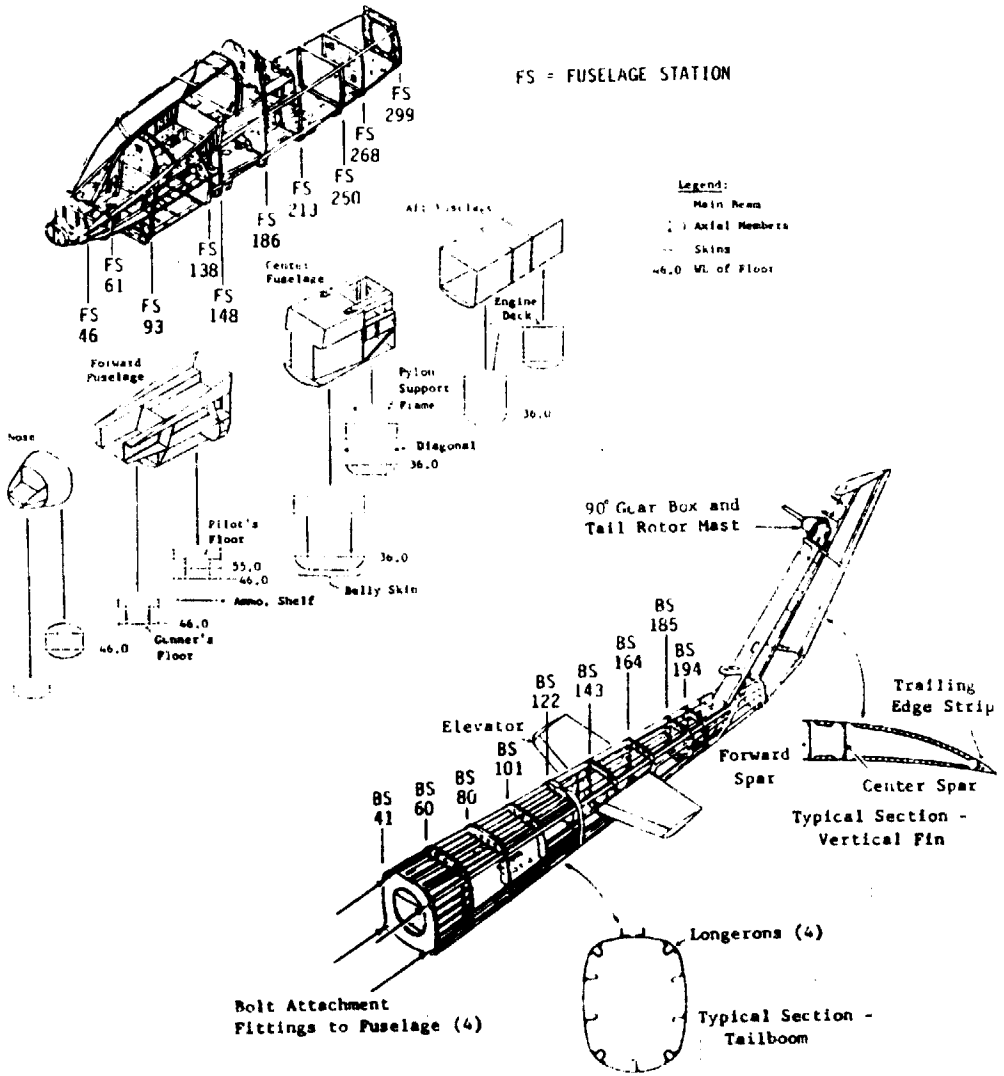

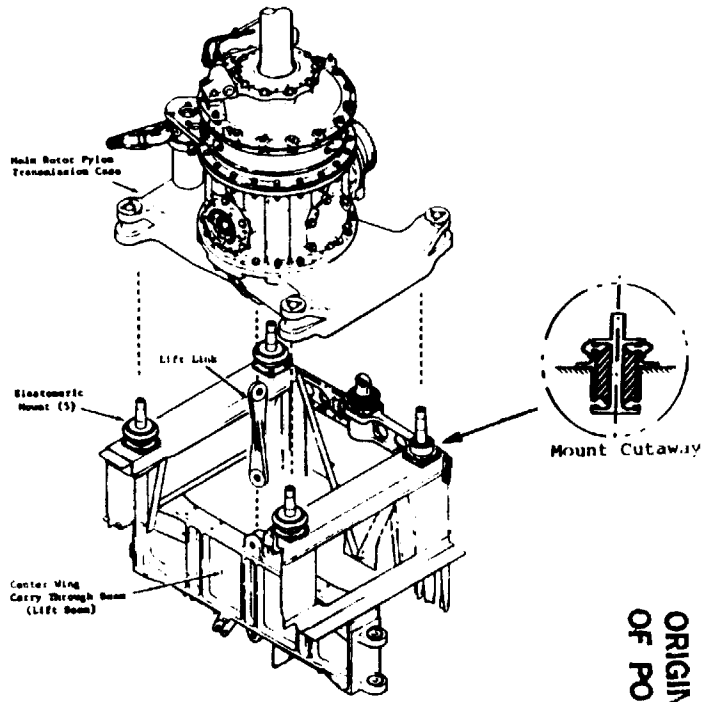

BS = BODY STATION

ORIGINAL PAGE IS
OF POOR QUALITY

STRUCTURAL IDEALIZATION

The emphasis in the structural idealization is on developing a finite element model adequately representing the low-frequency (≤30 Hz) vibration modes of the airframe with the fewest degrees of freedom possible. Therefore, only the primary structure is modeled. Details of the model approach and structural idealization appear in Reference 2. Representation of the fuselage and wing structures in the areas of the XM-28 gun turret and the wing stores is given special attention. The gun turret and stores themselves are represented as rigid masses, as are the main and tail rotors, the engine, and useful weight items such as the crew, fuel, and ammunition.

STRUCTURAL IDEALIZATION

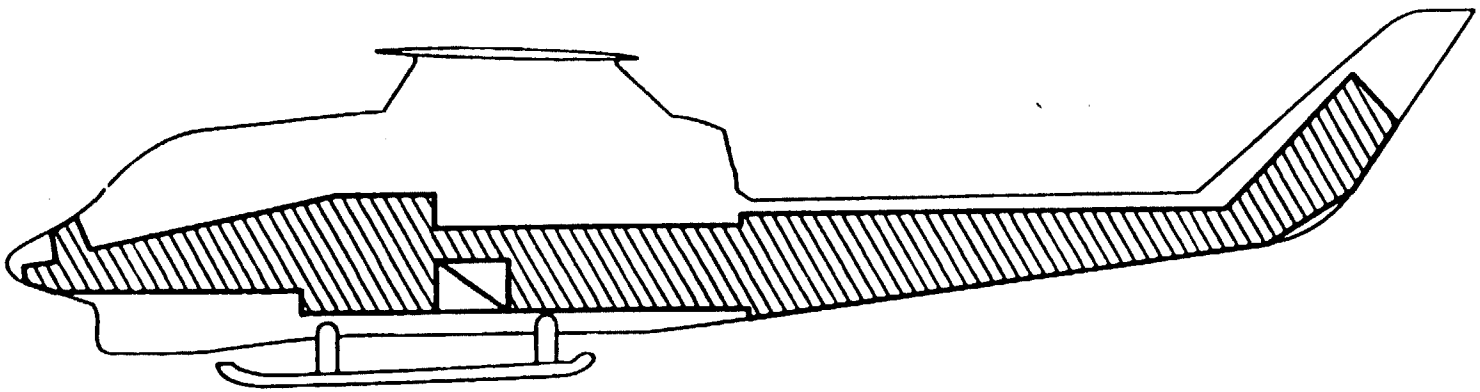

- PRIMARY STRUCTURE IN NASTRAN MODEL
- REPRESENTED AS LUMPED MASSES IN FEM:
  - DOORS AND ACCESS PANELS
  - FAIRINGS, CANOPY, COWLING, SECONDARY STRUCTURE, COVERS
  - COMPONENTS (ENGINES, STORES, ARMAMENT, CREW, FUEL, AVIONICS, INSTRUMENT PANELS, SHAFTING, TRANSMISSION, GEARBOXES)

NASTRAN VIBRATION MODEL OF THE AH-1G HELICOPTER AIRFRAME

The AH-1G FEM described in Reference 1 was the starting point for this investigation. The complete model consists of structural elements from the NASTRAN library, such as scalar springs, rods, bars, shear panels, and triangular and quadrilateral membranes. There was no use of General Elements, substructuring, or DMAPing in the model. Symmetry could not be used because of unsymmetrical sections in the fuselage and the tail rotor offset to the starboard side. The table below shows the degrees of freedom existing in the original FEM before and after constraints and partitioning were applied.

Stiffness Matrix	Degrees of Freedon	Description
K_{gg}	2940	Unreduced size
K_{nn}	2699	After applying MPC equations
K_{ff}	1714	After applying SPCs
K_{aa}	241	After partitioning with OMITs
K_{ll}	235	After applying free body SUPPORTS

NASTRAN VIBRATION MODEL OF THE AH-1G HELICOPTER AIRFRAME

NASTRAN
FINITE ELEMENT MODEL

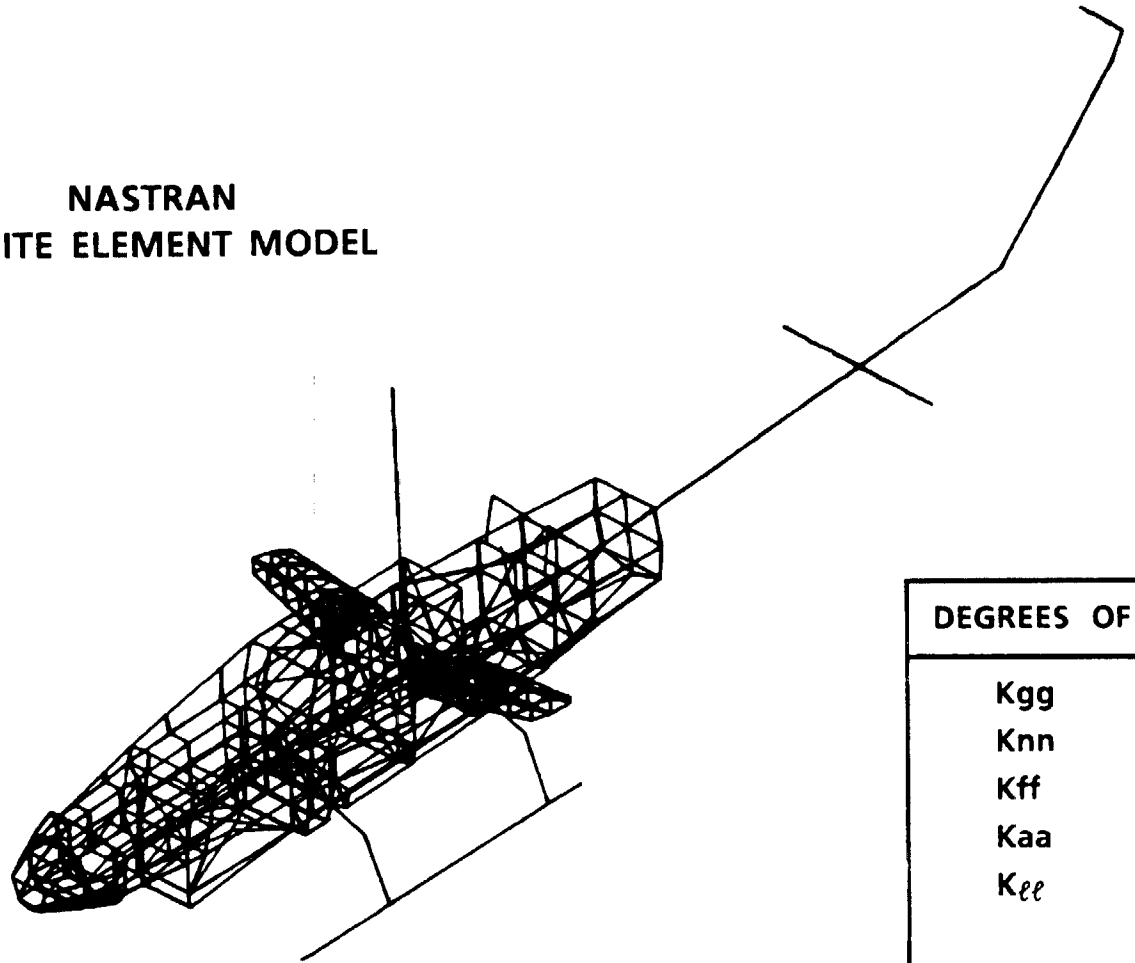

DEGREES OF FREEDOM		ELEMENTS	
Kgg	2940	BAR	197
Knn	2699	ROD	2012
Kff	1714	SHEAR	340
Kaa	241	QDMEM	160
$K_{\ell\ell}$	235	TRMEM	243
		ELAS2	13

PREVIOUS AH-1G MODELING AND CORRELATION EFFORTS

Previous test programs initiated prior to the NASA DAMVIBS program served to evaluate the mathematical representation of the stiffness and mass models for the BHTI AH-1G helicopter airframe. The math model was developed and analyzed using the NASTRAN structural analysis computer program (Ref. 3). Following the development and documentation of the AH-1G dynamic FEM, a correlation with static and vibration tests was performed to assess the validity of the model. Static load deflection tests of the fuselage, wings, tailboom, and vertical fin were performed to verify the stiffness model, and two separate sinusoidal vibration tests were performed to verify the dynamic characteristics of the model. Further correlations were performed by comparing the results of an analysis using NASTRAN for level-flight airframe vibration at main rotor frequencies and effective skin calculations with test data.

The DAMVIBS program required a review of all previous work conducted on the AH-1G as well as a new correlation with shake test data obtained at the Kaman Aerospace Corporation. The review and the new correlation work represent a significant amount of verification for the airframe model (Ref. 1). The validated airframe model was then combined with a rotor program (Ref. 4) to provide coupled rotor/airframe analysis results for comparison with OLS flight test data.

The finite element model was developed for the purpose of representing the low-frequency vibration response of the airframe and the structure deflections due to weapon firing.

PREVIOUS AH-1G MODELING AND CORRELATION EFFORTS

- **NASA / ARMY CONTRACT (1973-76)**
  - MODELING
  - STATIC AND GROUND VIBRATION TEST CORRELATIONS
  - FLIGHT VIBRATION TEST CORRELATION
  - TAILBOOM EFFECTIVE SKIN INVESTIGATION

- **NASA DAMVIBS PROGRAM (1984–86)**
  - REVIEW PAST CORRELATIONS AND INCLUDE CORRELATION WITH KAC GROUND VIBRATION TEST DATA
  - ROTOR / AIRFRAME COUPLING AND FLIGHT VIBRATIONS CORRELATION

EXAMPLE OF PREVIOUS AH-IG FREQUENCY RESPONSE CORRELATIONS

Two examples of representative frequency response functions are presented in semi-log format. The response magnitudes normalized by input force are presented for the pilot location as a function of frequency from 0-30 Hz. Pilot response is shown for both vertical and lateral excitation. The range of good correlation between test and NASTRAN calculations is highlighted on each frequency response plot. These correlations were used as the basis for determining which areas needed to be studied under this task. The details of proposed action to improve correlation are presented later.

VERTICAL TAIL SHAKE - CLEAN WING

Mode	Test	NASTRAN
Main rotor pylon fore/aft rocking (pylon pitch)	3.9	3.0
First fuselage vertical bending	8.0	8.0
Fuselage torsion	15.5	15.7
Second fuselage vertical bending	18.0	17.5
Third fuselage vertical bending	-	25.0

LATERAL TAIL SHAKE - CLEAN WING

Mode	Test	NASTRAN
First fuselage lateral bending	7.1	7.2
Fuselage torsion	15.5	15.7
Second fuselage lateral bending	18.9	17.5
Fuselage roll/engine lateral	-	18.8
Fuselage torsion/wing yaw	-	21.5
Main rotor mast lateral bending	-	25.3
Third fuselage lateral bending	24.4	25.8

EXAMPLE OF PREVIOUS AH-1G FREQUENCY RESPONSE CORRELATIONS

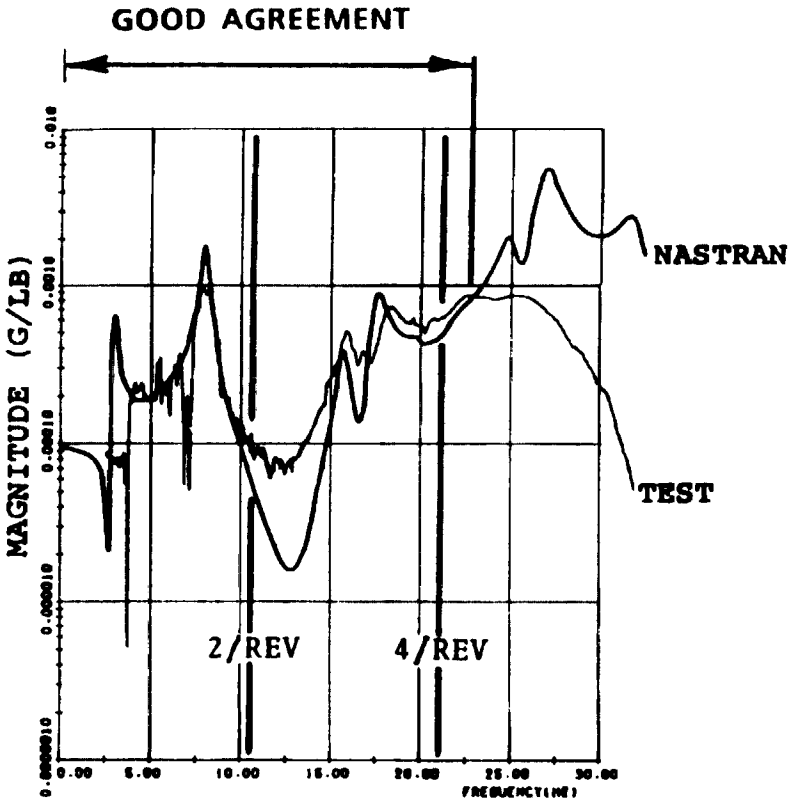

PILOT VERTICAL RESPONSE - TAIL VERTICAL SHAKE

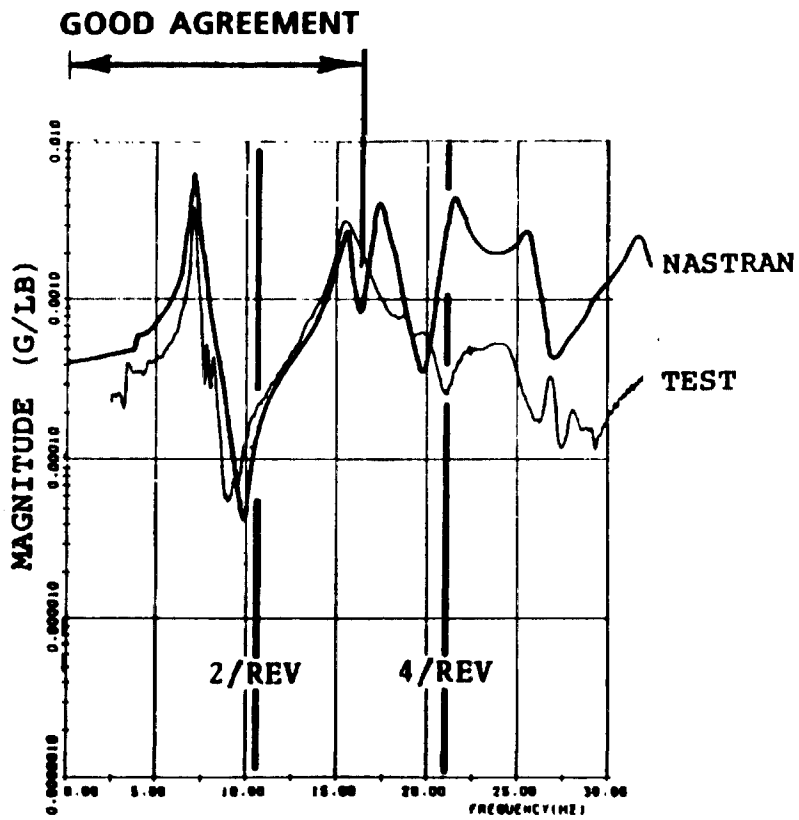

PILOT LATERAL RESPONSE - TAIL LATERAL SHAKE

3. NASTRAN FEM(s) FOR CORRELATION WITH TEST

NASTRAN FEM(s) FOR CORRELATION WITH TEST - OVERVIEW

The steps required to modify the existing AH-1G FEM to correspond to the various shake test configurations and investigate component effects are outlined below. The preliminary correlations represent pre-test NASTRAN predictions for the selected configurations. After these initial comparisons, several updates were made to the FEM. These updates included replacement of the original elastic line FEM with a built-up rod and shear panel tailboom, secondary structure effects, and better modal damping estimates. The new FEM was used for the final correlation effort.

NASTRAN FEM (s) FOR CORRELATION WITH TEST - OVERVIEW

EXISTING AH-1G
NASTRAN FEM

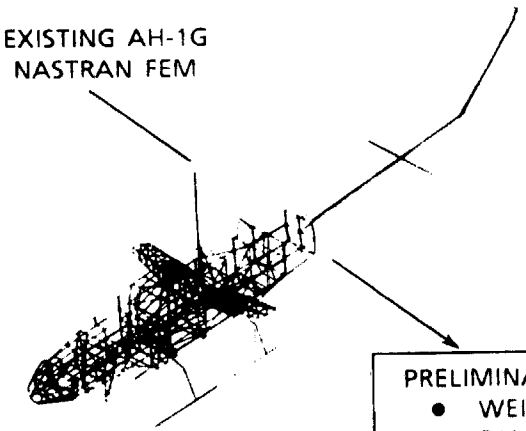

PRELIMINARY FEM UPDATES
- WEIGHTS
- DIAGNOSTIC CHECKOUT

PRELIMINARY CORRELATION
- REMOVE WEIGHTS
- REMOVE COMPONENTS

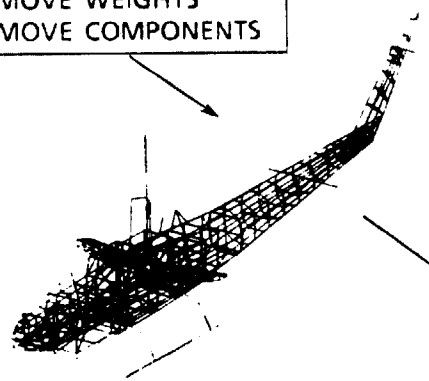

- BUILT-UP TAILBOOM
- SECONDARY STRUCTURE STIFFNESS
- MODAL DAMPING IMPROVED

FINAL NASTRAN FEM
FOR CORRELATION

FINAL CORRELATION

NASTRAN FEM CHECKOUT AND UPDATE

Prior to any comparisons, the AH-1G FEM was analyzed for its basic physical representation of strain energy, rigid body motion, and constraints. A multilevel strain energy DMAP alter written by McDonnell Douglas Helicopters (Ref. 5) and NASTRAN SPC force checks during normal modes analysis (Rigid Format 3) were used to evaluate the FEM. The DMAP provides information for SPC and MPC constraint effects on rigid body motion. The DMAP identified excessive SPC force levels in the canted canopy frame panels. The forces were a result of small kinks in the layout of the panels which generated out-of-plane forces. Small adjustments to the grid point coordinate locations removed the majority of the SPC problems. The DMAP also showed MPC force level problems in three areas: engine mounts, wing lugs, and transmission cg attachment to support structure. These problems resulted from small changes made to the original grid point locations and not implemented in the original MPC equations. Correction of the affected MPC equations eliminated the problem. Finally, mass distribution was checked for improper placement of mass at unsupported (out-of-plane) DOF using an SPC force check. Seven locations were identified as requiring minor redistribution of masses to grids with stiffness in all translational DOF. They included the gunner floor contour mass (8 lb) at FS 70 and 85, the interior mass (100 lb) at bulkhead FS 93, the ammo floor contour mass (14 lb) at FS 115, the main beam mass (12 lb) at FS 156, the fuel cell cover mass (40 lb) at FS 164, and the contour mass (28 lb) at the tailboom junction bulkhead FS 299. The SPC force problems were eliminated and no significant change in the global cg or inertia representation was experienced.

A comparison of the effect of these minor changes on rigid body mode approximations is given.

A comparison of the updated FEM predictions with the AH-1G FEM in Reference 1 is also shown for pilot vertical and lateral responses.

NASTRAN FEM CHECKOUT AND UPDATE

ELIMINATION OF CONSTRAINT FORCES

- SLIGHT REALIGNMENT OF CANOPY PANEL GEOMETRY TO REDUCE SPC FORCE LEVELS
- MINOR MASS REDISTRIBUTION TO REMOVE SPC FORCES
- RIGID BODY MODE FREQUENCIES
- WEIGHT DISTRIBUTION UPDATES TO REFLECT AH-1G TEST ARTICLE (6929 LB GW)

	BEFORE	AFTER
1	1.04-3	1.33-3
2	7.42-3	1.61-3
3	2.15-2	3.26-3
4	9.75-2	5.59-3
5	2.97-1	2.82-2
6	2.05 + 00	1.12-1

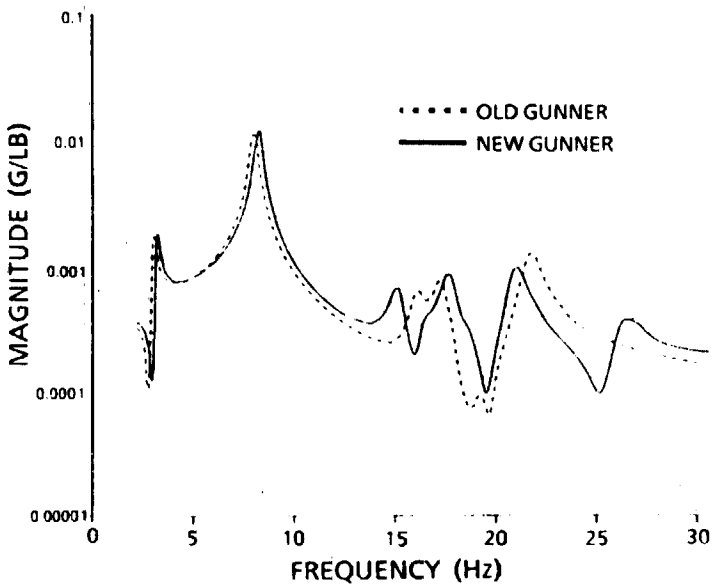

VERTICAL AT TAIL -
VERTICAL RESPONSE AT GUNNER

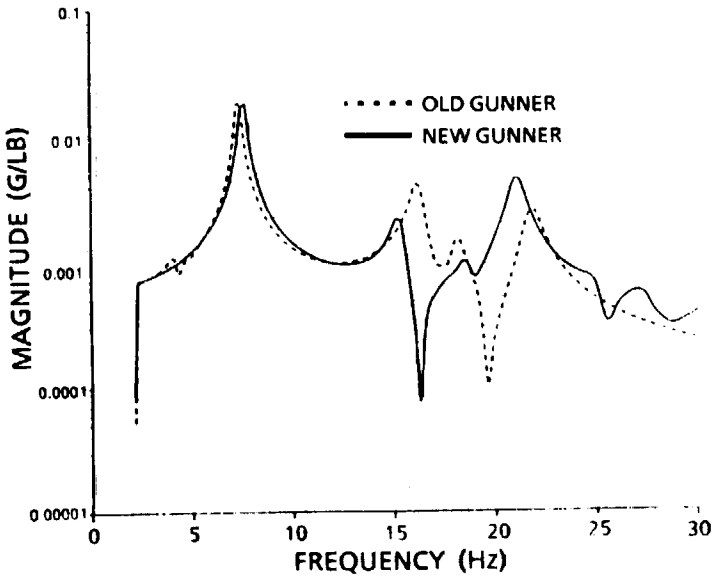

LATERAL AT TAIL -
LATERAL RESPONSE AT GUNNER

FEM TEST CONFIGURATIONS WEIGHT SUMMARY

During the shake test work conducted under this program, specific weight items were removed from the AH-1G helicopter. In order to correlate with the shake test data, the same corresponding weight items were removed from the AH-1G NASTRAN model. Generally, at BHTI a detailed weights tape of the empty flight configuration is generated by the Weight and Value Engineering System (WAVES). The mass data are then automatically distributed to existing NASTRAN mass grids on CONM2 (concentrated mass) cards using the SDSB01 program. However, since no WAVES tape had ever been developed for the AH-1G, a method was developed that enabled the existing CONM2 cards in the NASTRAN model to be converted over to $DWI (direct weight input) cards for use in SDSB01, thereby eliminating the need for a WAVES tape. Of course, to execute SDSB01 a WAVES tape must still be read; however, an $XCLUDE card can be used to eliminate all of the weight on the WAVES tape. The known weight of the item removed during the shake test can then be put on a $DWI card as a negative weight at the proper station, buttline, and waterline. After executing SDSB01, a new set of CONM2 cards will be generated representing the AH-1G configuration with the weight item removed.

A FORTRAN 77 program to convert the existing CONM2 cards to $DWI cards has been developed. The program reads a COSMIC or MSC/NASTRAN deck with 10,000 or fewer lines in standard single field format. There is no interactive user input. The weight from the CONM2 cards and the geometry on the associated GRID cards are extracted and punched onto $DWI cards. The output file uses an LRECL of 80 (i.e., 80 column output). Currently, the program does not account for rotational inertia on CONM2 continuation cards. The user must manually account for this rotational inertia as well as all weight data on CONM2 cards, density on MAT1 cards, and nonstructural mass on PBAR cards. In addition, the program does not interpret non-basic coordinate systems. In order to reduce the program's execution time, a large NASTRAN data deck should be copied to a temporary file and those sections of the data not containing CONM2 or GRID cards should be deleted.

FEM TEST CONFIGURATIONS WEIGHT SUMMARY

CONFIGURATION	GROSS WEIGHT		CG			I_{11}	I_{22}	I_{33}
	NASTRAN	TEST	FS	BL	WL			
1. ORIGINAL (FULL-UP)	6929	6928	197.4	–.06	75.6	1.06 + 7	5.65 + 7	4.79 + 7
2. M/R PYLON REMOVED	5119	5116	198.2	–.06	59.0	2.93 + 6	4.78 + 7	4.69 + 7
3. SECONDARY STRUCTURE REMOVED	4863	4857	198.3	–.06	59.2	2.77 + 6	4.65 + 7	4.56 + 7
4. T/R DRIVE SHAFTS REMOVED	4777	4771	197.9	–.06	59.0	2.74 + 6	4.46 + 7	4.37 + 7
5. SKID LANDING GEAR REMOVED	4676	4663	198.2	–.06	59.8	2.44 + 6	4.42 + 7	4.34 + 7
6. ENGINE REPLACED BY RIGID ENGINE	4676	4663	198.2	–.06	59.8	2.44 + 6	4.42 + 7	4.34 + 7
7. RIGID ENGINE REMOVED	3767	3755	197.4	–.08	54.8	1.84 + 6	3.94 + 7	3.91 + 7
8. FUEL DRAINED AND SUMPED	3202	3190	196.9	–.09	55.3	1.84 + 6	3.88 + 7	3.85 + 7

FEM MODIFICATIONS - A SUMMARY

A summary of the modifications made to the AH-1G FEM in order to obtain each test configuration is given below. Affected NASTRAN elements are cataloged in Appendix A. Removal of component elements (mass and stiffness) represents direct removal of existing elements only - no modifications.

Configuration	Modifications to FEM to Obtain Test Configuration			
	Structural Elements		Mass Elements	
	Remove	Add	Remove	Add
1	None	None	Small fairings and access panels	Pilot ballast (450 lb) and fuel (565 lb) Replace M/R and T/R with test fixtures weight
2	M/R pylon, elastomeric mounts, controls, lift link	Quad-brace hoist	M/R pylon, ballast (100 lb), access panels, input D/S, hydraulic pump, etc.	None
3	None	None	Secondary panel mass (359 lb)	Ballast (100 lb)
4	None	None	T/R drive shaft (26 lb), ballast (50 lb)	None
5	Skid tube elements	None	Skid (108 lb)	None
6	None. Mock engine has same properties as original NASTRAN FEM	None	None	None
7	Engine mount RBE2 equations	None	Engine mass/inertia, ballast (300 lb)	None
8	None	None	Fuel mass (565 lb)	None

FEM MODIFICATIONS - A SUMMARY

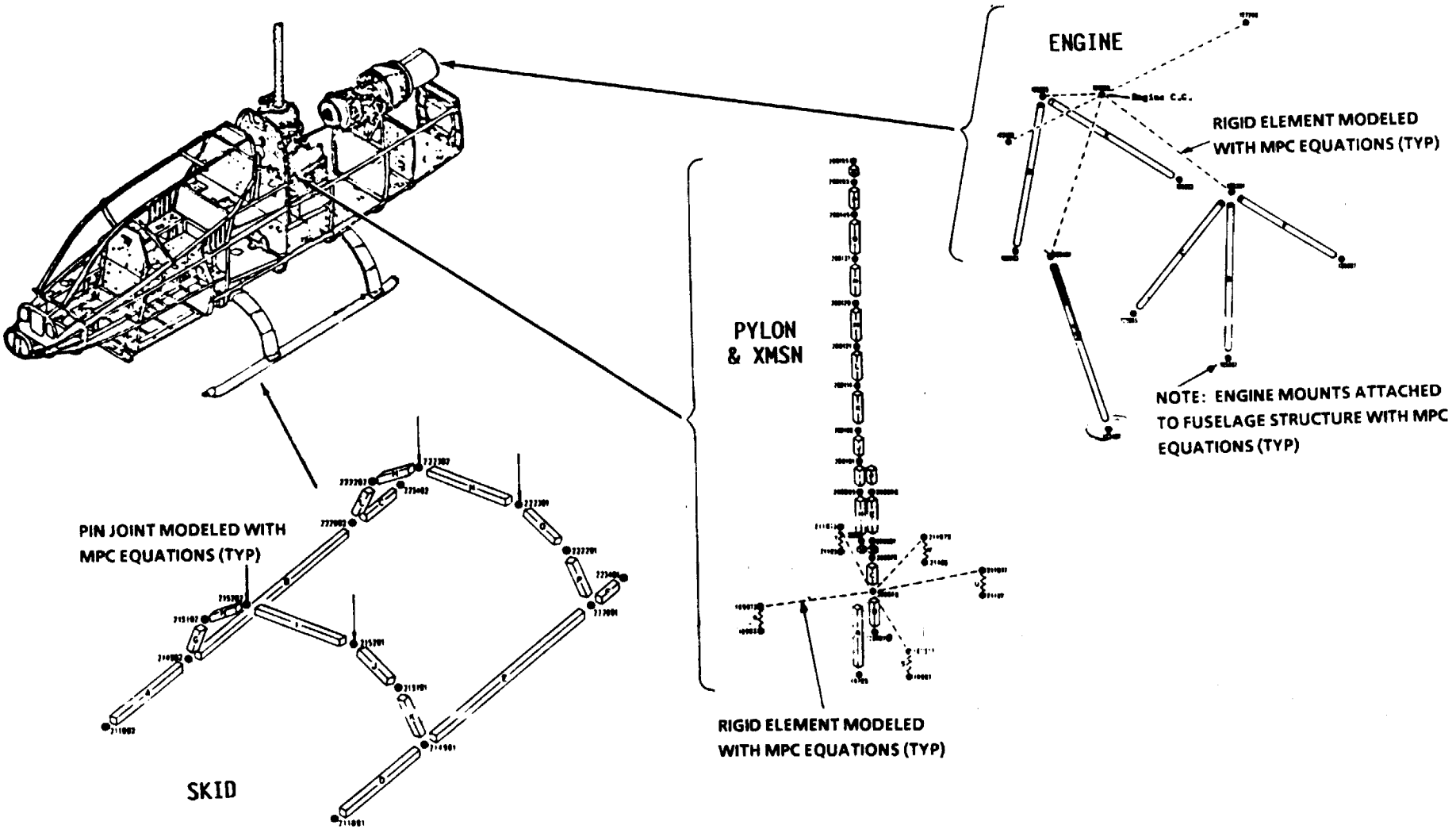

NORMAL MODE IDENTIFICATION - EXAMPLE

One of the single, most important efforts in determining the effect of each component was to identify the experimental and analytical modal characteristics. Modal Plus* is an SDRC modal analysis software package for the determination of the dynamic characteristics of a structure from frequency response functions. It provides interactive analysis and the validation and display of test data to extract modal parameters. Typical static and dynamic displays from Modal Plus of modal deformation are shown. The theory behind the extraction techniques is in the theory section of the Modal Plus User's manual (Ref. 6, Chapter 6). NASTRAN normal mode deformed plots, a kinetic energy DMAP from Hughes (Ref. 7), and modal strain energy output are used to identify the modes. A sample NASTRAN modal deformed plot is also shown.

*Product of Structural Dynamics Research Corporation (SDRC).

NORMAL MODE IDENTIFICATION – EXAMPLE

MODAL PLUS STATIC DISPLAY

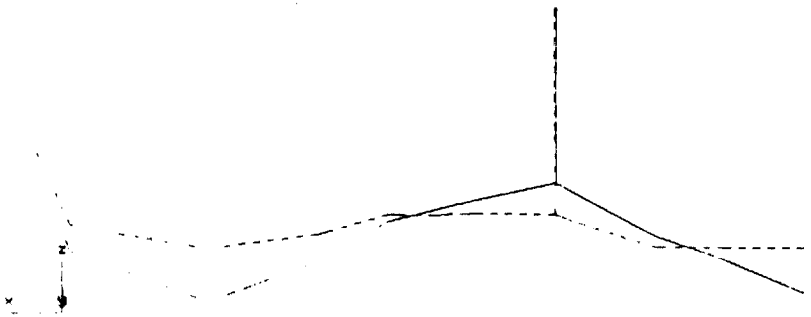

NASTRAN NORMAL MODES DEFORMED PLOTS

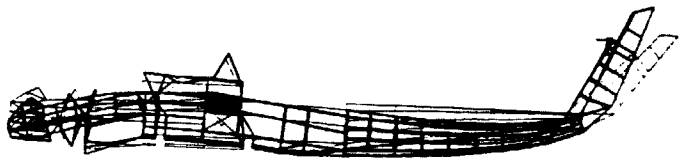

MODAL PLUS DYNAMIC DISPLAY

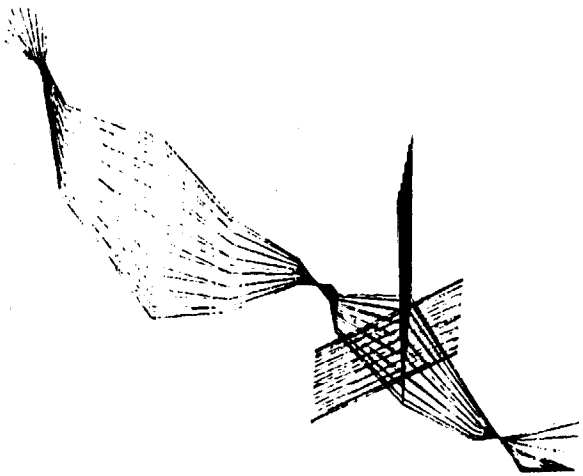

PRELIMINARY COMPARISON OF TEST/ANALYSIS FREQUENCY PLACEMENT

Natural frequencies extracted from Modal Plus* for seven dominant elastic modes are compared with frequencies obtained from a NASTRAN normal modes analysis (Rigid Format 3) for six of the eight configurations tested. NASTRAN results represent initial predictions obtained with the FEM by direct removal of the mass and stiffness properties associated with those components removed in test (see Volume I of this report for details of the components removed). These initial comparisons were used to identify trends in the percentage of error between analysis and test natural frequency placement. The test values were used as the basis for the error calculations shown in the tables and on the fan plot, which brackets 0% to 20% error. A significant error increase was evident in several modes when the secondary structure was removed (i.e., between Configurations 2 and 3). Therefore, the general assumption in FEM that the secondary structure is ineffective became suspect. Investigations into this and other suspect components are detailed on the following several pages.

*Product of Structural Dynamics Research Corporation (SDRC).

PRELIMINARY COMPARISON* OF TEST/ANALYSIS FREQUENCY PLACEMENT

CONFIGURATIONS 1, 2, AND 3

MODE†	CONFIGURATION 1 FULL-UP			CONFIGURATION 2 PYLON REMOVED			CONFIGURATION 3 SECONDARY STRUCTURE REMOVED		
	TEST ω_n (Hz)	NASTRAN ω_n (Hz)	ω_n ERROR (%)	TEST ω_n (Hz)	NASTRAN ω_n (Hz)	ω_n ERROR (%)	TEST ω_n (Hz)	NASTRAN ω_n (Hz)	ω_n ERROR (%)
FIRST LATERAL BENDING	7.3	7.4	1.4	7.5	7.4	-1.3	7.3	7.5	2.7
FIRST VERTICAL BENDING	8.0	8.2	2.5	8.3	8.4	1.2	7.9	8.5	7.6
SECOND LATERAL BENDING	16.0	16.7	4.4	15.9	16.9	6.3	14.6	17.0	16.4
SECOND VERTICAL BENDING	16.6	17.7	6.6	17.4	18.9	8.6	15.9	19.1	20.0
FUSELAGE TORSION	23.5	23.7	0.9	23.2	23.9	3.0	20.1	21.3	5.9
THIRD VERTICAL BENDING	24.7	28.2	14.1	25.1	28.3	12.7	23.5	28.6	21.7
THIRD LATERAL BENDING	32.4	32.8	1.2	32.5	33.0	1.5	30.2	32.6	7.9

*NASTRAN RESULTS REPRESENT DIRECT REMOVAL OF COMPONENT STIFFNESS AND MASS PROPERTIES.

†IMPORTANT GLOBAL AIRFRAME MODES PICKED AS REPRESENTATIVE TO STUDY TRENDS - ALL MODES NOT INCLUDED.

PRELIMINARY COMPARISON* OF TEST/ANALYSIS FREQUENCY PLACEMENT

CONFIGURATIONS 5, 7, AND 8

MODE†	CONFIGURATION 5 SKID GEAR REMOVED			CONFIGURATION 7 ENGINE REMOVED			CONFIGURATION 8 FUEL REMOVED		
	TEST ω_n (Hz)	NASTRAN ω_n (Hz)	ω_n ERROR (%)	TEST ω_n (Hz)	NASTRAN ω_n (Hz)	ω_n ERROR (%)	TEST ω_n (Hz)	NASTRAN ω_n (Hz)	ω_n ERROR (%)
FIRST LATERAL BENDING	7.4	7.6	1.3	8.2	8.4	2.4	8.2	8.5	2.4
FIRST VERTICAL BENDING	7.9	8.6	8.8	8.6	9.1	5.8	8.7	9.4	8.0
SECOND LATERAL BENDING	14.9	17.3	16.1	16.2	18.9	16.7	16.6	18.6	12.0
SECOND VERTICAL BENDING	16.0	19.1	19.4	16.9	19.9	17.8	17.3	20.3	17.3
FUSELAGE TORSION	20.3	20.6	1.5	21.3	24.6	15.5	21.3	24.4	14.6
THIRD VERTICAL BENDING	22.9	29.0	26.6	24.6	30.3	23.2	25.3	31.5	24.5
THIRD LATERAL BENDING	30.9	33.0	6.8	29.8	33.3	11.7	30.9	33.8	9.4

*NASTRAN RESULTS REPRESENT DIRECT REMOVAL OF COMPONENT STIFFNESS AND MASS PROPERTIES.

†IMPORTANT GLOBAL AIRFRAME MODES PICKED AS REPRESENTATIVE TO STUDY TRENDS - ALL MODES NOT INCLUDED.

PRELIMINARY NATURAL FREQUENCY COMPARISONS

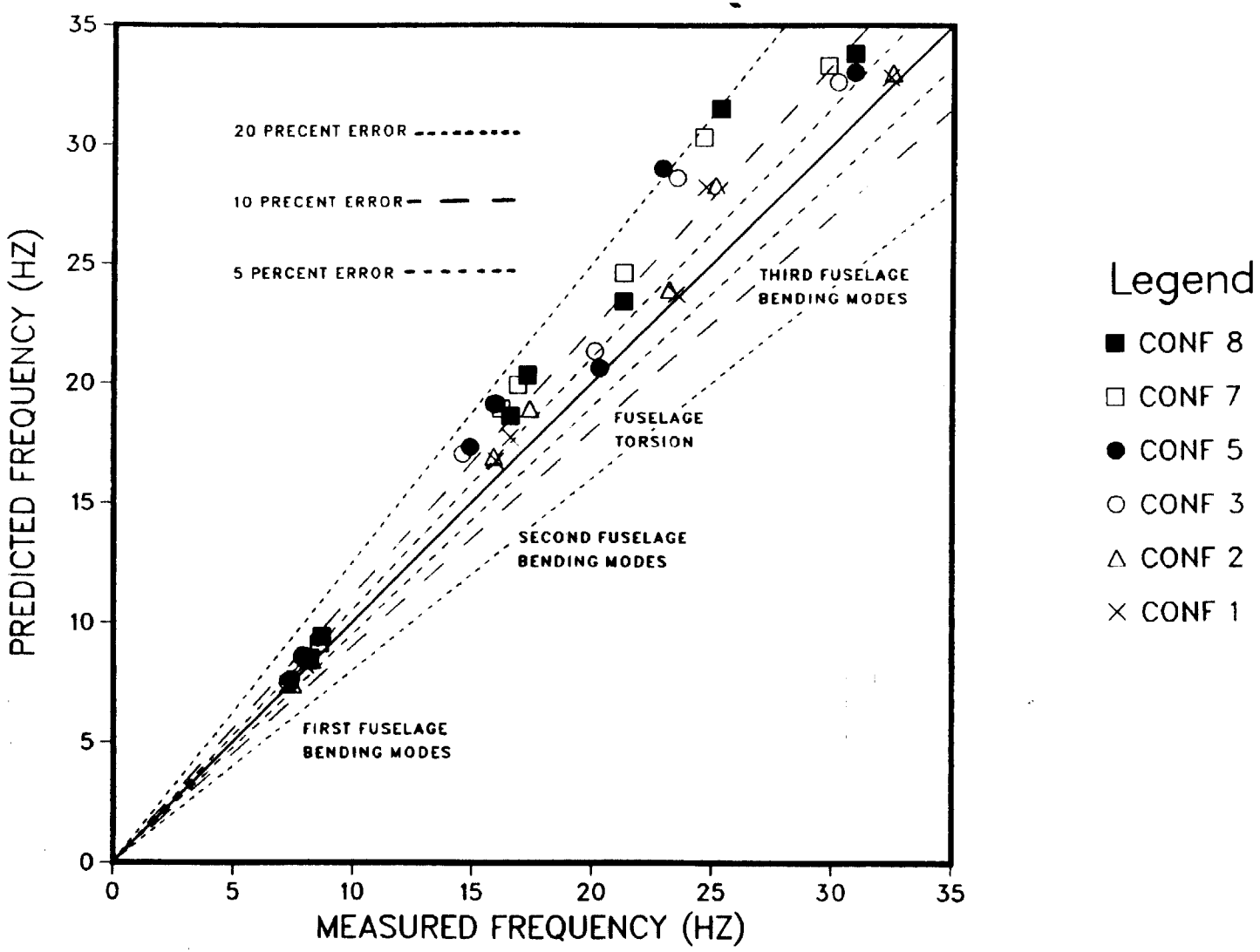

ESTABLISH BASELINE (CONFIGURATION 8) NASTRAN FEM FOR CORRELATIONS

The intent of the initial comparison is to establish the level of correlation between test and analysis in Configuration 8, which represents primary airframe structure only, since this configuration will be used as the baseline to determine the effect of each component on overall vibratory response.

The FEM of Configuration 8 was obtained by applying all the diagnostic, weight, and element updates detailed on the previous 16 pages to the original full-up FEM. These updates were required to obtain a realistic representation of the stripped-down aircraft shake test article.

ESTABLISH BASELINE (CONFIGURATION 8) NASTRAN FEM FOR CORRELATIONS

- BASELINE (CONFIGURATION 8) INVESTIGATIONS
  - SECONDARY STRUCTURE EFFECTS
  - ELASTIC LINE TAILBOOM vs BUILT-UP TAILBOOM
  - MODAL DAMPING EFFECTS
- NASTRAN FEM UPDATES BASED ON INVESTIGATIONS
- FINAL BASELINE (CONFIGURATION 8) FEM CORRELATION
  - COMPARISON OF NATURAL FREQUENCIES
  - FREQUENCY RESPONSE COMPARISONS
  - FORCED RESPONSE MODE SHAPE COMPARISONS

SECONDARY PANEL EFFECTIVE STIFFENING INVESTIGATION (CONFIGURATION 8)

A significant global stiffness variation was evident in the test modal response when the secondary structure was removed from the AH-1G (see Volume I, page 82). The structure removed between tests of Configurations 2 and 3 included 359 pounds of cowlings, fairings, hinged pilot and copilot doors, and assumed nonstructural panels on the contour of the ship from FS 61 (just aft of the nose) to FS 186 (just forward of the wings). In the NASTRAN FEM, however, only four of the members (panels located on the fuselage belly and tailboom bottom skin) had their stiffness accounted for while the remainder of the elements were only represented by mass. Therefore, the assumed nonstructural panels became suspect as members that actually do contribute stiffness to the fuselage. These contour panels are attached with screws and help to support the wedge-shaped canopy frame and gunner/pilot consoles. It was determined by analytical investigations that in tests without the contour panels the canopy frame and console members became ineffective. The unique cross section of the AH-1G from FS 61 to FS 148 is highlighted in the figure. In this area, the main beams cant inward and create a 4- to 8-inch area between the main beam and contour skin panels in question for controls and wiring access.

Essentially because of the nature of this cross section, the contour panels provide shear transfer, close the cross section, and hence contribute stiffness that cannot be neglected. The remedy in this case was to add some relatively thin (t = 0.01 inch) shear panels to Configurations 1 and 2 to allow for some shear transfer. This had the most significant effect on the second lateral bending mode (+0.5 Hz) and the fuselage torsion mode (+1.3 Hz), as expected, while leaving the other modes relatively unaffected. In addition to removing these shear panels from the FEM for Configurations 3 through 8, the NASTRAN elements for the canopy frame and console webs were removed because they are ineffective without the contour panels in place. To highlight the effects of these changes, a table of the natural frequency variation due to stiffness removed by the original four belly panels and the updated shear panel/canopy frame elements is provided.

It should be noted that the results found in this study are configuration dependent and do not suggest a panacea for modeling secondary structure.

SECONDARY PANEL EFFECTIVE STIFFENING INVESTIGATION (CONFIGURATION 8)

FS	①	②	③	④
61	L = 0"	5"	14"	4"
70	L = 1.5"	6"	14"	5"
85	L = 4"	7"	14"	7"
93	L = 6"	8"	15"	8"
115	L = 8"	8"	16"	8"
138	L = 11"	8"	17"	8"
148	L = 14"	8"	17.5"	8"

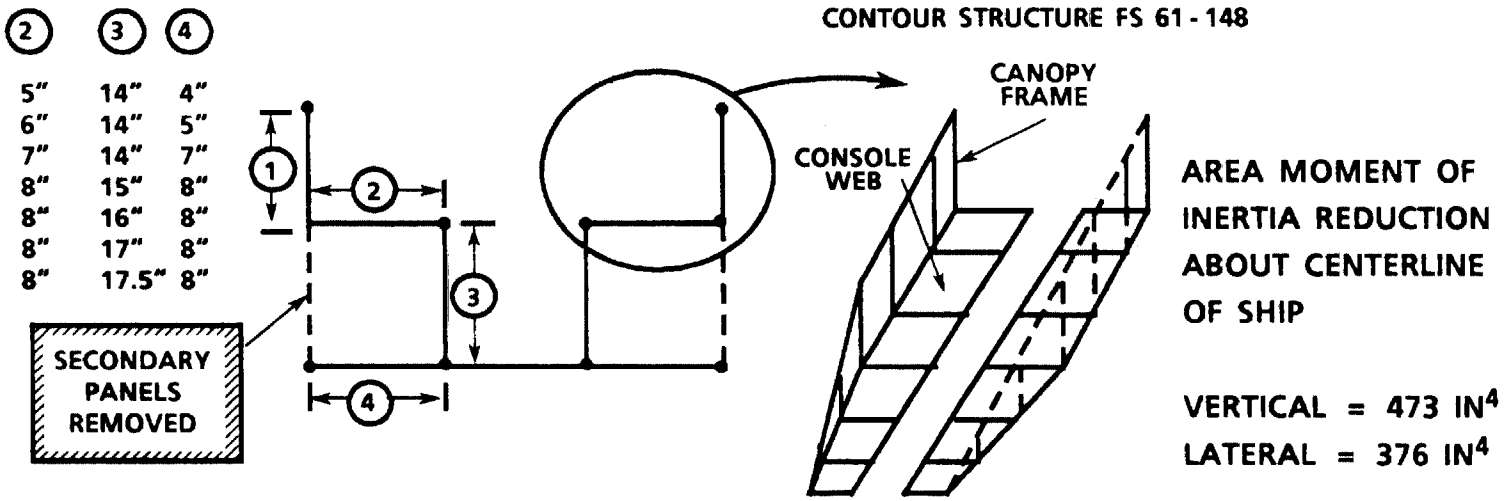

AREA MOMENT OF INERTIA REDUCTION ABOUT CENTERLINE OF SHIP

VERTICAL = 473 IN^4

LATERAL = 376 IN^4

TEST – NONSTRUCTURAL PANELS REMOVED; CONTOUR SECONDARY STRUCTURE BECOMES INEFFECTIVE

PRELIMINARY FEM – ONLY NONSTRUCTURAL PANEL MASS REMOVED

FINAL FEM – NONSTRUCTURAL PANEL MASS AND EFFECTIVE SECONDARY STRUCTURE STIFFNESS REMOVED

SECONDARY PANEL EFFECTIVE STIFFENING INVESTIGATION (CONFIGURATION 8)

MODE	PRELIMINARY FEM ω_n (Hz)	CONTOUR STRUCTURE REMOVED		BELLY PANELS REMOVED		TEST ω_n (Hz)
		ω_n (Hz)	DELTA ω_n (Hz)	ω_n (Hz)	TOTAL DELTA ω_n (Hz)	
FIRST LATERAL	8.5	8.5	–	8.3	-0.2	8.2
FIRST VERTICAL	9.4	9.1	-0.3	8.9	-0.5	8.7
SECOND LATERAL	18.6	17.5	-1.1	17.1	-1.5	16.6
SECOND VERTICAL	20.3	18.2	-2.1	17.9	-2.4	17.3
TORSION	24.4	22.9	-1.5	22.5	1.9	21.3
THIRD VERTICAL	31.5	29.1	-2.4	28.9	-2.6	25.3
THIRD LATERAL	33.8	31.5	-1.8	30.5	-2.8	30.9

ELASTIC LINE VS BUILT-UP TAILBOOM INVESTIGATION (CONFIGURATION 8)

NASTRAN frequency response and normal modes analyses were performed with two different tailboom representations, an elastic line model and a built-up model, to investigate the effects on vibration predictions. This investigation was conducted on the primary structure model (Configuration 8) since direct relationships of tailboom effects on primary bending modes are most evident on the stripped configuration. The two representative frequency response function comparison plots shown indicate that the built-up FEM agrees better with the test results, particularly in the antiresonant area before 15 Hz and for torsion and third vertical bending above 20 Hz.

Mode	Test	NASTRAN		% Error	
		Elastic	Built-Up	Elastic	Built-Up
First lateral	8.2	8.3	8.5	1.2	3.6
First vertical	8.7	8.9	9.1	2.3	4.6
Second lateral	16.6	17.1	16.0	3.0	3.8
Second vertical	17.3	17.9	17.2	3.5	0.6
Torsion	21.3	22.5	21.4	5.6	0.5
Third vertical	25.3	28.9	26.3	14.2	3.9
Third lateral	30.9	30.5	29.3	1.3	5.2

ELASTIC LINE vs BUILT-UP TAILBOOM INVESTIGATION (CONFIGURATION 8)

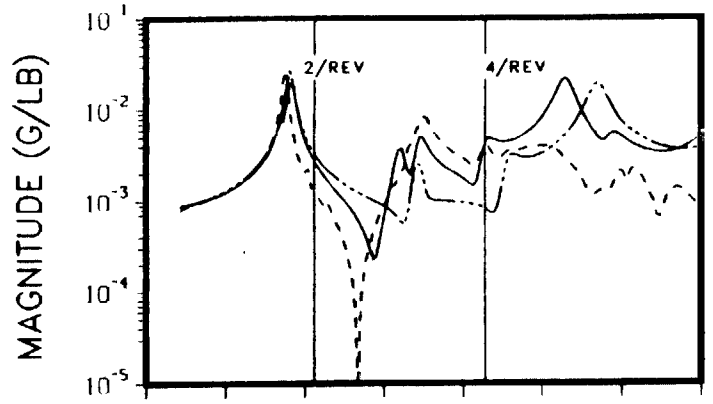

NOSE (FS 48) VERTICAL RESPONSE

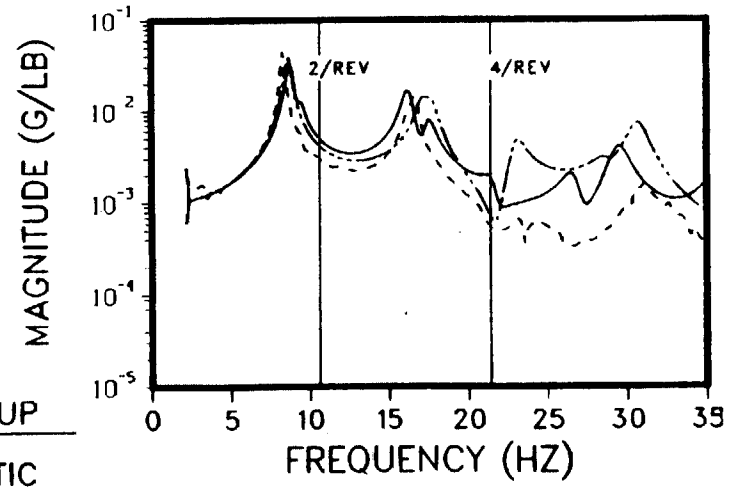

BUILTUP

ELASTIC

TEST

NOSE (FS 48) LATERAL RESPONSE

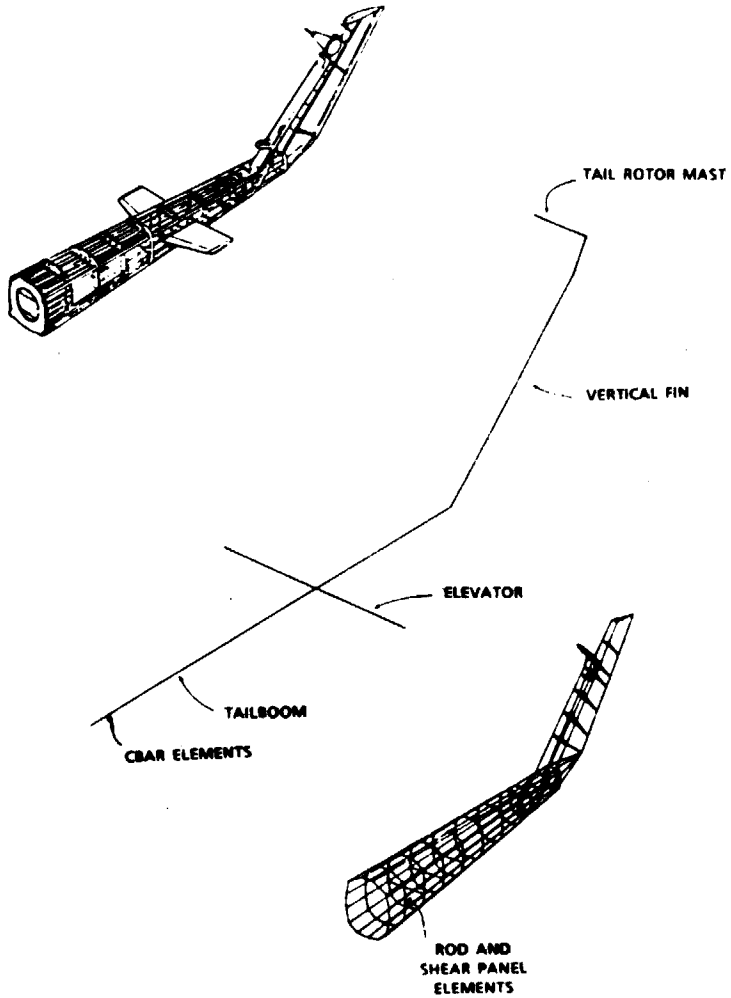

MODAL DAMPING INVESTIGATION (CONFIGURATION 8)

All NASTRAN results, unless otherwise stated, assume a constant 4% structural (or 2% critical) damping value in the frequency range of interest. Modal Plus has the ability to estimate modal damping (critical viscous damping) using the 1/2 power method technique (Ref. 6). These estimates of damping extracted from the frequency response functions measured in test were input to NASTRAN in step-function tabular format (via TABDMP) to study their effect on vibration prediction. Modal Plus damping values for modes identified in Configuration 8 are listed below and the resultant frequency response function comparisons of NASTRAN and test for vertical and lateral response with and without variable damping are shown on the figure.

Mode	Test Frequency (Hz)	Damping (% critical)	Amplitude	Phase
First lateral	8.2	1.09	2.56-2	1.441
First vertical	8.7	1.02	4.63-3	-1.475
Second lateral	16.6	1.4	2.31-2	-1.514
Second vertical	17.3	3.1	1.56-2	-1.864
Torsion	21.3	1.9	8.83-4	1.083
Third vertical	25.3	3.5	6.6 -3	1.333
Third lateral	30.9	2.2	3.54-3	1.668

MODAL DAMPING INVESTIGATION (CONFIGURATION 8)

VERTICAL LOAD AT THE TAIL SKID

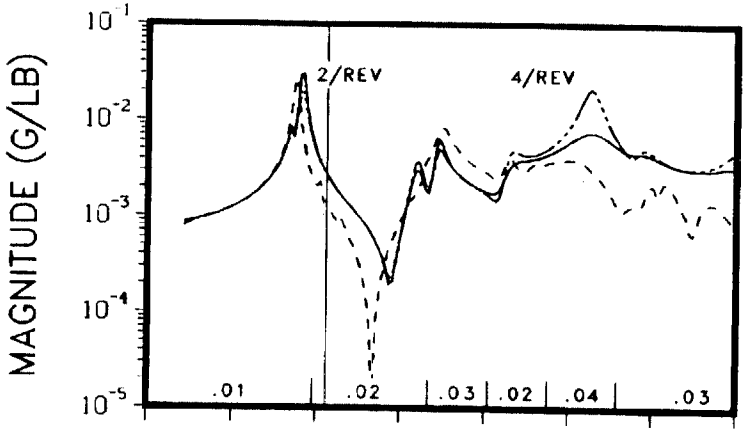

NOSE (FS 48) VERTICAL RESPONSE

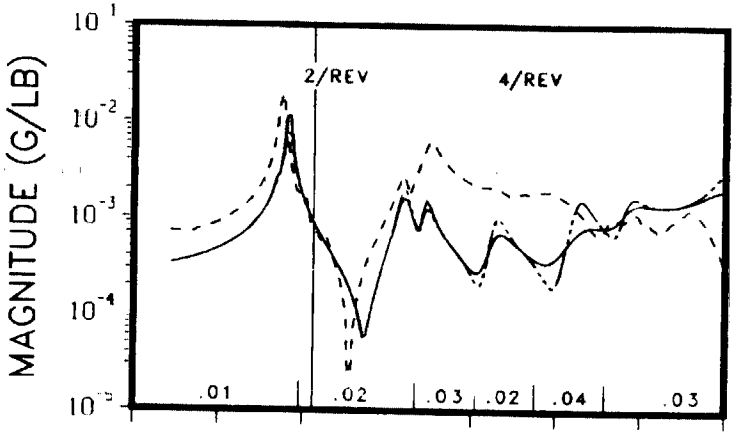

CG (FS 196) VERTICAL RESPONSE

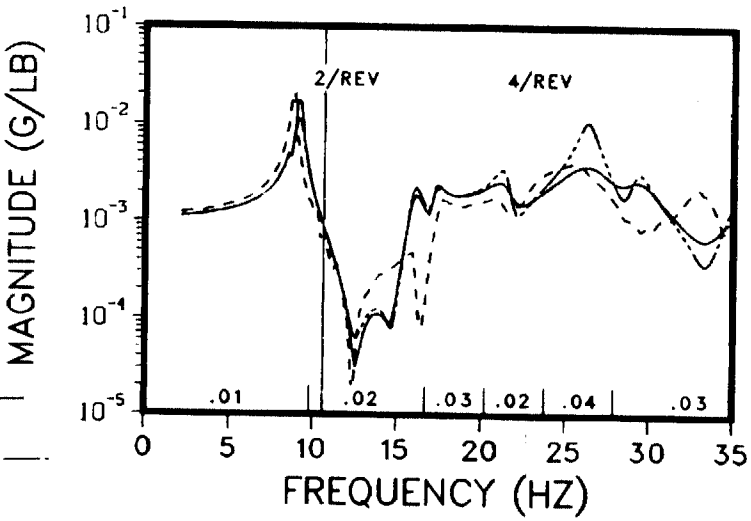

T/B JUNCTION (FS 296) VERTICAL RESPONSE

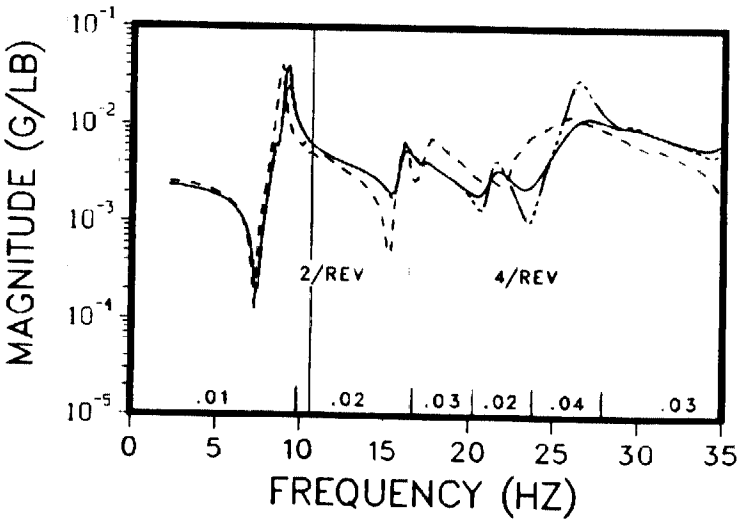

TAIL SKID (FS 485) VERTICAL RESPONSE

BUILTUP

ELASTIC

TEST

MODAL DAMPING INVESTIGATION (CONFIGURATION 8)

LATERAL LOAD AT THE TAIL ROTOR

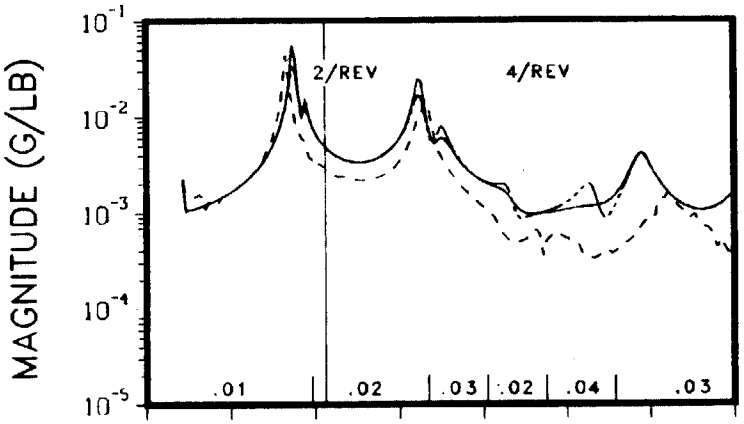

NOSE (FS 48) LATERAL RESPONSE

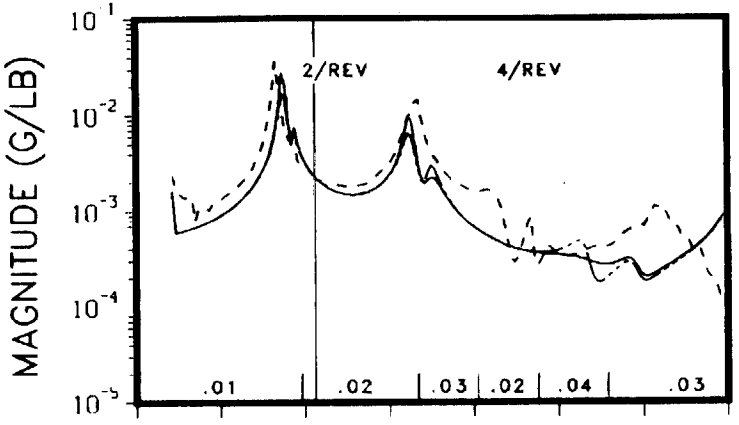

CG (FS 196) LATERAL RESPONSE

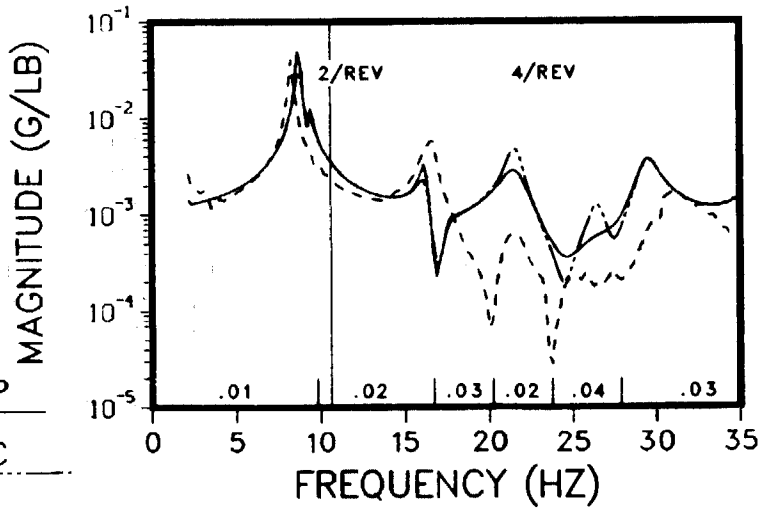

T/B JUNCTION (FS 296) LATERAL RESPONSE

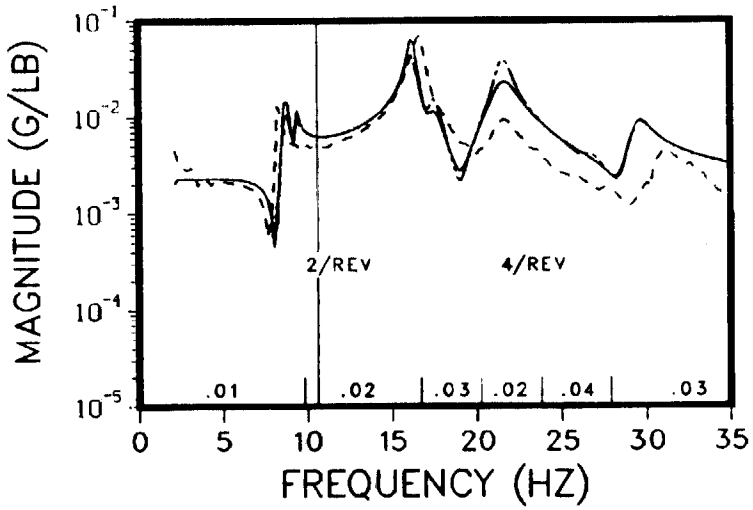

TAIL SKID (FS 485) LATERAL RESPONSE

FINAL NASTRAN FEM USED FOR CORRELATIONS

As a result of the investigations into preliminary comparisons between test and analysis, three major areas were identified immediately and updates included in the eight airframe configurations FEM(s).

Each of these topics has been discussed on previous pages. The resultant FEM for Configuration 1 is shown below with the number of degrees-of-freedom and elements highlighted in the table. The increased number of elements over the original FEM (page 13) is a direct result of the built-up tailboom model. The updated FEM was used in the remainder of the comparisons and represents the starting point for isolated component investigations. Variable modal damping values are only used in selected cases to demonstrate its effect. However, in general, a uniform value of 2% critical is still used to simplify comparisons and reduce the number of variables.

FINAL NASTRAN FEM USED FOR CORRELATIONS

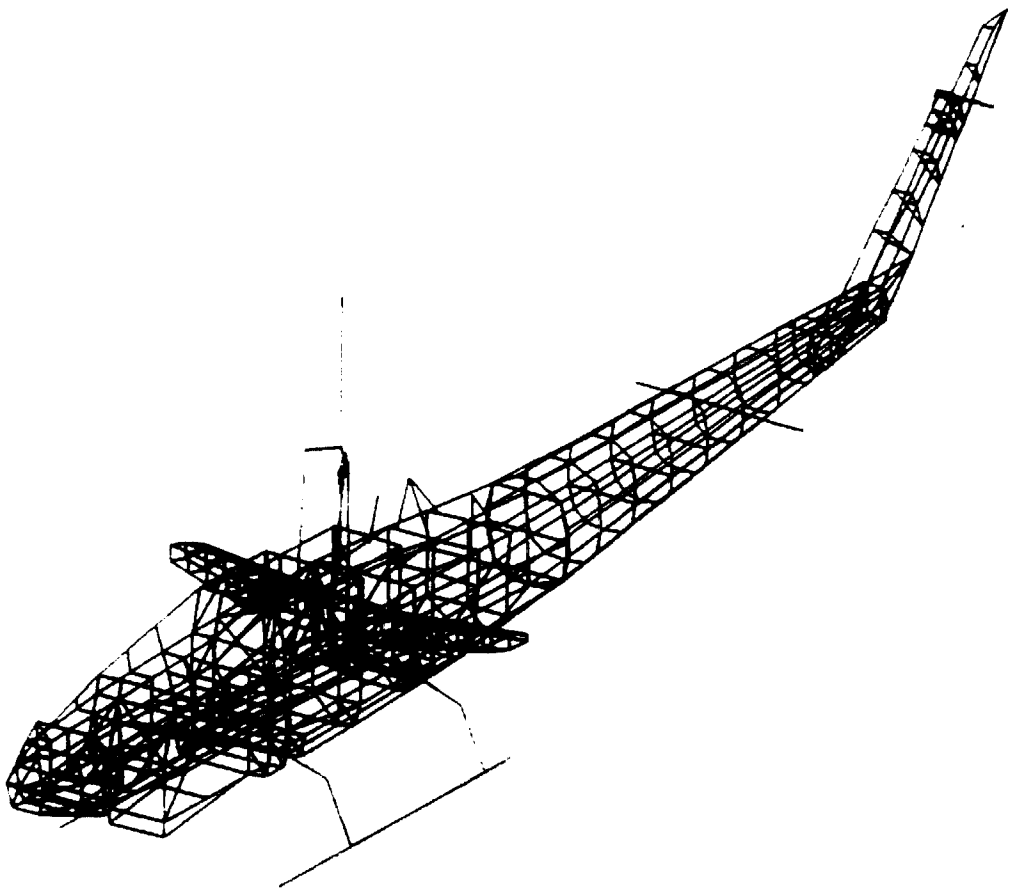

DEGREES OF FREEDOM		ELEMENTS	
K_{gg}	4611	BAR	358
K_{nn}	4223	ROD	3072
K_{ff}	2965	SHEAR	540
K_{aa}	241	QDMEM	160
$K_{\ell\ell}$	235	TRMEM	243

- CONTOUR STRUCTURE (FS 61 – 148) STIFFNESS REMOVED FROM CONFIGURATIONS 3 – 8
- BUILT-UP TAILBOOM REPLACES ELASTIC LINE ON ALL CONFIGURATIONS
- MODAL DAMPING
  - UNIFORM DAMPING ASSUMED FOR SIMPLICITY (2% LOSS)
  - WOULD BE MODIFIED ACCORDINGLY FOR ACTUAL RESPONSE PREDICTION

NASTRAN DEFORMED SHAPES - CONFIGURATION 1 VS CONFIGURATION 8

Two examples of NASTRAN normal mode graphical output for the first and third vertical bending modes are shown for Configuration 1 (full-up) and Configuration 8 (stripped down) to demonstrate the mode shapes exhibited for these natural frequencies.

NASTRAN DEFORMED SHAPES - CONFIGURATION 1 vs CONFIGURATION 8

FIRST VERTICAL BENDING

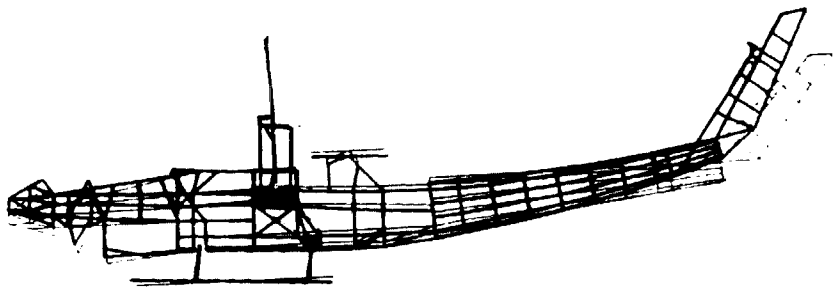

CONFIGURATION 1: ω = 8.3 Hz

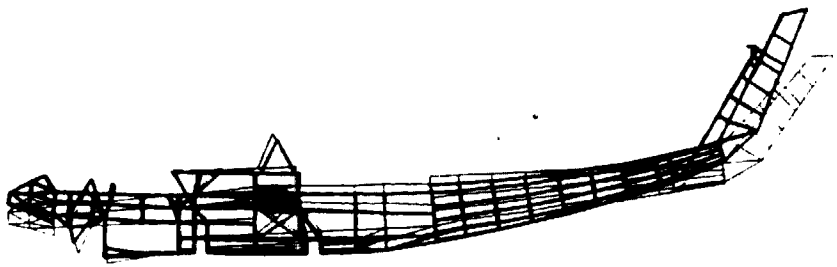

CONFIGURATION 8: ω = 9.1 Hz

THIRD VERTICAL BENDING

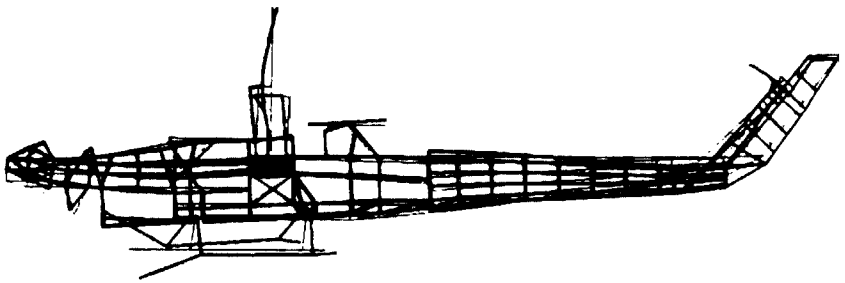

CONFIGURATION 1: ω = 25.8 Hz

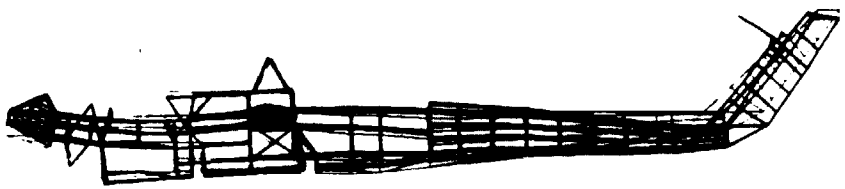

CONFIGURATION 8: ω = 26.3 Hz

FINAL COMPARISON OF TEST/ANALYSIS FREQUENCY PLACEMENT

Natural frequencies extracted from Modal Plus are compared with frequencies obtained from a NASTRAN normal modes analysis (Rigid Format 3) in the table for six of the eight configurations tested. NASTRAN results now reflect FEM predictions for each configuration with the following updates:

1. Secondary panel stiffening effects removed (e.g., canopy frame, gunner/pilot console web and belly; panels removed)

2. Gun turret mass moments of inertia added

3. Built-up tailboom replaces elastic line version of tailboom

Calculations of percentage error between NASTRAN and test natural frequencies indicate a much improved correlation of the FEM with test. All configurations exhibit approximately 5% error or less for the seven predominant flexible modes below 35 Hz once the built-up tailboom is added and the secondary panel stiffening effects are properly accounted for, as is evident when comparing this plot with the preliminary error comparison mode on page 33.

FINAL COMPARISON* OF TEST/ANALYSIS FREQUENCY PLACEMENT

CONFIGURATIONS 1, 2, AND 3

MODE†	CONFIGURATION 1 FULL-UP			CONFIGURATION 2 PYLON REMOVED			CONFIGURATION 3 SECONDARY STRUCTURE REMOVED		
	TEST ω_n (Hz)	NASTRAN ω_n (Hz)	ω_n ERROR‡ (%)	TEST ω_n (Hz)	NASTRAN ω_n (Hz)	ω_n ERROR‡ (%)	TEST ω_n (Hz)	NASTRAN ω_n (Hz)	ω_n ERROR‡ (%)
FIRST LATERAL BENDING	7.3	7.7	5.5	7.5	7.7	2.7	7.3	7.6	4.1
FIRST VERTICAL BENDING	8.0	8.4	5.0	8.3	8.7	4.8	7.9	8.3	5.1
SECOND LATERAL BENDING	16.0	15.1	-5.6	15.9	15.4	-3.1	14.6	14.1	-3.4
SECOND VERTICAL BENDING	16.6	17.7	6.6	17.4	18.3	5.2	15.9	15.7	-1.2
FUSELAGE TORSION	23.5	21.5	8.5	23.2	22.0	-5.2	20.1	19.6	-2.5
THIRD VERTICAL BENDING	24.7	25.9	4.9	25.1	26.1	3.9	23.5	23.8	1.3
THIRD LATERAL BENDING	32.4	32.1	-1.0	32.5	31.9	-1.8	30.2	29.2	-3.3

*NASTRAN RESULTS REPRESENT DIRECT REMOVAL OF SECONDARY PANEL STIFFENING EFFECTS AND INCLUDE BUILT-UP TAILBOOM.

†GLOBAL AIRFRAME MODES PICKED AS REPRESENTATIVE TO STUDY TRENDS - ALL MODES NOT INCLUDED.

‡TEST ω_n USED AS BASE FOR ERROR CALCULATIONS.

FINAL COMPARISON* OF TEST/ANALYSIS FREQUENCY PLACEMENT

CONFIGURATIONS 5, 7, AND 8

MODE†	CONFIGURATION 5 SKID GEAR REMOVED			CONFIGURATION 7 ENGINE REMOVED			CONFIGURATION 8 FUEL REMOVED		
	TEST ω_n (Hz)	NASTRAN ω_n (Hz)	ω_n ERROR‡ (%)	TEST ω_n (Hz)	NASTRAN ω_n (Hz)	ω_n ERROR‡ (%)	TEST ω_n (Hz)	NASTRAN ω_n (Hz)	ω_n ERROR‡ (%)
FIRST LATERAL BENDING	7.4	7.7	4.1	8.2	8.4	2.4	8.2	8.5	3.7
FIRST VERTICAL BENDING	7.9	8.3	5.1	8.6	8.9	3.5	8.7	9.1	4.6
SECOND LATERAL BENDING	14.9	14.5	-2.7	16.2	15.7	-3.1	16.6	16.0	-3.6
SECOND VERTICAL BENDING	16.0	15.9	-0.6	16.9	16.9	0.0	17.3	17.2	-0.6
FUSELAGE TORSION	20.3	20.3	0.0	21.3	21.1	-0.9	21.3	21.4	0.5
THIRD VERTICAL BENDING	22.9	24.0	4.8	24.6	25.7	4.5	25.3	26.3	3.9
THIRD LATERAL BENDING	30.9	28.9	-6.5	29.8	28.6	-4.0	30.9	29.3	-5.2

*NASTRAN RESULTS REPRESENT DIRECT REMOVAL OF SECONDARY PANEL STIFFENING EFFECTS AND INCLUDE BUILT-UP TAILBOOM.

†GLOBAL AIRFRAME MODES PICKED AS REPRESENTATIVE TO STUDY TRENDS - ALL MODES NOT INCLUDED.

‡TEST ω_n USED AS BASE FOR ERROR CALCULATIONS.

NATURAL FREQUENCY COMPARISONS

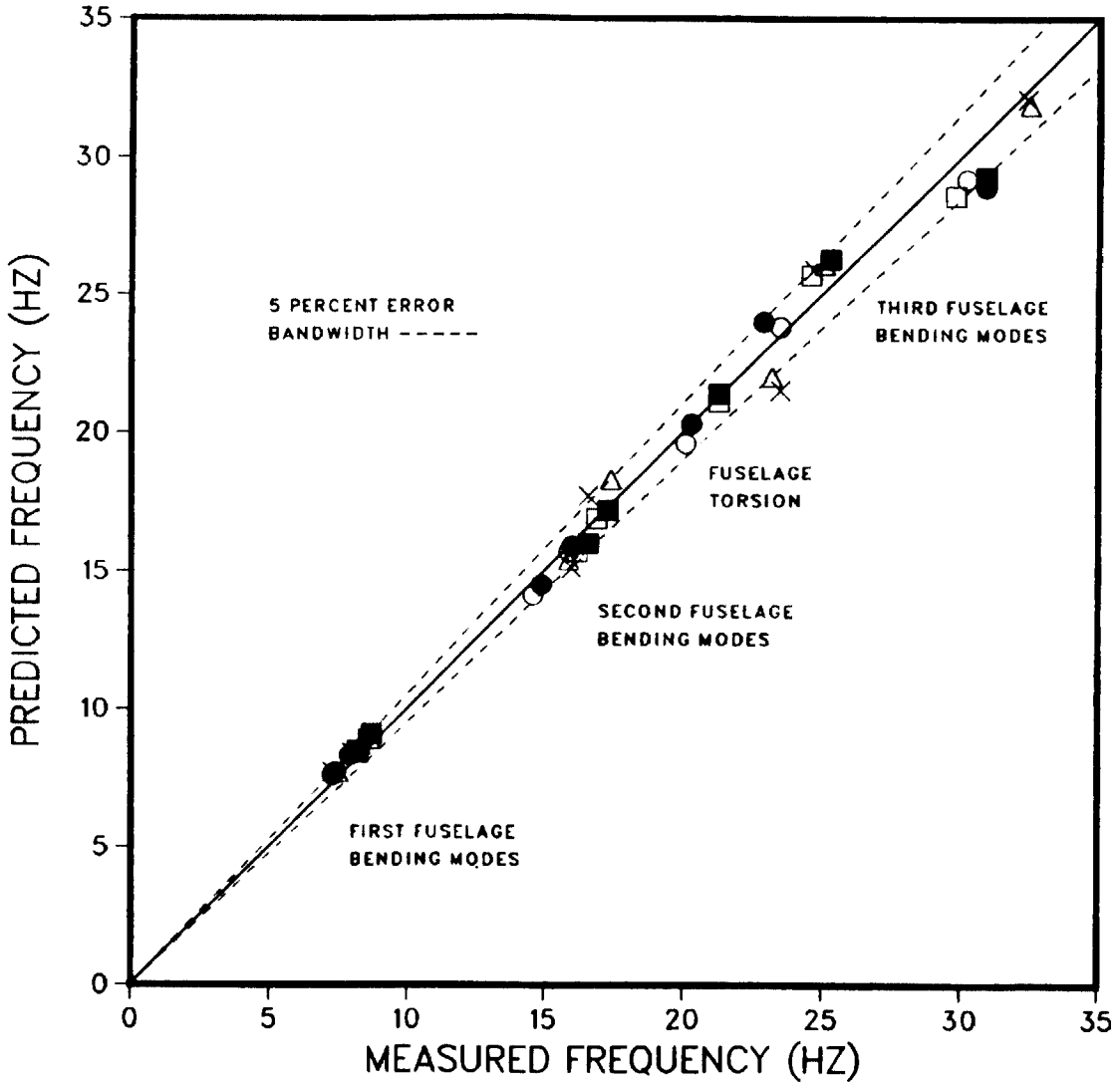

Legend

- ■ CONF 8
- □ CONF 7
- ● CONF 5
- ○ CONF 3
- △ CONF 2
- × CONF 1

VERTICAL FREQUENCY RESPONSE COMPARISONS (CONFIGURATION 8)

A comparison of measured frequency response functions with those predicted by NASTRAN is presented for eight accelerometer locations in semi-log format. The response magnitudes, normalized by input force, are presented for a vertical excitation at the tail skid (FS 485) as a function of frequency from 0-35 Hz. Modal damping estimates from test data are input as shown.

VERTICAL FREQUENCY RESPONSE COMPARISONS (CONFIGURATION 8)

FUSELAGE RESPONSE

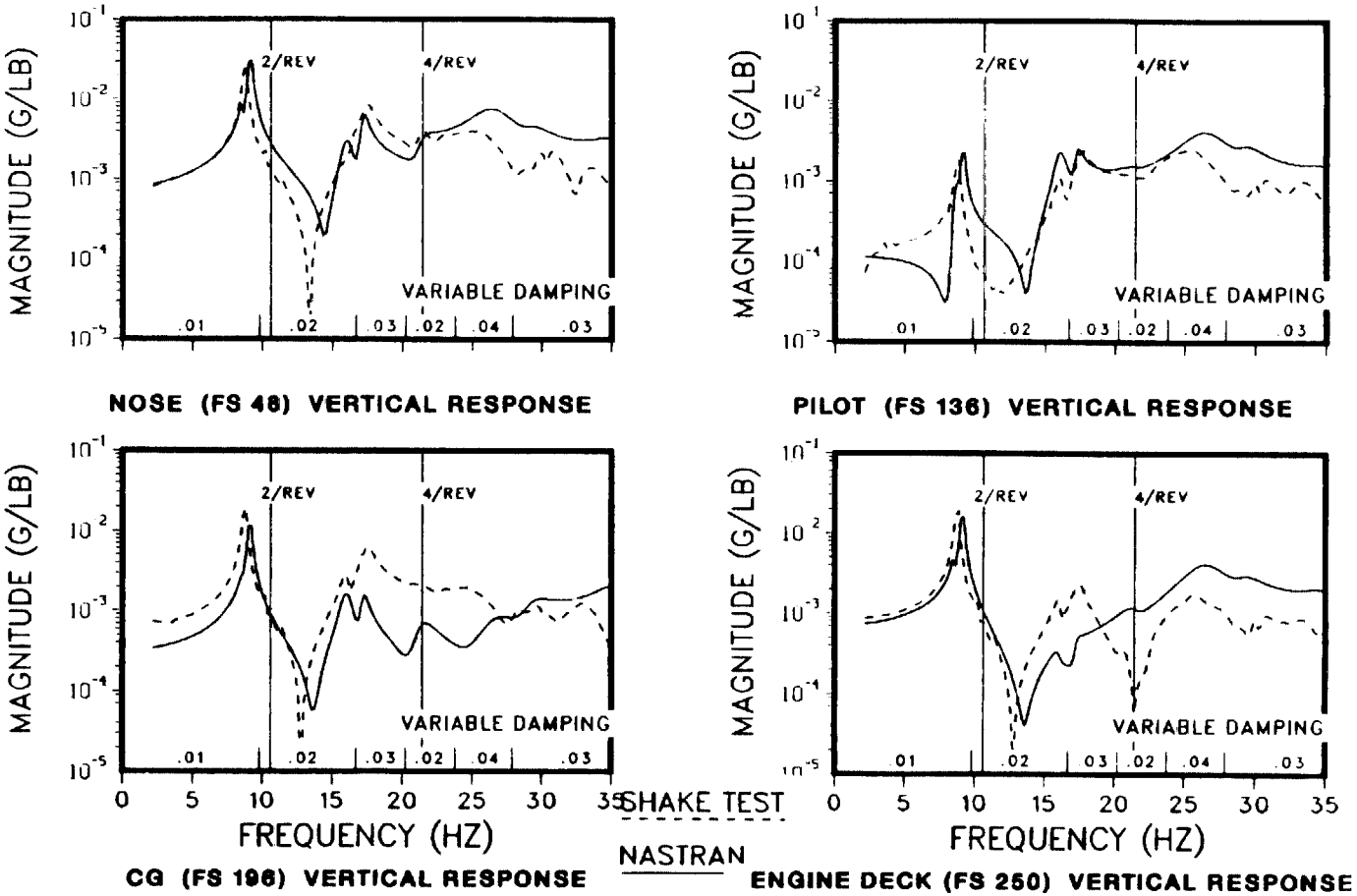

VERTICAL FREQUENCY RESPONSE COMPARISONS (CONFIGURATION 8)

TAILBOOM RESPONSE

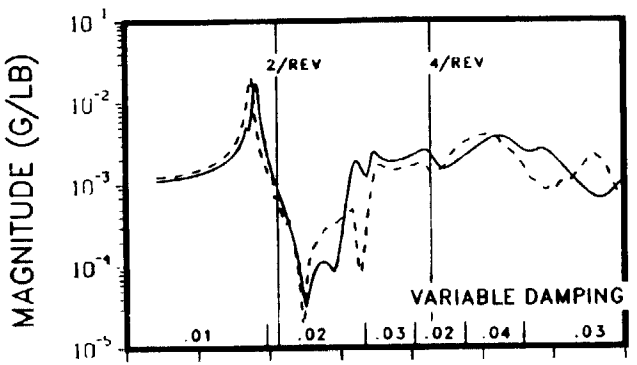

T/B JUNCTION (FS 296) VERTICAL RESPONSE

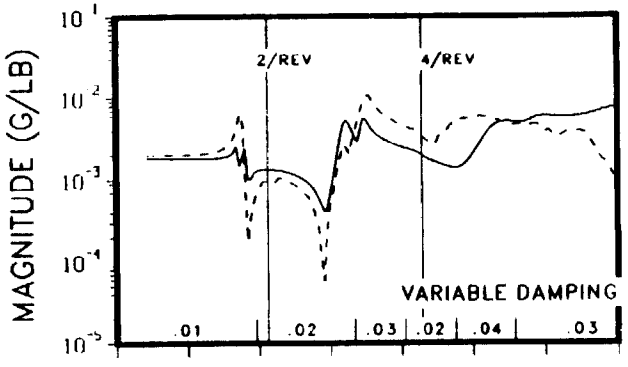

ELEVATOR (FS 402) VERTICAL RESPONSE

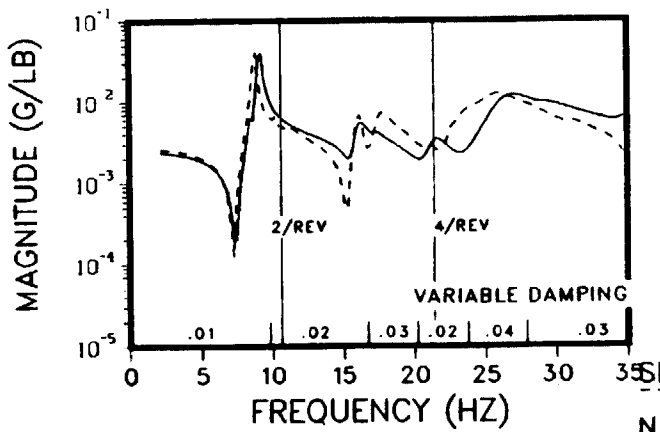

TAIL SKID (FS 485) VERTICAL RESPONSE

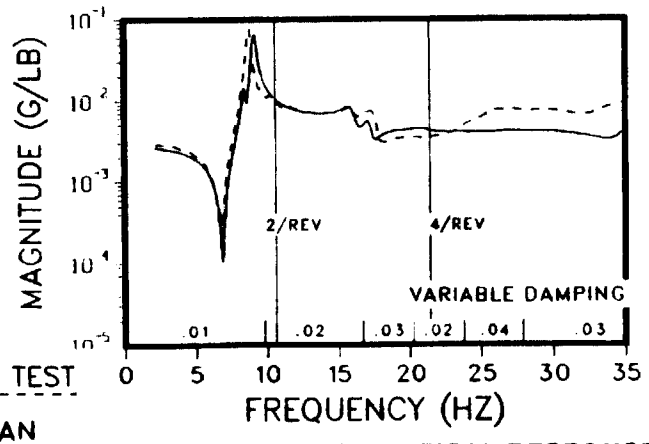

90 GEARBOX (FS 521) VERTICAL RESPONSE

SHAKE TEST

NASTRAN

LATERAL FREQUENCY RESPONSE COMPARISONS (CONFIGURATION 8)

A comparison of measured frequency response functions with those predicted by NASTRAN is presented for eight accelerometer locations in semi-log format. The response magnitudes, normalized by input force, are presented for a lateral excitation at the tail rotor hub (FS 521) as a function of frequency from 0-35 Hz. Modal damping estimates from test data are input as shown.

LATERAL FREQUENCY RESPONSE COMPARISONS (CONFIGURATION 8)

FUSELAGE RESPONSE

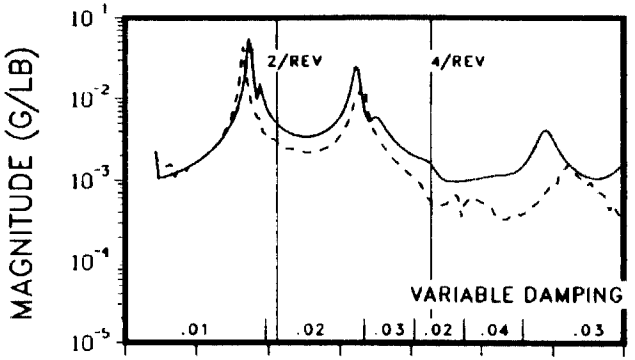

NOSE (FS 48) LATERAL RESPONSE

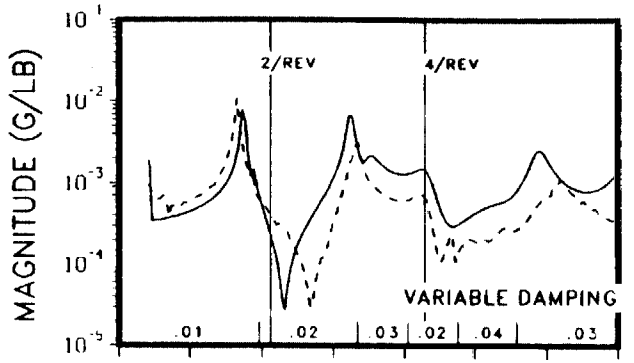

PILOT (FS 136) LATERAL RESPONSE

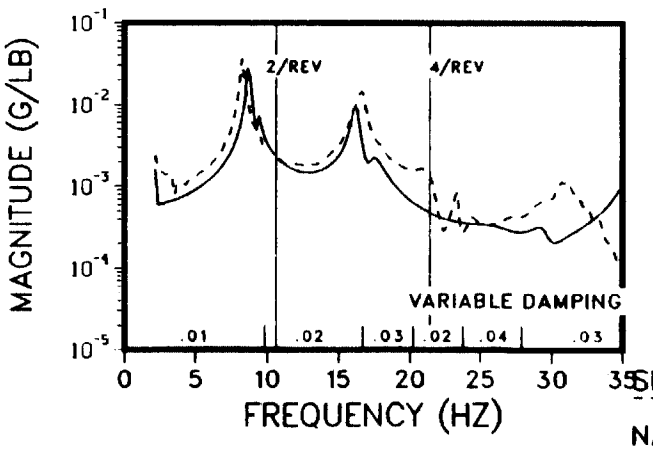

CG (FS 196) LATERAL RESPONSE

SHAKE TEST

NASTRAN

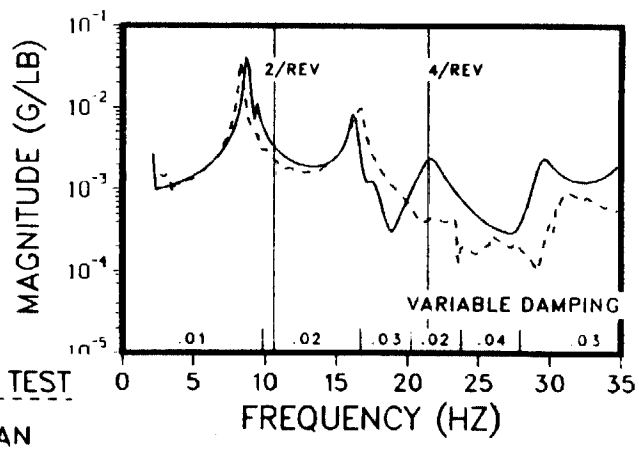

ENGINE DECK (FS 250) LATERAL RESPONSE

LATERAL FREQUENCY RESPONSE COMPARISONS (CONFIGURATION 8)

TAILBOOM RESPONSE

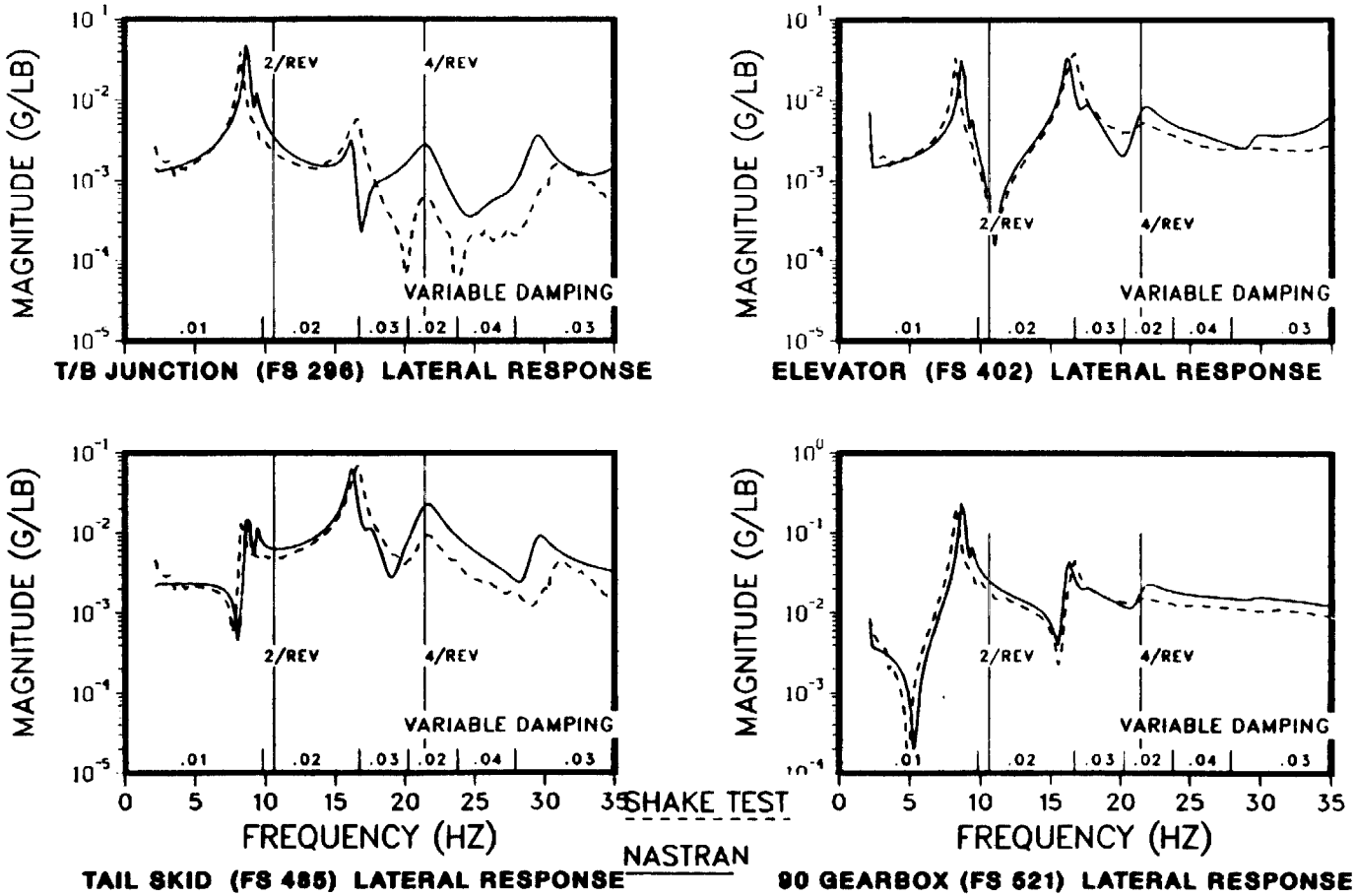

FORCED RESPONSE MODE SHAPE COMPARISONS (CONFIGURATION 8)

Forced response mode shape comparisons at discrete frequencies measured during the test using elastic line tailboom and built-up tailboom are shown for the first three global fuselage bending modes. Test data come from dwells at natural frequencies identified in the test. The NASTRAN forced response calculations are based on the same excitation magnitude as used in the test. The amplitudes are not scaled since absolute response is presented. Test and analysis frequency placement and amplitudes (servo-controlled shaker) used to excite the response are listed in the table.

MODE	Test		NASTRAN Frequency ω_n (Hz)
	Frequency ω_n (Hz)	Amplitude (lb)	
First lateral bending	7.91	6.07	8.70
First vertical bending	8.81	7.13	9.30
Second lateral bending	16.48	13.93	16.40
Second vertical bending	17.66	27.59	17.50
Third vertical bending	26.61	26.56	26.50
Third lateral bending	31.22	29.23	30.30

FORCED RESPONSE MODE SHAPE COMPARISONS (CONFIGURATION 8)

VERTICAL BENDING MODES

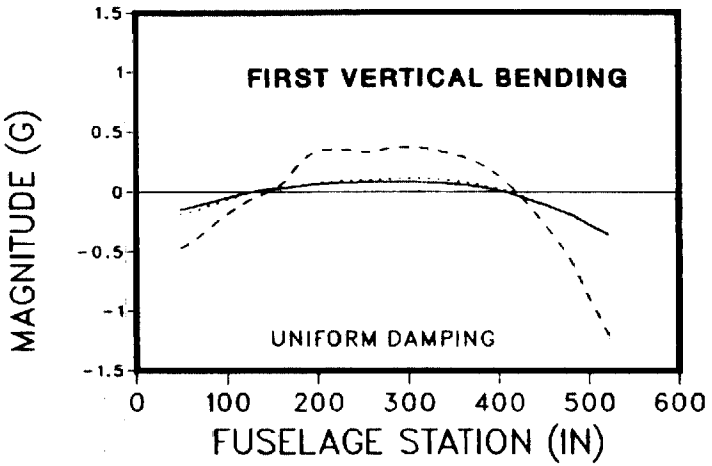

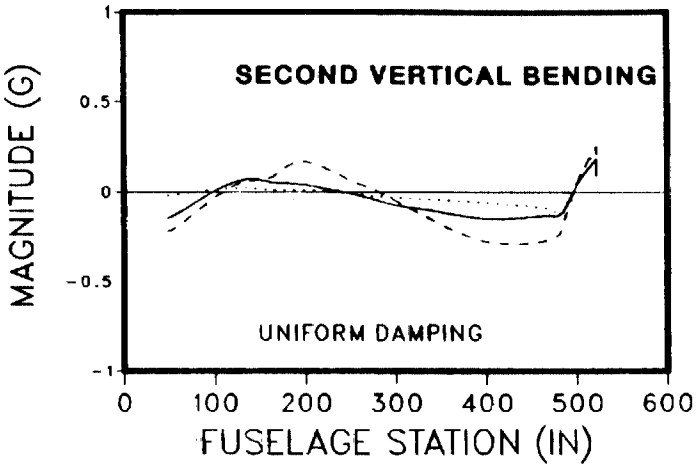

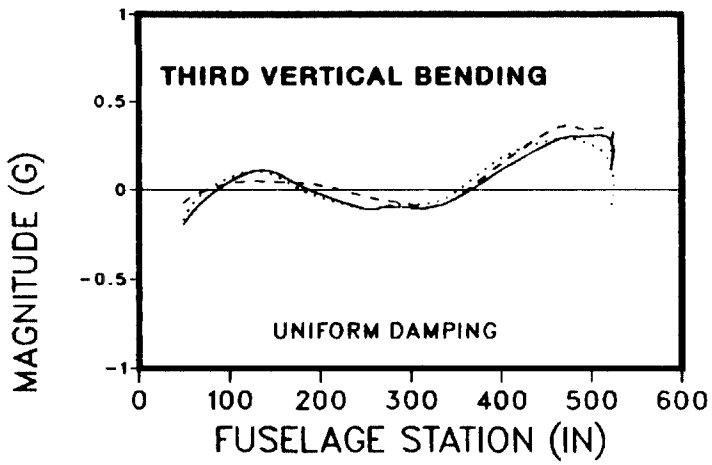

SHAKE TEST

NAST–ELASTIC

NAST–BUILT

FORCED RESPONSE MODE SHAPE COMPARISONS (CONFIGURATION 8)

LATERAL BENDING MODES

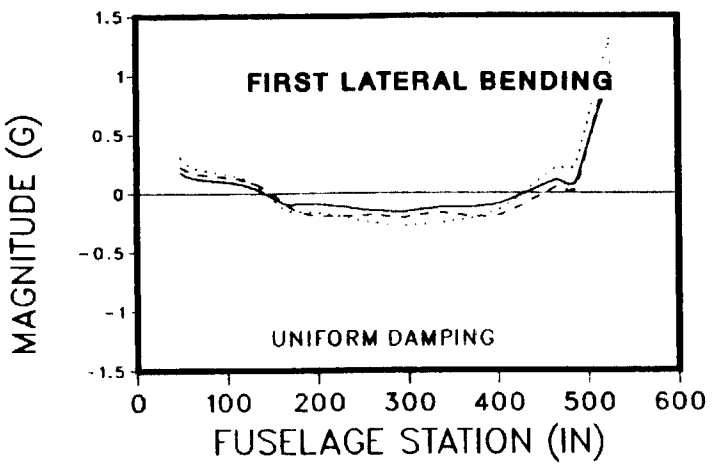

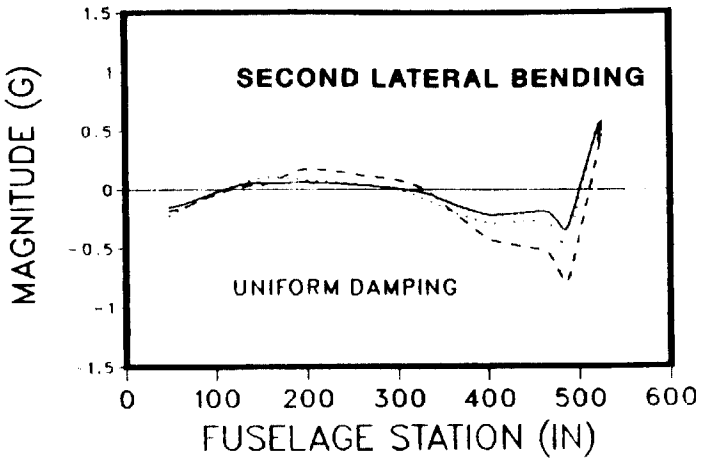

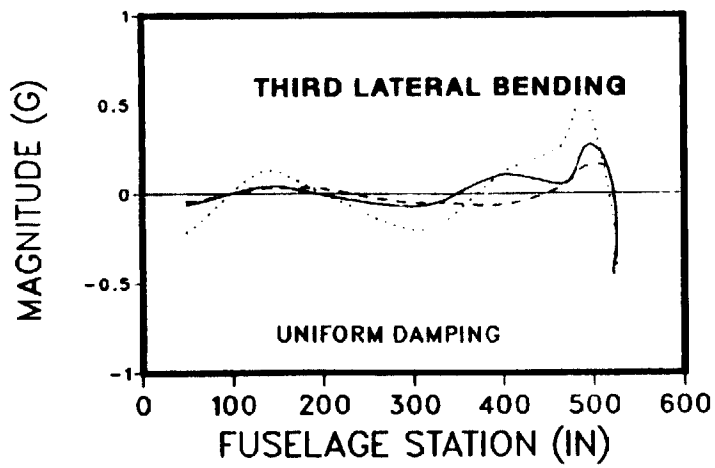

SHAKE TEST

NAST–ELASTIC

NAST–BUILT

4. TEST CORRELATION AND DIFFICULT COMPONENT INVESTIGATIONS

AIRFRAME COMPONENT EFFECTS - TEST VS ANALYSIS

Once the baseline correlation (Configuration 8) was established, the measured and predicted response of each successive configuration, in reverse order, was used to isolate and identify the effect of each component. Several techniques were used to identify the effects on overall vibratory response for each component. These techniques include the following:

1. Tracking variations in frequency placement and establishing the associated stiffness and mass effects for each component.

2. Overplotting of FRF from each successive configuration to identify modal contributors.

3. Component test to identify modal response.

AIRFRAME COMPONENT EFFECTS - TEST vs ANALYSIS

- TRACK VARIATIONS IN FREQUENCY RESPONSE FUNCTIONS AND NATURAL FREQUENCY PLACEMENT WITH OVERPLOTS OF TEST - TEST AND NASTRAN - NASTRAN :

CONFIGURATION	DIFFICULT COMPONENT
8	CANOPY GLASS & ELECTRONIC BOXES
8 VS 7	FUEL
7 VS 5	ENGINE
5 VS 4	LANDING GEAR
4 VS 3	T/R DRIVE SHAFT
3 VS 2	SECONDARY STRUCTURE
2 VS 1	MAIN ROTOR PYLON ASSEMBLY

SUBCOMPONENT INVESTIGATIONS - CONFIGURATION 8

Subcomponents (sealed canopy glass, electronic boxes in tailboom, and stub wings) were sequentially removed from Configuration 8 to determine their effects. Frequency response comparison plots at two selected locations showing test versus test and NASTRAN versus NASTRAN response are presented on the next three pages for one test load condition: vertical at the tail. Natural frequency variations are shown in the table below for each subcomponent.

The canopy glass appears in test to have an effect on the fuselage torsion mode near the 4p and higher frequency (20-30 Hz) responses. The black boxes also have an effect on higher frequency response. These components are not included in the NASTRAN FEM and therefore become candidates for improving correlation in the higher frequency range of interest. The most significant effect of the wings is seen on the NASTRAN response for the torsion mode. Connectivity of the wing to the fuselage is suspect.

Mode	Test				NASTRAN			
	Conf 8 ω_n (Hz)	Glass Removed ω_n (Hz)	Black Boxes Removed ω_n (Hz)	Wings Removed ω_n (Hz)	Conf 8 ω_n (Hz)	Glass Removed ω_n (Hz)	Black Boxes Removed ω_n (Hz)	Wings Removed ω_n (Hz)
First vertical bending	8.7	8.7	8.9	9.0	9.1	9.0	9.1	9.2
Second vertical bending	17.3	17.3	17.5	17.7	17.2	17.4	17.7	17.9
Fuselage torsion	21.3	20.4	20.5	21.1	21.4	23.1	23.3	24.9
Third vertical bending	25.3	25.4	25.5	25.7	26.3	27.7	28.2	28.5

SUBCOMPONENT INVESTIGATIONS - CONFIGURATION 8

CANOPY GLASS EFFECTS

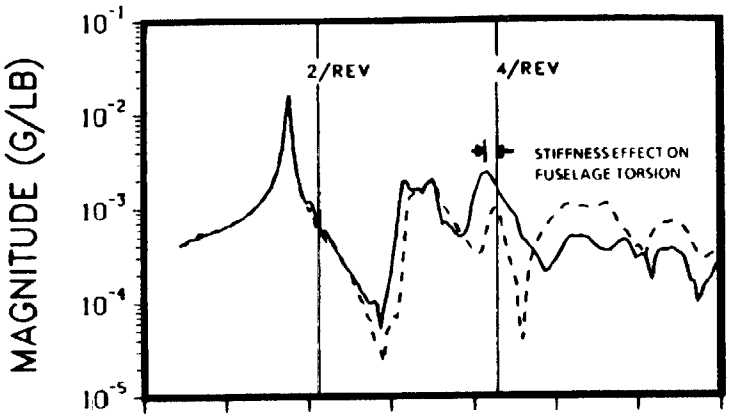

TEST DATA-GUNNER VERTICAL RESPONSE

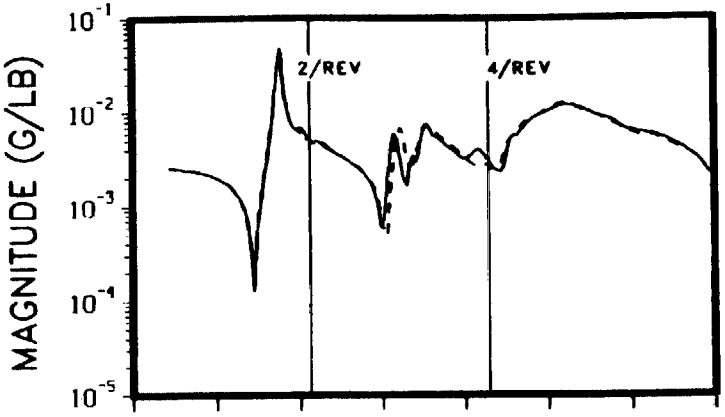

TEST DATA-TAIL SKID VERTICAL RESPONSE

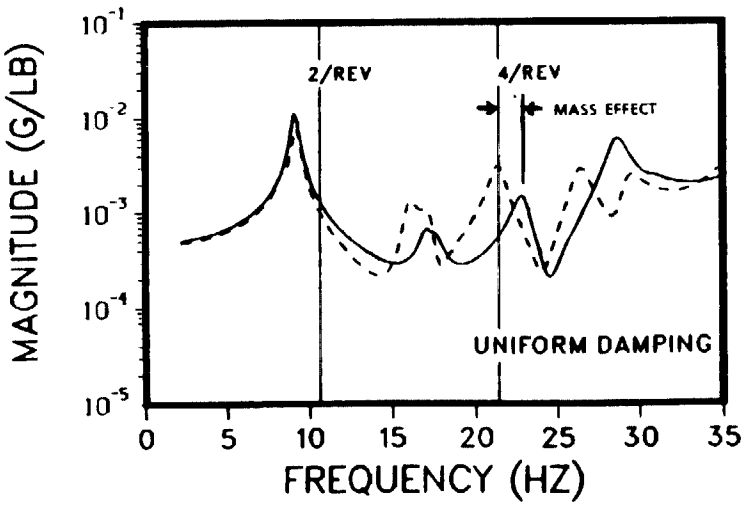

NASTRAN-GUNNER VERTICAL RESPONSE

W/GLASS

NO GLASS

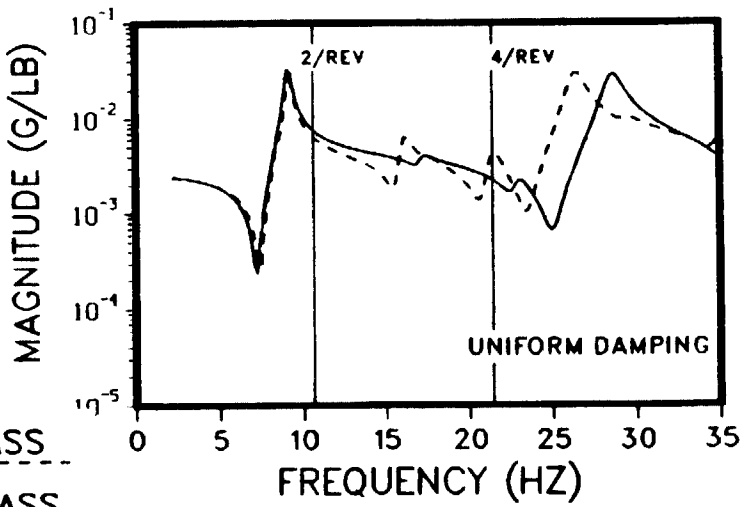

NASTRAN-TAIL SKID VERTICAL RESPONSE

SUBCOMPONENT INVESTIGATIONS - CONFIGURATION 8

BLACK BOX EFFECTS

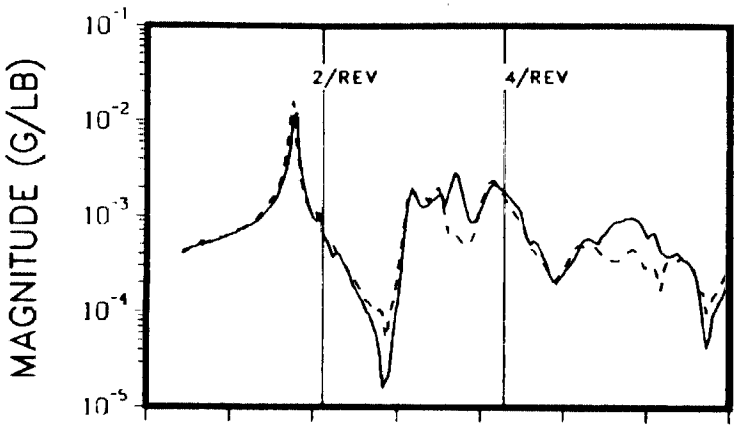

TEST DATA-GUNNER VERTICAL RESPONSE

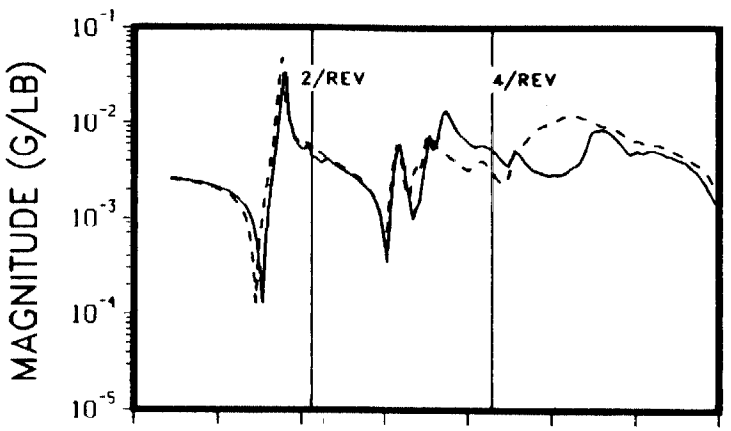

TEST DATA-TAIL SKID VERTICAL RESPONSE

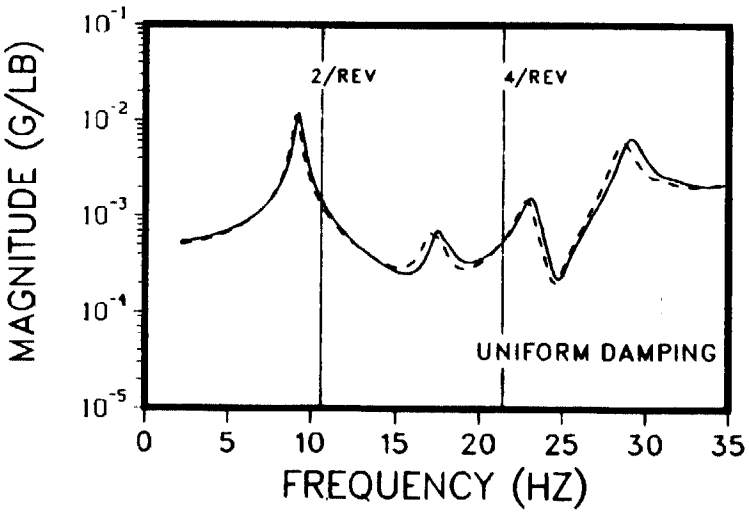

NASTRAN-GUNNER VERTICAL RESPONSE

W/BOXES

NO BOXES

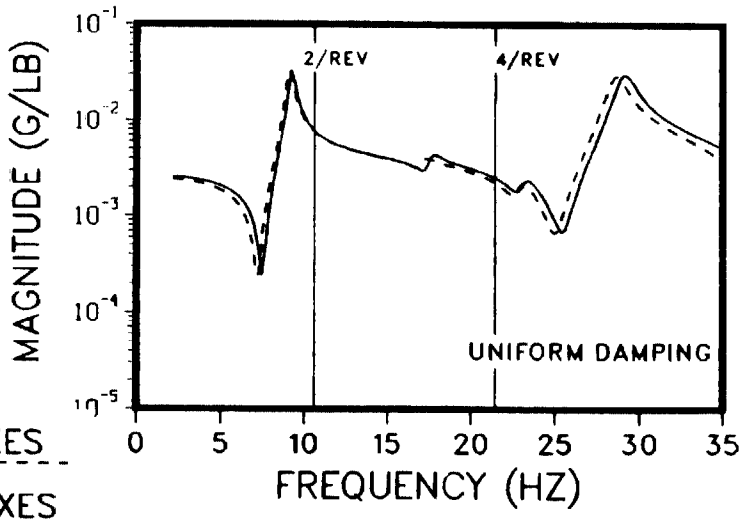

NASTRAN-TAIL SKID VERTICAL RESPONSE

SUBCOMPONENT INVESTIGATIONS - CONFIGURATION 8

STUB WING EFFECTS

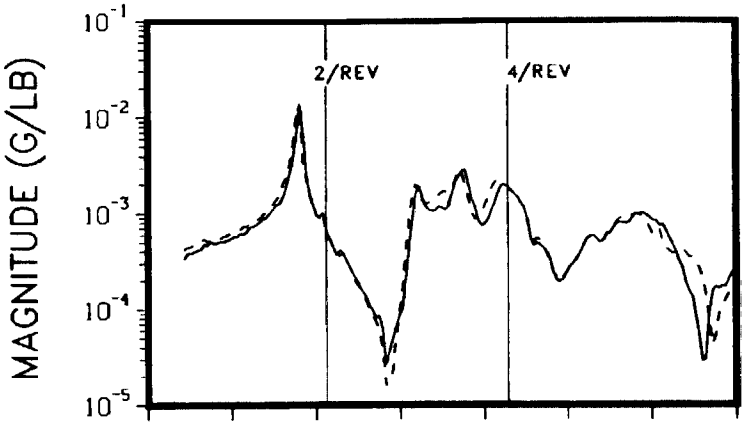

TEST DATA-GUNNER VERTICAL RESPONSE

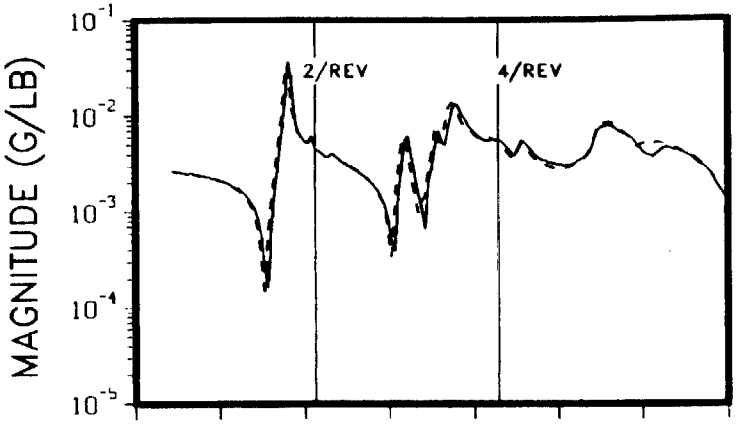

TEST DATA-TAIL SKID VERTICAL RESPONSE

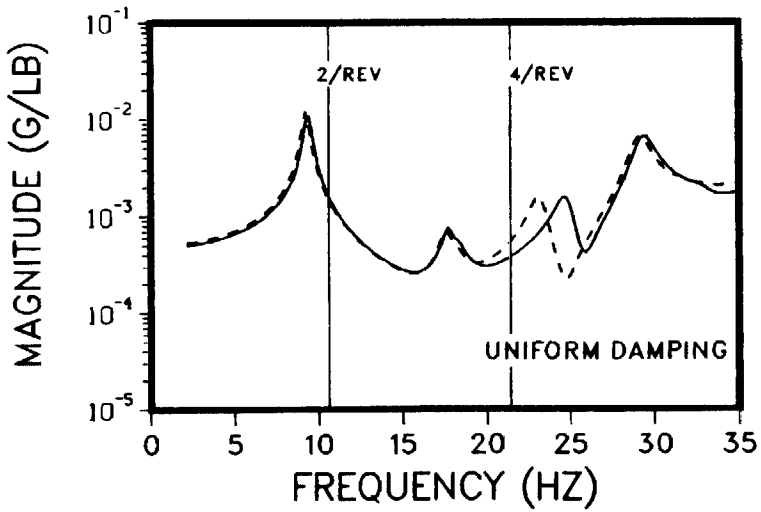

NASTRAN-GUNNER VERTICAL RESPONSE

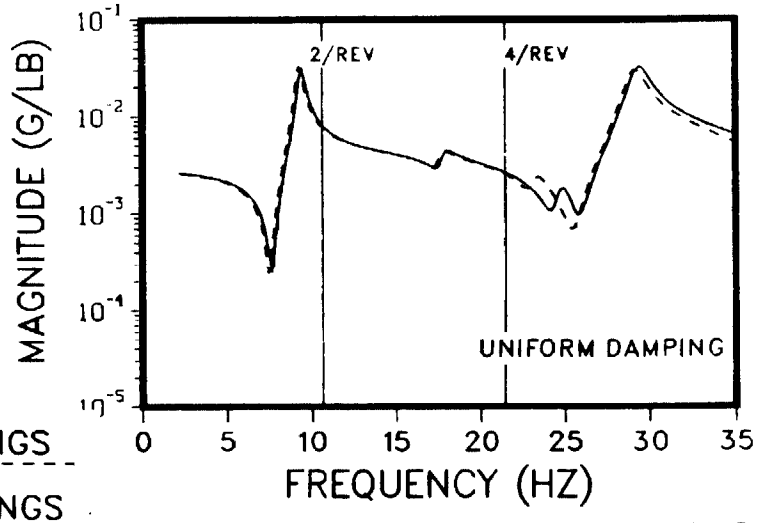

NASTRAN-TAIL SKID VERTICAL RESPONSE

W/WINGS

NO WINGS

FUEL EFFECTS - CONFIGURATION 7 VS 8

Direct comparisons of the test frequency response data from each configuration for the gunner and tail skid locations are shown in the top portion of the figure. NASTRAN frequency response comparisons at the same locations are shown in the bottom portion.

Natural frequency variations are summarized in the table for the seven most prominent flexible modes below 35 Hz.

As expected, the variation in frequency response for all test and analysis modes is characteristic of a pure mass effect, since only fuel mass was added. Higher frequency test response (>4p) also exhibits some other effects, as evidenced by the gunner response, that require some further investigation.

Test	Test			NASTRAN		
	Config 8 ω_n (Hz)	Config 7 ω_n (Hz)	Delta ω_n (Hz)	Config 8 ω_n (Hz)	Config 7 ω_n (Hz)	Delta ω_n (Hz)
First lateral bending	8.2	8.2	-	8.5	8.4	-0.1
First vertical bending	8.7	8.6	-0.1	9.1	8.9	-0.2
Second lateral bending	16.6	16.2	-0.4	16.0	15.7	-0.3
Second vertical bending	17.3	16.9	-0.4	17.2	16.9	-0.3
Fuselage torsion	21.3	21.3	-	21.4	21.1	-0.3
Third vertical bending	25.3	24.5	-0.8	26.3	25.7	-0.6
Third lateral bending	30.9	29.8	-1.1	29.3	28.6	-0.7

FUEL EFFECTS - CONFIGURATION 7 vs 8
VERTICAL LOAD AT TAIL SKID

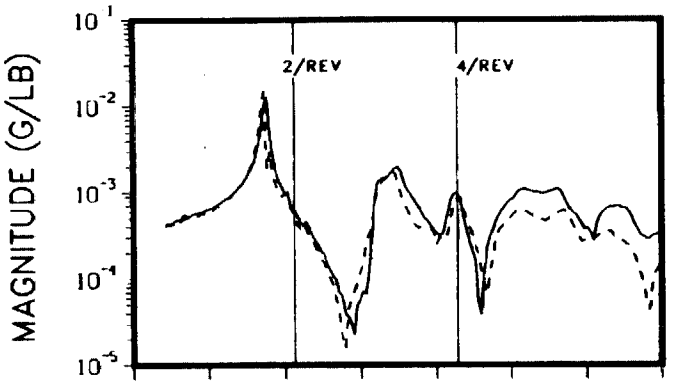

TEST DATA-GUNNER VERTICAL RESPONSE

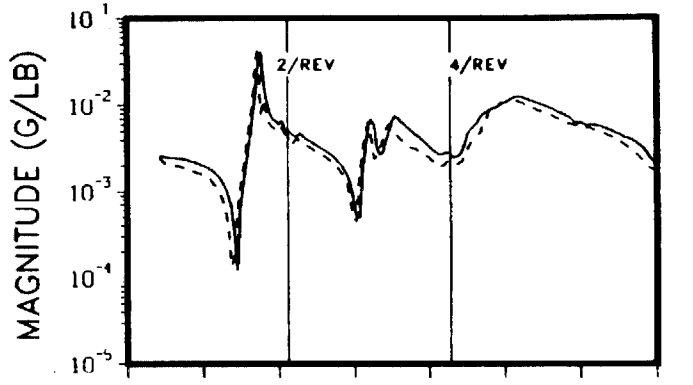

TEST DATA-TAIL SKID VERTICAL RESPONSE

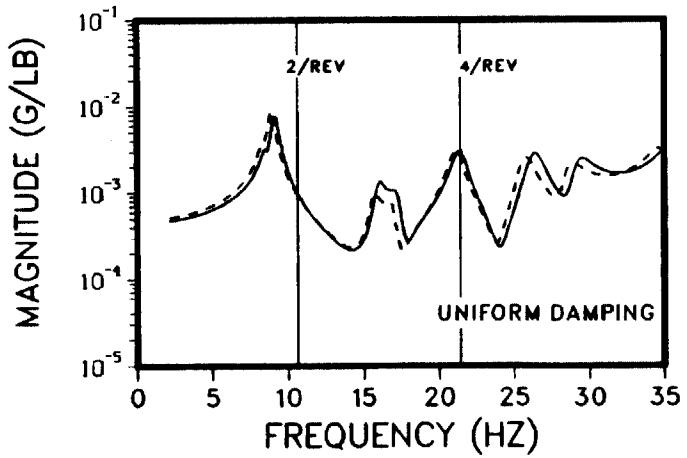

NASTRAN-GUNNER VERTICAL RESPONSE

CONF 7

CONF 8

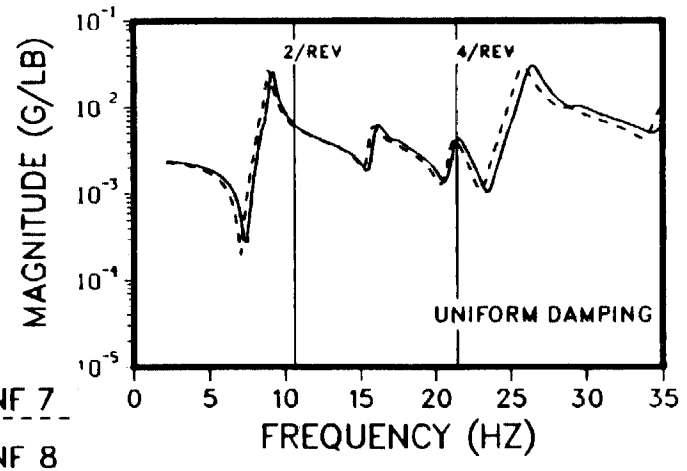

NASTRAN-TAIL SKID VERTICAL RESPONSE

FUEL EFFECTS - CONFIGURATION 7 vs 8
LATERAL LOAD AT TAIL ROTOR

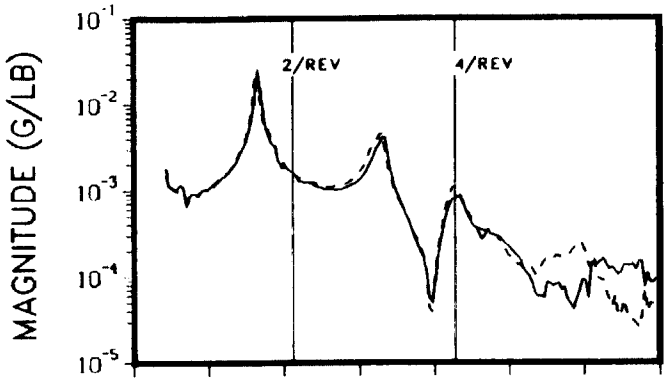

TEST DATA-GUNNER LATERAL RESPONSE

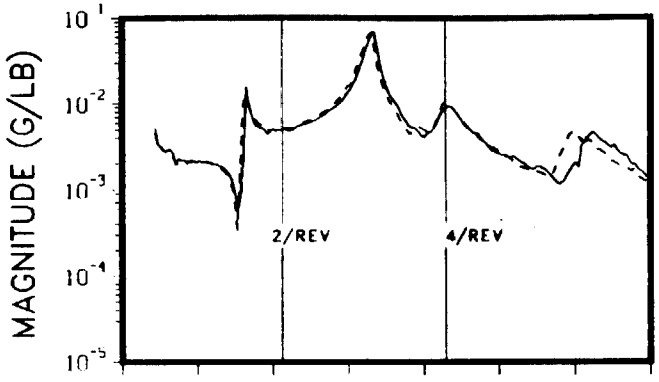

TEST DATA-TAIL SKID LATERAL RESPONSE

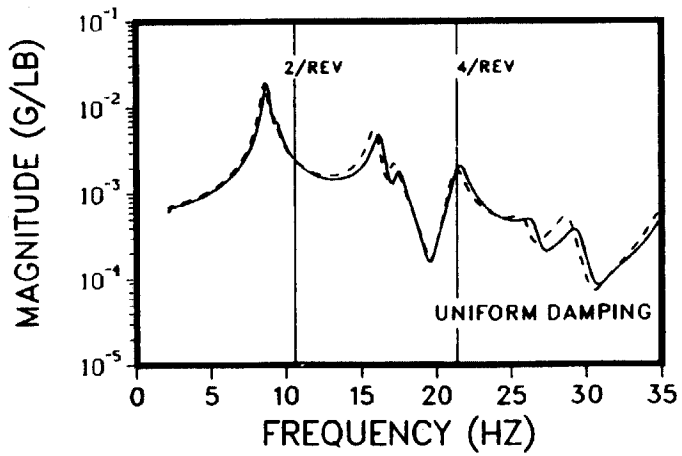

NASTRAN-GUNNER LATERAL RESPONSE

CONF 7

CONF 8

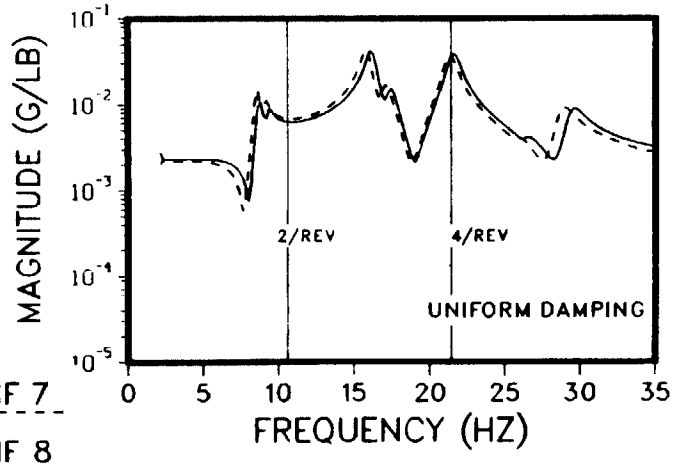

NASTRAN-TAIL SKID LATERAL RESPONSE

ENGINE EFFECTS - CONFIGURATION 5 VS 7

Direct comparisons of the test frequency response data from each configuration for the gunner and tail skid locations are shown in the top portion of the figure. NASTRAN frequency response comparisons at the same locations are shown in the bottom portion.

Natural frequency variations are summarized in the table for the seven most prominent flexible modes below 35 Hz.

For frequencies less than 25 Hz, engine rigid modes in the 22-26 Hz range cause flexible natural frequencies to shift down; above 25 Hz, the flexible natural frequencies shift up in both test and analysis. Neither of the chosen response points clearly portrays the engine modes themselves; however, their effect on the other flexible modes is seen. Each point depicts the downward shift in natural frequencies below 25 Hz when the engine is added and the neutral or upward shift in natural frequency above 25 Hz.

Test	Test			NASTRAN		
	Config 7 ω_n (Hz)	Config 5 ω_n (Hz)	Delta ω_n (Hz)	Config 7 ω_n (Hz)	Config 5 ω_n (Hz)	Delta ω_n (Hz)
First lateral bending	8.2	7.4	-0.8	8.4	7.7	-0.7
First vertical bending	8.6	7.9	-0.7	8.9	8.3	-0.6
Second lateral bending	16.2	14.9	-1.3	15.7	14.5	-1.2
Second vertical bending	16.9	16.0	-0.9	16.9	15.9	-1.0
Fuselage torsion	21.3	20.3	-1.0	21.1	20.3	-0.8
Third vertical bending	24.5	22.9	-1.6	25.7	24.0	-1.7
Third lateral bending	29.8	30.9	+1.1	28.6	28.9	+0.3

ENGINE EFFECTS - CONFIGURATION 5 vs 7

VERTICAL LOAD AT TAIL SKID

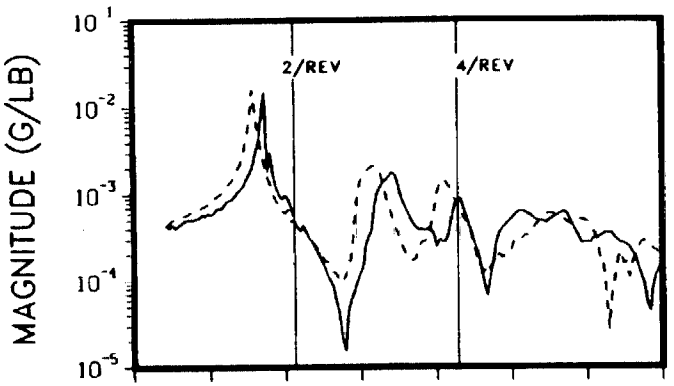

TEST DATA-GUNNER VERTICAL RESPONSE

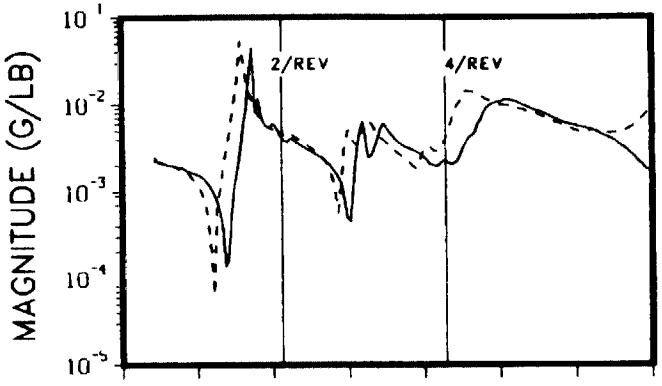

TEST DATA-TAIL SKID VERTICAL RESPONSE

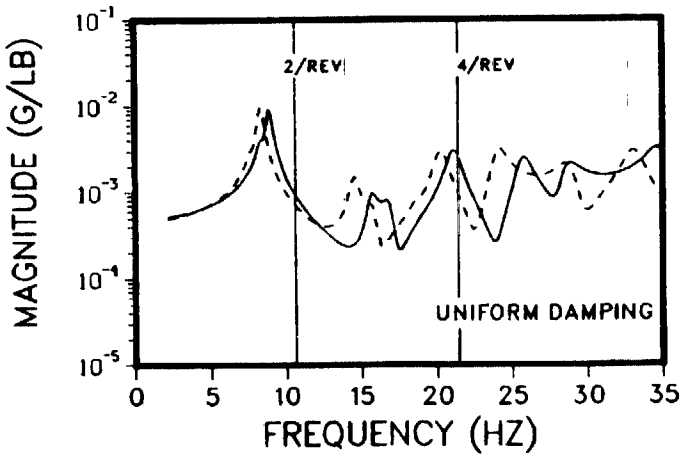

NASTRAN-GUNNER VERTICAL RESPONSE

CONF 5

CONF 7

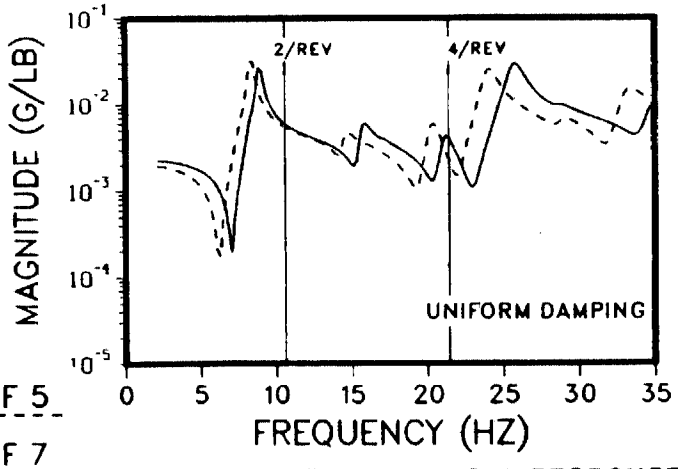

NASTRAN-TAIL SKID VERTICAL RESPONSE

ENGINE EFFECTS - CONFIGURATION 5 vs 7

LATERAL LOAD AT TAIL ROTOR

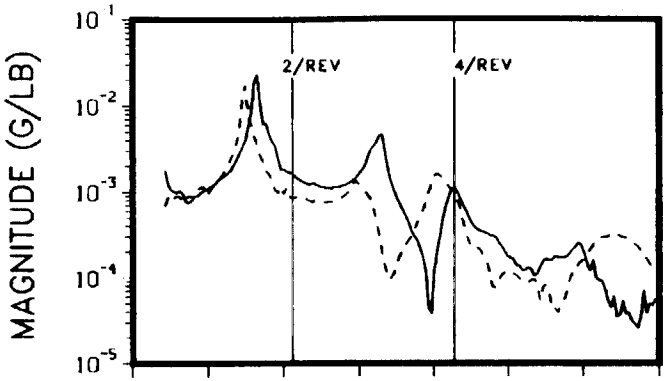

TEST DATA-GUNNER LATERAL RESPONSE

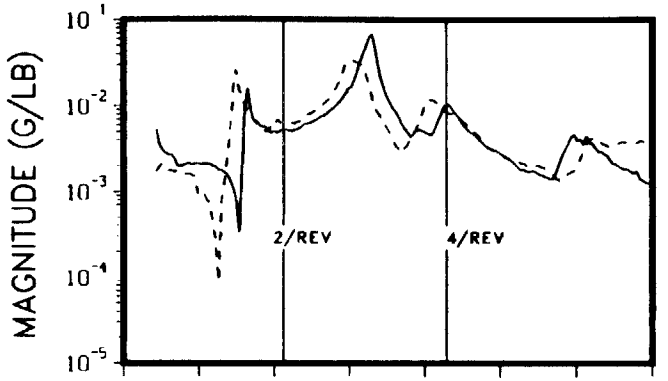

TEST DATA-TAIL SKID LATERAL RESPONSE

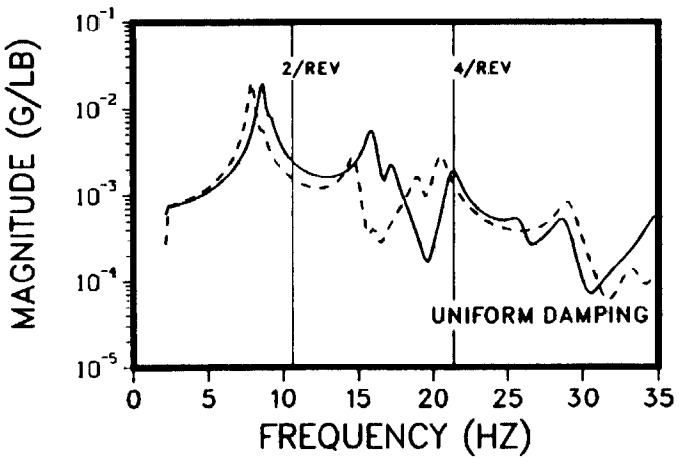

NASTRAN-GUNNER LATERAL RESPONSE

CONF 5

CONF 7

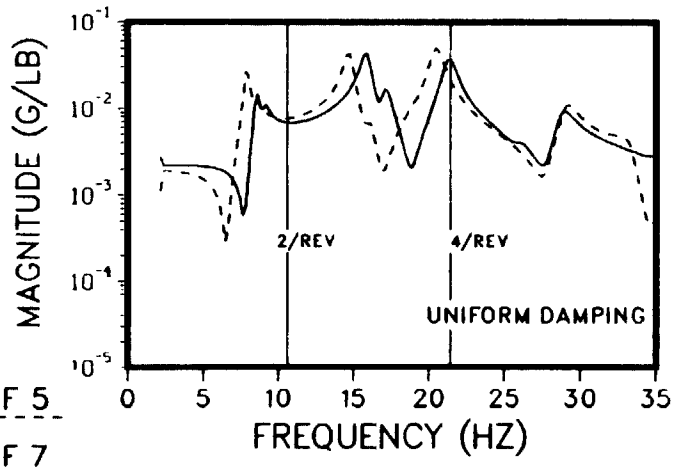

NASTRAN-TAIL SKID LATERAL RESPONSE

SKID GEAR EFFECTS - CONFIGURATION 4 VS 5

Direct comparisons of the test frequency response data from each configuration for the gunner and tail skid locations are shown in the top portion of the figure. NASTRAN frequency response comparisons at the same locations are shown in the bottom portion.

Natural frequency variations are summarized in the table for the seven most prominent flexible modes below 35 Hz.

Three skid modes are clearly identified in the comparison plots. A symmetric skid mode at 14.6 Hz and two symmetric skid modes (17.0 and 24.5 Hz) are labeled in the test and analysis comparisons. Trends in the effects of the skid gear are quite similar between test and analysis.

Test	Test			NASTRAN		
	Config 5 ω_n (Hz)	Config 4 ω_n (Hz)	Delta ω_n (Hz)	Config 5 ω_n (Hz)	Config 4 ω_n (Hz)	Delta ω_n (Hz)
First lateral bending	7.4	7.5	+0.1	7.7	7.7	-
First vertical bending	7.9	7.9	-	8.3	8.4	+0.1
Second lateral bending	14.9	14.5	-0.4	14.5	14.4	-0.1
Second vertical bending	16.0	15.9	-0.1	15.9	15.9	-
Fuselage torsion	20.3	20.1	-0.2	20.3	19.9	-0.4
Third vertical bending	22.9	23.7	+0.8	24.0	24.2	+0.2
Third lateral bending	30.9	29.7	-1.2	28.9	29.4	+0.5

SKID GEAR EFFECTS – CONFIGURATION 4 vs 5

VERTICAL LOAD AT TAIL SKID

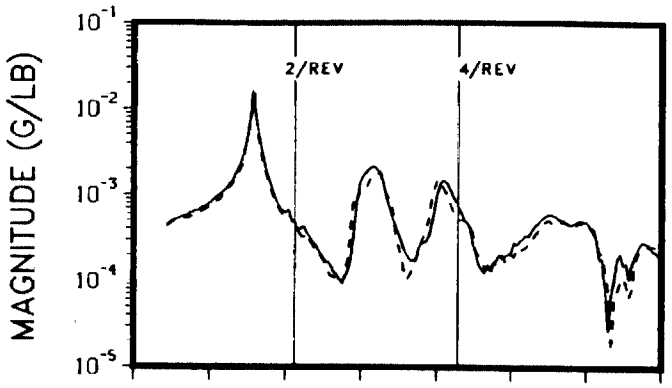

TEST DATA-GUNNER VERTICAL RESPONSE

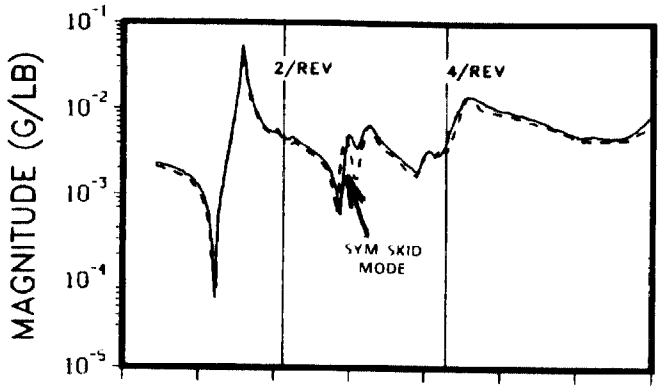

TEST DATA-TAIL SKID VERTICAL RESPONSE

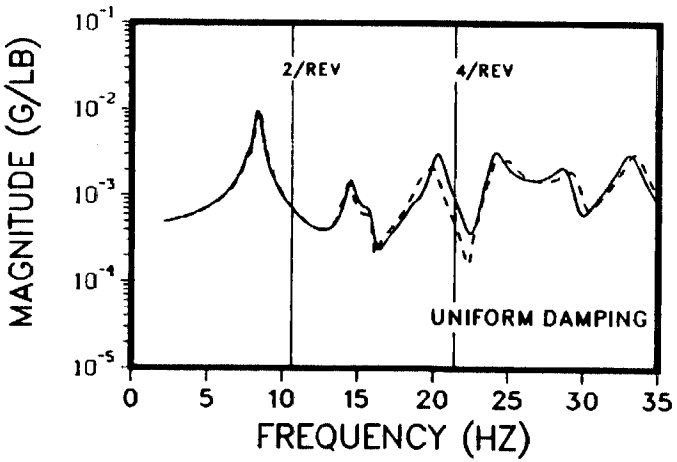

NASTRAN-GUNNER VERTICAL RESPONSE

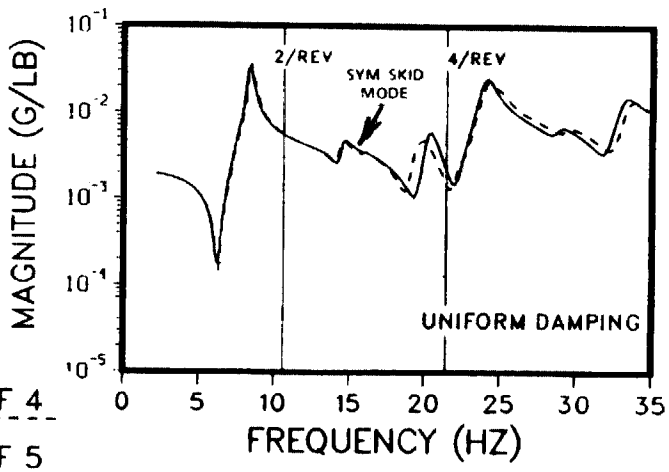

CONF 4 - - - - -

CONF 5 ———

NASTRAN-TAIL SKID VERTICAL RESPONSE

SKID GEAR EFFECTS – CONFIGURATION 4 vs 5

LATERAL LOAD AT TAIL ROTOR

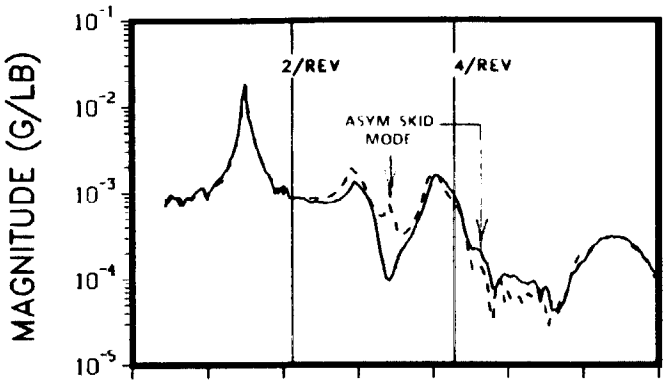

TEST DATA-GUNNER LATERAL RESPONSE

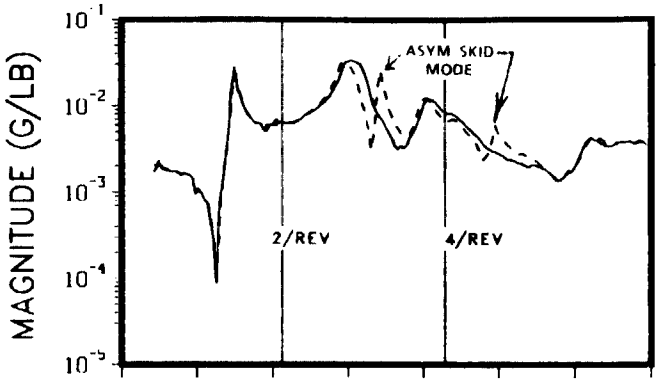

TEST DATA-TAIL SKID LATERAL RESPONSE

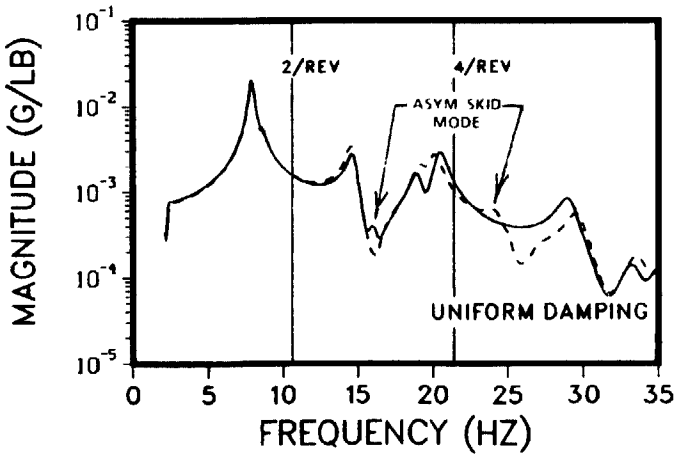

NASTRAN-GUNNER LATERAL RESPONSE

CONF 4

CONF 5

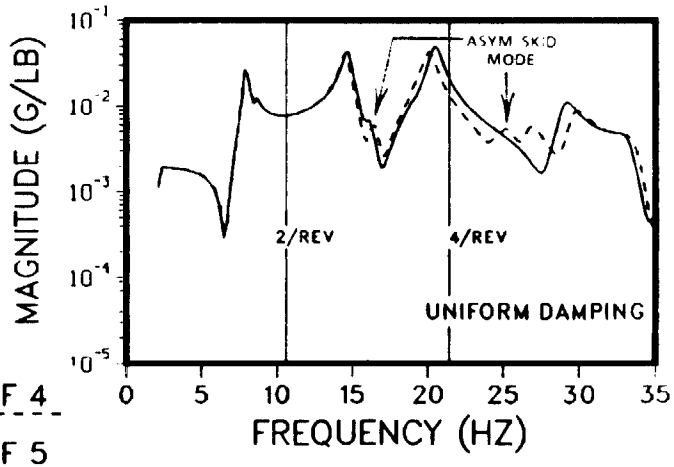

NASTRAN-TAIL SKID LATERAL RESPONSE

TAIL ROTOR DRIVE-SHAFT EFFECTS - CONFIGURATION 3 VS 4

Direct comparisons of the test frequency response data from each configuration at the gunner and tail skid locations are shown in the top portion of the figure. NASTRAN frequency response comparisons at the same locations are shown in the bottom portion.

Natural frequency variations are summarized in the table for the seven most prominent flexible modes below 35 Hz.

The variation in frequency response in test is minimal. The most notable change is seen in third lateral bending. The mass effects appear to be counteracted by some stiffening to result in no effective change in natural frequency. NASTRAN response shows a downward trend associated with a pure mass effect. Some slight stiffening effects may need to be represented, particularly when the shaft is torqued up.

Test	Test			NASTRAN		
	Config 4 ω_n (Hz)	Config 3 ω_n (Hz)	Delta ω_n (Hz)	Config 4 ω_n (Hz)	Config 3 ω_n (Hz)	Delta ω_n (Hz)
First lateral bending	7.5	7.3	-0.2	7.7	7.6	-0.1
First vertical bending	7.9	7.9	-	8.4	8.3	-0.1
Second lateral bending	14.5	14.6	+0.1	14.4	14.1	-0.3
Second vertical bending	15.9	15.9	-	15.9	15.7	-0.2
Fuselage torsion	20.1	20.1	-	29.9	19.6	-0.3
Third vertical bending	23.7	23.5	-0.2	24.2	23.8	-0.4
Third lateral bending	29.7	30.2	+0.5	29.4	29.2	-0.2

TAIL ROTOR DRIVE-SHAFT EFFECTS - CONFIG. 3 vs 4

VERTICAL LOAD AT TAIL SKID

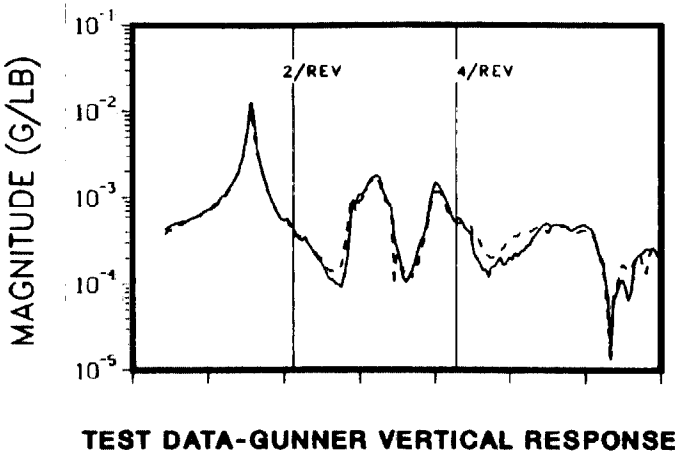

TEST DATA-GUNNER VERTICAL RESPONSE

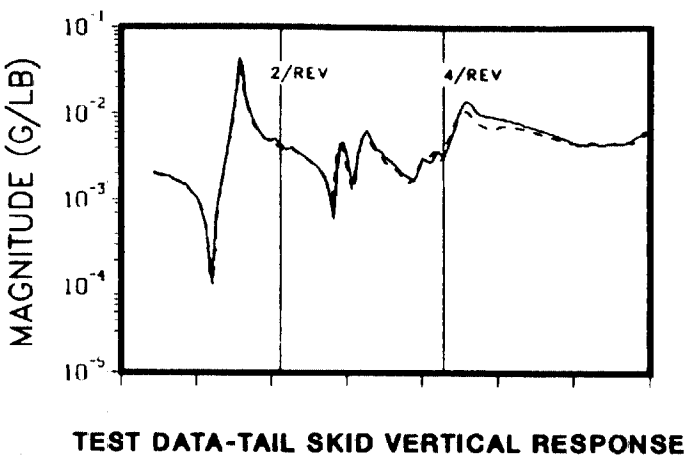

TEST DATA-TAIL SKID VERTICAL RESPONSE

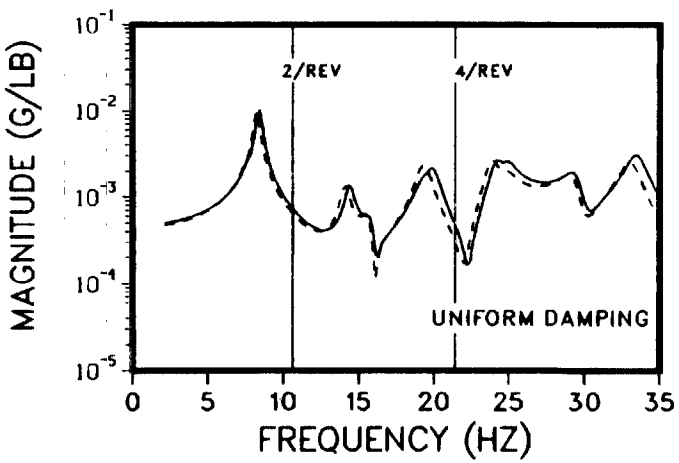

NASTRAN-GUNNER VERTICAL RESPONSE

CONF 3

CONF 4

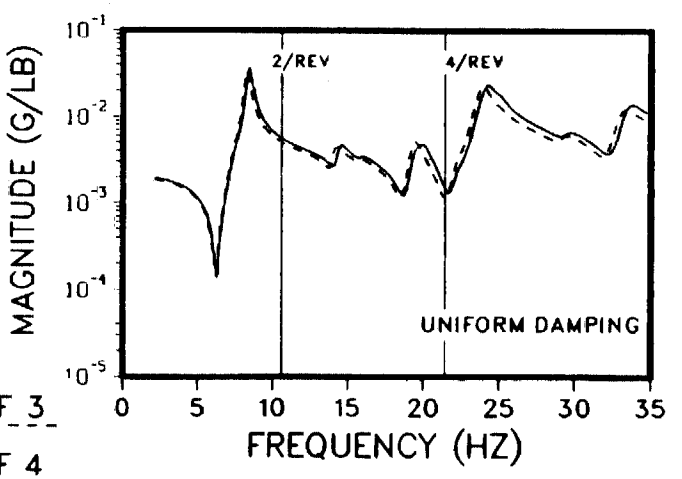

NASTRAN-TAIL SKID VERTICAL RESPONSE

TAIL ROTOR DRIVE-SHAFT EFFECTS - CONFIG. 3 vs 4

LATERAL LOAD AT TAIL ROTOR

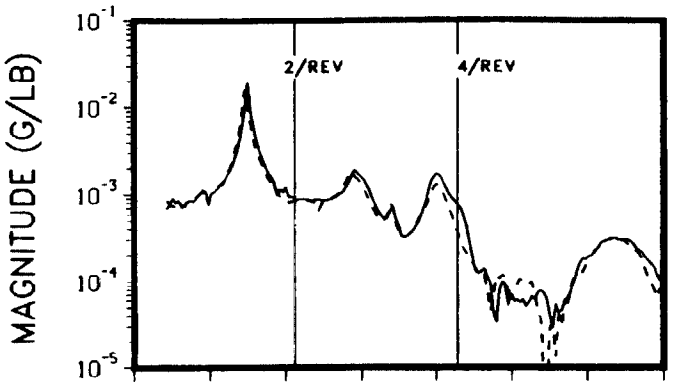

TEST DATA-GUNNER LATERAL RESPONSE

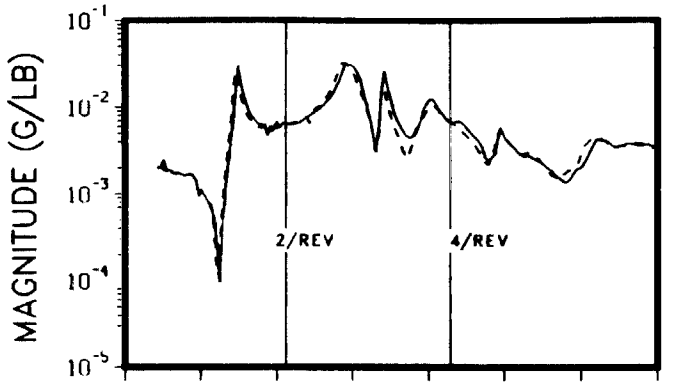

TEST DATA-TAIL SKID LATERAL RESPONSE

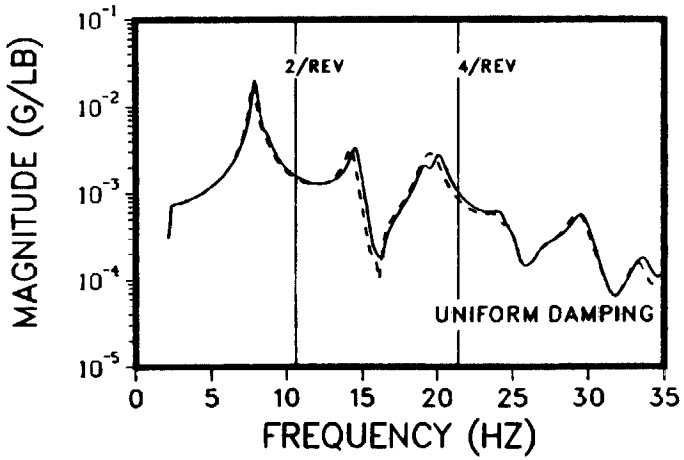

NASTRAN-GUNNER LATERAL RESPONSE

CONF 3

CONF 4

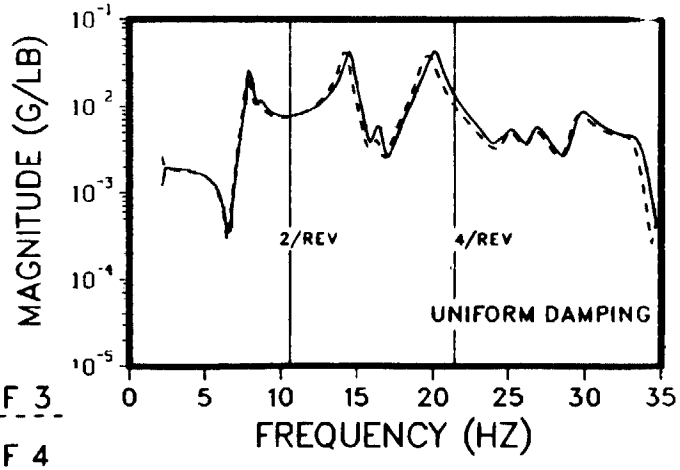

NASTRAN-TAIL SKID LATERAL RESPONSE

SECONDARY STRUCTURE EFFECTS - CONFIGURATION 2 VS 3

Direct comparisons of the test frequency response data from each configuration at the gunner and tail skid locations are shown in the top portion of the figure. NASTRAN comparisons at the same locations are shown in the bottom portion.

Natural frequency variations are summarized in the table for the seven most prominent flexible modes below 35 Hz.

The variation in frequency response in test shows a significant increase in stiffness when the panels are added. This is attributed to the effective stiffening of the canopy frame, as discussed earlier on pages 37-39. NASTRAN variations are similar once the panel stiffness was properly modeled. Unfortunately, each airframe may require a unique modeling approach.

Test	Test			NASTRAN		
	Config 3 ω_n (Hz)	Config 2 ω_n (Hz)	Delta ω_n (Hz)	Config 3 ω_n (Hz)	Config 2 ω_n (Hz)	Delta ω_n (Hz)
First lateral bending	7.3	7.5	+0.2	7.6	7.7	+0.1
First vertical bending	7.9	8.3	+0.4	8.3	8.6	+0.3
Second lateral bending	14.6	15.9	+1.3	14.1	14.9	+0.8
Second vertical bending	15.9	17.4	+1.5	15.7	18.3	+2.6
Fuselage torsion	20.1	23.2	+3.1	19.6	20.7	+1.1
Third vertical bending	23.5	25.1	+1.6	23.8	26.1	+2.3
Third lateral bending	30.2	32.5	+2.3	29.2	31.9	+2.7

SECONDARY STRUCTURE EFFECTS – CONFIG. 2 vs 3

VERTICAL LOAD AT TAIL SKID

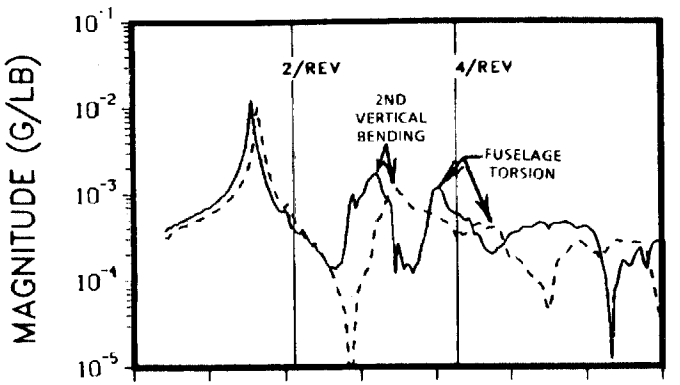

TEST DATA-GUNNER VERTICAL RESPONSE

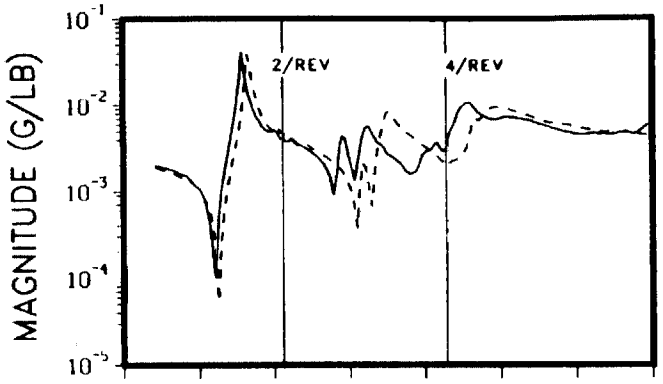

TEST DATA-TAIL SKID VERTICAL RESPONSE

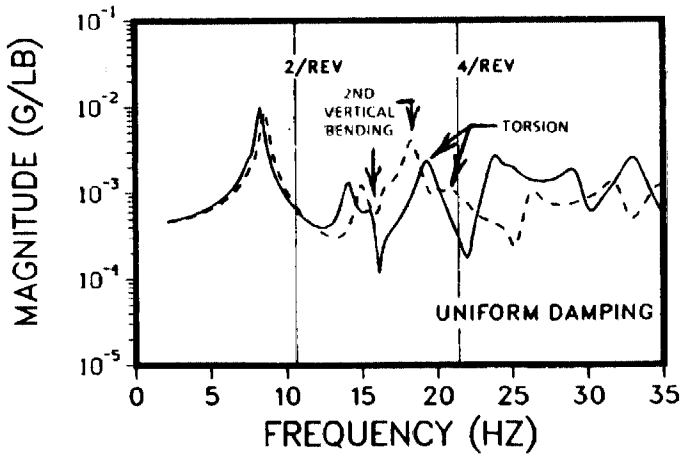

NASTRAN-GUNNER VERTICAL RESPONSE

CONF 2

CONF 3

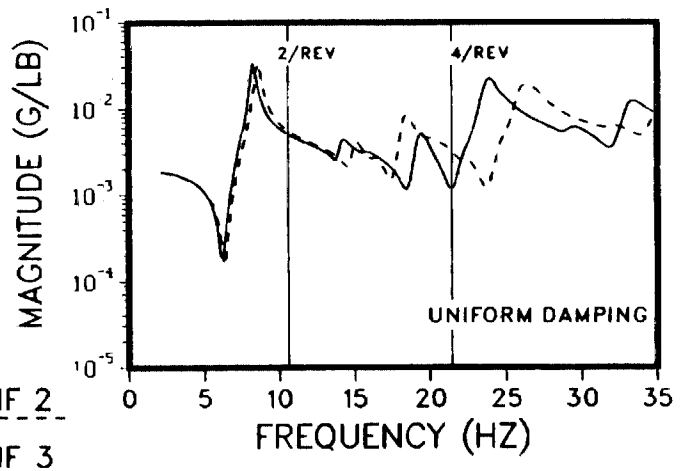

NASTRAN-TAIL SKID VERTICAL RESPONSE

SECONDARY STRUCTURE EFFECTS – CONFIG. 2 vs 3

LATERAL LOAD AT TAIL ROTOR

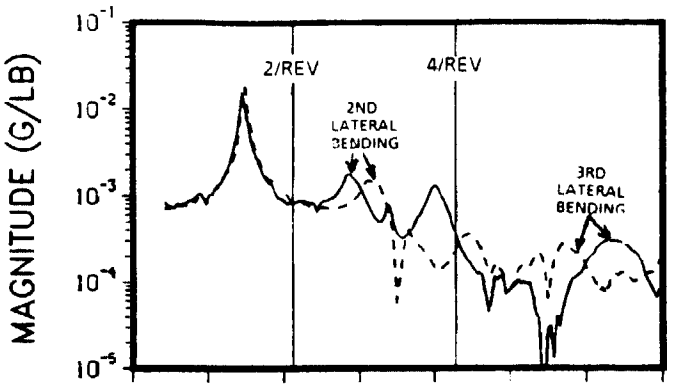

TEST DATA-GUNNER LATERAL RESPONSE

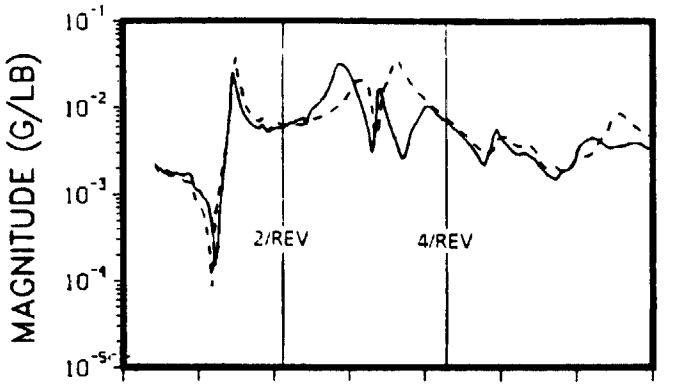

TEST DATA-TAIL SKID LATERAL RESPONSE

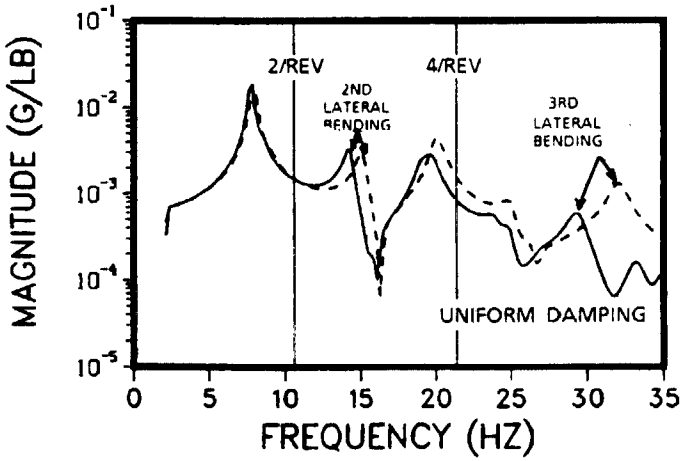

NASTRAN-GUNNER LATERAL RESPONSE

CONF 2

CONF 3

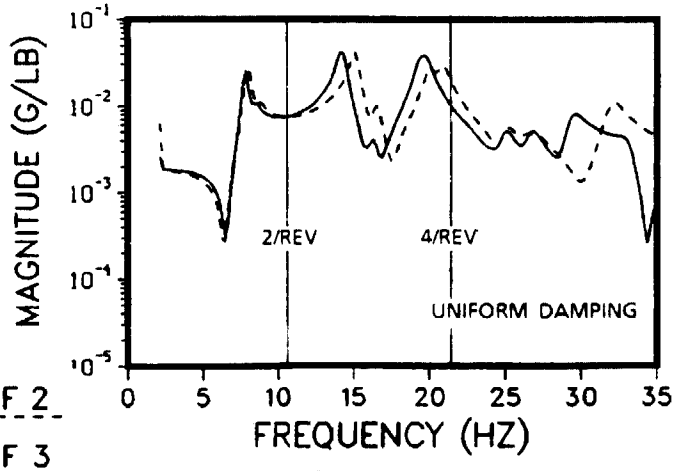

NASTRAN-TAIL SKID LATERAL RESPONSE

MAIN ROTOR PYLON EFFECTS - CONFIGURATION 1 VS 2

Direct comparisons of the test frequency response data from each configuration at the gunner and tail skid locations are shown in the top portion of the figure. NASTRAN frequency response comparisons at the same locations are shown in the bottom portion.

Natural frequency variations are cataloged in the table for the seven most prominent flexible modes below 35 Hz.

The variation in frequency response in test suggests that the pylon assembly has some stiffening effect on the fuselage torsion mode. Pylon component tests are discussed in detail in the following section.

Test	Test			NASTRAN		
	Config 2 ω_n (Hz)	Config 1 ω_n (Hz)	Delta ω_n (Hz)	Config 2 ω_n (Hz)	Config 1 ω_n (Hz)	Delta ω_n (Hz)
First lateral bending	7.5	7.3	-0.2	7.7	7.7	-
First vertical bending	8.3	8.0	-0.3	8.6	8.3	-0.3
Second lateral bending	15.9	16.0	+0.1	14.9	14.6	-0.3
Second vertical bending	17.4	16.6	-0.8	18.3	17.4	-0.9
Fuselage torsion	23.2	23.5	+0.3	20.7	20.2	-0.5
Third vertical bending	25.1	24.7	-0.4	26.1	25.8	-0.3
Third lateral bending	32.5	32.4	-0.1	31.9	31.8	-0.1

MAIN ROTOR PYLON EFFECTS – CONFIG. 1 vs 2

VERTICAL LOAD AT TAIL SKID

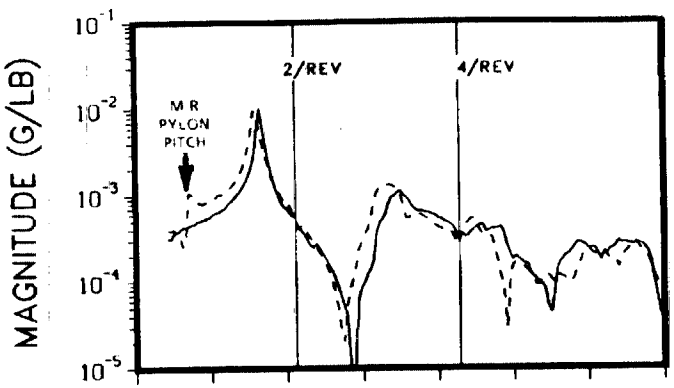

TEST DATA-GUNNER VERTICAL RESPONSE

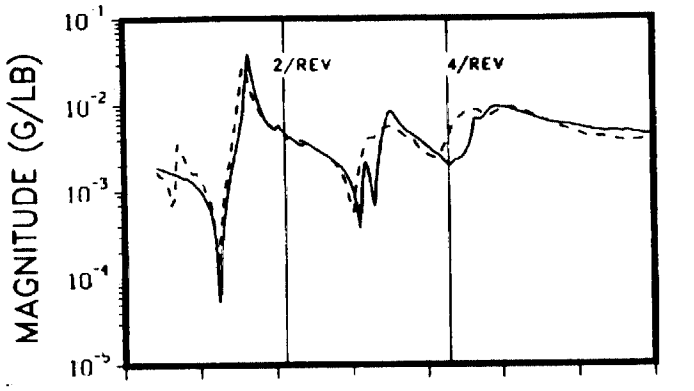

TEST DATA-TAIL SKID VERTICAL RESPONSE

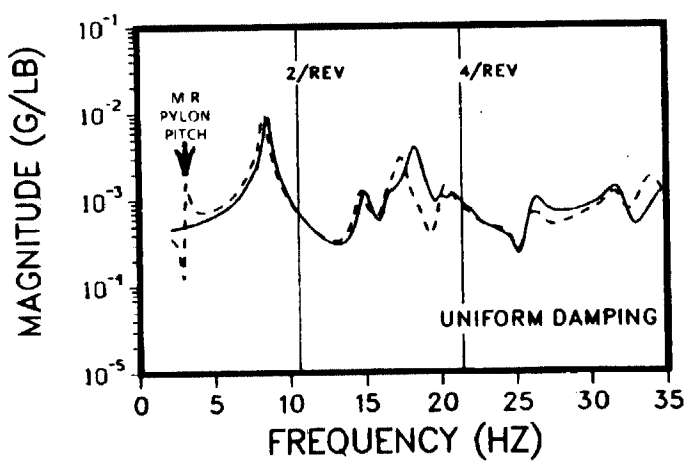

NASTRAN-GUNNER VERTICAL RESPONSE

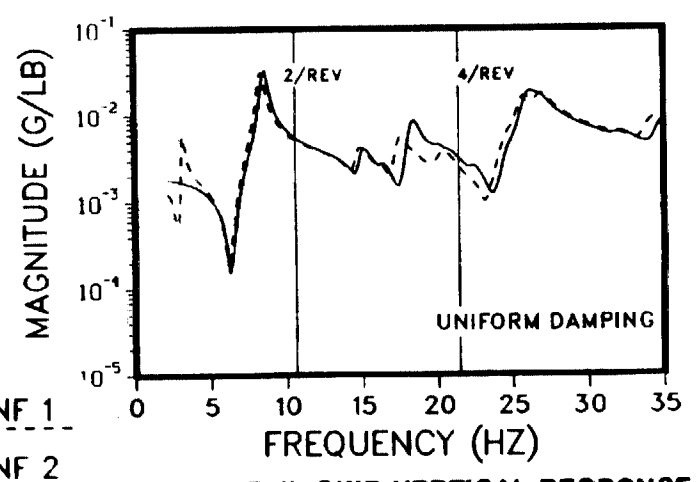

CONF 1

CONF 2

NASTRAN-TAIL SKID VERTICAL RESPONSE

MAIN ROTOR PYLON EFFECTS – CONFIG. 1 vs 2

LATERAL LOAD AT TAIL ROTOR

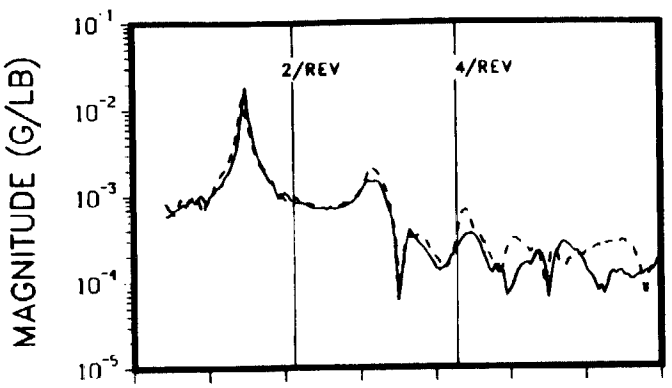

TEST DATA-GUNNER LATERAL RESPONSE

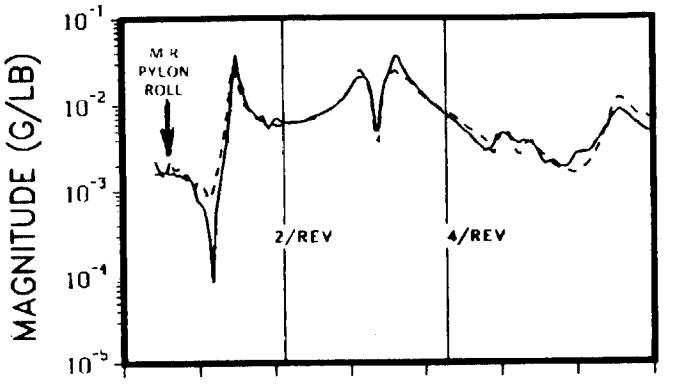

TEST DATA-TAIL SKID LATERAL RESPONSE

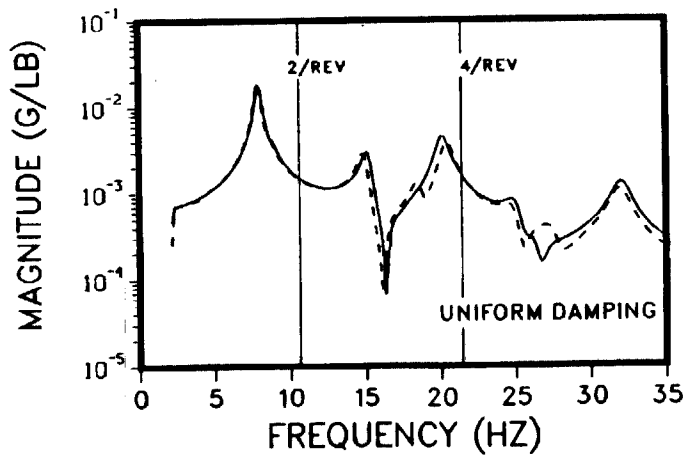

NASTRAN-GUNNER LATERAL RESPONSE

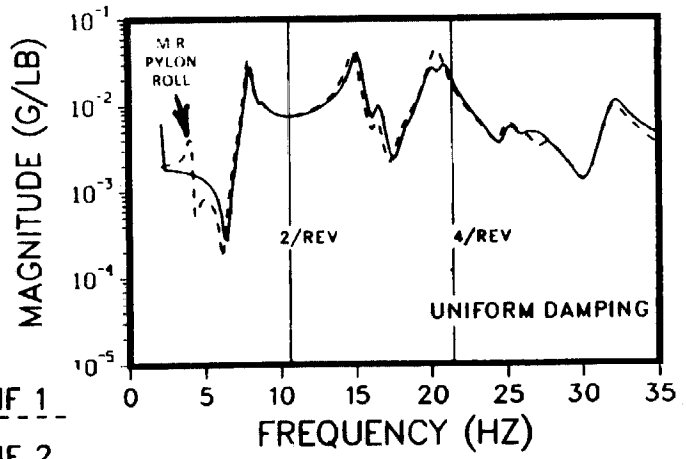

CONF 1

CONF 2

NASTRAN-TAIL SKID LATERAL RESPONSE

COMPONENT TEST CORRELATIONS

In addition to the full-scale airframe tests used to isolate the effect of various components, separate static and dynamic tests were performed on the suspension system and main rotor pylon. Results of the two isolated component tests are compared with special NASTRAN FEM(s) of these components in the following section to determine the relationship between measured and predicted response of these components. In particular, the responses are presented to highlight various effects, such as thrust, damping, and differential stiffness, that were not included in the original FEM.

COMPONENT TEST CORRELATIONS

- **IN-PLANE STATIC AND DYNAMIC TESTS**
  - GROUNDED MAIN ROTOR PYLON ASSEMBLY
    - THRUST EFFECTS, DAMPER EFFECTS, ELASTOMERIC MOUNT EFFECTS
  - STEEL CABLE SUSPENSION SYSTEM
    - DIFFERENTIAL STIFFNESS EFFECTS
- **VERTICAL (OUT-OF-PLANE) STATIC TEST**
  - STEEL CABLE SUSPENSION SYSTEM
    - STIFFNESS EFFECTS

PYLON COMPONENT TEST SETUP

The details of the tests performed on the pylon (main rotor mast, transmission) and elastomeric mounts are described in Volume I of this report. The pylon was supported on a test stand and tested statically and dynamically to determine the mass and stiffness characteristics of this component individually. The elastomeric mounts were also subjected to static and dynamic tests to determine their static and dynamic characteristics.

This section is intended to quantify the discrepancies between the existing FEM and test in order to provide a basis for recommending improved modeling techniques in future FEM(s). The elastic line FEM representation of the main rotor pylon, rotor thrust effects, damper characteristics, and elastomeric mount nonlinearities are investigated.

PYLON COMPONENT TEST SETUP

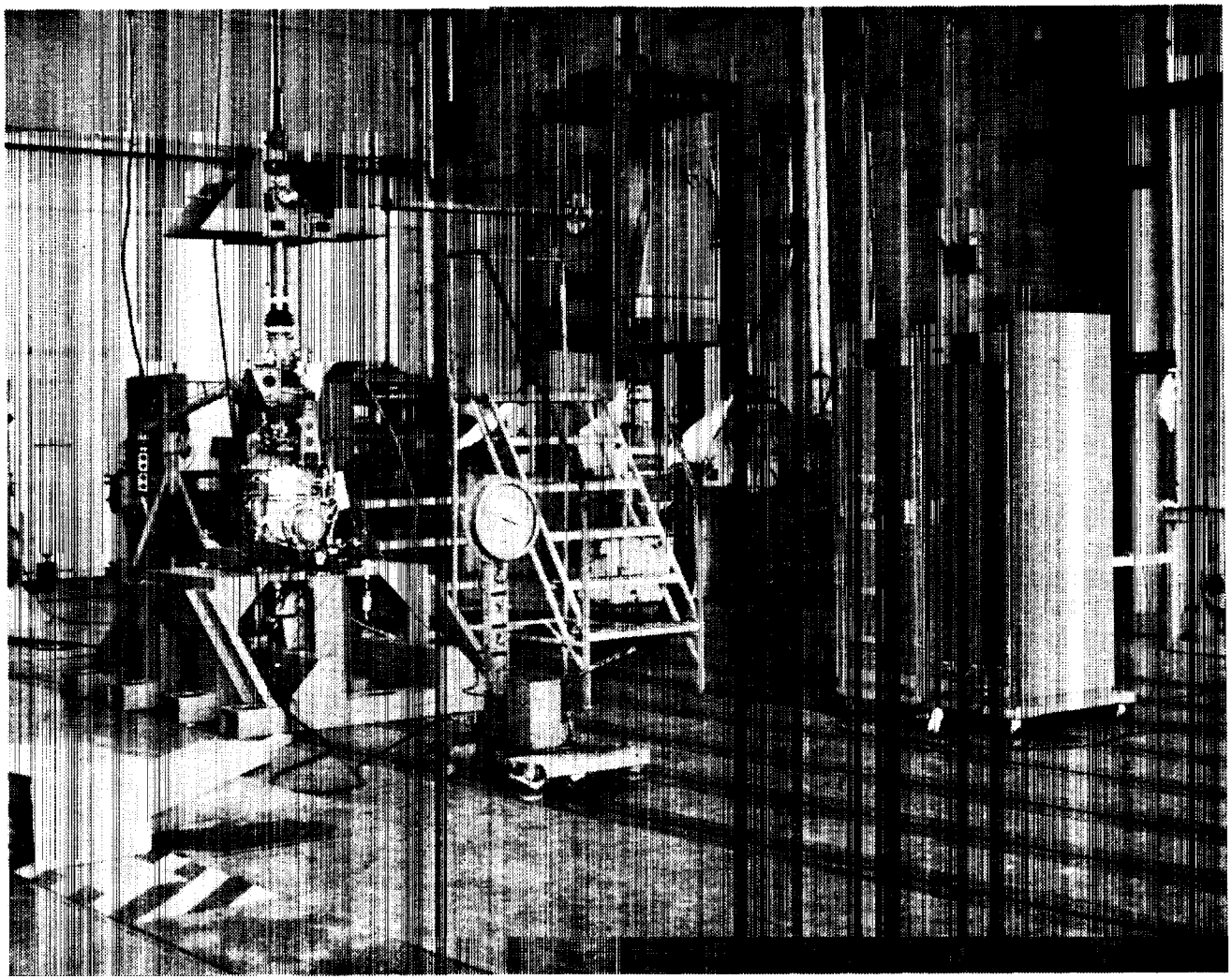

STATIC
(LATERAL & F/A)
0 - 1500 LB
(WITH & WITHOUT LIFT)

DYNAMIC
(LATERAL & F/A)
0 - 50 Hz
(WITH & WITHOUT LIFT)
(WITH & WITHOUT DAMPERS)

PYLON STATIC TEST CORRELATION - ROTATION AT TRANSMISSION CG

Pylon rotation, measured at the transmission, is compared to predicted NASTRAN results using the nonlinear geometry solution (SOL 64) in the calculations. The pylon rotation was actually calculated from the differential vertical displacements at the pylon mounts. The test/NASTRAN correlation is shown in the opposite figure for longitudinally and laterally applied loads at the hub. There is a good correlation for the lateral deflection results but poor correlation for the longitudinal deflection results. The good correlation in the lateral direction indicates that the four-corner pylon mount stiffnesses are accounted for correctly. Close examination of the static test results indicated discrepancies between test and analysis in the displacements at the lift link and fifth mount locations. For instance, a deflection of 0.038 inch was measured at the lift link location due to a 7,000-lb thrust, compared to 0.013 inch predicted by NASTRAN. Therefore, the combined flexibility of the lift link, test fixture, and lift link joint is three times larger than that of the NASTRAN model. Also, the displacement indicator on the hinge joint that connects the fifth mount to the pylon structure showed a differential deflection between the fifth mount and the hinge joint. The original NASTRAN FEM did not account for this flexibility. The stiffness of the fifth mount joint was calculated and found to be equivalent to a spring with a coefficient of 53,100 lb in series with the fifth mount.

PYLON STATIC TEST CORRELATION – ROTATION AT TRANSMISSION CG

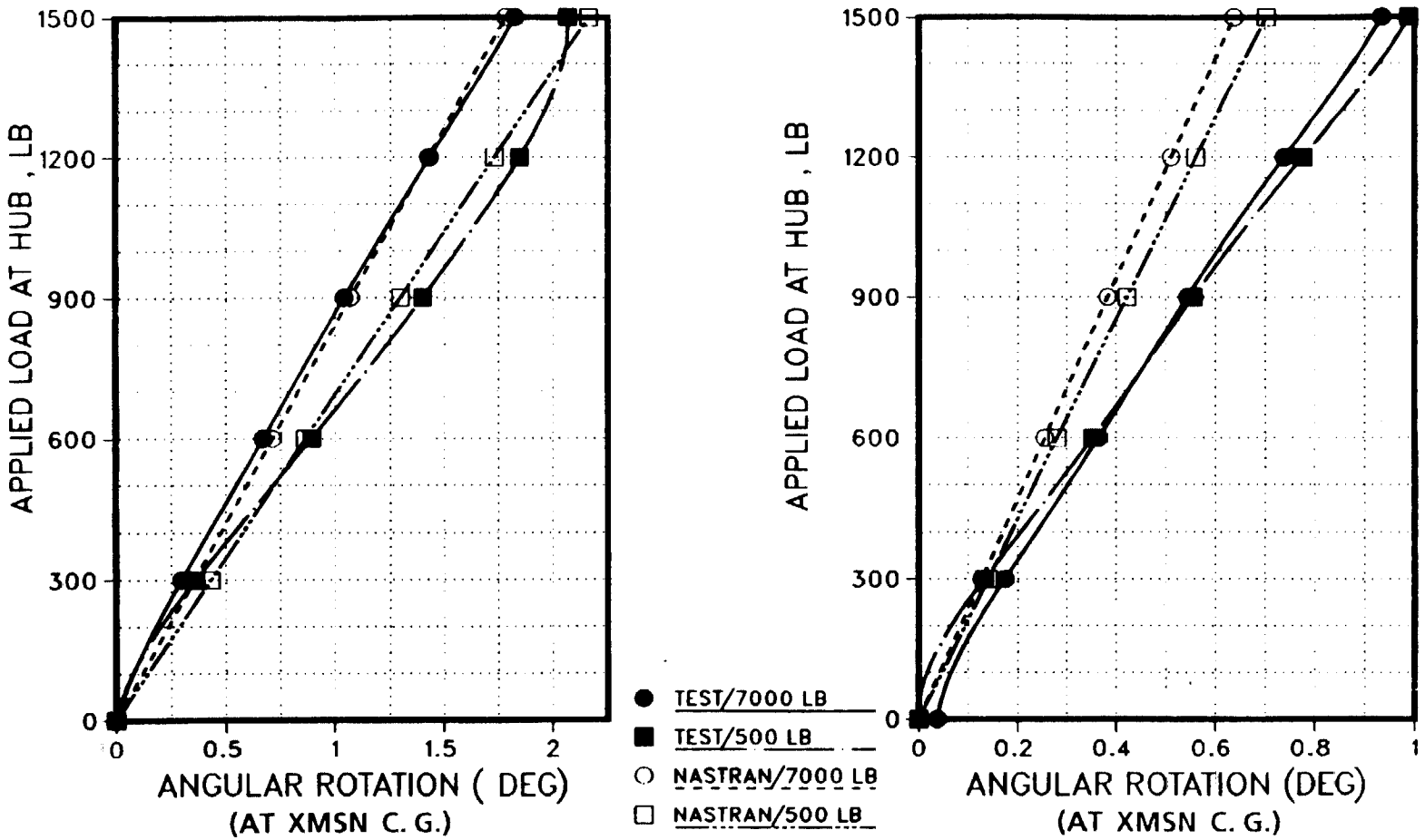

PYLON LONGITUDINAL ROTATION

PYLON LATERAL ROTATION

PYLON STATIC TEST CORRELATION - TRANSLATIONS

The additional apparent flexibilities in the lift link/test fixture and in the fifth mount hinge joint are included here in the calculation of the hub deflection in the lateral and longitudinal directions, in order to examine the overall integrity of the NASTRAN model. These results include a check on the mast stiffness, which is 1726 lb/in as measured at the hub using NASTRAN. The correlation between the test and the analysis is good in both directions. This confirms that the pylon mounts and the elastic line mast stiffness were appropriately modeled in the original FEM. The additional flexibilities of the fifth mount and lift link to test fixture connectivity are not included in the ensuing dynamic analyses.

PYLON STATIC TEST CORRELATION – TRANSLATIONS

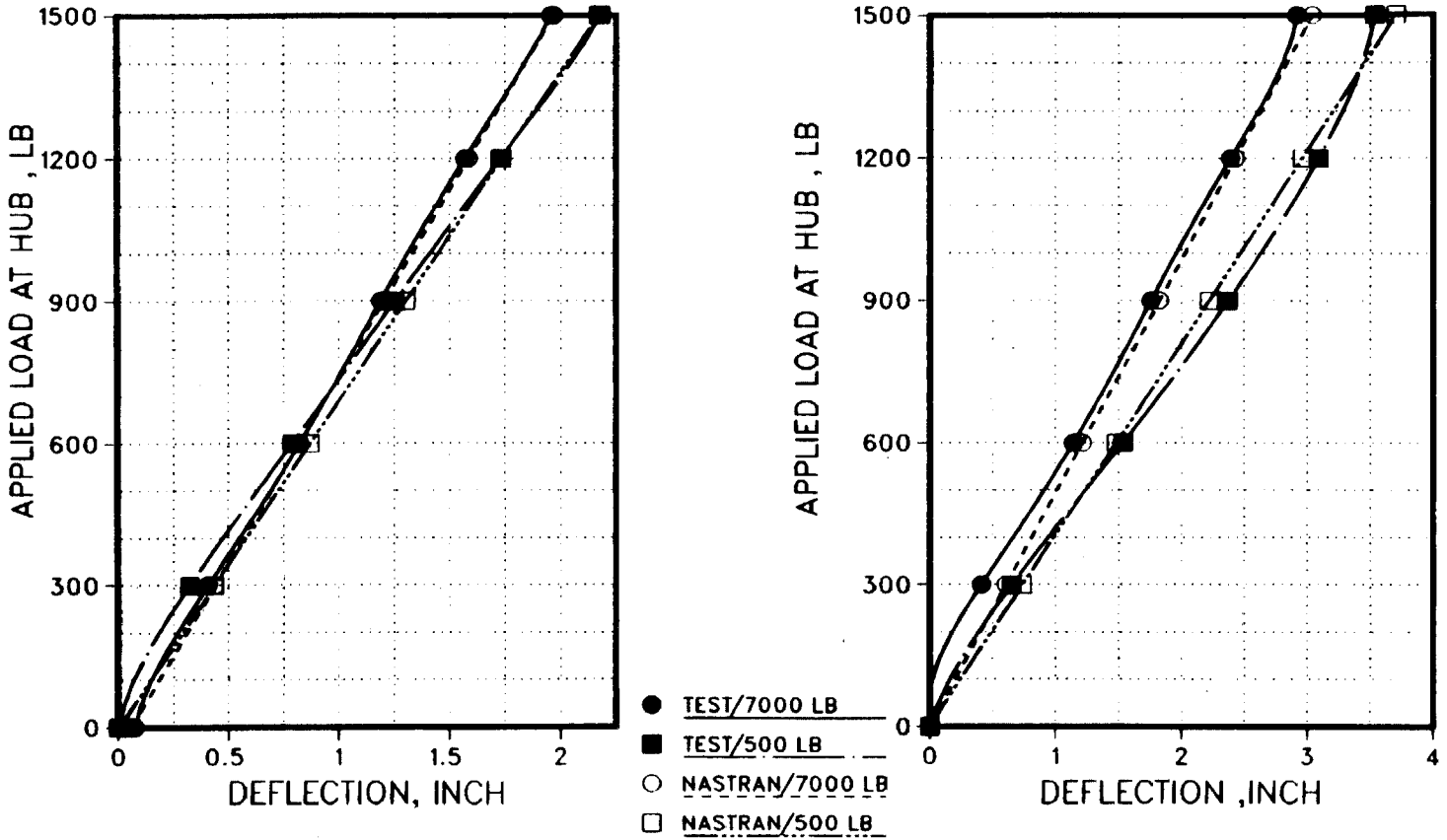

HUB LONGITUDINAL DEFLECTION

HUB LATERAL DEFLECTION

CALCULATION OF PYLON MOUNT STIFFNESS FOR FORCED RESPONSE CORRELATION

The pylon rocking modes and, to a lesser extent, the main rotor mast bending modes are controlled by the stiffness of the elastomeric mounts.

Approximate static and dynamic stiffnesses for the four pylon elastomeric mounts were calculated from the test data documented in Volume I of this report. Test data were obtained at two frequencies, 2 and 5 Hz, proximate to the pylon roll mode ($\approx$ 2.5 Hz) and pylon pitch mode ($\approx$ 3.0 Hz) of the AH-1G. Based on these test results, individual mount dynamic stiffnesses for the 2-4 Hz frequency range were interpolated by applying shake test level forces to the NASTRAN FEM hub and determining the static reactions of each pylon mount. These static force levels were compared to the dynamic stiffness data in Volume I to provide representative values for dynamic stiffness at the desired frequency, as shown in the table below.

Unfortunately, no test data existed near the mast bending modes frequency range (25-30 Hz) to provide similar data for correlation with the mast bending modes.

CALCULATION OF PYLON MOUNT STIFFNESS FOR FORCED RESPONSE CORRELATION

	PYLON PITCH SHAKE TEST*				PYLON ROLL SHAKE TEST†			
	± 100 AT HUB		± 200 LB AT HUB		± 100 LB AT HUB		± 200 LB AT HUB	
	REACTION‡ (lb)	STIFFNESS (LOSS) (lb/in)	REACTION (lb)	STIFFNESS (LOSS) (lb/in)	REACTION‡ (lb)	STIFFNESS (LOSS) (lb/in)	REACTION (lb)	STIFFNESS (LOSS) (lb/in)
R. H. FORWARD	29	6428	58	6147	160	5446	320	5056
R. H. AFT	57	5230	114	4959	150	4751	300	4459
L. H. FORWARD	29	5926	58	5874	160	5088	320	4747
L. H. AFT	56	5440	12	5117	150	4876	300	4550
FIFTH MOUNT	310	22677	620	21646	1.5	50560	3	50560

*STIFFNESS VALUES USED ARE THE AVERAGE VALUES AT 2 Hz AND 5 Hz (PYLON PITCH ≈ 3 Hz).

†STIFFNESS VALUES USED ARE VALUES AT 2 Hz (PYLON ROLL ≈ 2 Hz).

‡REACTIONS AT THE PYLON MOUNTS ARE CALCULATED FROM STATIC NASTRAN ANALYSIS WITH STATIC STIFFNESS VALUES.

PYLON NORMAL MODE CORRELATION

The difference in the pylon and mast modes for lateral excitation from those given in the F/A excitation configuration is mainly due to the different reaction at the pylon mounts to a lateral load applied at the hub from the reactions calculated to the same load applied in the F/A direction. As can be seen in the following tables, the two cases with 1000 lb lift and with/without the dampers installed produced different pylon roll modes in the test results. The NASTRAN results for both cases are identical since the dampers are modeled with zero spring coefficient in the NASTRAN analysis. The calculated mast lateral mode is 1 Hz (4%) higher than the test results without dampers and 1 Hz (4%) lower than the test results with dampers. The correlation between the calculated mast lateral bending and test results based on the case without damper is good even with the NASTRAN model not employing a damper stiffness model. The correlation between the calculated pylon roll mode and test results is relatively poor, with an error as high as 17% for the case with damper, 1000 lb lift, and 200 lb shake force. Since this error extends to the case without dampers (13% errors), the neglected dampers in the NASTRAN model are not the only reason for the poor correlation for the pylon roll mode. The calculated spring constants for the pylon mounts at 2 Hz are probably lower than the actual dynamic stiffness of these mounts.

The lift load was found to be an effective parameter on the pylon roll mode where the frequency of this mode increased from 2.03 Hz to 2.21 Hz (9%) when the lift load was increased from 1000 lb to 7000 lb.

The analysis started by evaluating the structural and geometrical stiffness using the nonlinear geometry solution (NASTRAN SOL 64). The superelement normal mode solution (SOL 63) was then restarted using the updated stiffness matrix, which accounts for the lift effect. The results of this normal mode analysis were used to identify and compare the peak responses in the test and NASTRAN results. The calculated pylon pitch modes for the different configurations agree well with test; however, the mast longitudinal bending for the cases with dampers is 2-3 Hz lower than the test values. Again, the apparent reason for the discrepancy is the negligence of the damper stiffness in the NASTRAN model.

The pylon vertical mode is placed at about 35 Hz in the test results and above 50 Hz in NASTRAN results. The high frequency of the pylon vertical mode is due to the large vertical stiffness introduced by the lift link. The dynamic analysis did not incorporate additional flexibility at the lift link and the fifth corner mount hinge to counter the static test observation of apparent additional flexibility at these two locations.

PYLON NORMAL MODE CORRELATION

		RESPONSE TO LATERAL EXCITATION (Hz)			
		1000-LB THRUST			7000-LB THRUST
		WITH DAMPERS		W/O DAMPERS	WITH DAMPERS
SHAKE TEST FORCE (LB):	2-6 Hz	100	200	100	100
	6-50 Hz	400	400	400	400
PYLON ROLL:	NASTRAN	2.03	1.98	2.03	2.21
	TEST	2.27	2.42	2.34	2.49
PYLON PITCH:	NASTRAN	3.33	3.32	3.33	3.47
	TEST	3.16	3.70	2.81	3.51
MAST LATERAL:	NASTRAN	24.07	25.50	24.07	24.31
	TEST	25.00	24.90	22.98	25.26
MAST F/A:	NASTRAN	30.17	29.84	30.17	30.34
	TEST	31.20	29.00	27.40	29.00

		RESPONSE TO F/A EXCITATION (Hz)					
		1000-LB THRUST				7000-LB THRUST	
		WITH DAMPERS		W/O DAMPERS		WITH DAMPERS	
SHAKE TEST FORCE (LB):	2-6 Hz	200	100	200	100	200	100
	6-50 Hz	200	400	200	400	200	400
PYLON ROLL:	NASTRAN	2.10	2.13	2.10	2.13	2.28	2.31
	TEST	2.60	2.63	2.46	2.38	2.35	2.35
PYLON PITCH:	NASTRAN	2.90	2.93	2.90	2.93	3.04	3.08
	TEST	2.81	2.71	2.81	2.71	3.15	3.22
MAST LATERAL:	NASTRAN	24.39	24.53	24.39	24.53	24.63	24.77
	TEST	24.04	23.20	23.86	23.48	24.70	24.21
MAST F/A:	NASTRAN	27.18	27.48	27.18	27.48	27.37	27.68
	TEST	30.90	29.50	28.80	27.73	30.90	30.50

PYLON COMPONENT FREQUENCY RESPONSE RESULTS
(Dampers Installed)

Frequency response at two different locations on the pylon-mast structure is presented for lateral and longitudinal excitation for a 7000-lb thrust load and with the dampers installed. A shake test force of 200 lb was applied at the main rotor hub. The stiffness of the pylon mounts was derived for frequencies near those of the pylon modes, which explains the good correlation between the test and NASTRAN results around the pylon modes. The forced response correlation around the mast bending modes is poor. The mast bending frequency correlations are poor because damper stiffness and mass coupling were neglected in the NASTRAN model. The test response clearly shows coupling between F/A and lateral mast bending modes. However, the lack of good correlation between force amplitudes is mainly related to the damping content provided by the elastomeric mounts at higher frequency. The analysis for each test configuration was conducted with specific values for pylon mount stiffness and damping, which were not changed over frequency. The analysis used the NASTRAN superelement direct frequency response (SOL 68) which was restarted from solution 64 with the updated stiffness matrix. A complete listing of forced response comparison plots is contained in Appendix B.

PYLON COMPONENT FREQUENCY RESPONSE RESULTS

(DAMPERS INSTALLED)

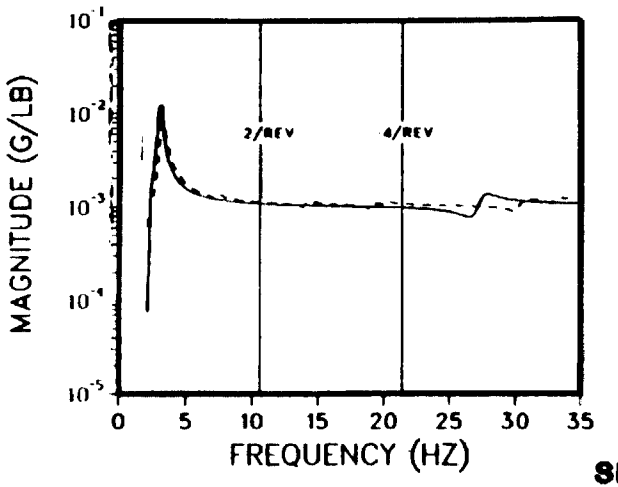

M/R HUB F/A RESPONSE

THRUST = 7000 LB.

SHAKER FORCE = 200 LB

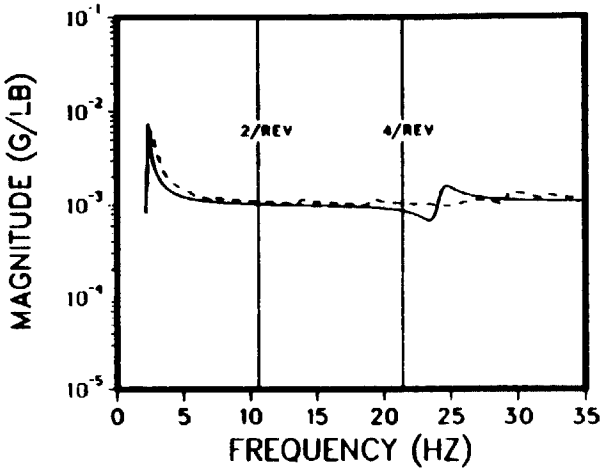

M/R HUB LATERAL RESPONSE

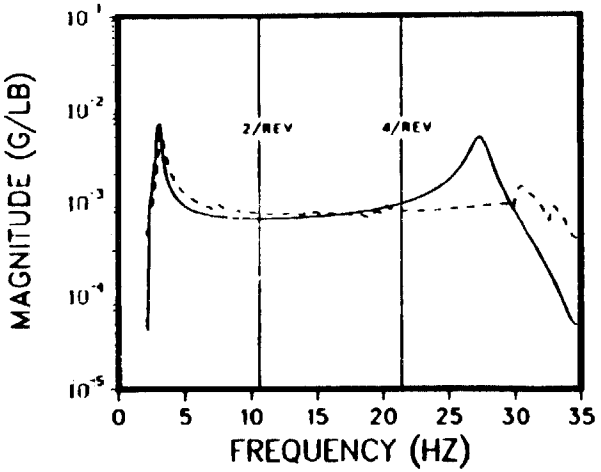

MID MAST (STA 22) F/A RESPONSE

SHAKE TEST

NASTRAN

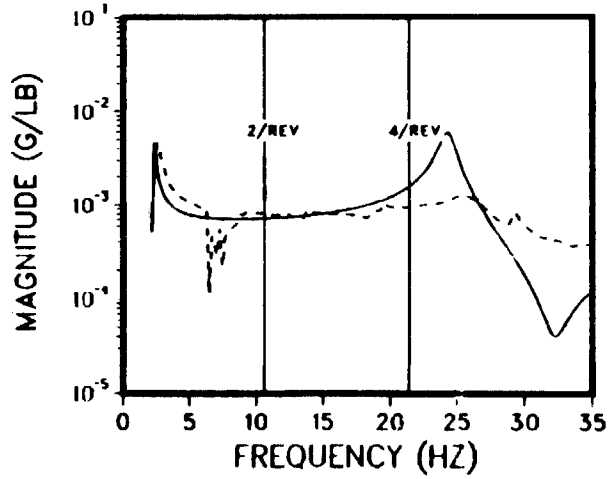

MID MAST (STA 22) LATERAL RESPONSE

CONCLUSIONS - PYLON COMPONENT CORRELATION

The following conclusions are based on the pylon static and dynamic tests and the NASTRAN comparative analysis:

1. Rotor thrust should be incorporated in the evaluation of the pylon modes.

2. Appropriate stiffness coefficients for the pylon elastomeric mounts significantly improves the pylon frequency predictions. However, such good frequency prediction will apply only in a narrow frequency band where the elastomeric mount stiffness is valid.

3. Simple finite element models of the pylon structure with accurate mast modeling are sufficient. The transmission mass moments of inertia with cross products of inertia are required for modeling enhancement and for evaluation of the pylon out-of-plane forced response.

4. The pylon dampers under the pylon aft mounts perform only with relatively large pylon deflection and their stiffness should be included in future dynamic analyses.

CONCLUSIONS - PYLON COMPONENT CORRELATION

- ROTOR THRUST DIFFERENTIAL STIFFENING EFFECTS ARE SIGNIFICANT TO PYLON MODAL RESPONSE.
- ELASTOMERIC MOUNT NONLINEARITIES ARE CRITICAL FOR PYLON MODES.
- ELASTIC LINE MODEL OF PYLON STRUCTURE APPEARS SUFFICIENT FOR STIFFNESS, BUT SIGNIFICANT IN-PLANE MASS COUPLING EFFECTS MUST BE INCLUDED.
- DAMPER CHARACTERISTICS NEED BETTER DEFINITION.

SUSPENSION SYSTEM TEST SETUP

Details of the tests performed on the cable suspension system are described in Volume I of this report. Two cable systems were used. The first had an 8-foot cable with a bunge isolation system in series to isolate vertical suspension effects during vertical tests. For in-plane tests, a 12-foot steel cable was used. The in-plane cable suspension system was modeled using the finite element technique illustrated in the figure. The load-deflection curve obtained from the static pull tests (vertical) was used in the FEM description as well as cable mass and lumped masses to develop a dynamic representation of the suspension system. This model was validated by comparing static out-of-plane stiffness and dynamic natural frequencies with those values obtained during the test.

STATIC TEST				DYNAMIC TEST		
Load (lb)		Deflection (in)			ω_n (Hz)	
Lateral	Tension	Test	NASTRAN	Mode	Test	NASTRAN
1000	7000	13.4	12.9	1	2.1	2.9
				2	5.1	4.7
1000	1000	30.6	30.2	3	11.6	13.7
				4	19.5	19.6

The cable FEM was then attached to the AH-1G airframe FEM as described on the next page to determine the cable differential stiffening effects during the test.

SUSPENSION SYSTEM TEST SETUP

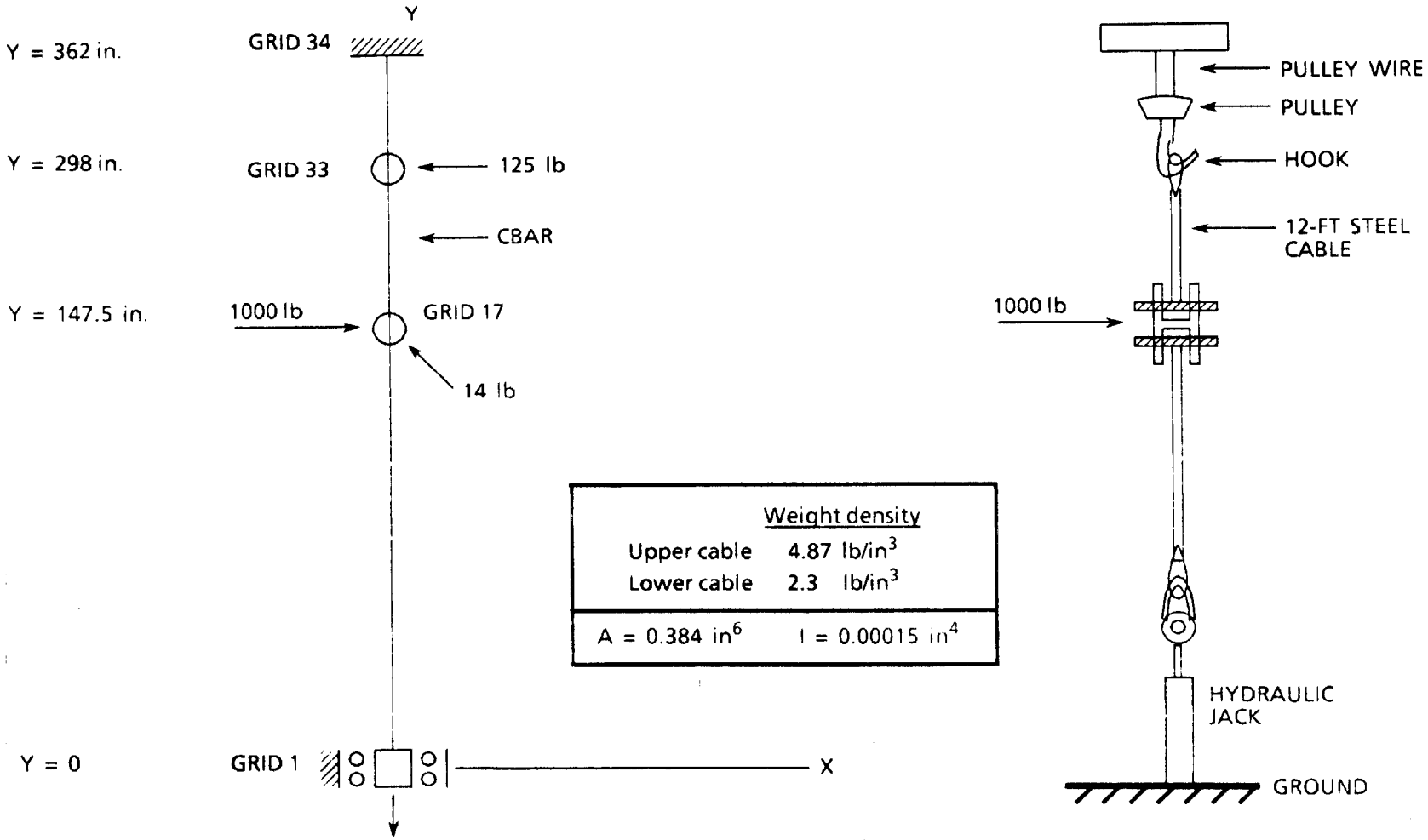

	Weight density
Upper cable	4.87 lb/in^3
Lower cable	2.3 lb/in^3

$A = 0.384\ in^6$	$I = 0.00015\ in^4$

CABLE SUSPENSION EFFECTS - CONFIGURATION 1

An investigation of the effects of adding the 12-foot steel cable suspension to Configuration 1 was performed by building a finite element model of the cable to determine the effects of differential stiffening on the frequency response predictions of NASTRAN. Initially, a nonlinear static superelement analysis (Rigid Format 64) is required to generate a differential stiffness matrix. This is accomplished with two subcases in SOL 64. Subcase 1 contains an enforced vertical displacement of the system to represent the cable lengthening that occurs when the ship is suspended. Subcase 2 is identical to Subcase 1 and enables SOL 64 to calculate a differential stiffness matrix. After SOL 64, SOL 63 is run to get the resultant normal mode output using the differential stiffness matrix from the database. Finally, the modal stiffness of the cable at the hub is enforced on the full NASTRAN FEM by a constraint equation (MPC) between the hub displacement (excitation location) and the generalized coordinates corresponding to the cable modes. Comparisons of frequency response predictions with and without the suspension differential stiffening effects and tests are shown.

CABLE SUSPENSION EFFECTS - CONFIGURATION 1

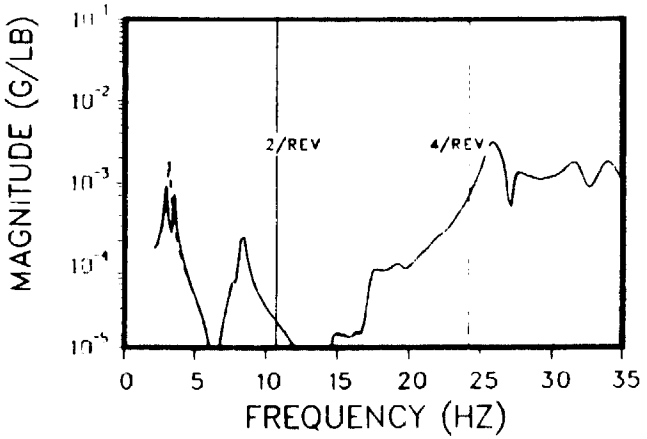

PILOT (FS 138) VERTICAL RESPONSE

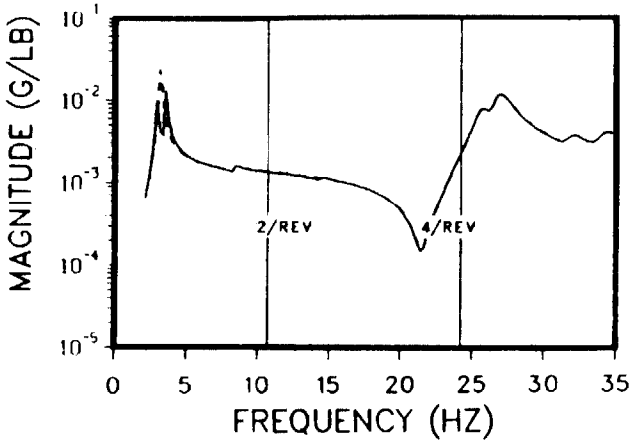

HUB (FS 200) F/A RESPONSE

CABLE FEM ANALYSIS

SOL 64 - GEOMETRIC NONLINEAR
⇌ GENERALIZED COORDINATE
RESPONSE AT HUB

SOL 63 - NORMAL MODES

CABLE MODES

FEM	TEST
2.4	2.7
6.9	7.2
19.2	18.2

INVESTIGATION OF SPECIAL EFFECTS

Nonlinearity and nonproportional damping effects were investigated to determine their effects on frequency response correlations.

INVESTIGATION OF SPECIAL EFFECTS

- NONLINEARITIES
- NONPROPORTIONAL DAMPING

NONLINEAR INVESTIGATION - CONFIGURATION 1

Comparisons of the frequency response functions obtained from tests at two different forcing amplitudes for three load cases on Configuration 1 are shown. No effect is seen. The force levels used during the test were limited to avoid damage to the aircraft. Higher force levels should be investigated, especially off-resonance force levels, in order to find nonlinear responses.

NONLINEAR INVESTIGATION – CONFIGURATION 1

VERTICAL LOAD AT MAIN ROTOR

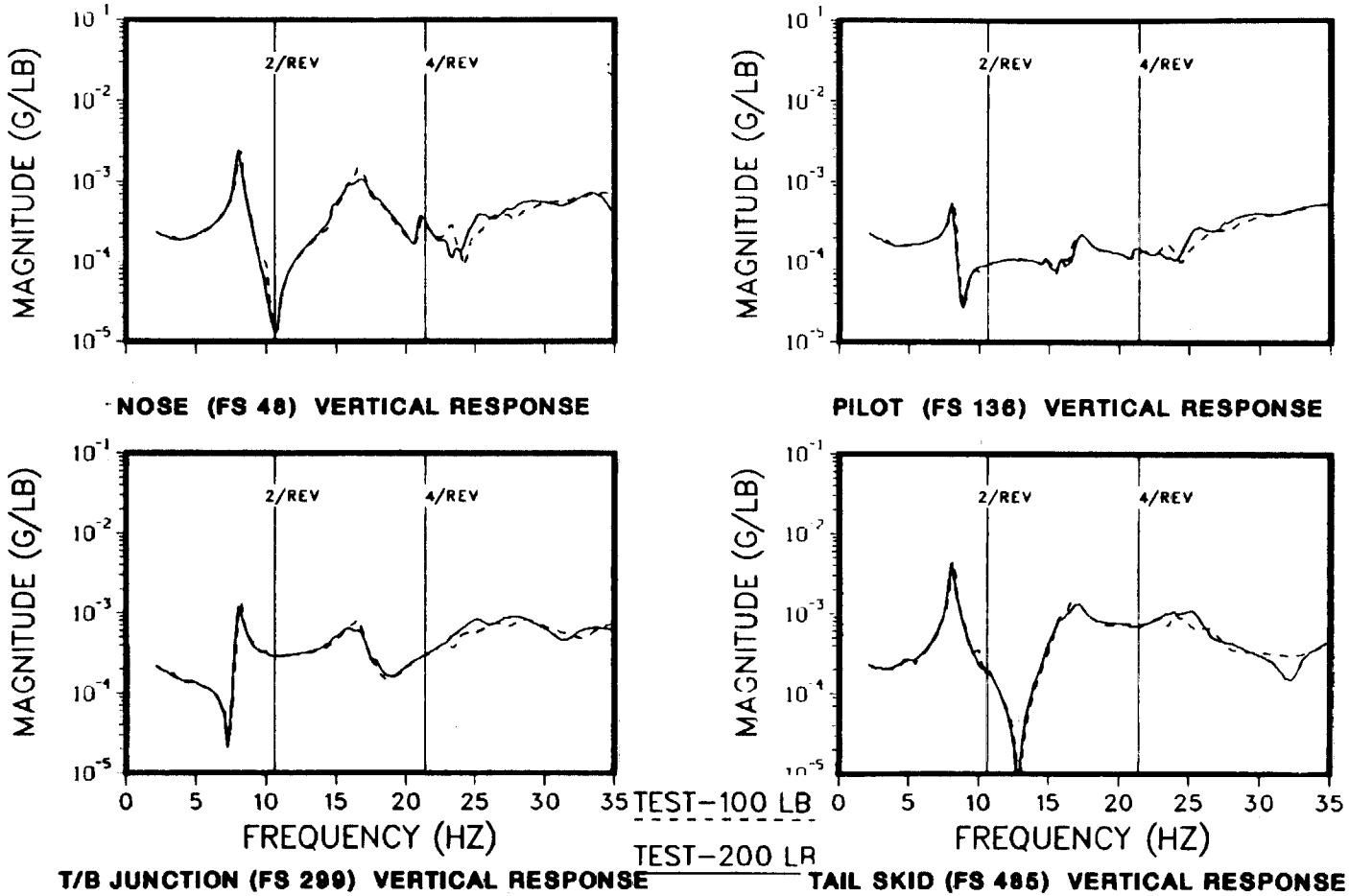

NONLINEAR INVESTIGATION – CONFIGURATION 1

VERTICAL LOAD AT TAIL SKID

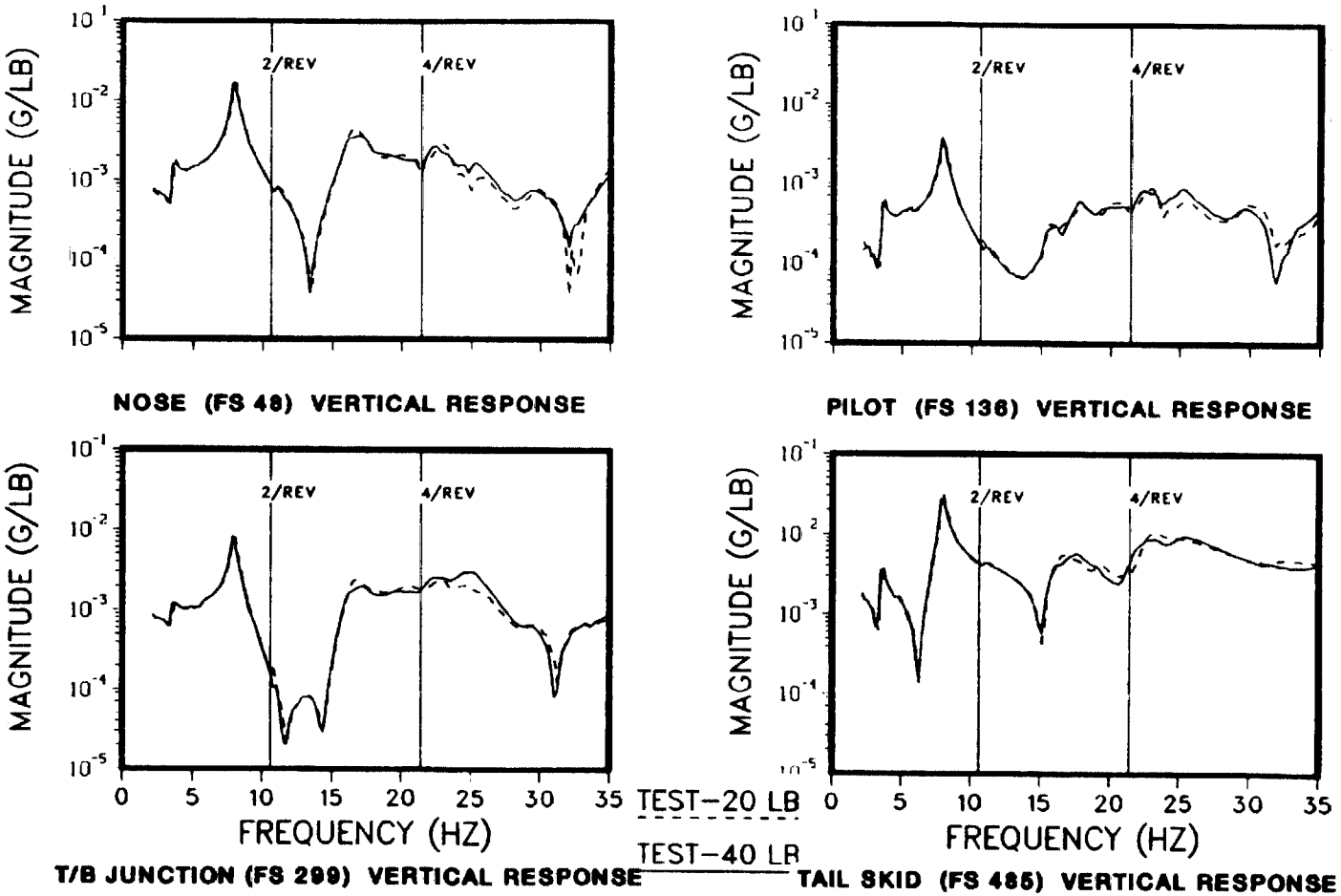

NONLINEAR INVESTIGATION – CONFIGURATION 1

LATERAL LOAD AT MAIN ROTOR

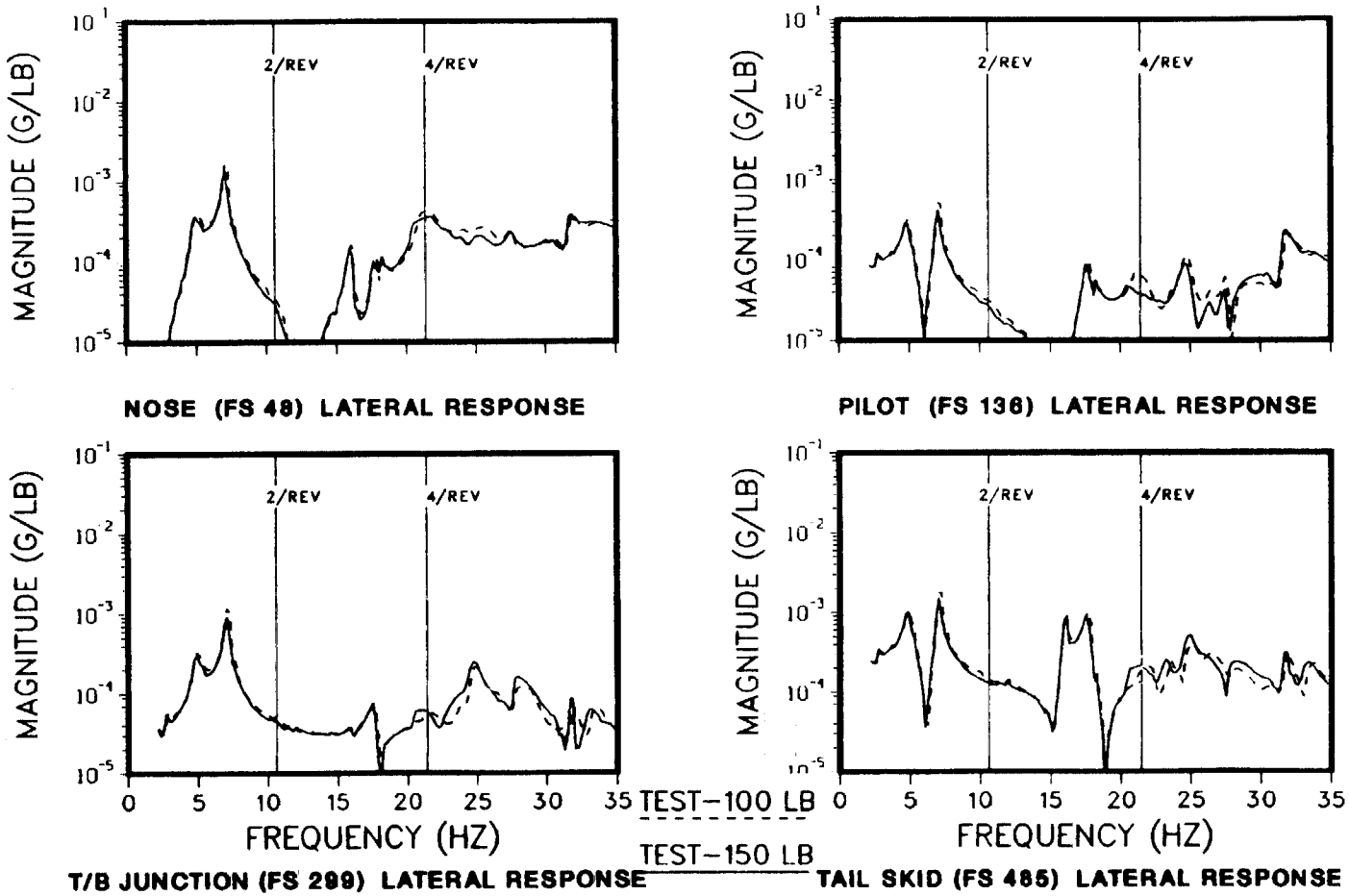

NONPROPORTIONAL DAMPING EFFECTS

Displacements in the structure will reach their peak simultaneously when a system is undamped or proportionally damped. However, as is illustrated in the figure, higher frequency bending modes were found to exhibit nonproportional damping effects and a varying phase angle between response points. These differences in phase cause the amplitudes of responses to vary quite significantly from those of a proportionally damped system. Forced response dwells were recorded for most of the natural frequencies identified in test. However, no capability existed for digital recording of this information and only hard copy files of real and imaginary or magnitude and phase response per channel are available. These data represent a voluminous collection of information that could not be presented in this report. It is available for future studies into the trends associated with nonproportional damping and frequency.

NONPROPORTIONAL DAMPING EFFECTS
LATERAL EXCITATION AT TAIL

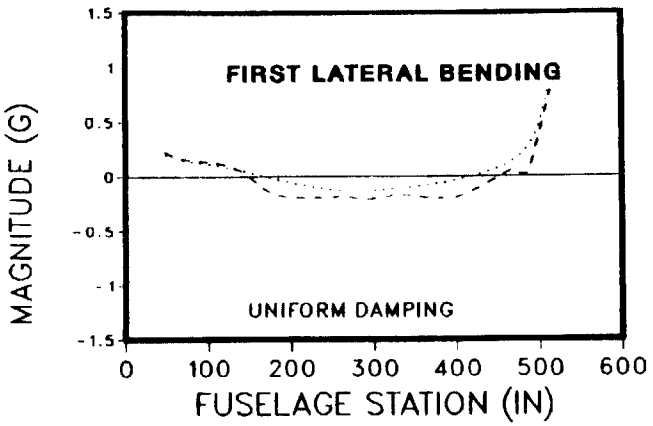

TEST

NASTRAN

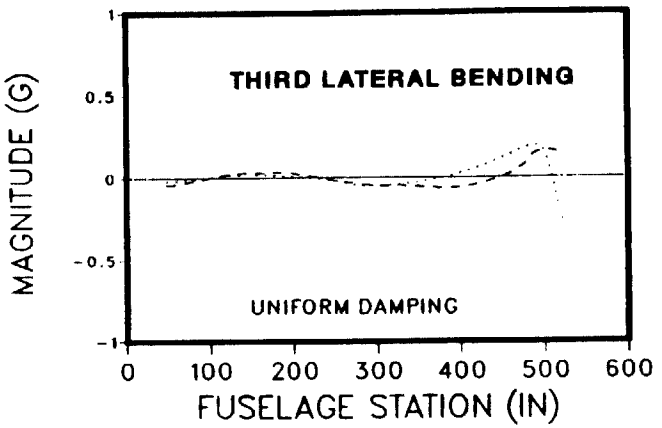

RESPONSE POINT	AMPLITUDE	PHASE	*	AMPLITUDE	PHASE	*
NOSE	.23	268	0	.04	281	0
GUNNER	.14	267	1	.004	263	18
PILOT	.06	266	2	.03	100	181
PILOT AFT	.09	81	187	.03	105	176
CG	.19	83	185	.03	92	176
ENG DECK	.19	85	183	.02	299	189
ENG DECK AFT	.19	85	183	.03	294	- 18
T/B JUNCT	.21	84	189	.05	286	- 15
T/B ANTENNAE	.17	87	181	.05	271	10
ELEVATOR	.20	85	183	.07	185	93
42° GEARBOX	.05	292	- 24	.04	93	188
TAIL SKID	.02	334	- 66	.13	115	166
MID FIN	.59	271	- 3	.16	8	273
90° GEARBOX	1.02	269	- 1	.31	350	- 69

* Phase relationsips normalized to response at the nose.

5. CONCLUSIONS

CONCLUSIONS

The procedure used in the study, known as the AH-1G difficult component investigation, consisted of the progressive and cumulative removal of individual components from the helicopter while various shake tests were performed at each stage of the removal process. In addition, analytical predictions were obtained for a similar removal of components, and discrepancies between the measured and predicted changes were noted. The findings from the difficult components investigation are summarized on the next several pages. Some key findings from this effort, in addition to the effects of individual components, include the following:

1. Incorporating secondary structure effects along with a built-up tailboom FEM, in lieu of the elastic line tailboom FEM, improved natural frequency correlations to within 5% for all flexible modes through 35 Hz.

2. The modal damping estimates from the test are between 1% and 3% for all airframe modes through 35 Hz, which is fairly consistent with the standard 2% estimates used in NASTRAN; but nonproportional damping effects seem to increase substantially in the higher frequency modes (>20 Hz), causing complex (phase dependent) responses.

3. Better analytic modal parameter diagnostics are needed to quantify mode shape or eigenvector correlations in the same manner as eigenvalue correlation is quantified.

SUMMARY OF AH-1G DIFFICULT COMPONENT CORRELATIONS

COMPONENT	FINDINGS	RECOMMENDED ACTION
PYLON		
THRUST	STIFFENING TRENDS CONSISTENT WHEN THRUST ADDED	INCLUDE EFFECTS OF THRUST
DAMPERS	REPRESENTED AS MODAL DAMPING	INVESTIGATE VISCOUS DAMPING EFFECTS
MOUNTS	VARIABLE STIFFNESS REQUIRED	INVESTIGATE ELASTOMERIC MOUNT NONLINEARITIES (FREQUENCY AND AMPLITUDE)
SECONDARY STRUCTURE	SIDE ACCESS PANELS AND BELLY PANELS PROVIDE STIFFNESS	PROBABLY CONFIGURATION DEPENDENT, BUT NEEDS TO BE INVESTIGATED FOR EACH AIRFRAME
T/R DRIVE SHAFT	MASS REPRESENTATION SUFFICIENT	INVESTIGATE STIFFENING/ DAMPING EFFECTS UNDER TORQUE
SKID LANDING GEAR	ELASTIC LINE FEM SUFFICIENT	NONE

SUMMARY OF AH-1G DIFFICULT COMPONENT CORRELATIONS (CONTINUED)

COMPONENT	FINDINGS	RECOMMENDED ACTION
ENGINE	MASS REPRESENTATION SUFFICIENT	IF ENGINE ELASTIC MODES IN FREQUENCY RANGE OF INTEREST, THEY NEED TO BE CONSIDERED
FUEL	MASS REPRESENTATION SUFFICIENT BELOW 4p	INVESTIGATE EFFECTS ABOVE 4p
CANOPY GLASS	AFFECTS FUSELAGE TORSION MODE AND FREQUENCY RESPONSE ABOVE 4p	STIFFNESS NEEDS TO BE DEFINED
SOFT-MOUNTED BLACK BOXES	HAS MINOR EFFECT ON FREQUENCY RESPONSE ABOVE 4p	LOCAL MODE CHARACTERISTICS NEED INVESTIGATION
TAILBOOM FEM (ELASTIC OR BUILT UP)	BUILT-UP FEM PROVIDES BETTER CORRELATION, PARTICULARLY ABOVE 4p	USE BUILT-UP FEM

SUMMARY OF AH-1G DIFFICULT COMPONENT CORRELATIONS (CONCLUDED)

COMPONENT	FINDINGS	RECOMMENDED ACTION
SUSPENSION	ONLY SIGNIFICANT BELOW 1p	INCLUDE EFFECTS IN FEM
AIRFRAME NONLINEARITIES	NOT SIGNIFICANT AT SHAKE TEST LOAD LEVELS (10 - 400 LB)	INVESTIGATE EFFECTS AT ROTOR LOAD LEVELS (400 - 1000 LB)
DAMPING		
PYLON MOUNTS	UNSATISFACTORY REPRESENTATION	INVESTIGATE MOUNT DAMPING
< 20 Hz, AIRFRAME	0 - 2 % CRITICAL PROVIDES GOOD CORRELATION	USE MODAL PLUS ESTIMATES
> 20 Hz, AIRFRAME	> 2 % CRITICAL PROVIDES GOOD CORRELATION	USE MODAL PLUS ESTIMATES
NONPROPORTIONAL	BECOMES MORE SIGNIFICANT AT HIGHER FREQUENCIES	SOURCE MUST BE DETERMINED

BHTI DAMVIBS SUGGESTED FOLLOW-ON EFFORTS

The DAMVIBS program at Bell Helicopter has consisted of five tasks performed over the period extending from 1984 to 1988. The difficult component work presented here is the culmination of these efforts geared towards assessing current industry standards for vibration prediction. Based on the experience gained by Bell personnel under DAMVIBS, the following areas of advanced research are highlighted as having the most potential for improving current industry standards:

1. ACAP difficult components (all composite rotorcraft)
2. Optimization applications
3. Damping determination
4. Force determination
5. Component modal synthesis
6. Test methodology and analysis interfaces

BHTI DAMVIBS SUGGESTED FOLLOW-ON EFFORTS

1. ACAP DIFFICULT COMPONENTS:

- USE EXISTING FEM
- TEST PLAN BASED ON AH-1G EXPERIENCES

2. OPTIMIZATION:

- DEFINE DESIGN PROCESS, APPLICATION TO LARGE FEMs
- NATURAL FREQUENCY PLACEMENT
- FORCED RESPONSE MINIMIZATION
- MODE SHAPING

3. DAMPING DETERMINATION:

- MODAL, NONPROPORTIONAL
- FEM ANALYSIS

4. OSCILLATORY LOADS DEFINITION:

- FORCE DETERMINATION (HUB LOADS, DOWNWASH, CONTROL LOADS)
- ROTOR/AIRFRAME COUPLING
- FEM DYNAMIC/AERODYNAMIC ROTOR LOADS ANALYSIS

BHTI DAMVIBS SUGGESTED FOLLOW-ON EFFORTS
(CONCLUDED)

5. COMPONENT MODAL SYNTHESIS:

- COUPLED TEST/FEM ANALYSIS
- REANALYSIS OF BATTLE-DAMAGED STRUCTURE
- CORRELATION OF SUBSTRUCTURING (SUPERELEMENTS) VS. MODAL SYNTHESIS

6. NONLINEARITIES:

- PYLON DYNAMIC (THRUST EFFECTS, ELASTOMERIC MOUNTS, BEARINGS)
- COMPONENT ATTACHMENTS (ELEVATOR, ENGINES, LANDING GEAR)
- STRUCTURAL RESPONSE AT VARYING FORCE LEVELS

TEST METHODS:

- SYSTEM PARAMETER IDENTIFICATION
- STRUCTURAL MODIFICATION
- FEM IMPROVEMENT
- QUANTITATIVE CORRELATION METHODS, DETERMINE MODAL CONTRIBUTORS

6. REFERENCES

REFERENCES

1. Cronkhite, J. D., Berry, V. L., and Dompka, R. V., "Summary of the Modeling and Test Correlations of a NASTRAN Finite Element Vibrations Model for the AH-1G Helicopter," NASA CR 178201, January 1987.

2. Cronkhite, J. D., Berry, V. L., and Brunken, J. E., "A NASTRAN Vibration Model of the AH-1G Helicopter Airframe," R-TR-74-045, U.S. Army Armament Command, June 1974.

3. "The NASTRAN User's Manual," NASA SP-221(05), December 1979.

4. Dompka, R. V., and Corrigan, J. J., "AH-1G Flight Vibration Correlations Using NASTRAN and the C81 Rotor/Airframe Coupled Analysis," 1986 AHS Forum Proceedings, Washington, D.C., June 1986.

5. Brown, J. J., and Parker, G. R., "DMAP Alters for Performing Basic Constraint Checks on Structural Models," NSC/NASTRAN User's Conference Proceedings, March 21-22, 1985, Pasadena, CA.

6. "Modal Plus User's Manuals - Theory Section," Structural Dynamics Research Corporation, 1983.

7. Parker, G. R., and Brown, J. J., "Kinetic Energy DMAP for Mode Identification," MSC/NASTRAN User's Conference Proceedings, March 18-19, 1982, Pasadena, CA.

APPENDIX A

MODIFIED NASTRAN FEM ELEMENTS FOR CONFIGURATIONS 1–8 AND SUBCOMPONENTS

MODIFIED NASTRAN ELEMENTS FOR CONFIGURATION 1

COMPONENT	GRIDS	CBARS	CONRODS	CELAS2	CONM2	MPC	PBARS	MAT1
FUEL ADDITION					917100 923100			
GUNNER BALLAST					908300 908533 908537			
PILOT BALLAST					913500 911543 911547			
90° G/B FAIRING					610057			
PITCH-LINKS					290145			
BATTERY ACCESS PANEL					116821 119921			
STINGER FAIRING					138445			

MODIFIED NASTRAN ELEMENTS FOR CONFIGURATION 2

COMPONENT	GRIDS	CBARS	CONRODS	CELAS2	CONM2	MPC	PBARS	MAT1
PYLON	200070	3530251			290070			
	200078	3530252			78			
	200079	3530253			79			
	200086	3530254			86			
	200087	3530255			87			
	200095	4500050			95			
	200096	4500070			290096			
	200101	4500071			290101			
	200106	4500072			106			
	200112	4500073			14			
	200114	4500074			21			
	200121	4500075			29			
	200129	4500076			37			
	200137	4500077			45			
	200145	4500078			290153			
	200153	4500079			290155			
	200153	4500080						
	200162	4500081						

MODIFIED NASTRAN ELEMENTS FOR CONFIGURATION 2 (CONTINUED)

COMPONENT	GRIDS	CBARS	CONRODS	CELAS2	CONM2	MPC	PBARS	MAT1	CSHEAR	CQDEM
TRANSMISSION SUPPORT CASE	18073 -77 211073 -77 214075					(30)				
M/R CYCLIC CONTROL LEVER	192111 193111 200111	4020011 4020012				(4)				
M/R COLL. CONTROL LEVER	194106 200105 211104	4060011 4060012				(4)				
M/R CYCLIC BOOST CYL.			0760211 0760212							
M/R COLL. CONT'L LEVER ATTACHMENT TO TRANSMISSION		4060014	0760213							

MODIFIED NASTRAN ELEMENTS FOR CONFIGURATION 2 (CONTINUED)

COMPONENT	GRIDS	CBARS	CONRODS	CELAS2	CONM2	MPC	PBARS	MAT1
QUAD-BRACED *LIFT	200015	18687 18683 21383 21387						
LIFT LINK		3570001						
PYLON MOUNTS				189831 189832 189833 189871 189872 189873 211831 211832 211833 211871 211872 211873 214853				
HUB & BLADE					291153 292153			

*DENOTES STRUCTURE ADDED TO MODEL.
( ) DENOTES THE NUMBER OF MPC CARDS ASSOCIATED WITH THIS COMPONENT.

MODIFIED NASTRAN ELEMENTS FOR CONFIGURATION 2 (CONCLUDED)

COMPONENT	GRIDS	CBARS	CONRODS	CELAS2	CONM2	MPC	PBARS	MAT1
42° G/B FAIRING					136445 138045			
DRIVESHAFT					124801			
TRANS. OIL					9200070			
GUNNER BALLAST					908300 908533 908537			
PILOT BALLAST					913500 911543 911547			
MISC.					10000000 Thru 10000098			

MODIFIED NASTRAN ELEMENTS FOR CONFIGURATION 3

COMPONENT	GRIDS	CBARS	CONRODS	CELAS2	CONM2	MPC	PBARS	MAT1
FUEL ADDITION					93331 93339 93349 93341 94661 94669 111361 111369 112703 112707 115003 115007 116801 116809 125945 128045 132245 134345 142045 305202 305201 312301 312302 100000 Thru 100297			
GUNNER BALLAST					908300 908533 908537			
PILOT BALLAST					913500 911543 911547			

MODIFIED NASTRAN ELEMENTS FOR CONFIGURATION 4

COMPONENT	GRIDS	CBARS	CONRODS	CELAS2	CONM2	MPC	PBARS	MAT1
T/R D/S & FAIRING					400000 Thru 400049			
GUNNER BALLAST					908300			
PILOT BALLAST					953500			

MODIFIED NASTRAN ELEMENTS FOR CONFIGURATION 5

COMPONENT	GRIDS	CBARS	CONRODS	CELAS2	CONM2	MPC	PBARS	MAT1
SKID GEAR	211002 214902 222002 223402 215102 215202 222202 222302 211001 214901 222001 223401 215101 215201 222201 222301	0020521 0020522 0020523 0020511 0020512 0020513 0020451 0020452 0020453 0020454 0020455 0020411 0020412 0020413 0020414 0020415			301002 304902 312002 313402 305102 305202 305201 312202 312301 312302 301001 304901 312001 313401 305101 312201			1720021 Thru 1720028 1720011 Thru 1720018
GUNNER BALLAST					908300 908533 908537			
PILOT BALLAST					913500 911543 911547			

MODIFIED NASTRAN ELEMENTS FOR CONFIGURATION 6

COMPONENT	GRIDS	CBARS	CONRODS	CELAS2	CONM2	MPC	PBARS	MAT1
ENGINE					124800			
STARTER					124801			
TACHOMETER					124804			
FUEL FILTER					124802			
BELL CRANK & PUSH ROD ASSY.					124803			
*DUMMY ENGINE					124800 124801 124804 124802 124803			

MODIFIED NASTRAN ELEMENTS FOR CONFIGURATION 7

COMPONENT	GRIDS	CBARS	CONRODS	CELAS2	CONM2	MPC	PBARS	MAT1
DUMMY ENGINE	122400 124800 127200				127800 124801 124802 124503 124804	(12)		
PILOT BALLAST					913500 911543 911547			
GUNNER BALLAST					908300 908533 908537			
ENGINE MOUNT	123457 125383 125387		109001 1070012 1060012 108001 1070011 1060011					

MODIFIED NASTRAN ELEMENTS FOR CONFIGURATION 8

COMPONENT	GRIDS	CBARS	CONRODS	CELAS2	CONM2	MPC	PBARS	MAT1
FUEL	17100 23100		0031071 0031072 0031073 0031074 0031081 0031082 0031083 0031084		917100 923100			

MODIFIED NASTRAN ELEMENTS FOR CANOPY GLASS SUBCOMPONENT

COMPONENT	GRIDS	CBARS	CONRODS	CELAS2	CONM2	MPC	PBARS	MAT1
CANOPY					80000000 Thru 80000078			

MODIFIED NASTRAN ELEMENTS FOR ELECTRONIC BOX SUBCOMPONENTS

COMPONENT	GRIDS	CBARS	CONRODS	CELAS2	CONM2	MPC	PBARS	MAT1
BLACK BOXES					90000000 Thru 90000023			
PILOT BALLAST					913500 911543 911547			
GUNNER BALLAST					908300 908533 908537			

MODIFIED NASTRAN ELEMENTS FOR WING SUBCOMPONENTS

COMPONENT	GRIDS	CBARS	CONRODS	CELAS2	CONM2	MPC	PBARS	MAT1	CSHEAR	CQDEM
RIGHT WING	61913	6222813	6222811		151912	HARD			6221119	6221121
	61917	-17	-12		-13	POINT			6281119	6281121
	61922	-21	6283411		-14	ATTACH			6241119	6341121
	61924	-24	-12		-16	(6)			6421119	6421121
	61926	-26	6344211		-17	RT FWD			6501119	6501121
	61928	-29	-12		-18	SPAR LUB			6223139	6222131
	61934	-31	6425011		-22	(20)			6283139	6282131
	61936	-39	-12		-23	CENTER			6343139	6342131
	62211	6131922	6505911		-24	RT SPAR			6423139	6422131
	62213	6171922	-12		-26	LUG			6503139	6502131
	62217	6221922	6222819		-27	(20)				6221929
	62219	6241922	-18		-28	AFT RT				6281929
	62221	6261922	6283419		-34	SPAR LUB				6341929
	62224	6281922	-18		-35	PIN				6421929
	62226	6341922	6344219		-36	(10)				6501929
	62229	6361922	-18		152211					6222939
	62231	7222839	4625019		-13					6282939
	62239		-18		-17					6342939
	62811		6505919		-19					6422939
	62819		-18		-21					
	62821		6222822		-24					
	62829		6282431		-26					
	62831		-22		-29					
	62839		6344221		-31					
	63411		-22		-39					
	63419		6425021		152811					
	63421		-22		-19					
	63429		6505921		-21					
	63431									
	63439									

MODIFIED NASTRAN ELEMENTS FOR WING SUBCOMPONENTS (CONTINUED)

COMPONENT	GRIDS	CBARS	CONRODS	CELAS2	CONM2	MPC	PBARS	MAT1	CSHEAR	CQDEM
RIGHT WING (CONTINUED)	64211 64219 64221 64229 64231 64239 65011 65019 65021 65029 65031 65039 65911 65919 65921 65929 65931 65939		6505922 6222129 6282129 6342129 6422129 6502129 6222828 6283429 6283428 6344229 -28 6425029 -28 6505929 -28 6222832 6283431 6283432 6344231 -32 6425031 -32 6505931 -32 6222838 6283439 -38 6344239 6344238 6425039 -38 6505939 -38		152829 -31 -39 153411 -19 -21 -29 -31 -39 154211 -19 -21 -29 -31 -39 155011 -19 -21 -29 -31 -39 155911 -19 -21 -29 -31 -39					6591129 6592139 6501129 6502139

MODIFIED NASTRAN ELEMENTS FOR WING SUBCOMPONENTS (CONTINUED)

COMPONENT	GRIDS	CBARS	CONRODS	CELAS2	CONM2	MPC	PBARS	MAT1	CSHEAR	CQDEM
LEFT WING	71913	7222813	7222811		161912	HARD			7221119	6502939
	-17	-17	-12		-13	POINT			7281119	6221124
	-22	-21	7283411		-14	ATTACH			7341119	6221326
	-24	-24	-12		-16	(6)			7421119	6221729
	-26	-26	7344211		-17	FWD LT			7501119	6222431
	-28	-29	-12		-18	SPAR			7222129	6222439
	-34	-31	7425011		-22	LUG PIN			7282129	6222639
	-36	7131922	-12		-23	(20)			7342129	6281129
	72211	7171922	7505911		-24	CENTER			7422129	6282139
	-13	7221922	-12		-26	LT SPAR			7502129	6341129
	-17	7241922	7222819		-27	LUG PIN			7223139	6342139
	-19	7261922	-18		-28	(20)			7283139	6421129
	-21	7281922	7283419		-34	AFT LT			7343139	6422139
	-24	7341922	-18		-35	SPAR			7423139	7221121
	-26	7361922	7344219		-36	LUG PIN			7503139	7281121
	-29		-18		162211	(10)				7341121
	-31		7425019		-13					7421121
	-39		-18		-17					7501121
	72811		7505919		-19					7222131
	-19		-18		-21					7282131
	-21		7222822		-24					7342131
	-29		7783421		-26					7422131
	-31		-22		-29					7502131
	-39		7344221		-31					7221929
	73411		-22		-39					7281929
	-19		7425021		162811					7341929
	-21		-22		-19					7421929
			7505921		-21					7501929

MODIFIED NASTRAN ELEMENTS FOR WING SUBCOMPONENTS (CONTINUED)

COMPONENT	GRIDS	CBARS	CONRODS	CELAS2	CONM2	MPC	PBARS	MAT1	CSHEAR	CQDEM
LEFT WING (CONTINUED)	73429		7505922		162829					7222939
	-31		7222828		-31					7282939
	-39		7283429		-39					7342939
	74211		-28		163411					7422939
	-19		7344229		-19					7502939
	-21		-28		-21					7221124
	-29		7425029		-29					7221326
	-31		-28		-31					7221729
	-39		7505929		-39					7222431
	75011		-28		164211					7222439
	-19		7222832		-19					7222639
	-21		7283431		-21					7281129
	-29		-32		-29					7282139
	-31		7344231		-31					7421129
	-39		-32		-39					7422139
	75911		7425031		165011					7501129
	-19		-32		-19					7502139
	-21		7505931		-21					7591129
	-29		-32		-29					7592139
	-31		7222838		-31					
	-39		7283439		-39					
			-38		165911					
			7344239		-19					
			-38		-21					
			7425039		-29					
			-38		-31					
			7505939		-39					
			7505938							

MODIFIED NASTRAN ELEMENTS FOR WING SUBCOMPONENTS (CONCLUDED)

COMPONENT	GRIDS	CBARS	CONRODS	CELAS2	CONM2	MPC	PBARS	MAT1	CSHEAR	CQDEM
WING PYLONS RIGHT OUTBOARD					965929					
WING PYLONS LEFT OUTBOARD					975929					
WING PYLONS LEFT OUTBOARD					964229					
WING PYLONS LEFT OUTBOARD					974229					

APPENDIX B

PYLON COMPONENT TEST AMPLITUDE AND PHASE RESPONSE

APPENDIX B

Table of Contents

F/A EXCITATION AT THE M/R HUB
THRUST = 1000 LB . DAMPERS INSTALLED
SHAKE TEST FORCE = 200 LB

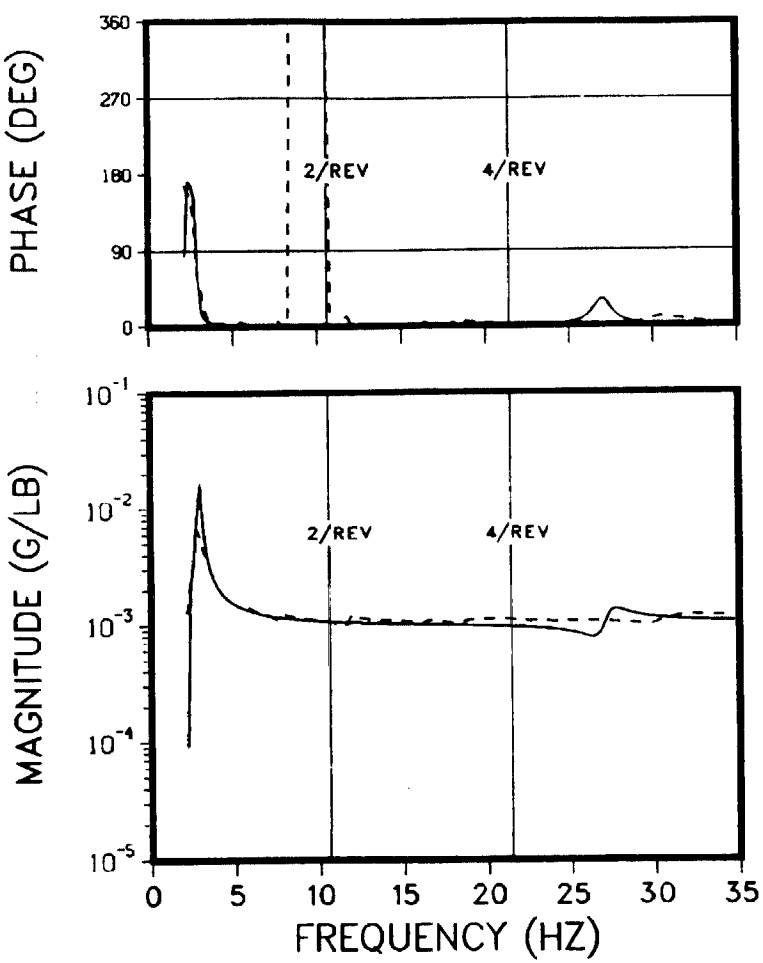

M/R HUB F/A RESPONSE

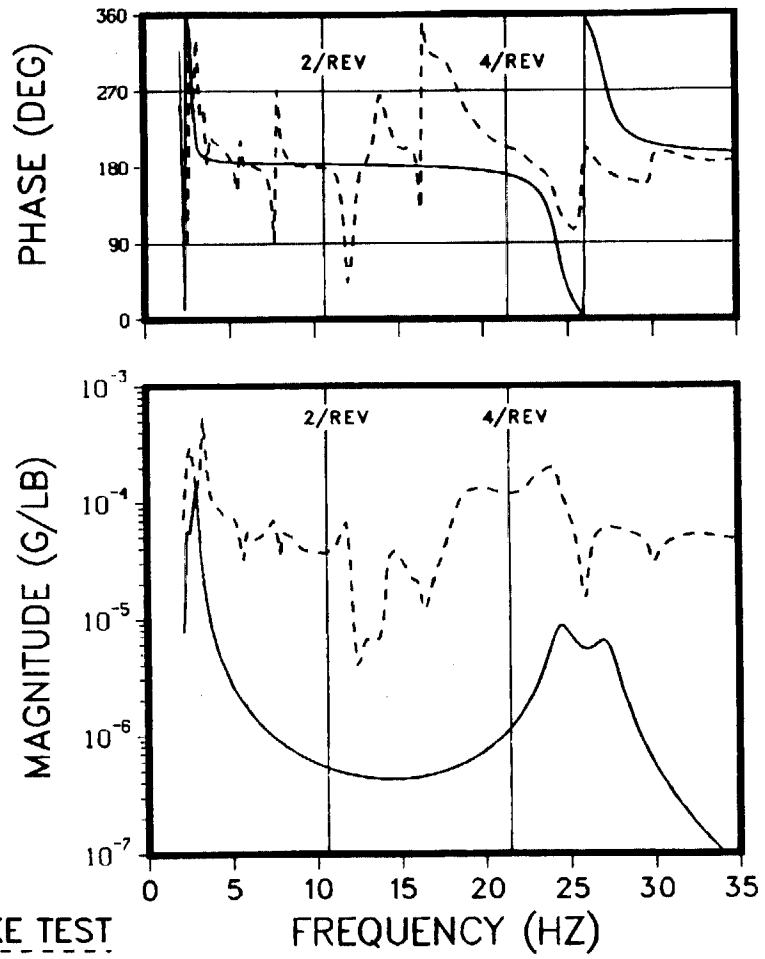

SHAKE TEST

NASTRAN

M/R HUB LATERAL RESPONSE

F/A EXCITATION AT THE M/R HUB
THRUST = 1000 LB . DAMPERS INSTALLED
SHAKE TEST FORCE = 200 LB

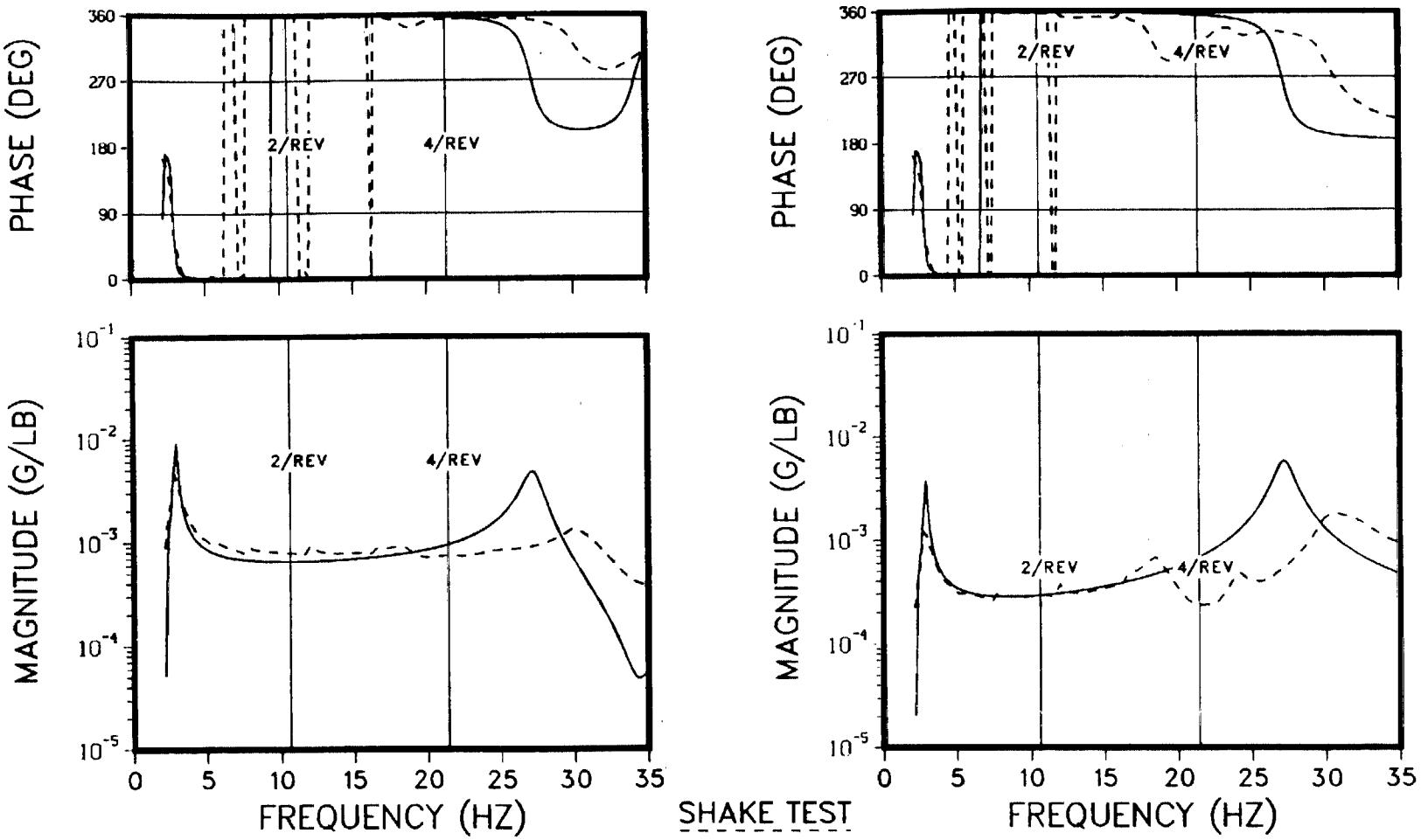

MID MAST (STA 22) F/A RESPONSE

TRANSMISSION UPPER BEARING F/A RESPONSE

F/A EXCITATION AT THE M/R HUB
THRUST = 1000 LB . DAMPERS INSTALLED
SHAKE TEST FORCE = 200 LB

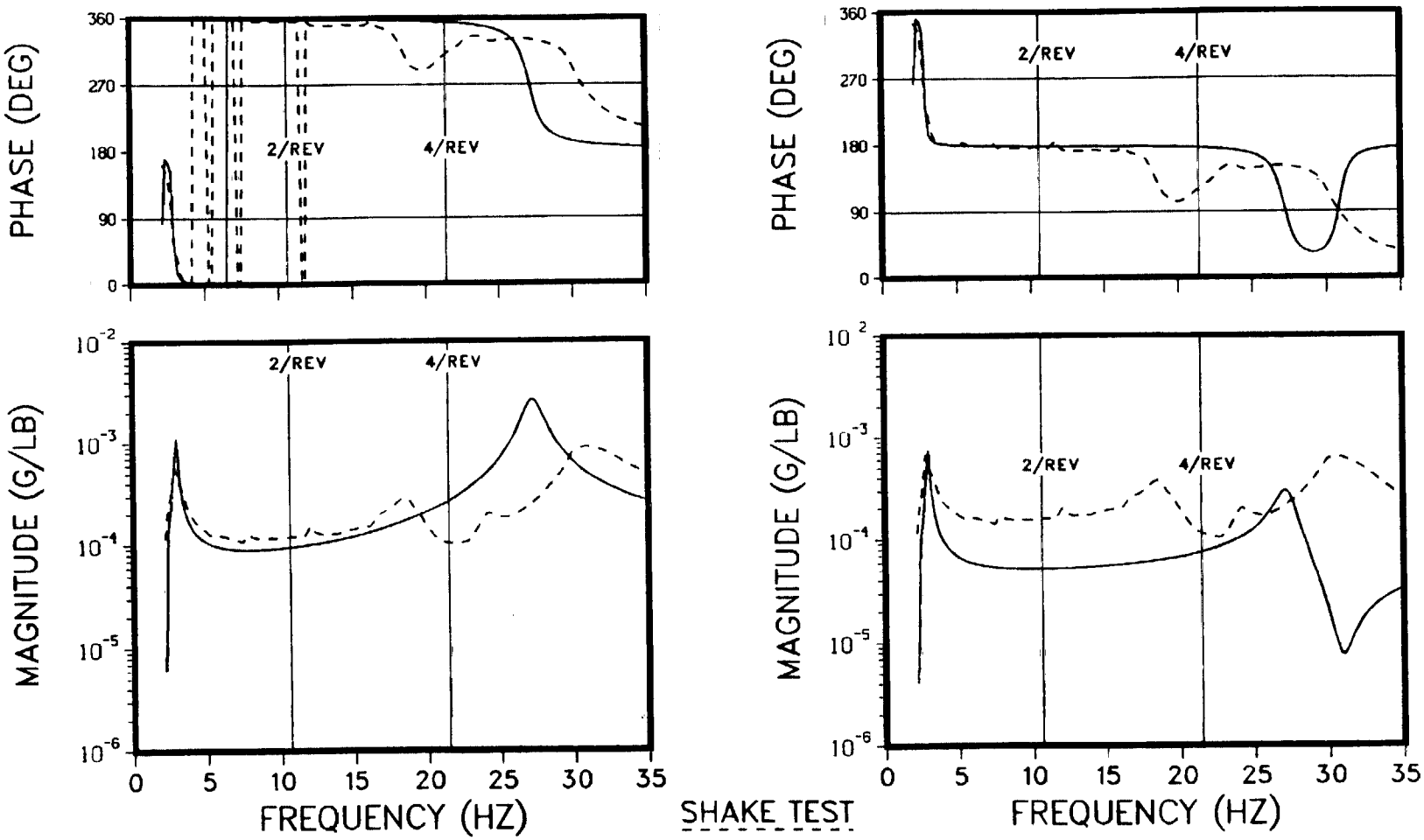

MID TRANSMISSION F/A RESPONSE

TRANSMISSION SUMP F/A RESPONSE

F/A EXCITATION AT THE M/R HUB
THRUST = 1000 LB . DAMPERS INSTALLED
SHAKE TEST FORCE = 200 LB

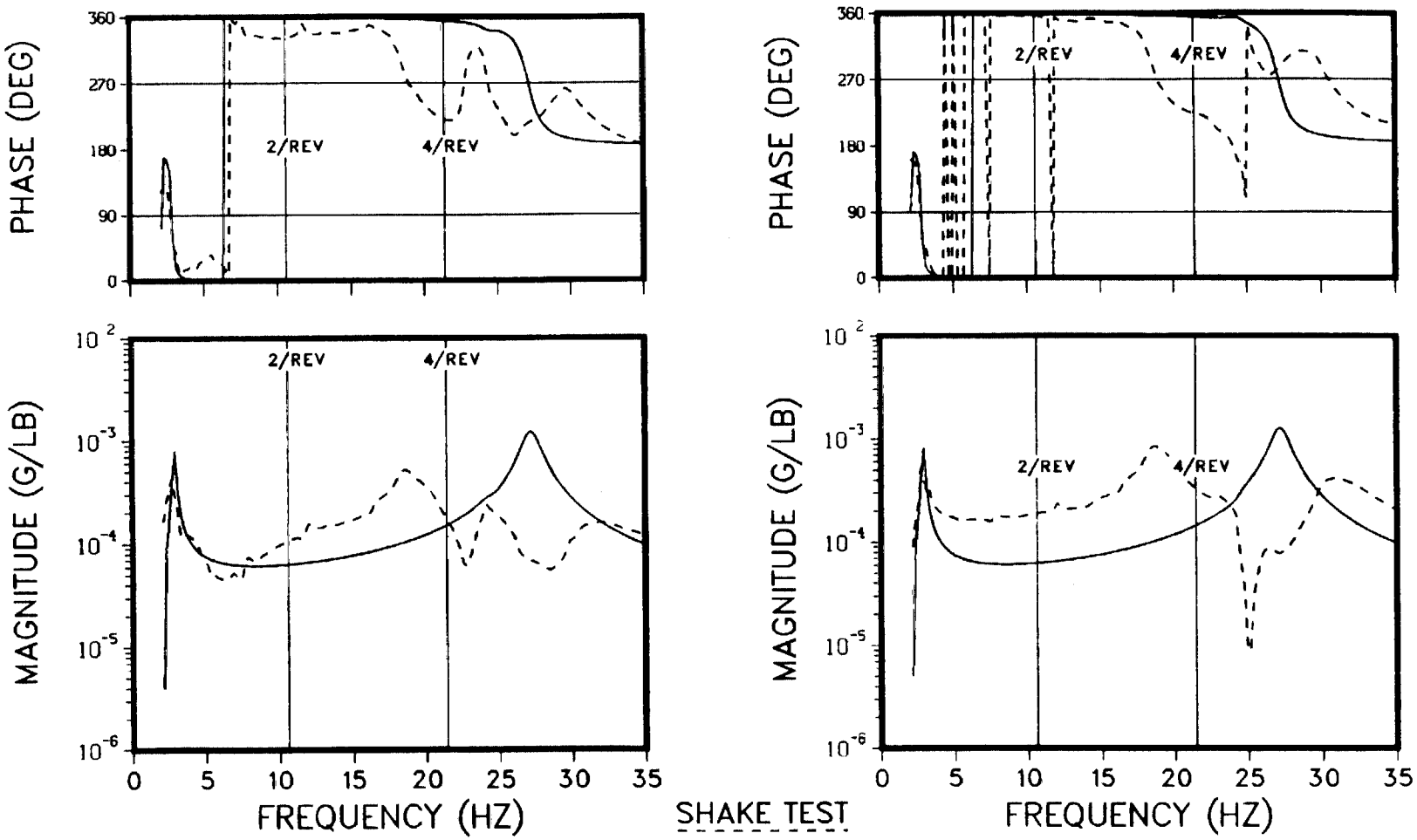

LEFT FORWARD MOUNT VERTICAL RESPONSE **RIGHT FORWARD MOUNT VERTICAL RESPONSE**

F/A EXCITATION AT THE M/R HUB
THRUST = 1000 LB . DAMPERS INSTALLED
SHAKE TEST FORCE = 200 LB

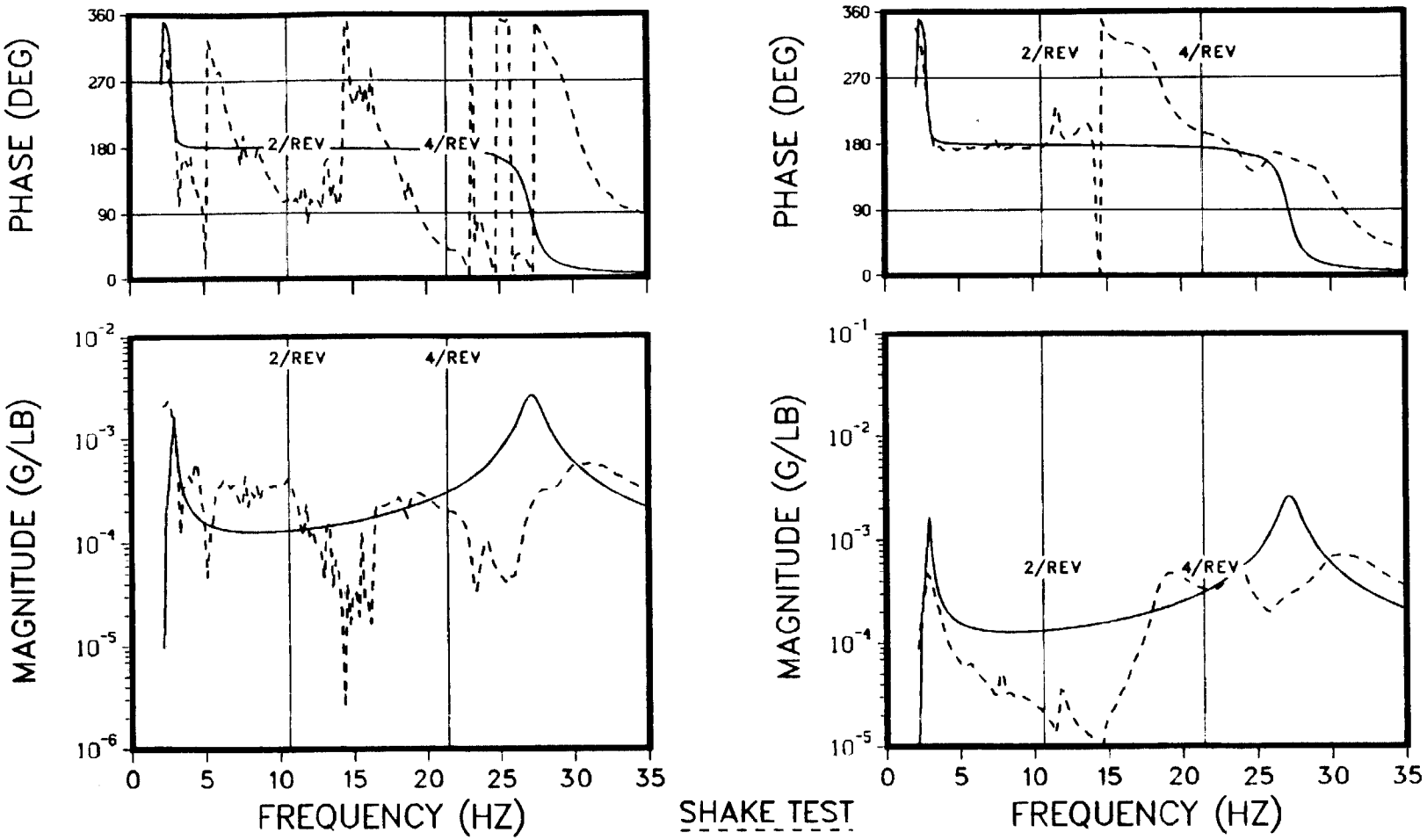

LEFT AFT MOUNT VERTICAL RESPONSE

RIGHT AFT MOUNT VERTICAL RESPONSE

F/A EXCITATION AT THE M/R HUB
THRUST = 1000 LB . DAMPERS INSTALLED
SHAKE TEST FORCE = 200 LB

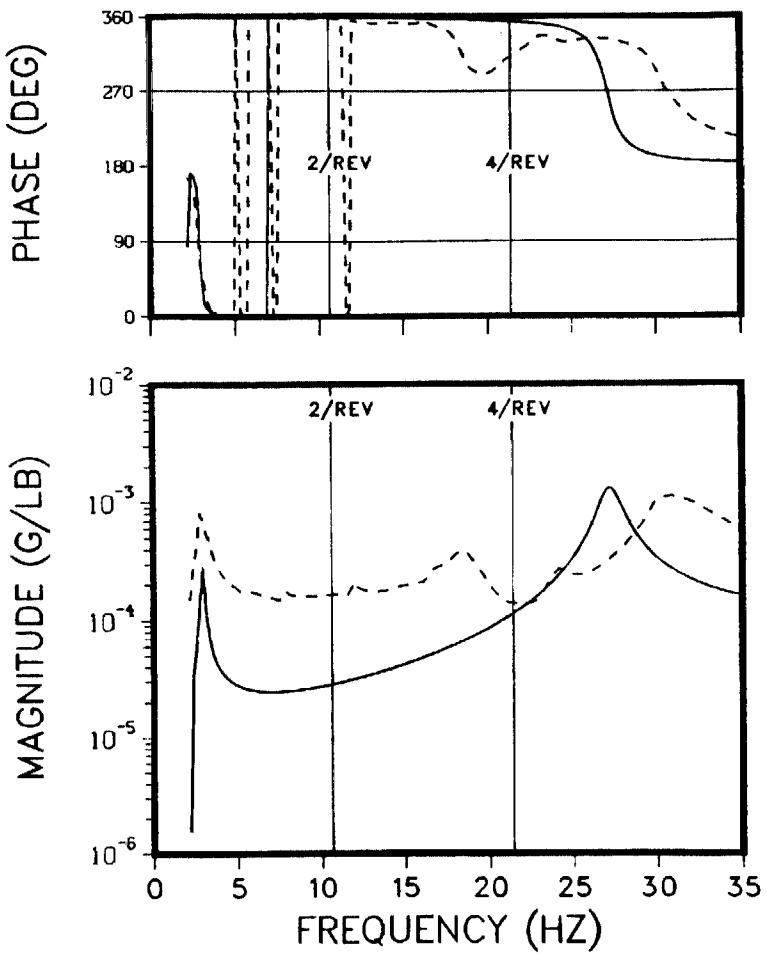

TRANSMISSION C.G. F/A RESPONSE

F/A EXCITATION AT THE M/R HUB
THRUST = 7000 LB . DAMPERS INSTALLED
SHAKE TEST FORCE = 200 LB

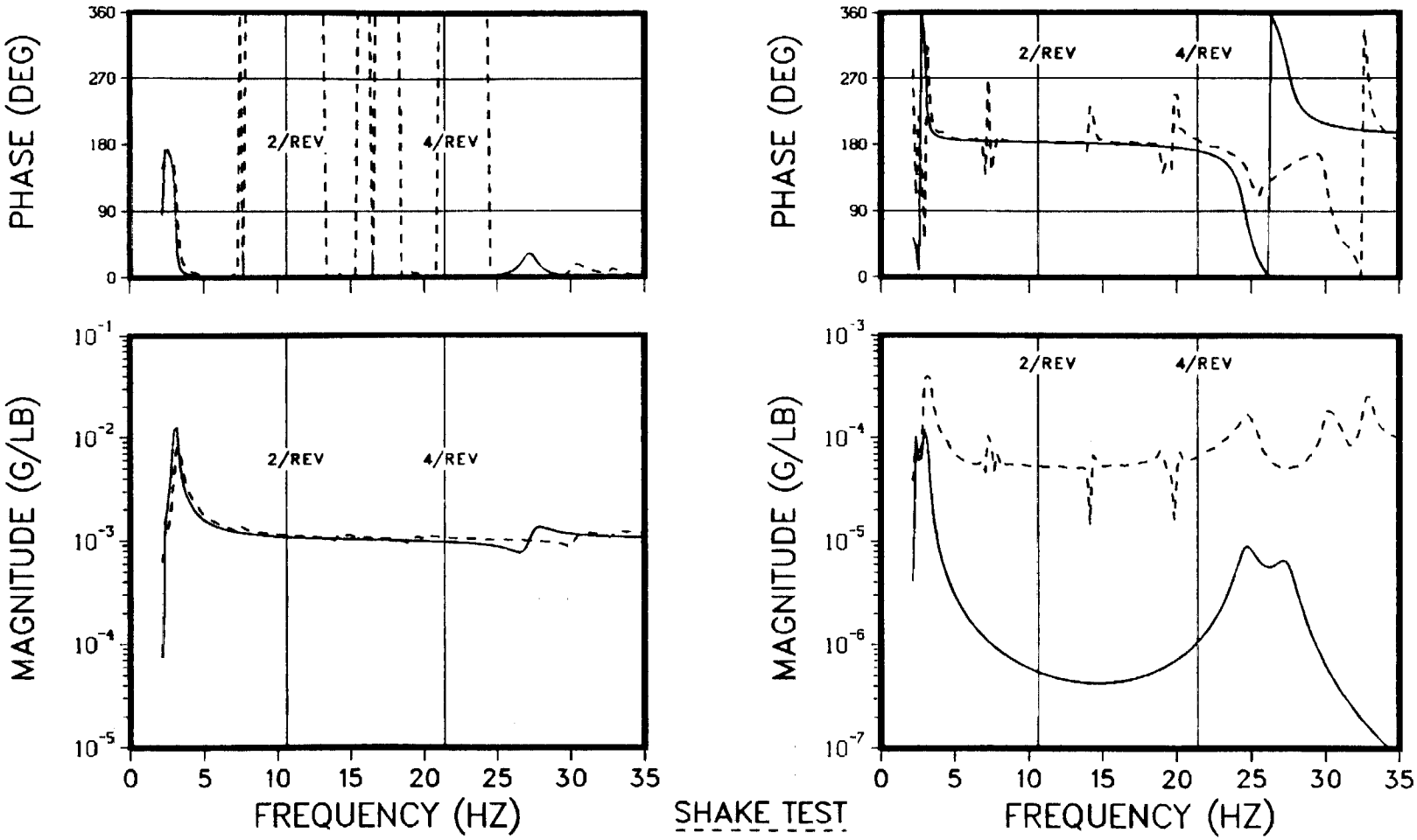

M/R HUB F/A RESPONSE

M/R HUB LATERAL RESPONSE

F/A EXCITATION AT THE M/R HUB
THRUST = 7000 LB . DAMPERS INSTALLED
SHAKE TEST FORCE = 200 LB

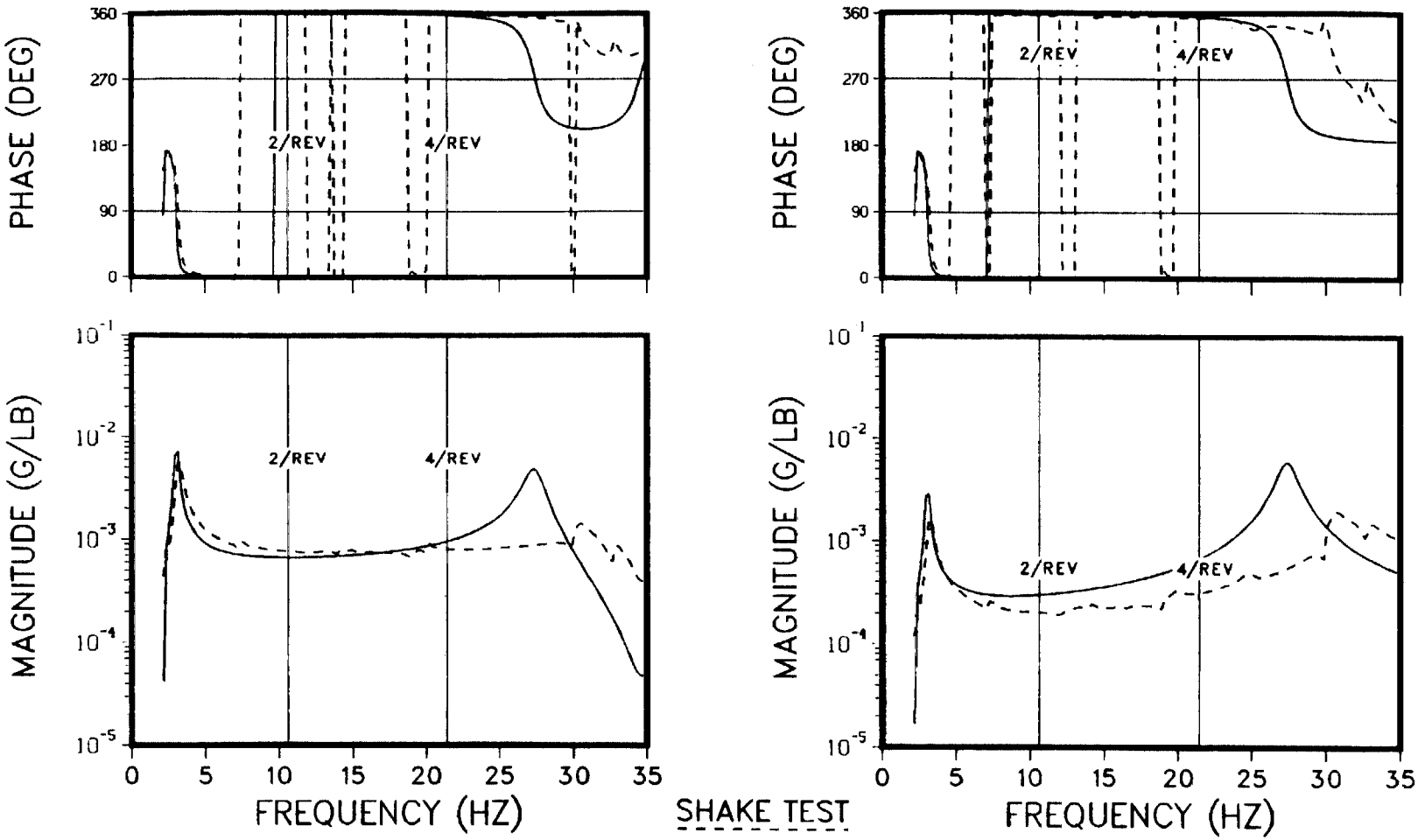

MID MAST (STA 22) F/A RESPONSE

TRANSMISSION UPPER BEARING F/A RESPONSE

F/A EXCITATION AT THE M/R HUB
THRUST = 7000 LB . DAMPERS INSTALLED
SHAKE TEST FORCE = 200 LB

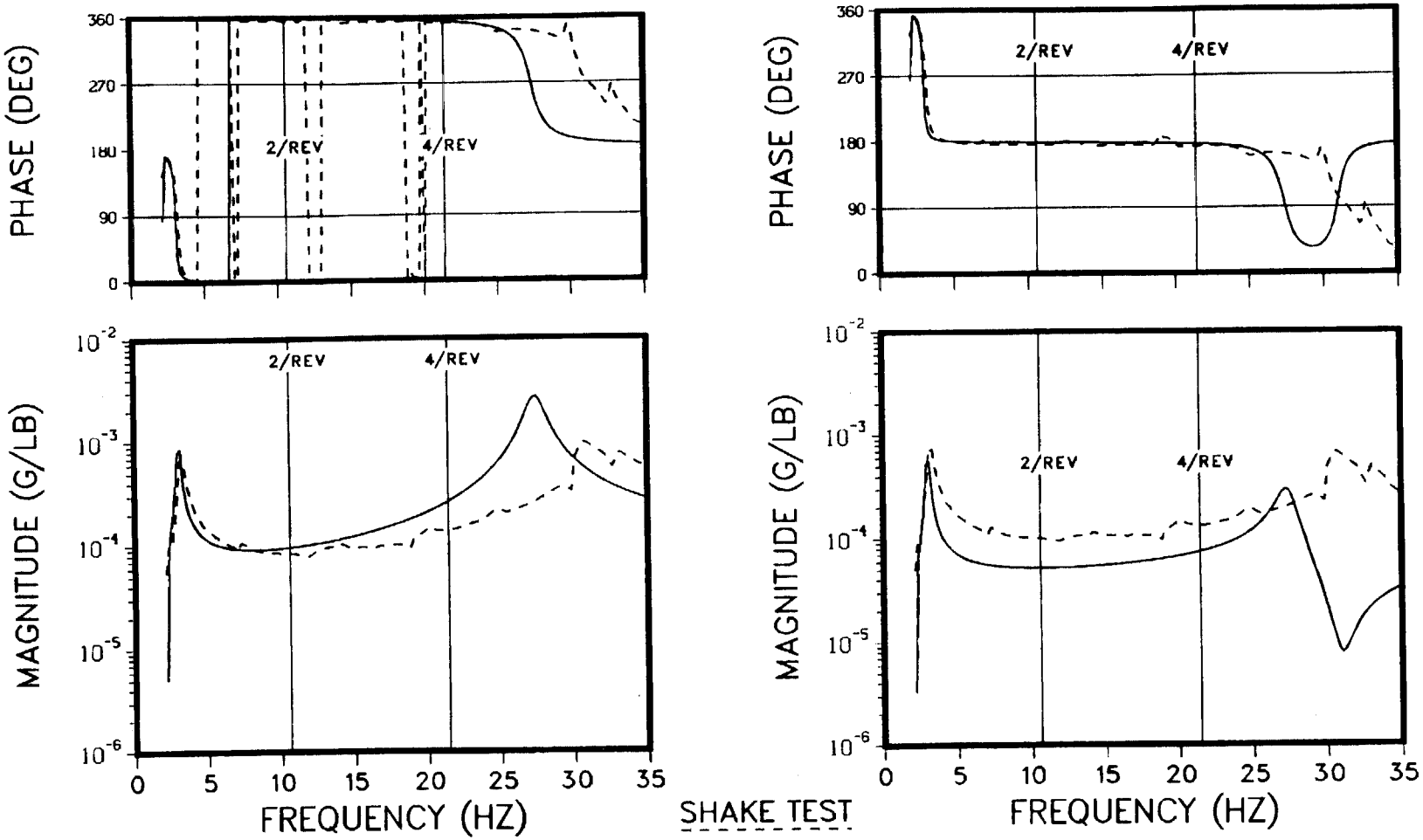

MID TRANSMISSION F/A RESPONSE

TRANSMISSION SUMP F/A RESPONSE

F/A EXCITATION AT THE M/R HUB
THRUST = 7000 LB . DAMPERS INSTALLED
SHAKE TEST FORCE = 200 LB

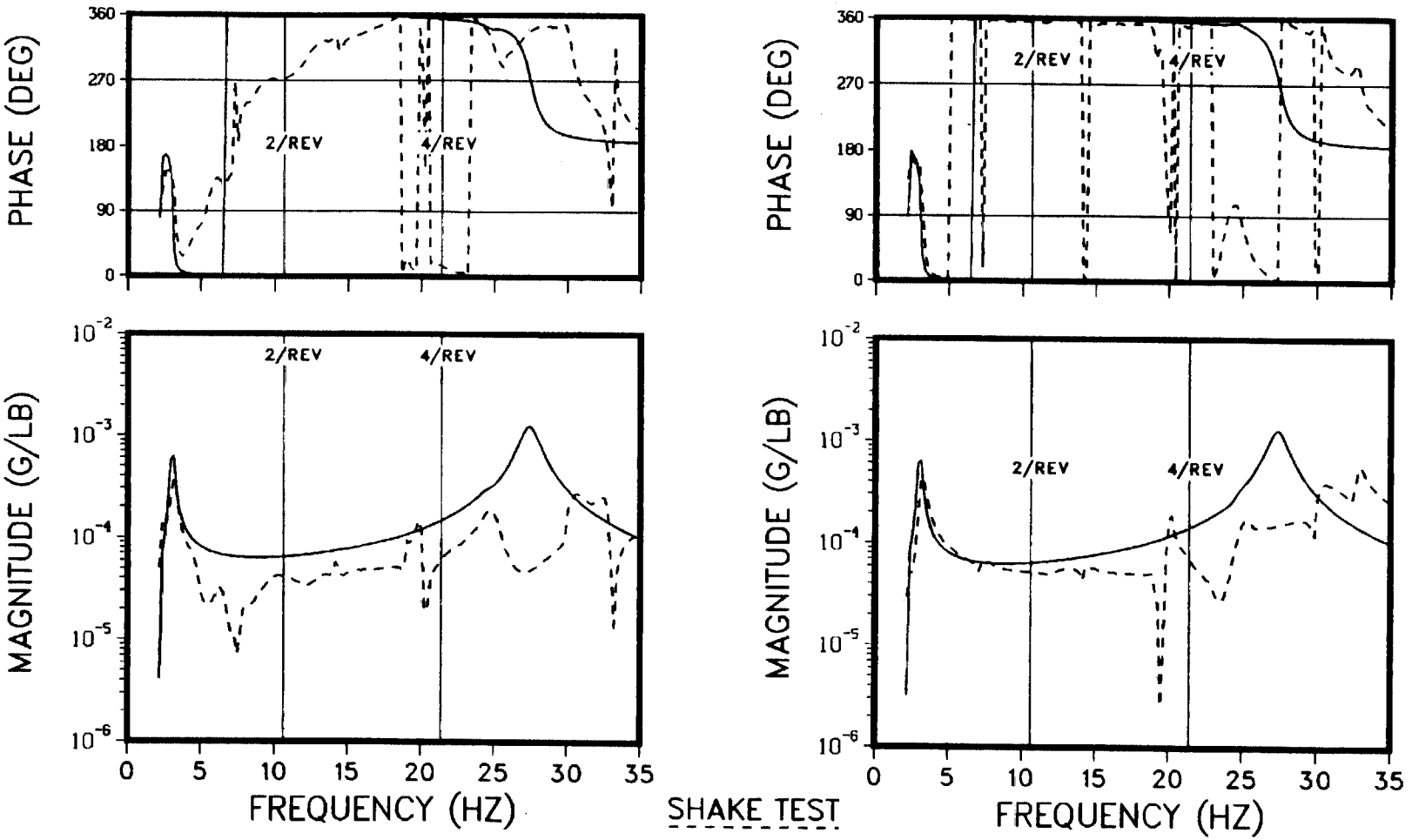

LEFT FORWARD MOUNT VERTICAL RESPONSE

RIGHT FORWARD MOUNT VERTICAL RESPONSE

F/A EXCITATION AT THE M/R HUB
THRUST = 7000 LB . DAMPERS INSTALLED
SHAKE TEST FORCE = 200 LB

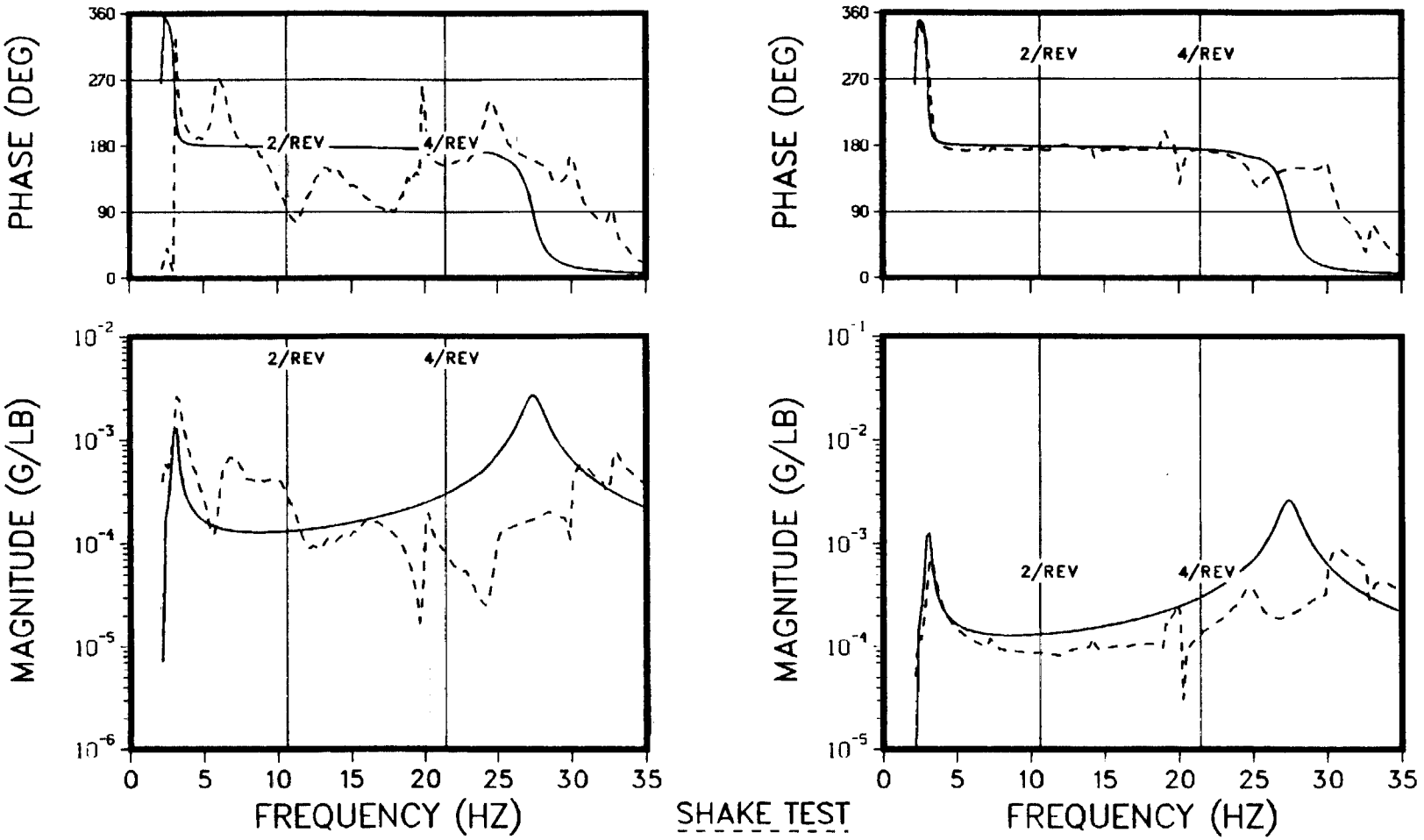

LEFT AFT MOUNT VERTICAL RESPONSE

RIGHT AFT MOUNT VERTICAL RESPONSE

F/A EXCITATION AT THE M/R HUB
THRUST = 7000 LB . DAMPERS INSTALLED
SHAKE TEST FORCE = 200 LB

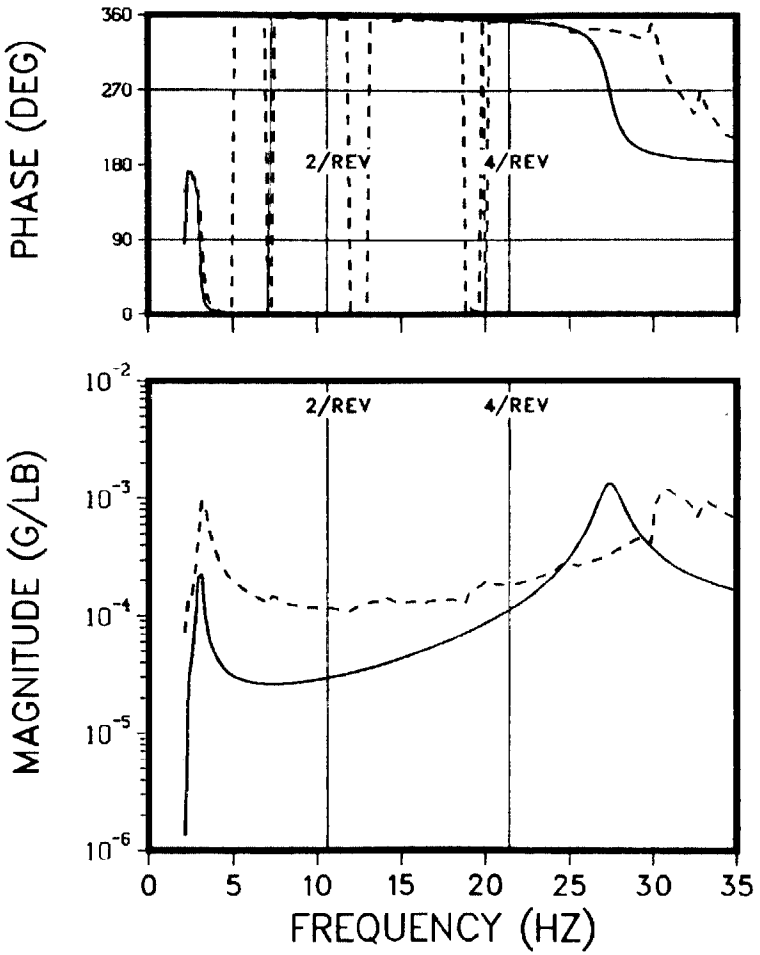

TRANSMISSION C.G. F/A RESPONSE

F/A EXCITATION AT THE M/R HUB
THRUST = 7000 LB . DAMPERS INSTALLED
SHAKE TEST FORCE = 100 LB FROM 2 TO 6 HZ

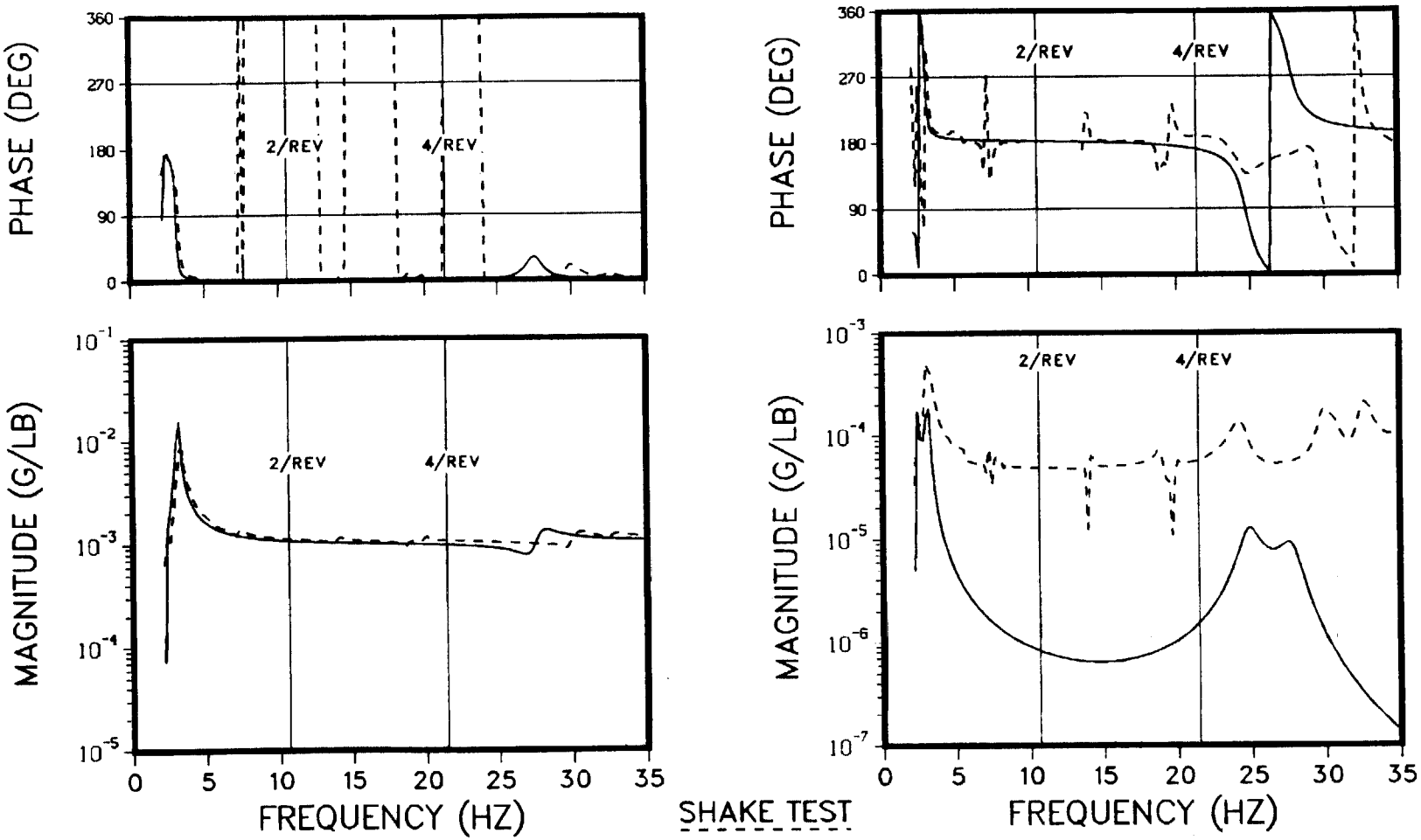

M/R HUB F/A RESPONSE

M/R HUB LATERAL RESPONSE

F/A EXCITATION AT THE M/R HUB
THRUST = 7000 LB . DAMPERS INSTALLED
SHAKE TEST FORCE = 100 LB FROM 2 TO 6 HZ

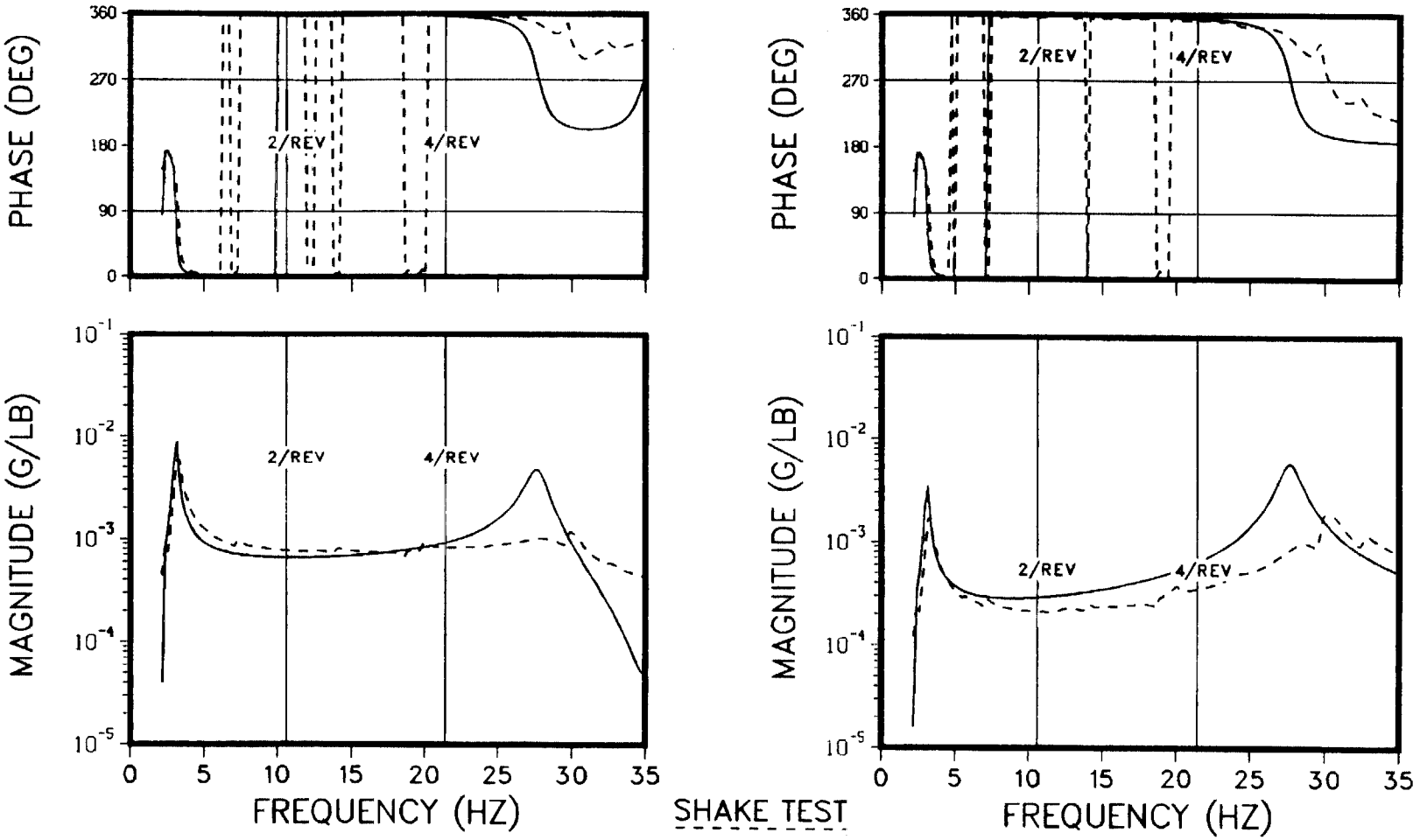

MID MAST (STA 22) F/A RESPONSE

TRANSMISSION UPPER BEARING F/A RESPONSE

F/A EXCITATION AT THE M/R HUB
THRUST = 7000 LB . DAMPERS INSTALLED
SHAKE TEST FORCE = 100 LB FROM 2 TO 6 HZ

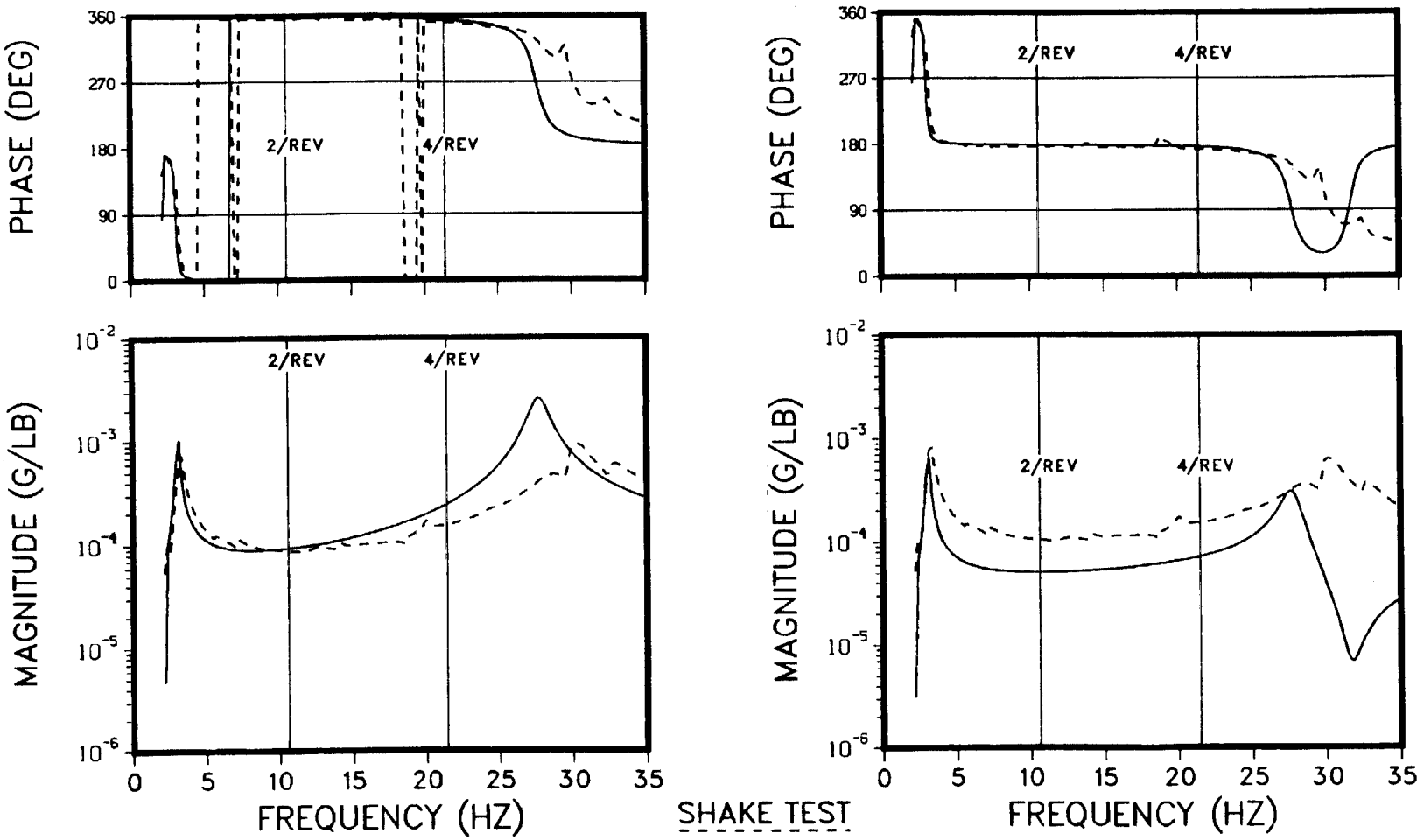

MID TRANSMISSION F/A RESPONSE

TRANSMISSION SUMP F/A RESPONSE

F/A EXCITATION AT THE M/R HUB
THRUST = 1000 LB . DAMPERS INSTALLED
SHAKE TEST FORCE = 100 LB FROM 2 TO 6 HZ

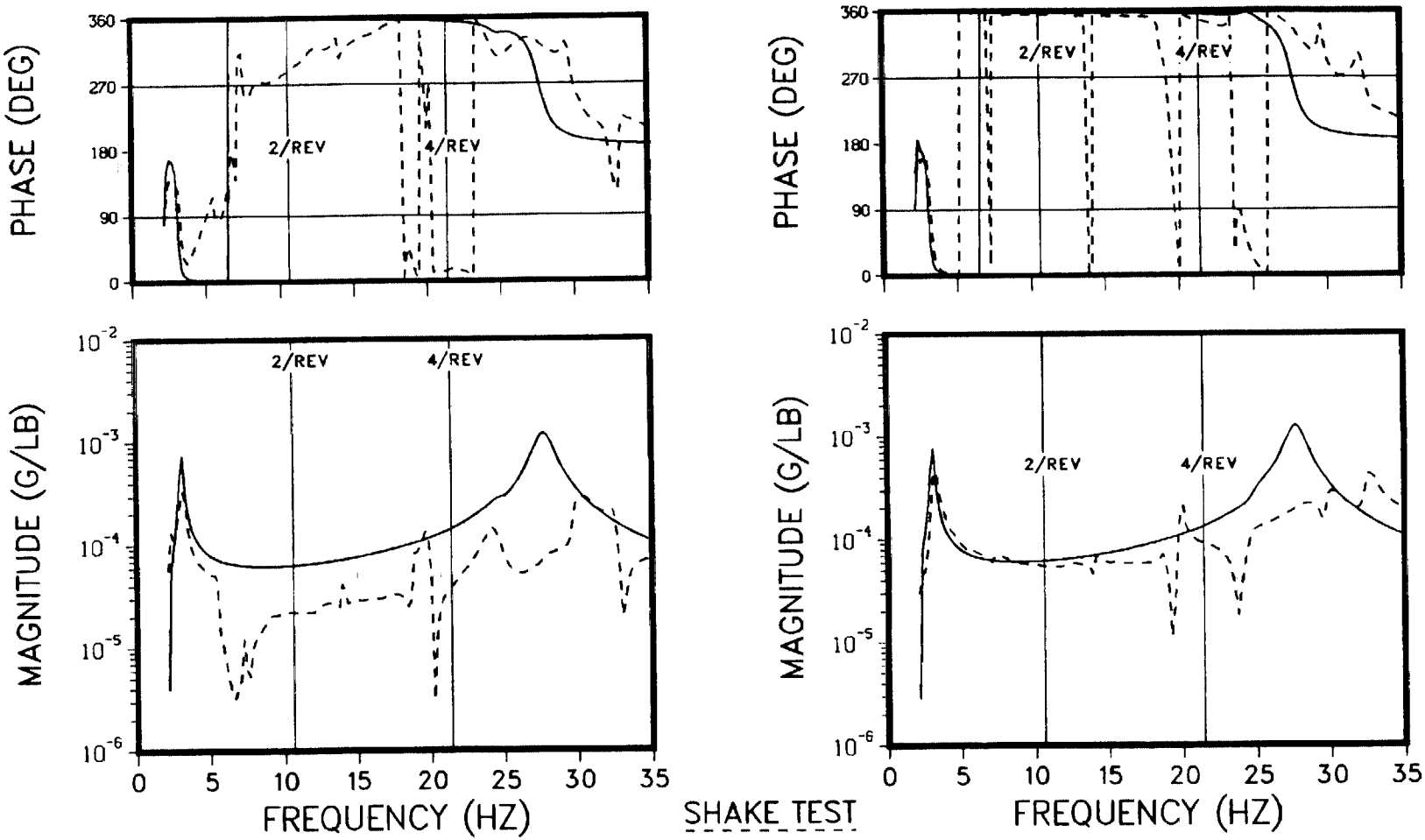

LEFT FORWARD MOUNT VERTICAL RESPONSE **RIGHT FORWARD MOUNT VERTICAL RESPONSE**

F/A EXCITATION AT THE M/R HUB
THRUST = 7000 LB . DAMPERS INSTALLED
SHAKE TEST FORCE = 100 LB FROM 2 TO 6 HZ

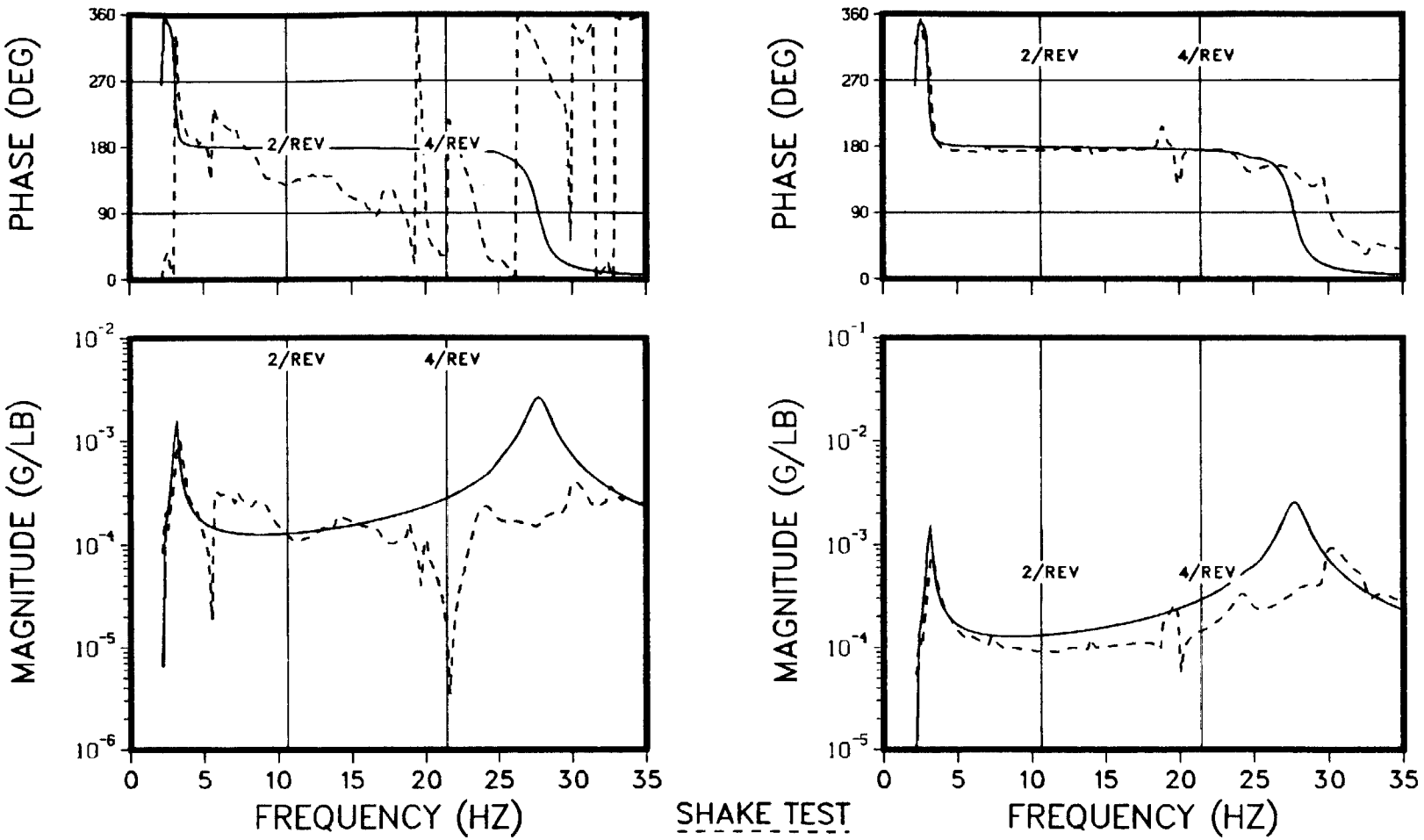

LEFT AFT MOUNT VERTICAL RESPONSE

RIGHT AFT MOUNT VERTICAL RESPONSE

F/A EXCITATION AT THE M/R HUB
THRUST = 7000 LB . DAMPERS INSTALLED
SHAKE TEST FORCE = 100 LB FROM 2 TO 6 HZ

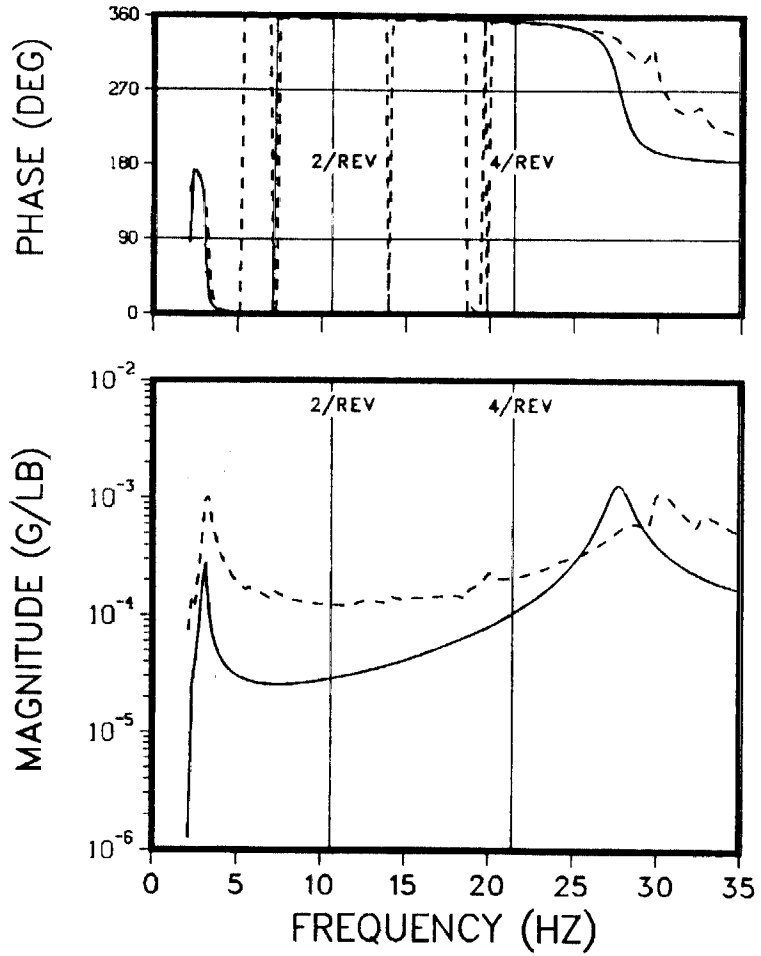

TRANSMISSION C.G. LATERAL RESPONSE

F/A EXCITATION AT THE M/R HUB
THRUST = 1000 LB . DAMPERS INSTALLED
SHAKE TEST FORCE = 100 LB FROM 2 TO 6 HZ

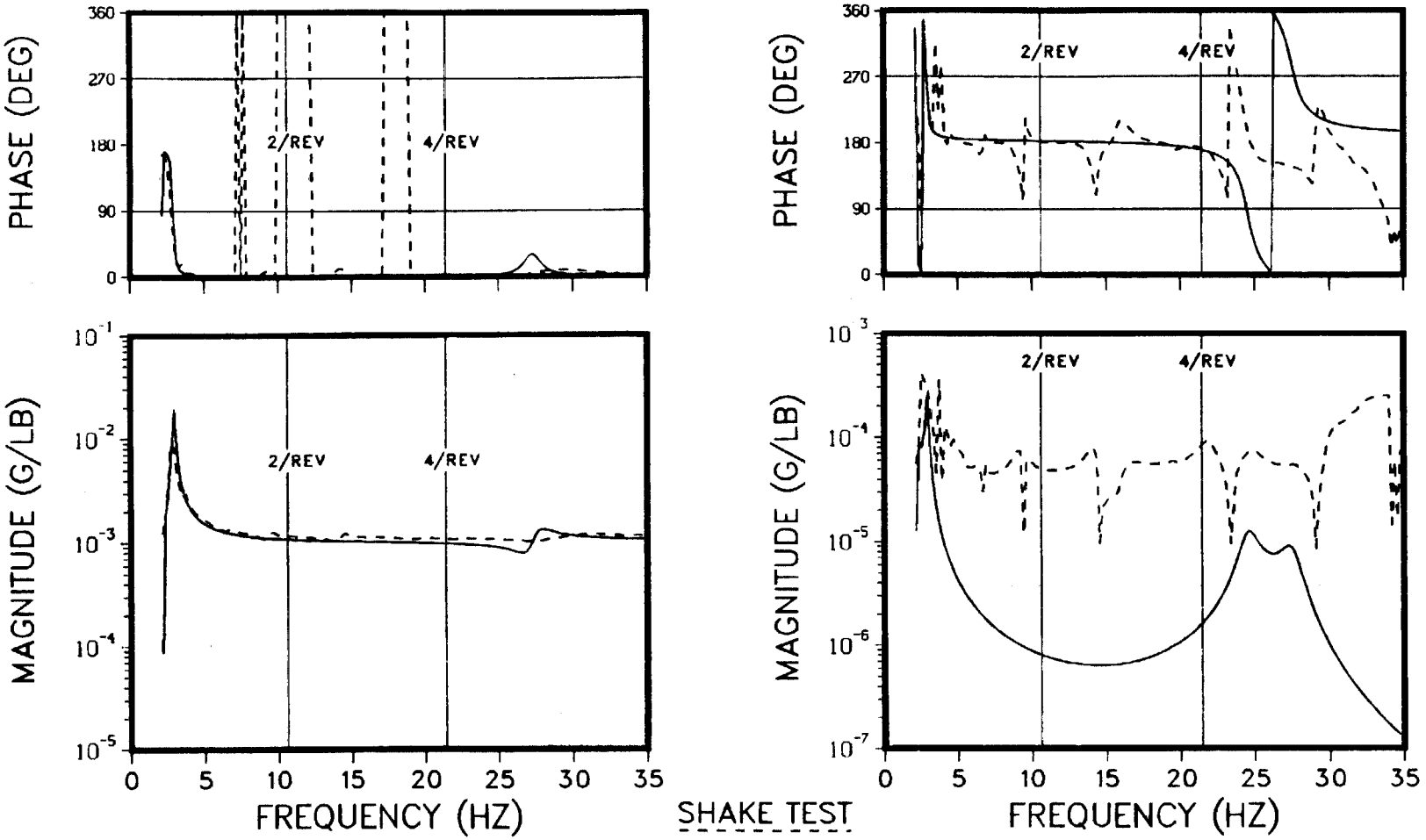

M/R HUB F/A RESPONSE

M/R HUB LATERAL RESPONSE

F/A EXCITATION AT THE M/R HUB
THRUST = 1000 LB . DAMPERS INSTALLED
SHAKE TEST FORCE = 100 LB FROM 2 TO 6 HZ

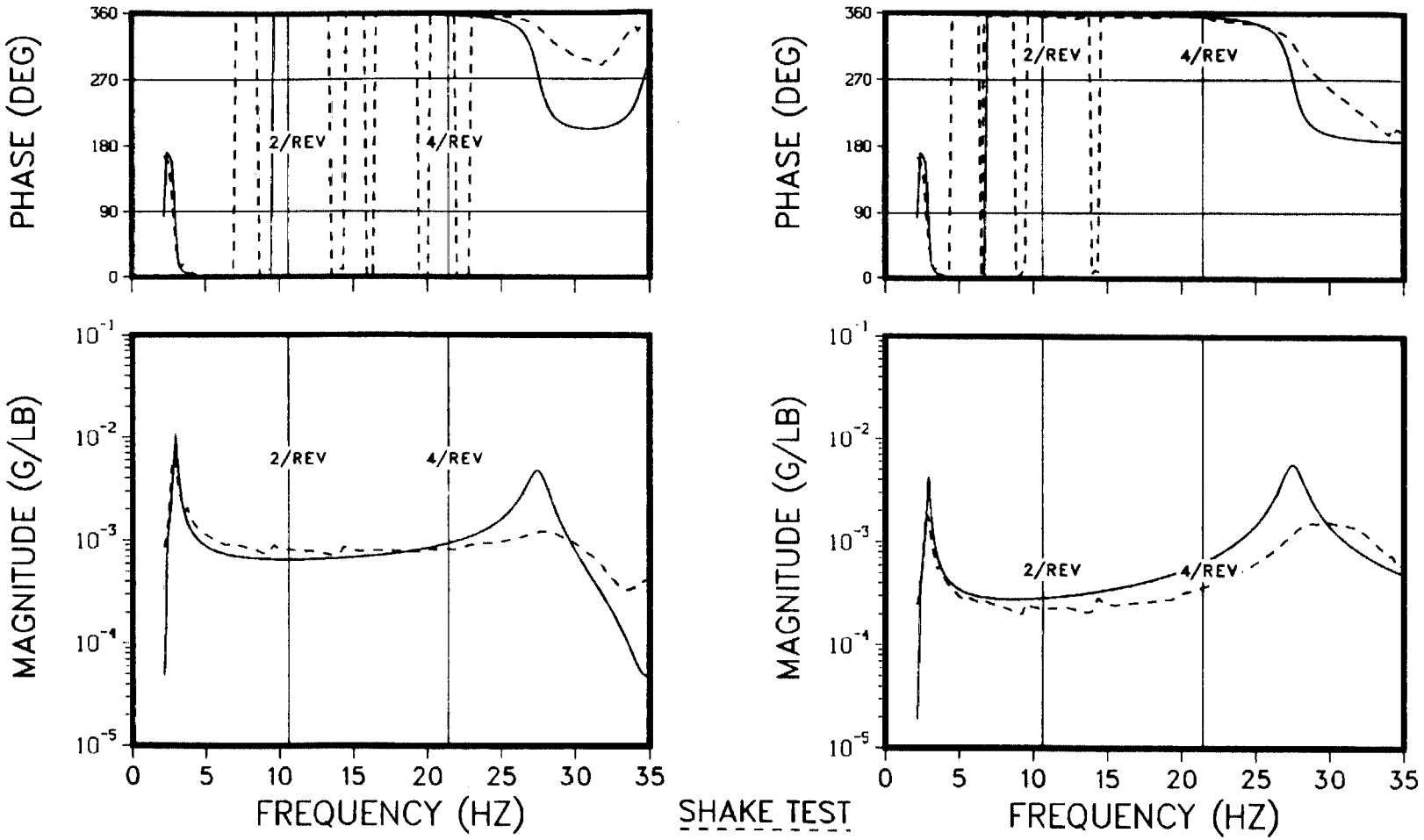

MID MAST (STA 22) F/A RESPONSE

TRANSMISSION UPPER BEARING F/A RESPONSE

F/A EXCITATION AT THE M/R HUB
THRUST = 1000 LB . DAMPERS INSTALLED
SHAKE TEST FORCE = 100 LB FROM 2 TO 6 HZ

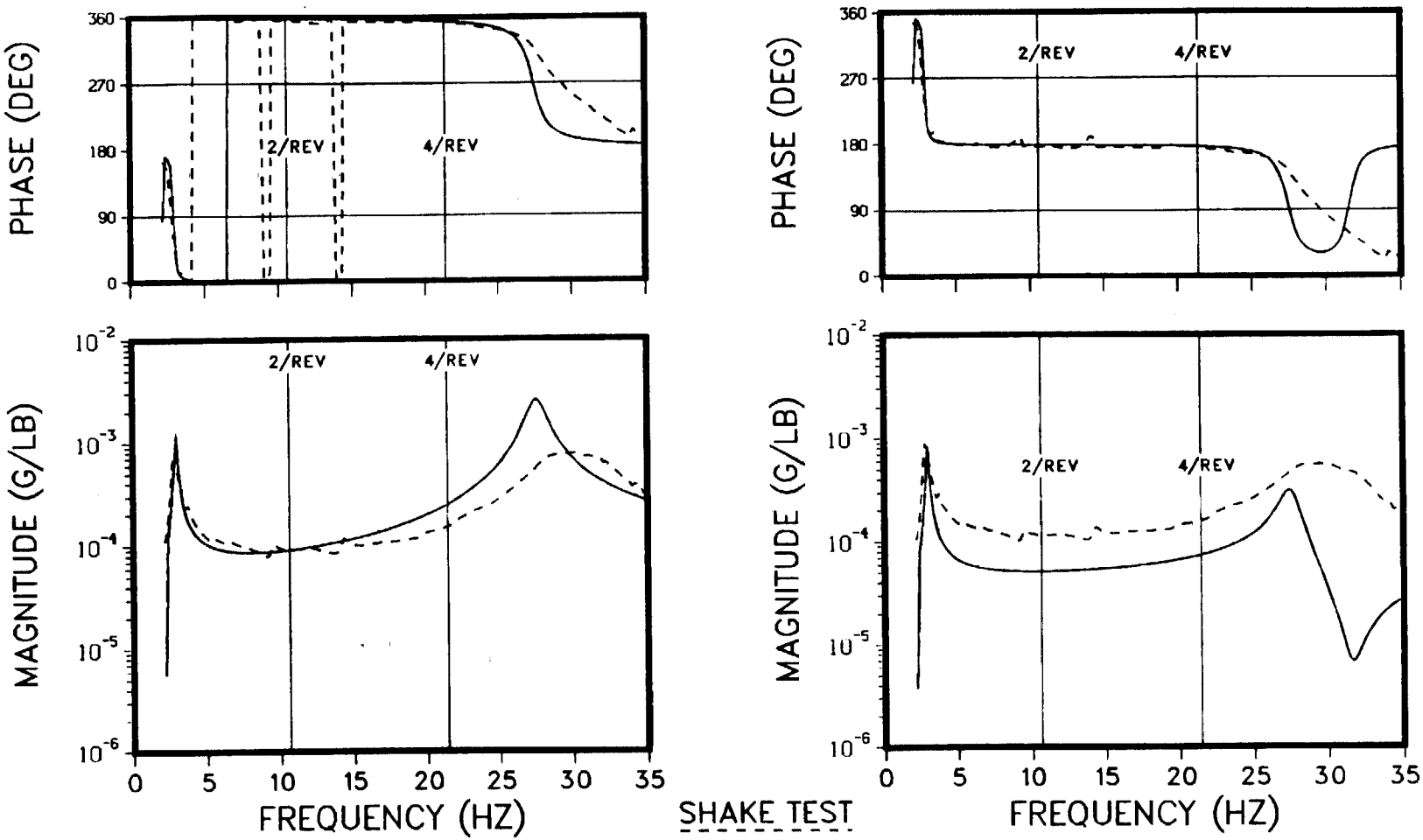

MID TRANSMISSION F/A RESPONSE

TRANSMISSION SUMP F/A RESPONSE

F/A EXCITATION AT THE M/R HUB
THRUST = 1000 LB . DAMPERS INSTALLED
SHAKE TEST FORCE = 100 LB FROM 2 TO 6 HZ

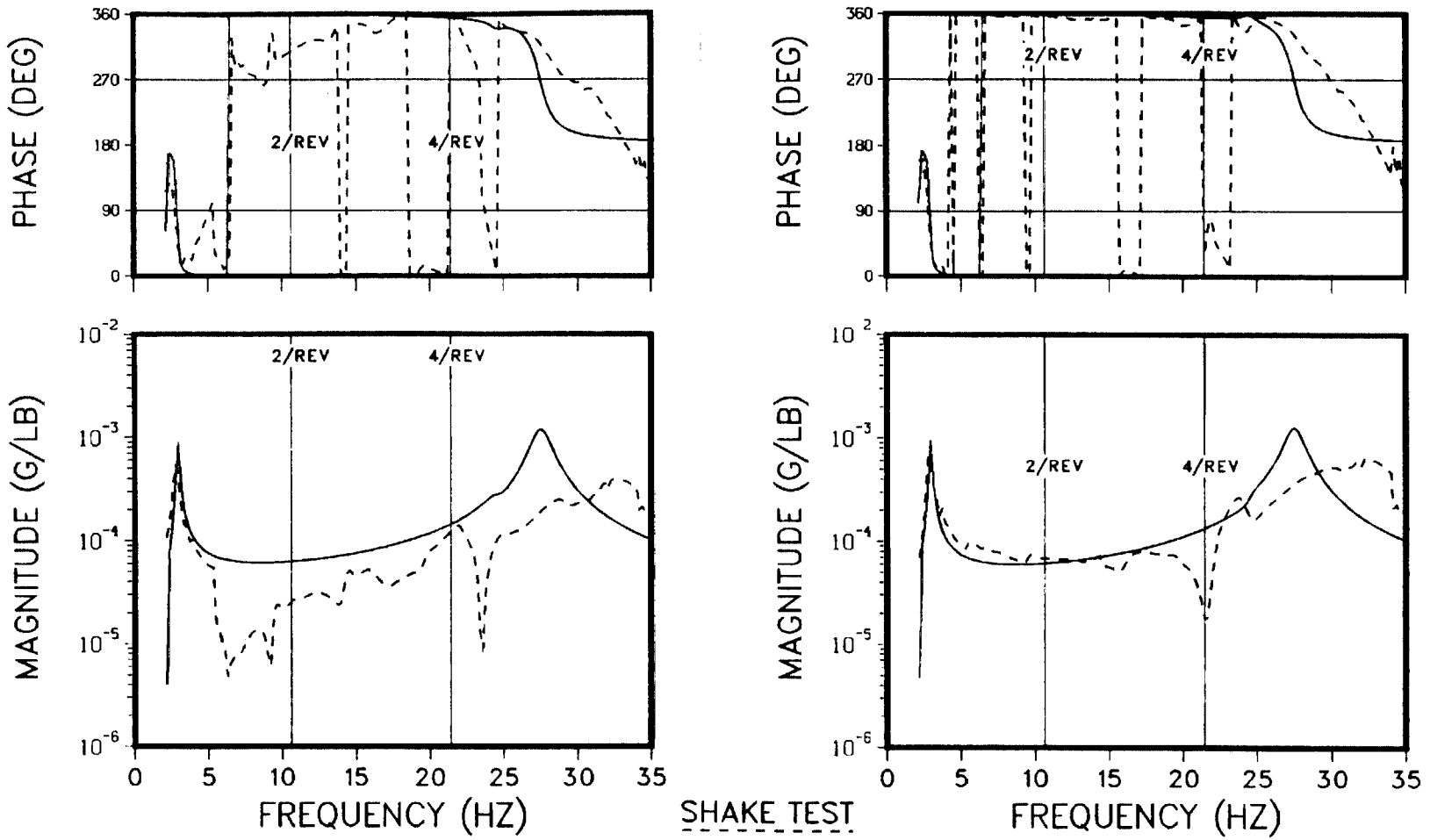

LEFT FORWARD MOUNT VERTICAL RESPONSE **RIGHT FORWARD MOUNT VERTICAL RESPONSE**

F/A EXCITATION AT THE M/R HUB
THRUST = 1000 LB . DAMPERS INSTALLED
SHAKE TEST FORCE = 100 LB FROM 2 TO 6 HZ

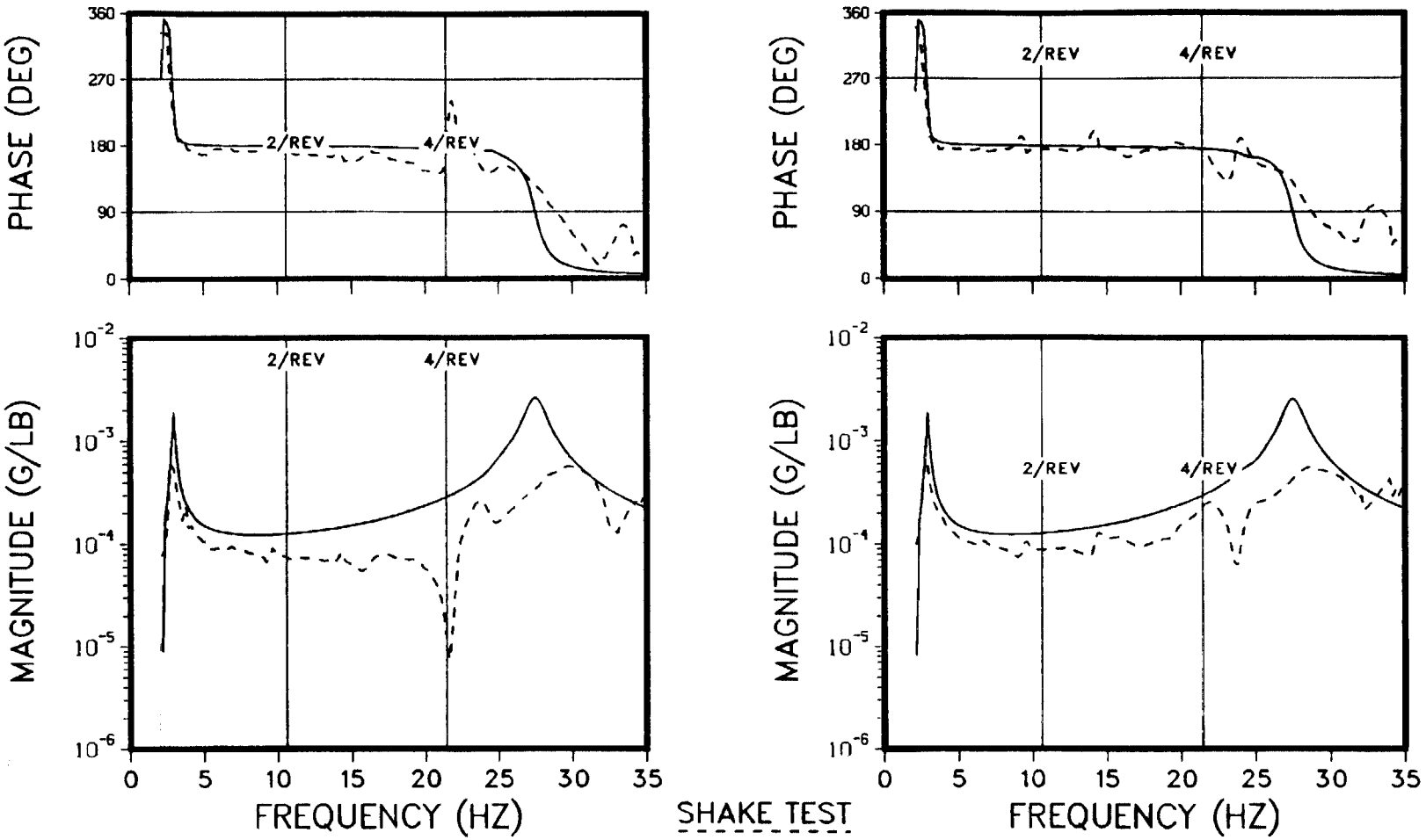

LEFT AFT MOUNT VERTICAL RESPONSE

RIGHT AFT MOUNT VERTICAL RESPONSE

F/A EXCITATION AT THE M/R HUB
THRUST = 1000 LB . DAMPERS INSTALLED
SHAKE TEST FORCE = 100 LB FROM 2 TO 6 HZ

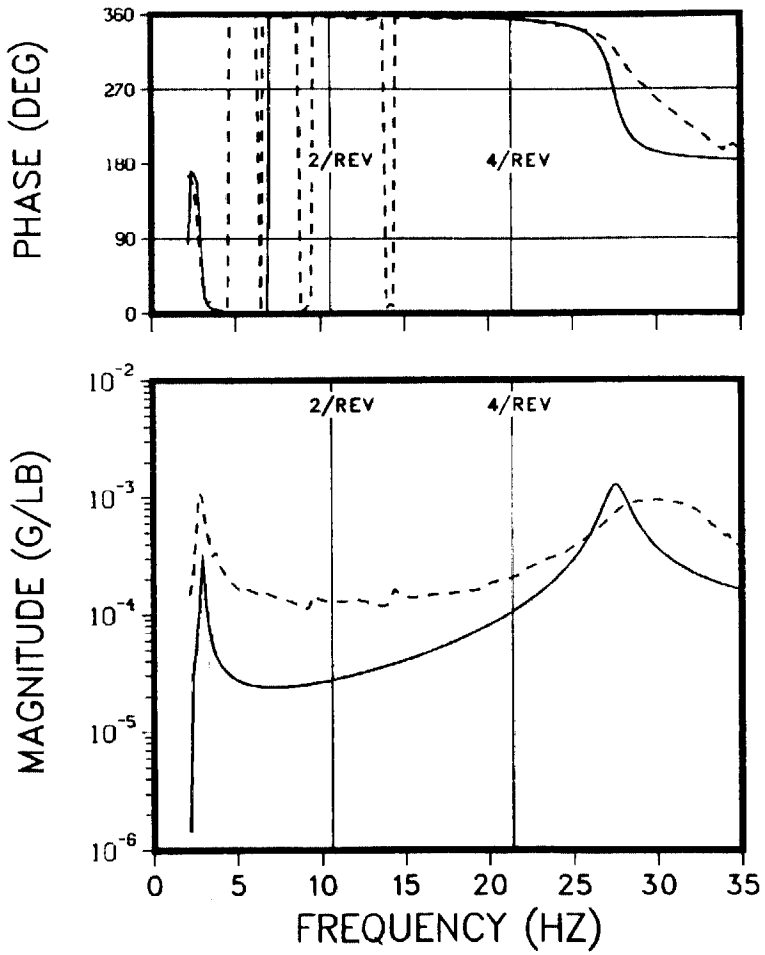

TRANSMISSION C.G. F/A RESPONSE

F/A EXCITATION AT THE M/R HUB
THRUST = 1000 LB .NO DAMPERS INSTALLED
SHAKE TEST FORCE = 200 LB

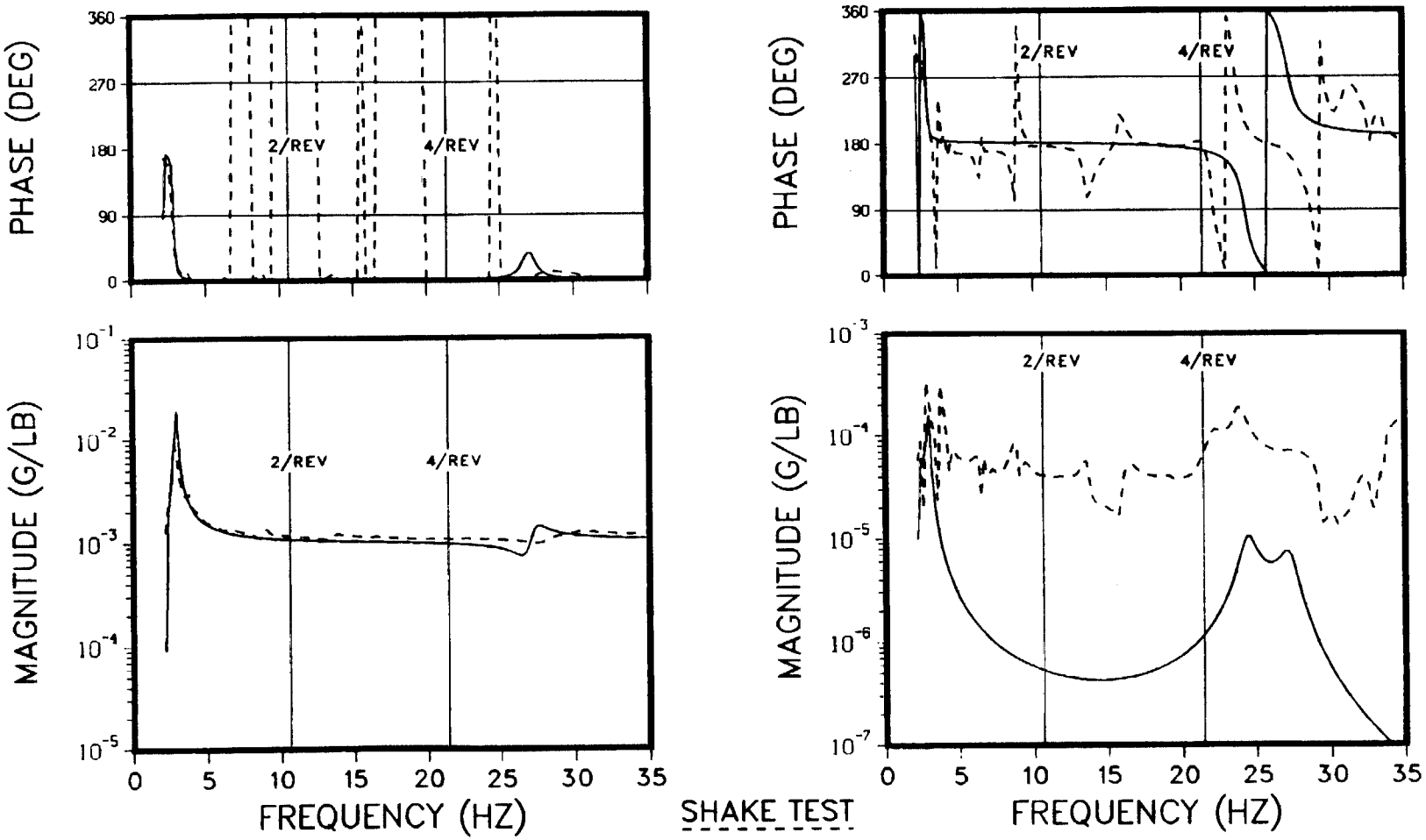

M/R HUB F/A RESPONSE

M/R HUB LATERAL RESPONSE

F/A EXCITATION AT THE M/R HUB
THRUST = 1000 LB .NO DAMPERS INSTALLED
SHAKE TEST FORCE = 200 LB

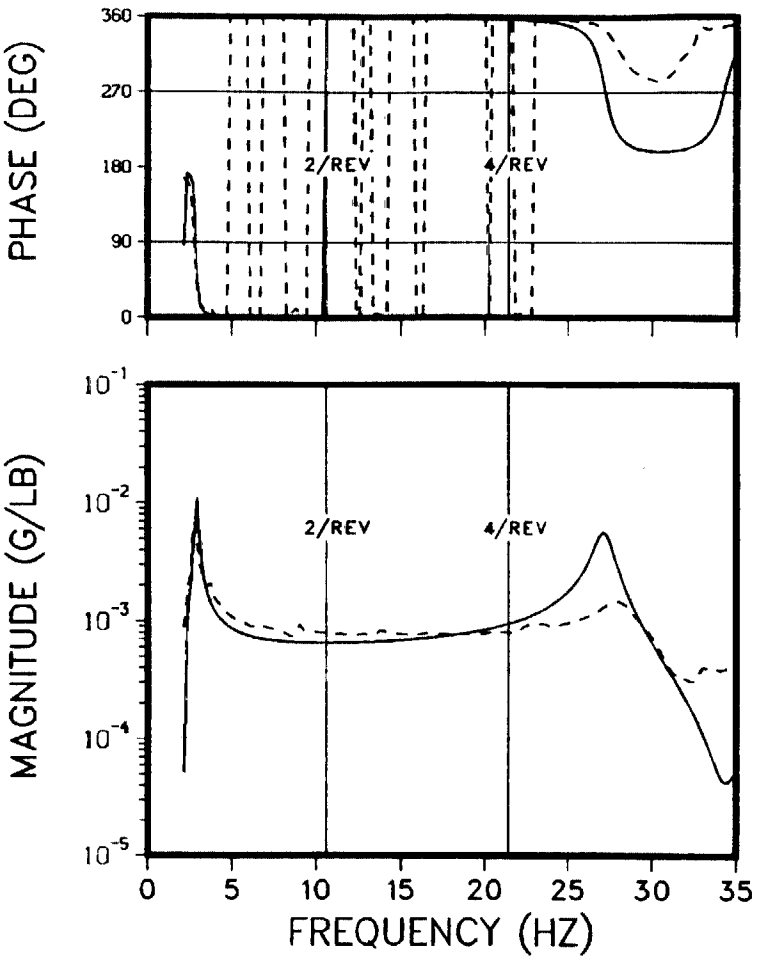

MID MAST (STA 22) F/A RESPONSE

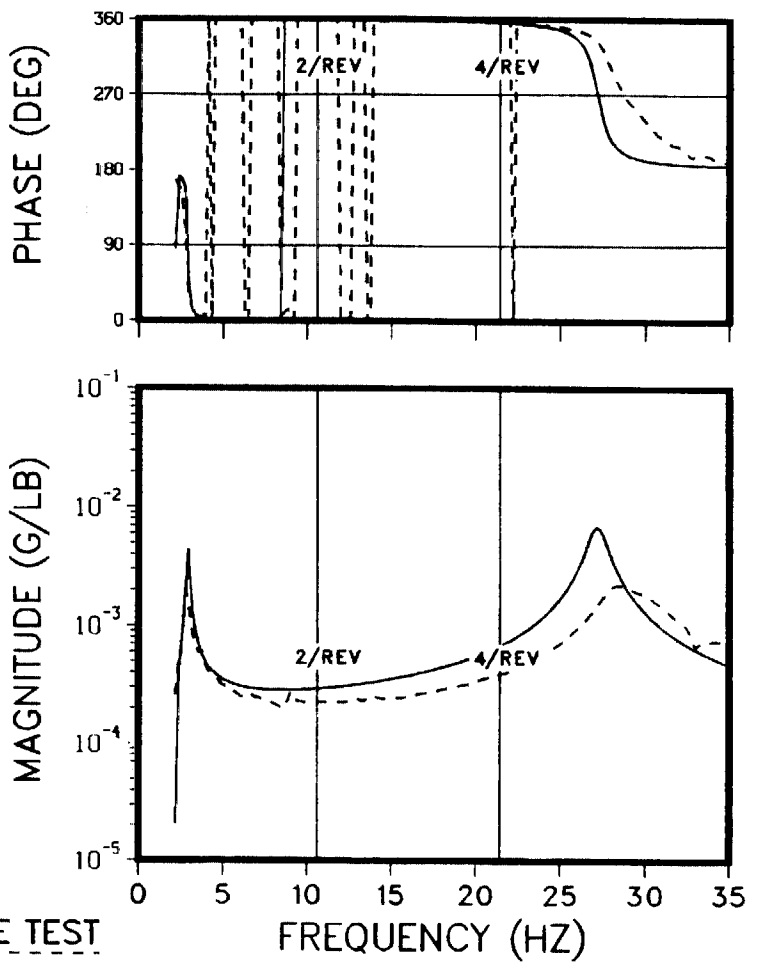

SHAKE TEST

NASTRAN

TRANSMISSION UPPER BEARING F/A RESPONSE

F/A EXCITATION AT THE M/R HUB
THRUST = 1000 LB .NO DAMPERS INSTALLED
SHAKE TEST FORCE = 200 LB

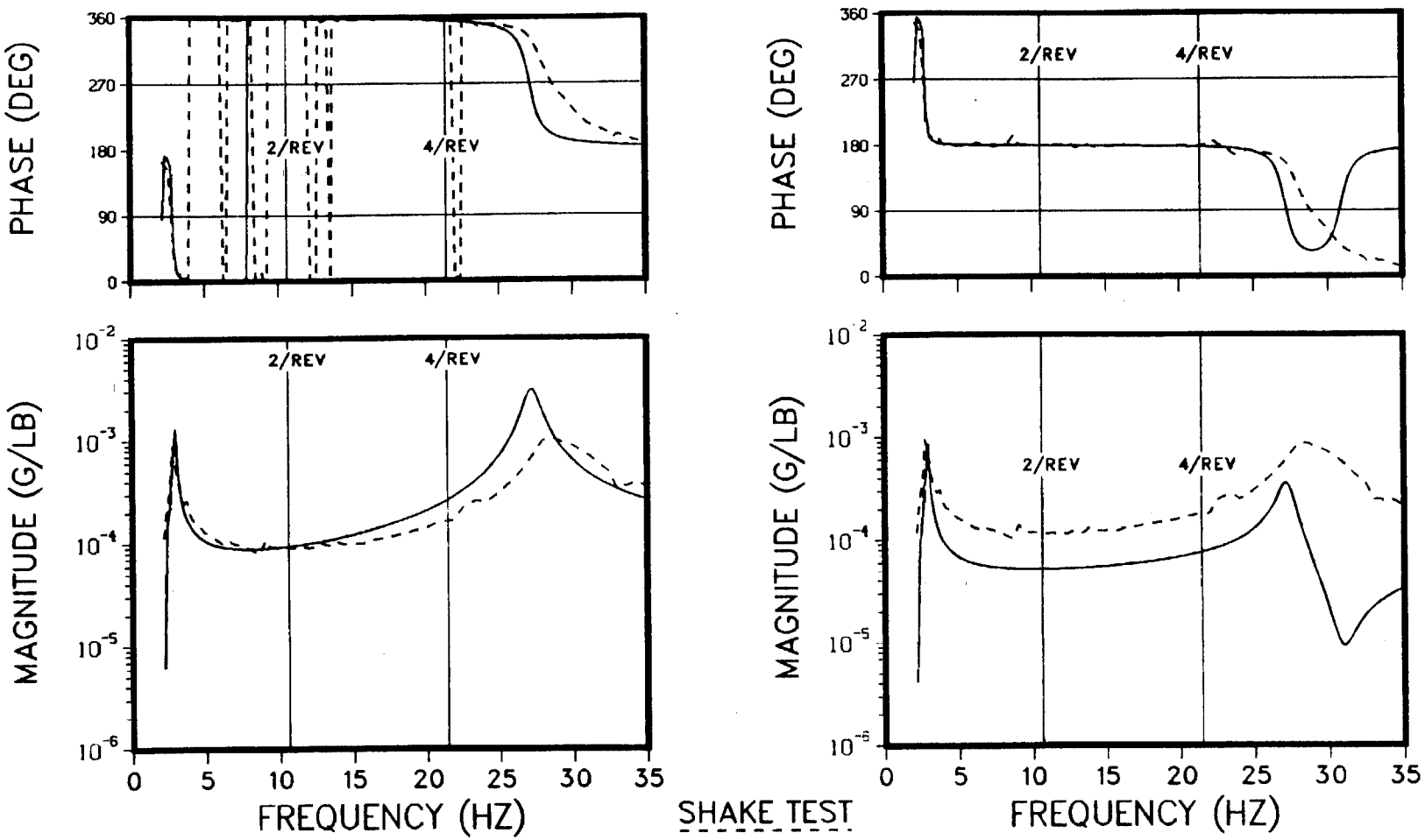

MID TRANSMISSION F/A RESPONSE

TRANSMISSION SUMP F/A RESPONSE

F/A EXCITATION AT THE M/R HUB
THRUST = 1000 LB .NO DAMPERS INSTALLED
SHAKE TEST FORCE = 200 LB

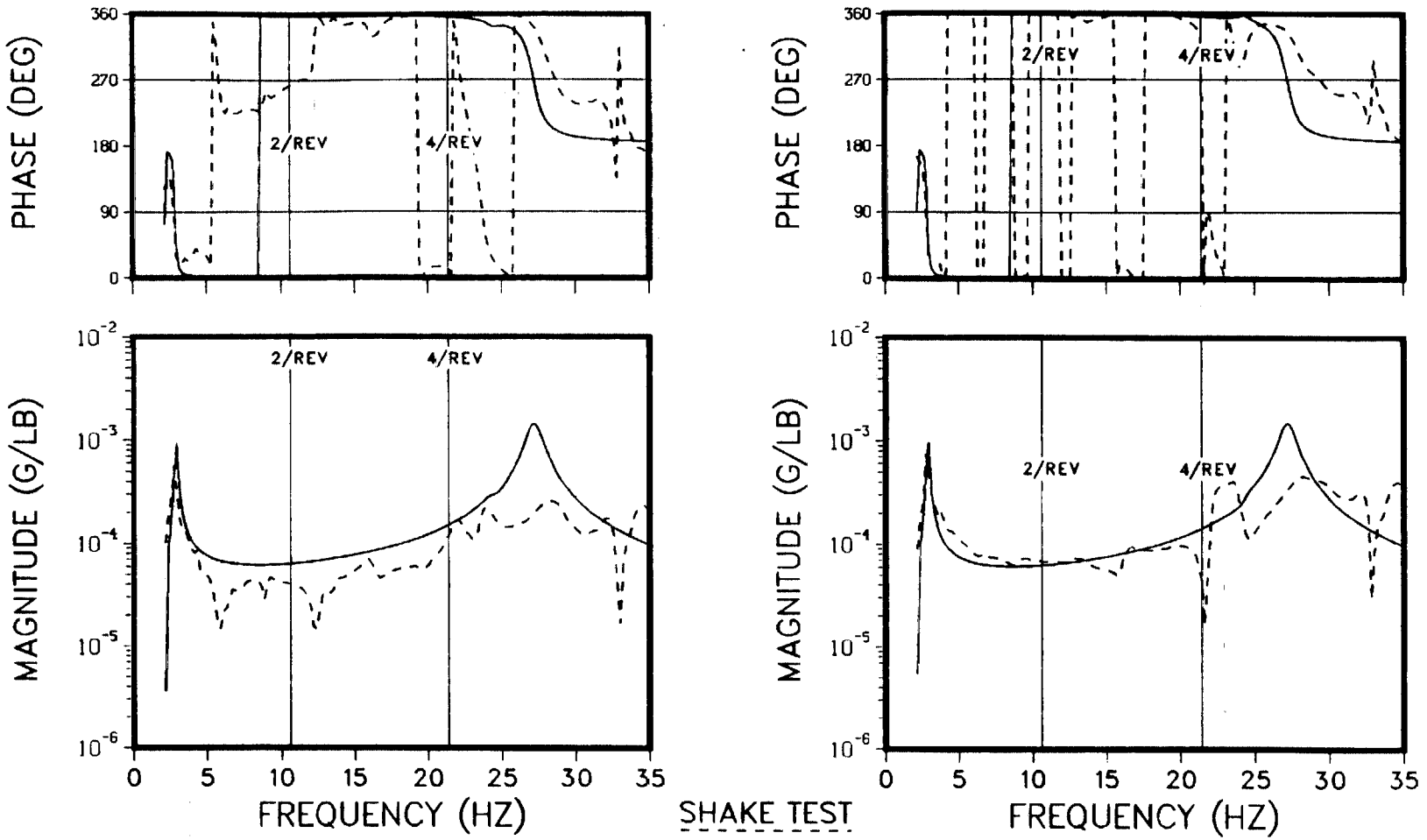

LEFT FORWARD MOUNT VERTICAL RESPONSE **RIGHT FORWARD MOUNT VERTICAL RESPONSE**

F/A EXCITATION AT THE M/R HUB
THRUST = 1000 LB .NO DAMPERS INSTALLED
SHAKE TEST FORCE = 200 LB

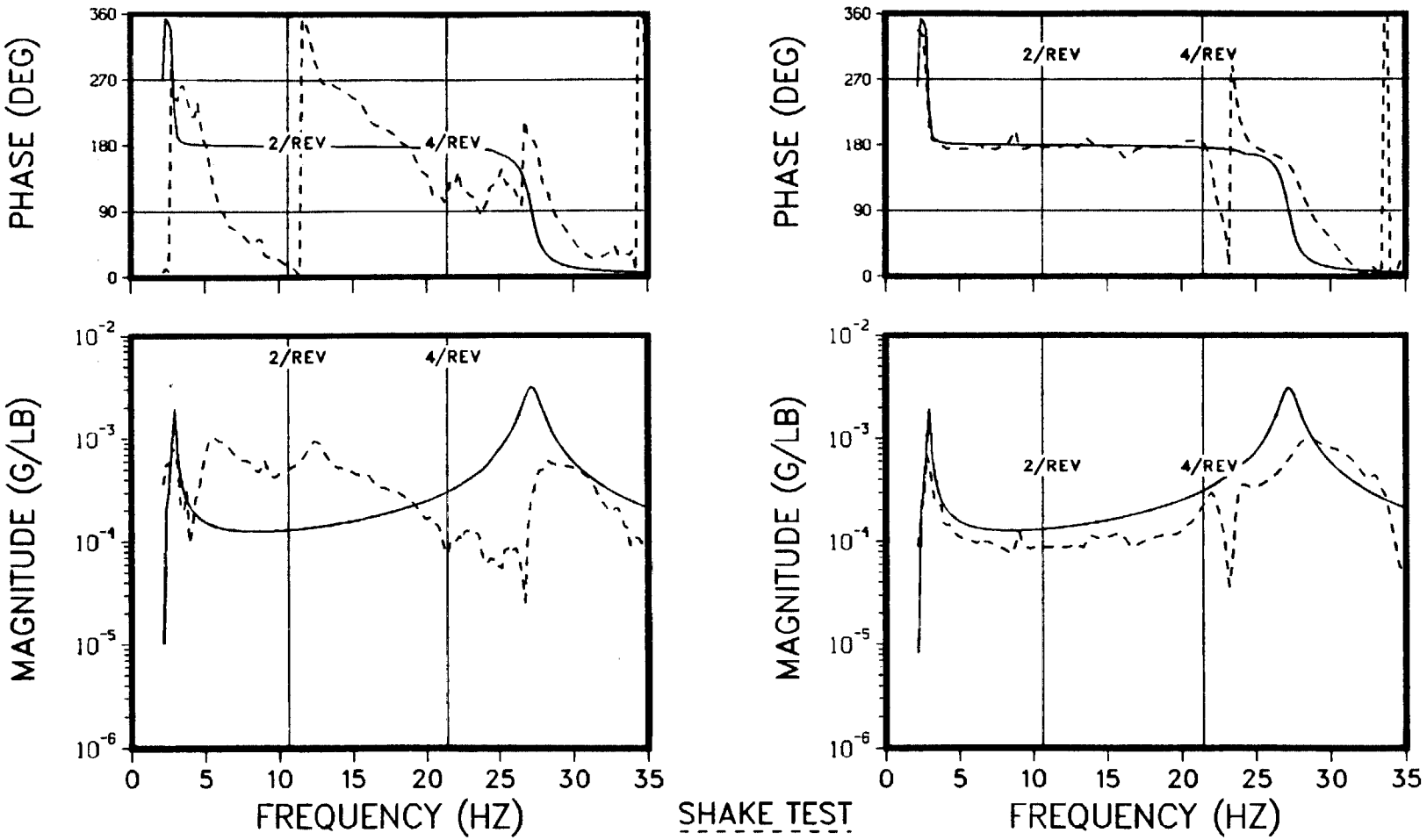

LEFT AFT MOUNT VERTICAL RESPONSE

RIGHT AFT MOUNT VERTICAL RESPONSE

F/A EXCITATION AT THE M/R HUB
THRUST = 1000 LB .NO DAMPERS INSTALLED
SHAKE TEST FORCE = 200 LB

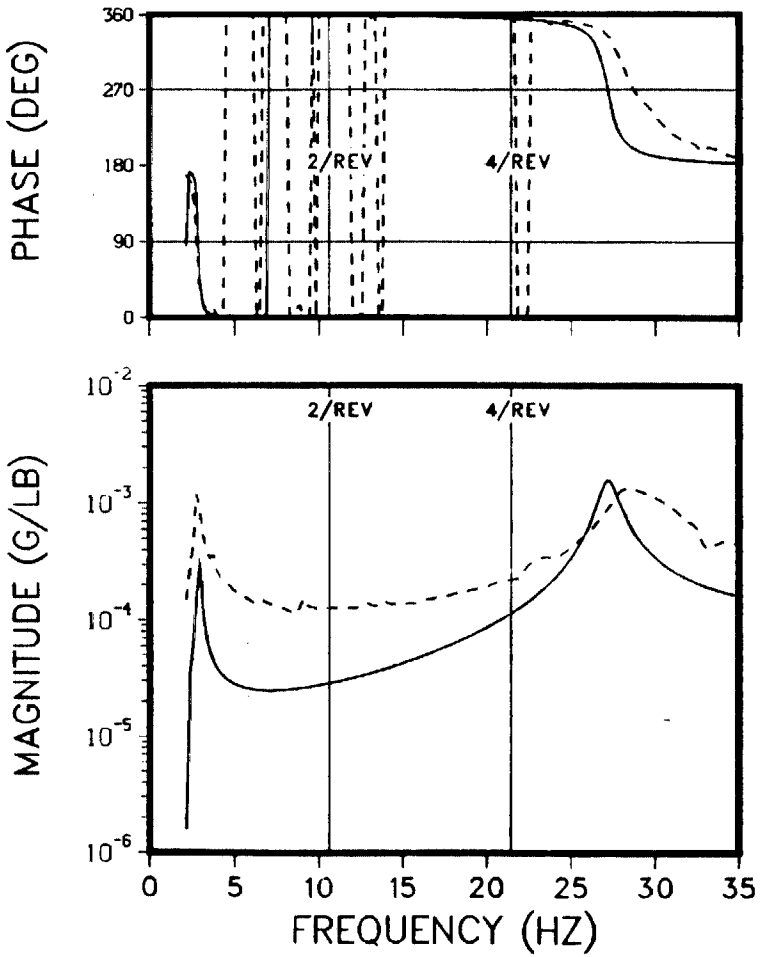

TRANSMISSION C.G. F/A RESPONSE

F/A EXCITATION AT THE M/R HUB
THRUST = 1000 LB .NO DAMPERS INSTALLED
SHAKE TEST FORCE = 100 LB FROM 2 TO 6 HZ

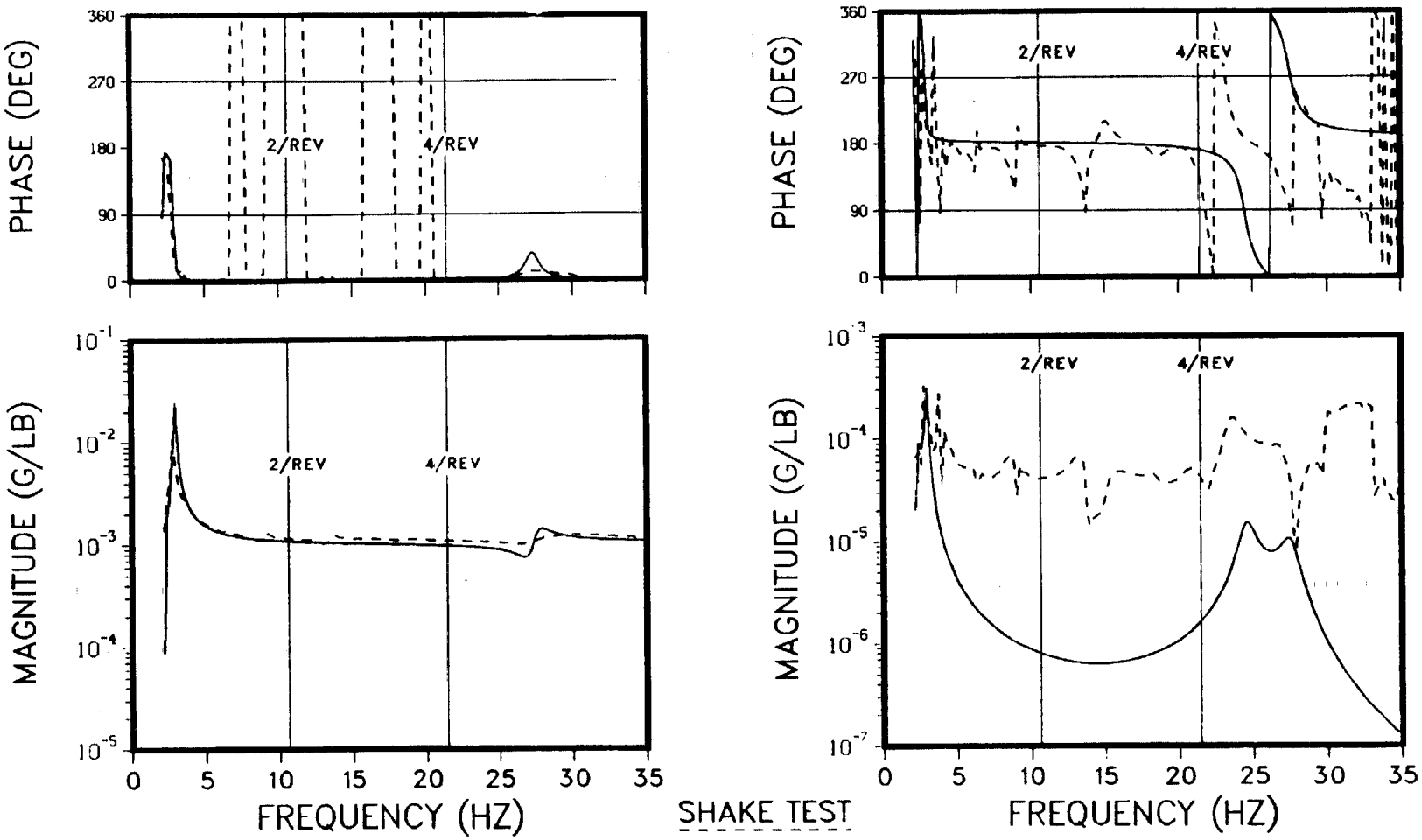

M/R HUB F/A RESPONSE

M/R HUB LATERAL RESPONSE

F/A EXCITATION AT THE M/R HUB
THRUST = 1000 LB .NO DAMPERS INSTALLED
SHAKE TEST FORCE = 100 LB FROM 2 TO 6 HZ

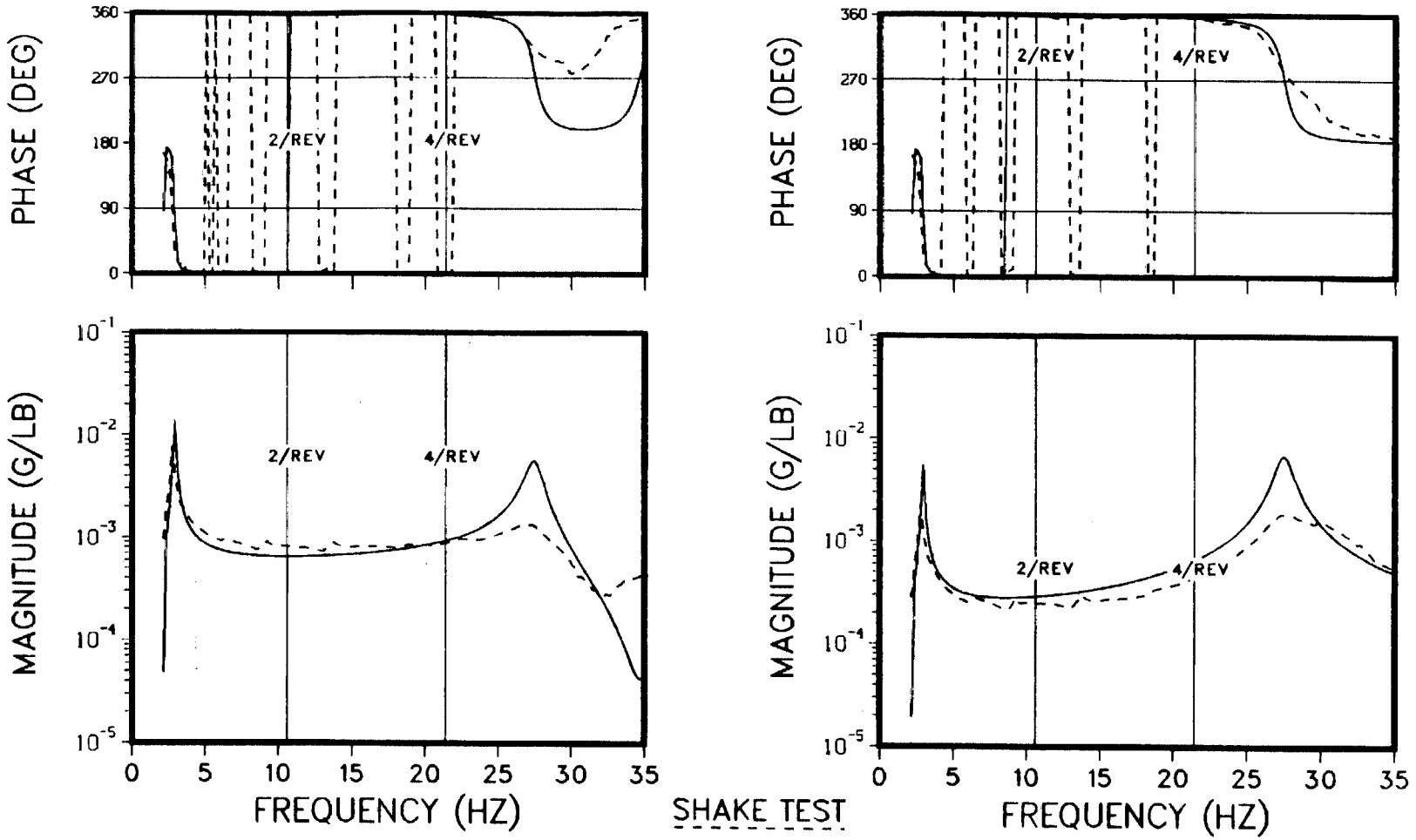

MID MAST (STA 22) F/A RESPONSE

TRANSMISSION UPPER BEARING F/A RESPONSE

F/A EXCITATION AT THE M/R HUB
THRUST = 1000 LB .NO DAMPERS INSTALLED
SHAKE TEST FORCE = 100 LB FROM 2 TO 6 HZ

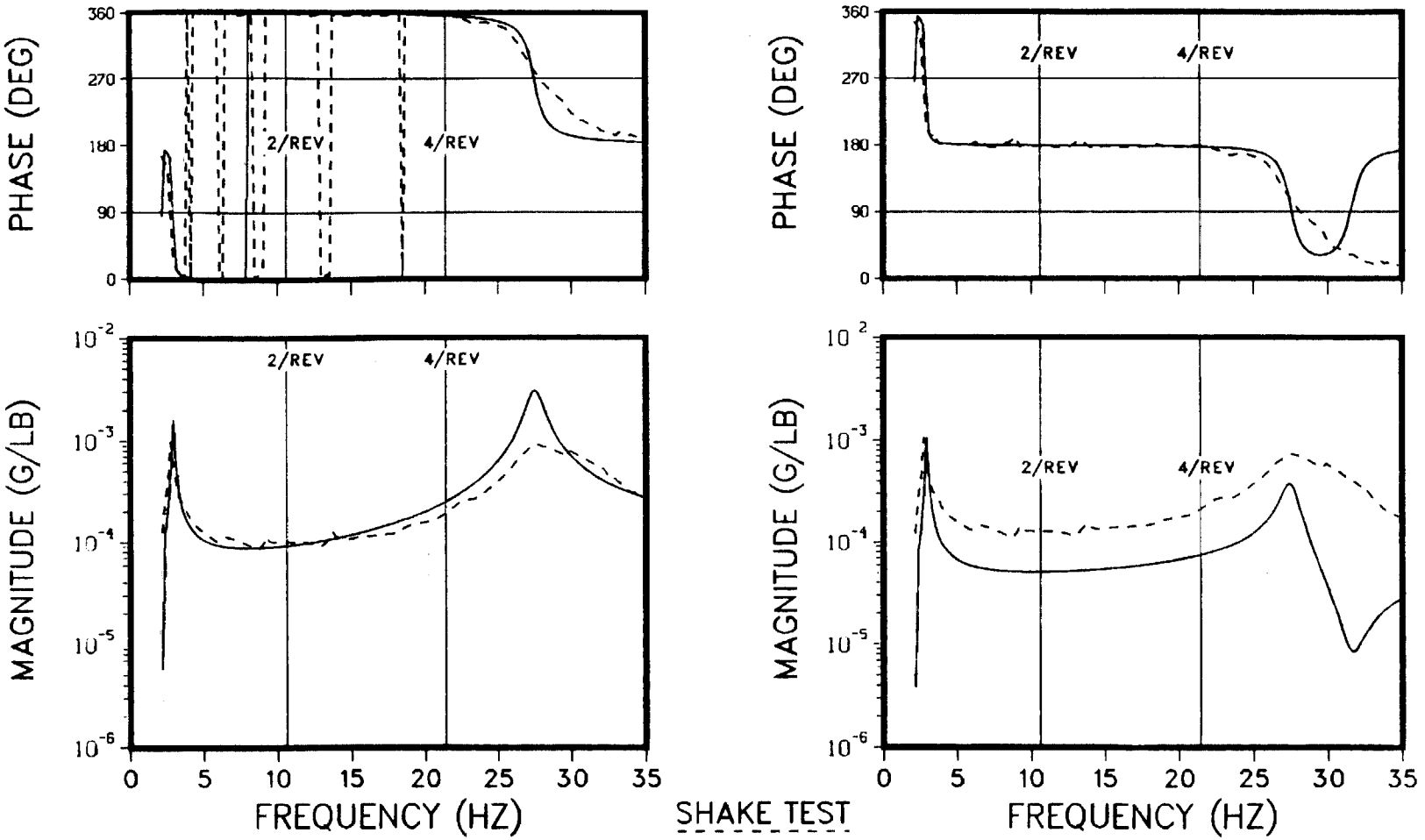

MID TRANSMISSION F/A RESPONSE

TRANSMISSION SUMP F/A RESPONSE

F/A EXCITATION AT THE M/R HUB
THRUST = 1000 LB .NO DAMPERS INSTALLED
SHAKE TEST FORCE = 100 LB FROM 2 TO 6 HZ

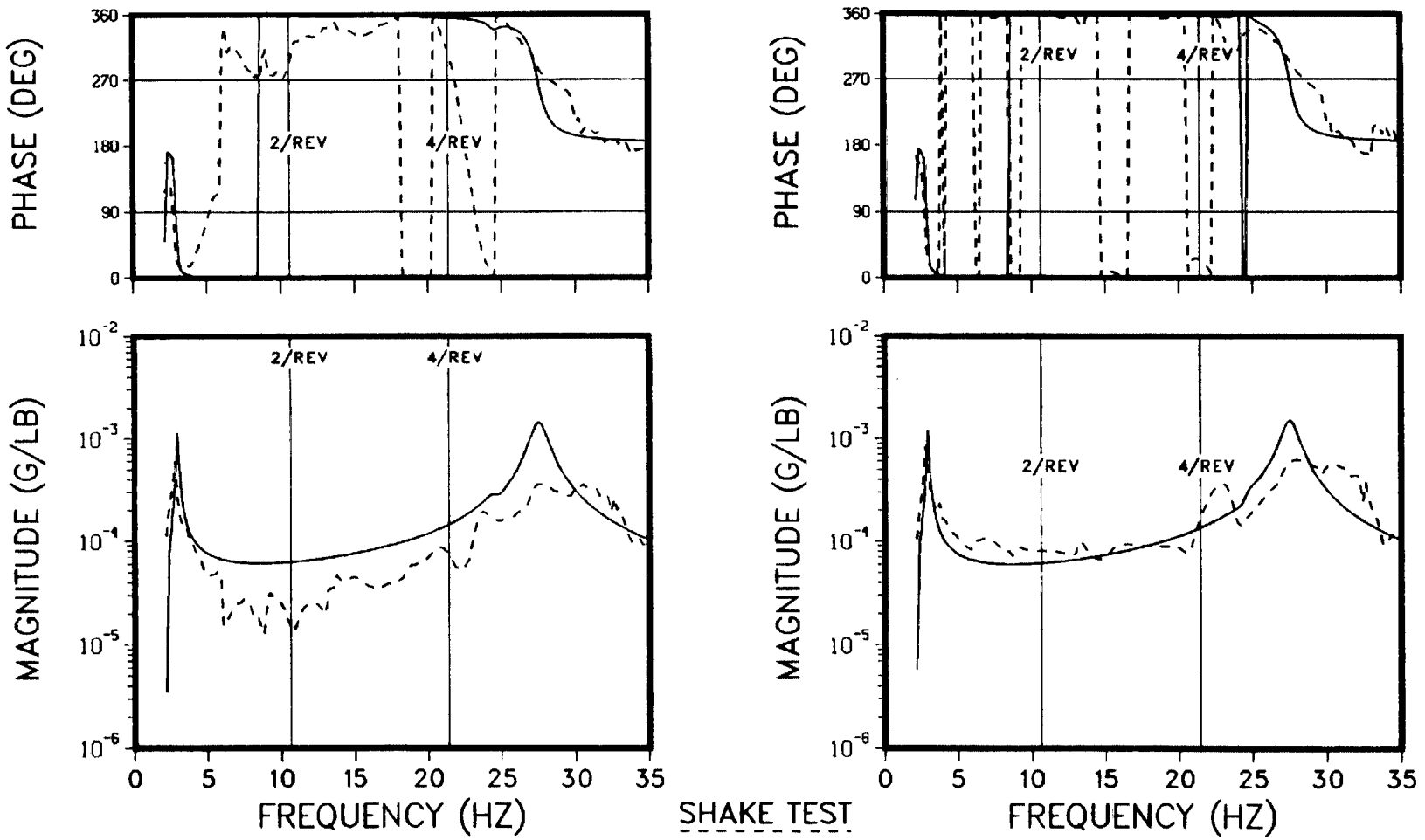

LEFT FORWARD MOUNT VERTICAL RESPONSE **RIGHT FORWARD MOUNT VERTICAL RESPONSE**

F/A EXCITATION AT THE M/R HUB
THRUST = 1000 LB .NO DAMPERS INSTALLED
SHAKE TEST FORCE = 100 LB FROM 2 TO 6 HZ

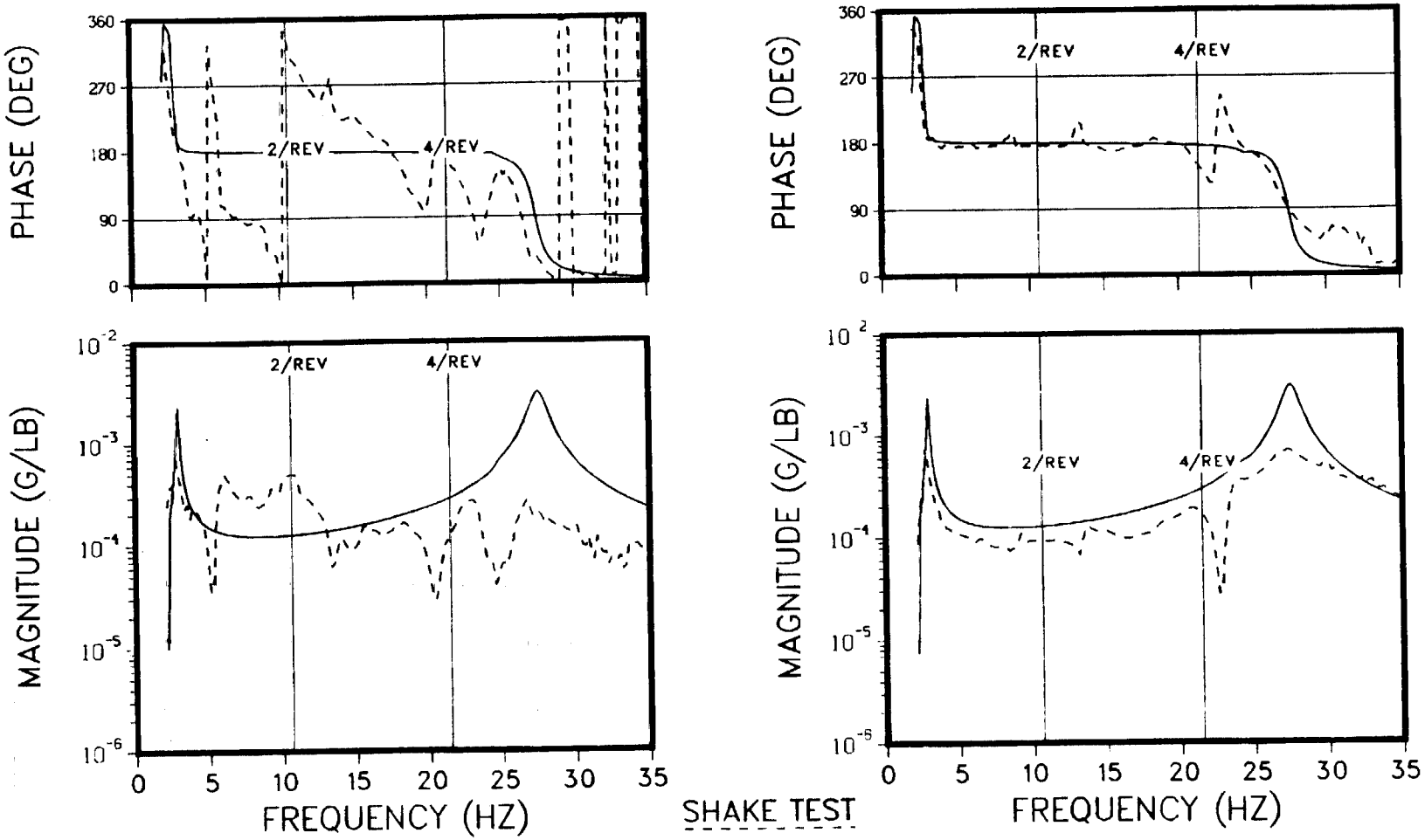

LEFT AFT MOUNT VERTICAL RESPONSE

RIGHT AFT MOUNT VERTICAL RESPONSE

F/A EXCITATION AT THE M/R HUB
THRUST = 1000 LB .NO DAMPERS INSTALLED
SHAKE TEST FORCE = 100 LB FROM 2 TO 6 HZ

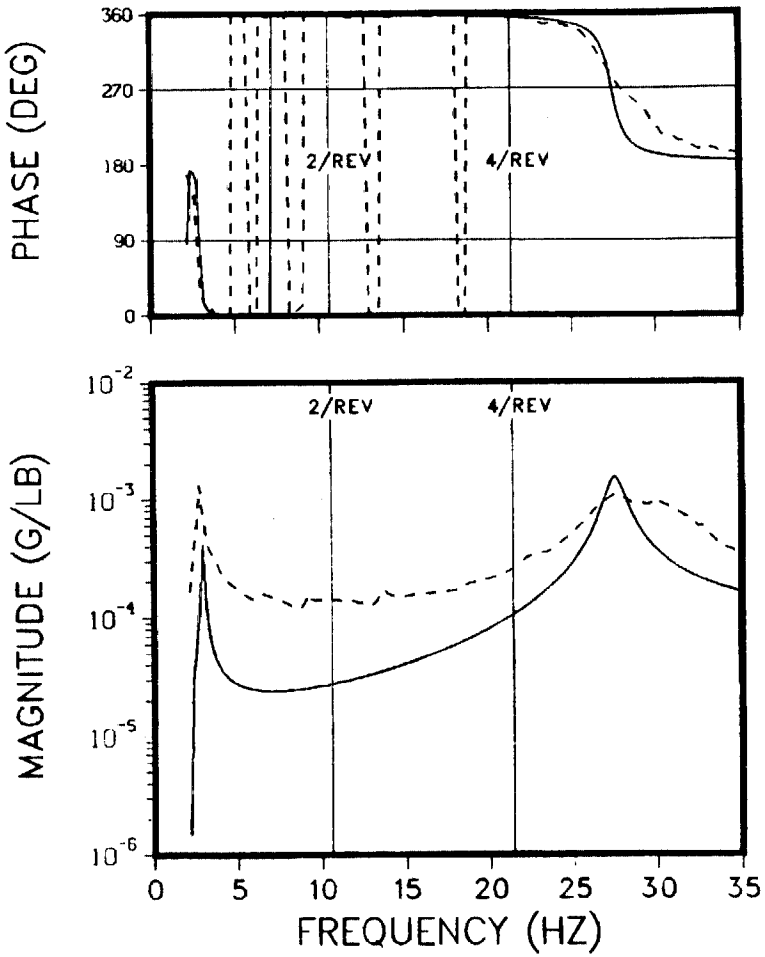

TRANSMISSION C.G. F/A RESPONSE

LATERAL EXCITATION AT THE M/R HUB
THRUST = 1000 LB .NO DAMPERS INSTALLED
SHAKE TEST FORCE = 100 LB FROM 2 TO 6 HZ

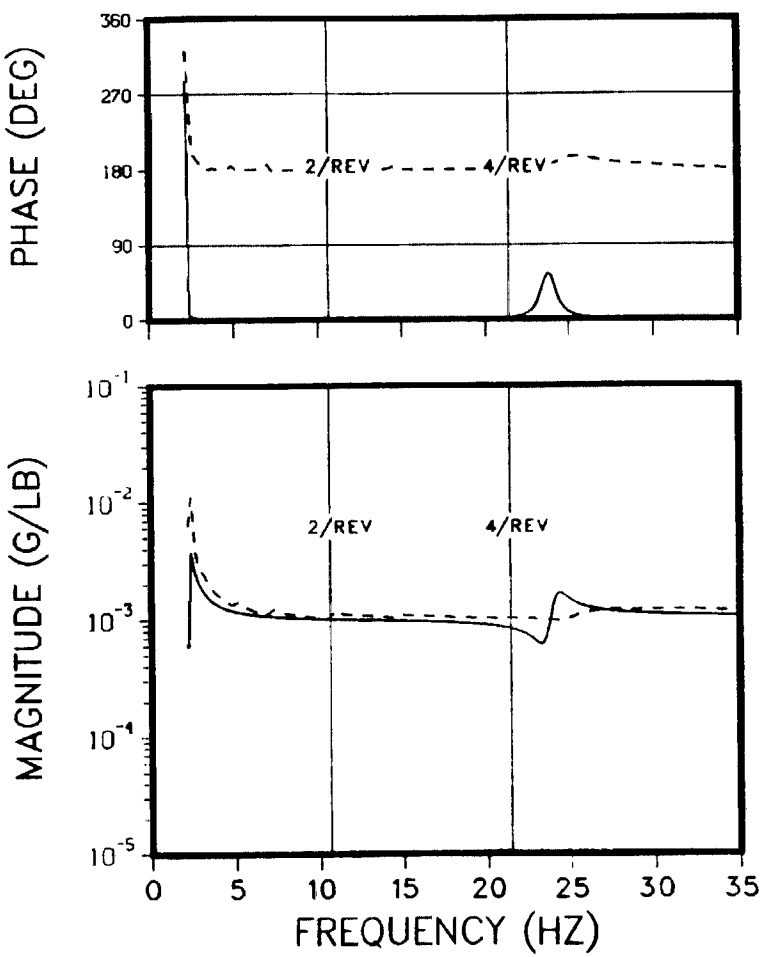

M/R HUB LATERAL RESPONSE

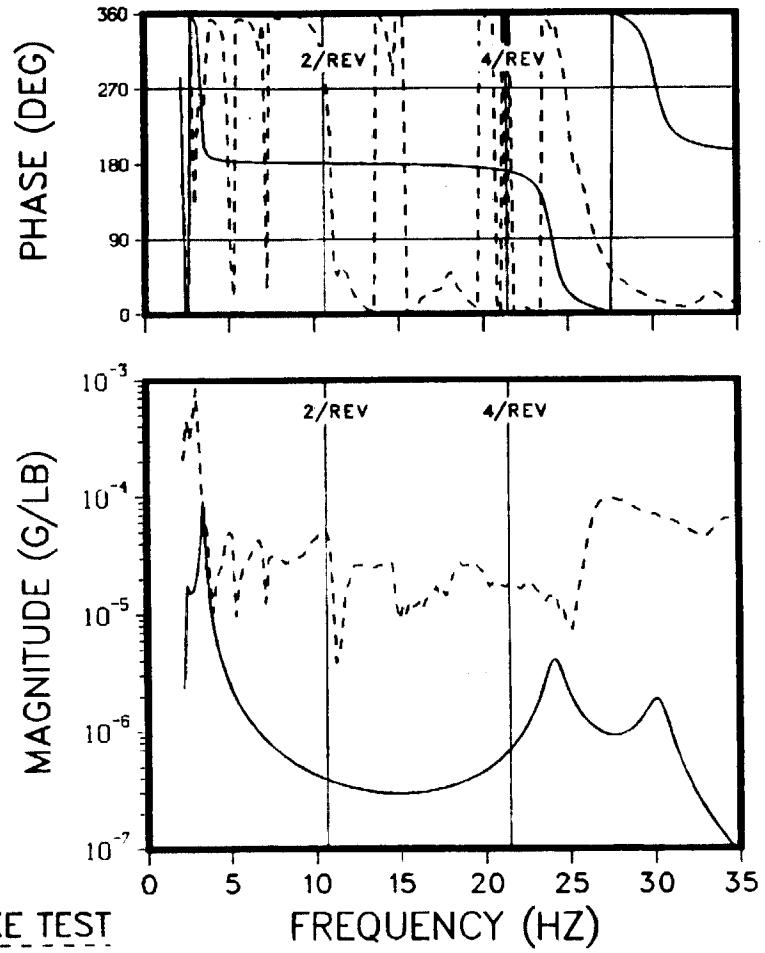

M/R HUB F/A RESPONSE

SHAKE TEST

NASTRAN

LATERAL EXCITATION AT THE M/R HUB
THRUST = 1000 LB .NO DAMPERS INSTALLED
SHAKE TEST FORCE = 100 LB FROM 2 TO 6 HZ

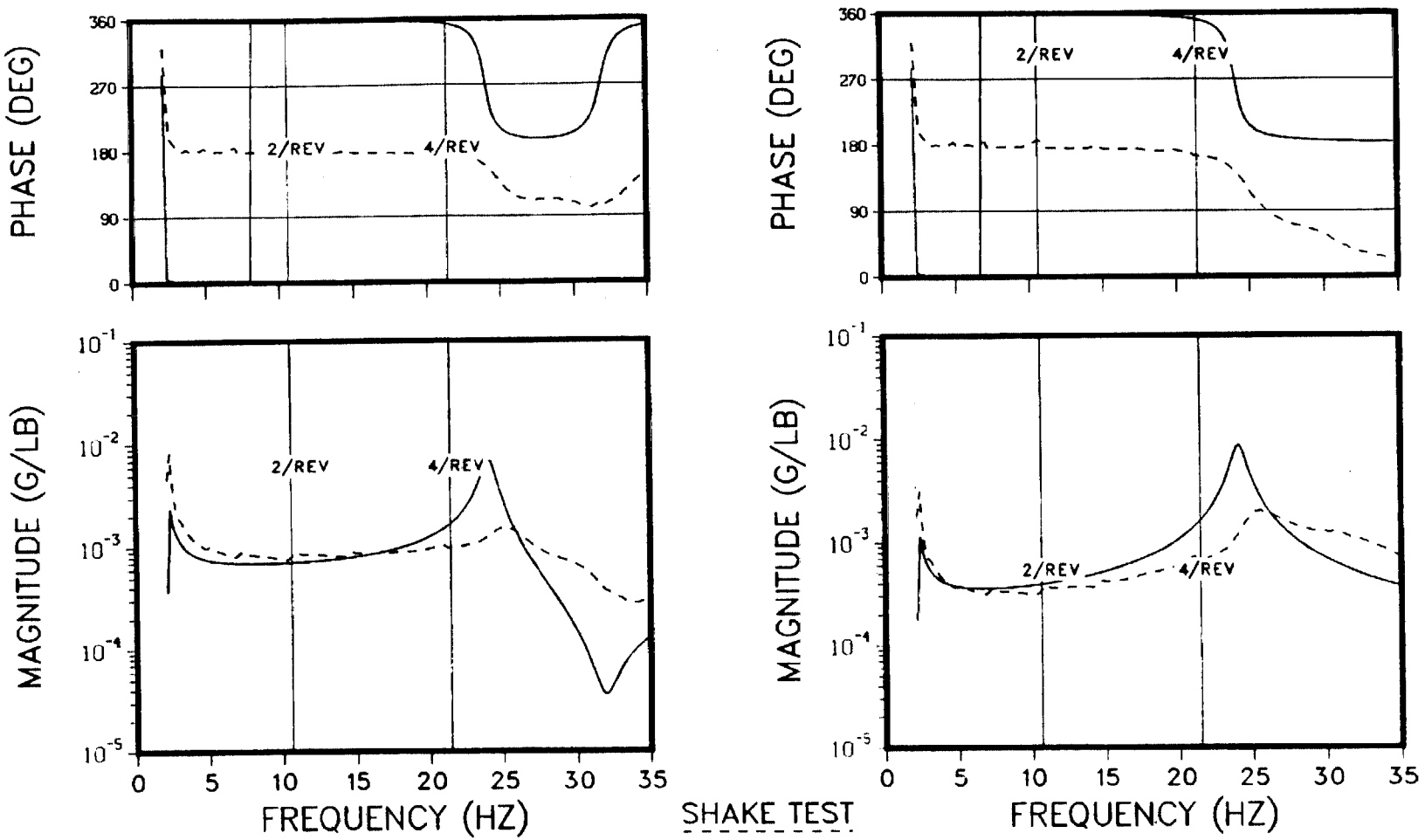

MID MAST (STA 22) LATERAL RESPONSE

TRANSMISSION UPPER BEARING LATERAL RESPONSE

LATERAL EXCITATION AT THE M/R HUB
THRUST = 1000 LB .NO DAMPERS INSTALLED
SHAKE TEST FORCE = 100 LB FROM 2 TO 6 HZ

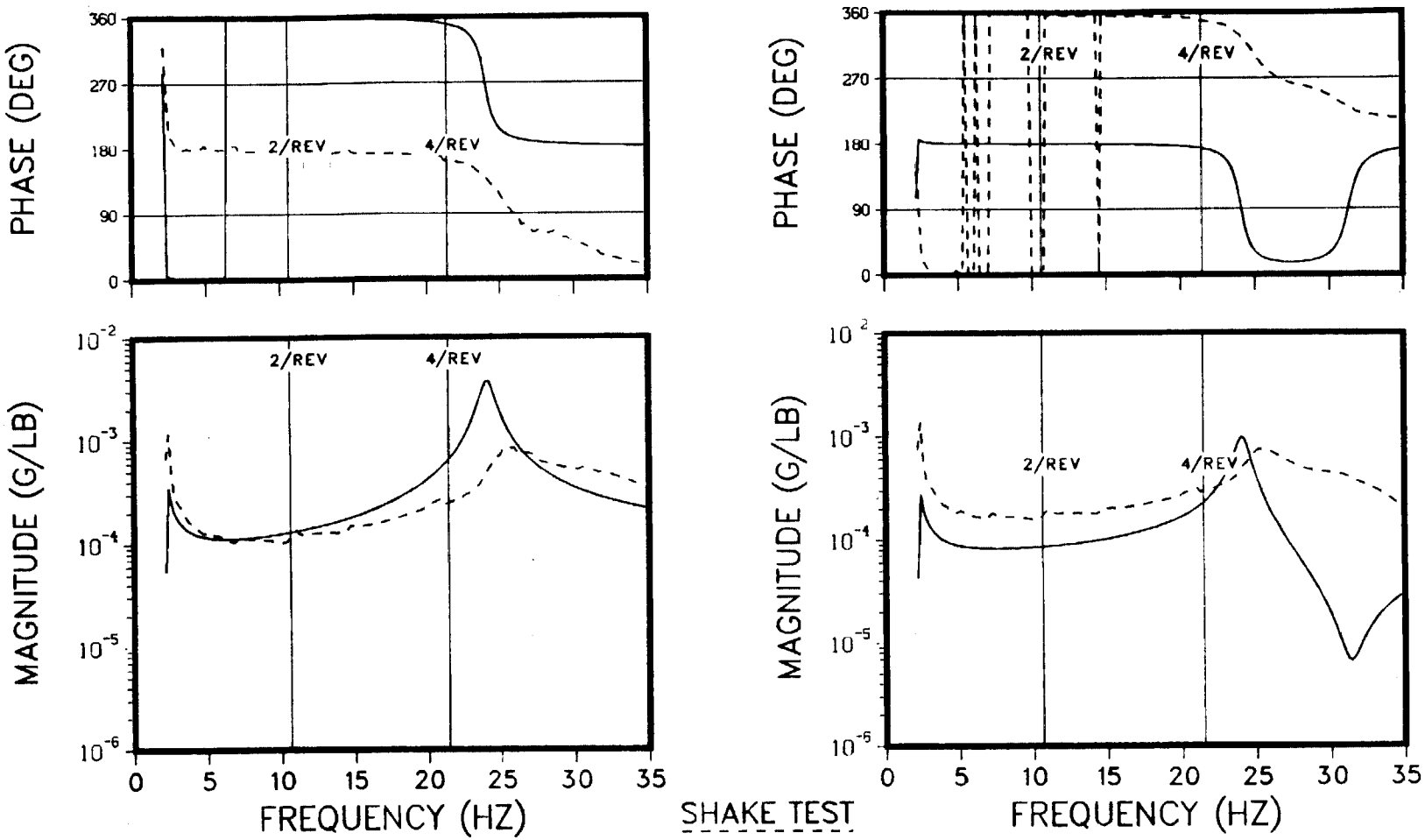

MID TRANSMISSION LATERAL RESPONSE

TRANSMISSION SUMP LATERAL RESPONSE

LATERAL EXCITATION AT THE M/R HUB
THRUST = 1000 LB .NO DAMPERS INSTALLED
SHAKE TEST FORCE = 100 LB FROM 2 TO 6 HZ

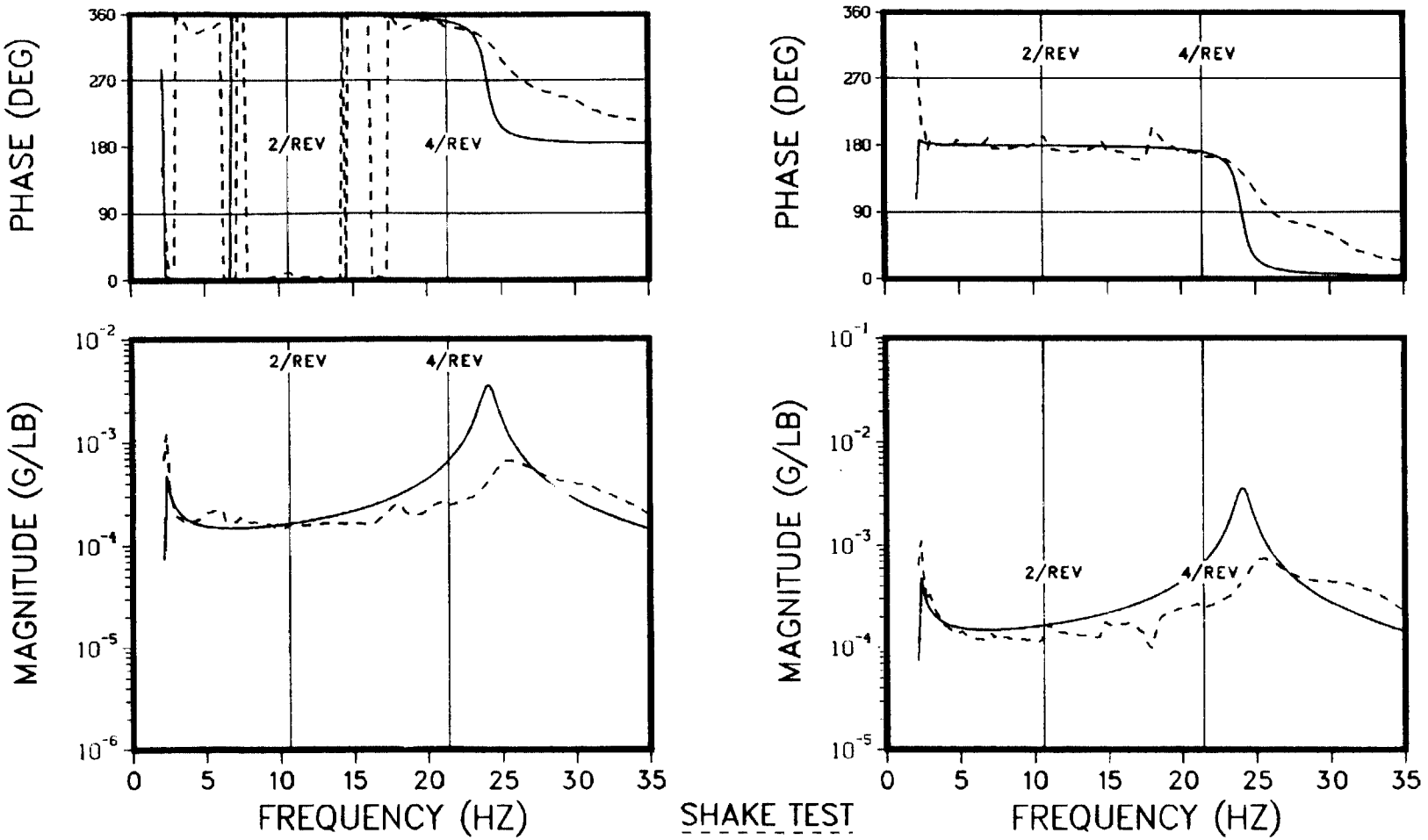

LEFT FORWARD MOUNT VERTICAL RESPONSE **RIGHT FORWARD MOUNT VERTICAL RESPONSE**

LATERAL EXCITATION AT THE M/R HUB
THRUST = 1000 LB .NO DAMPERS INSTALLED
SHAKE TEST FORCE = 100 LB FROM 2 TO 6 HZ

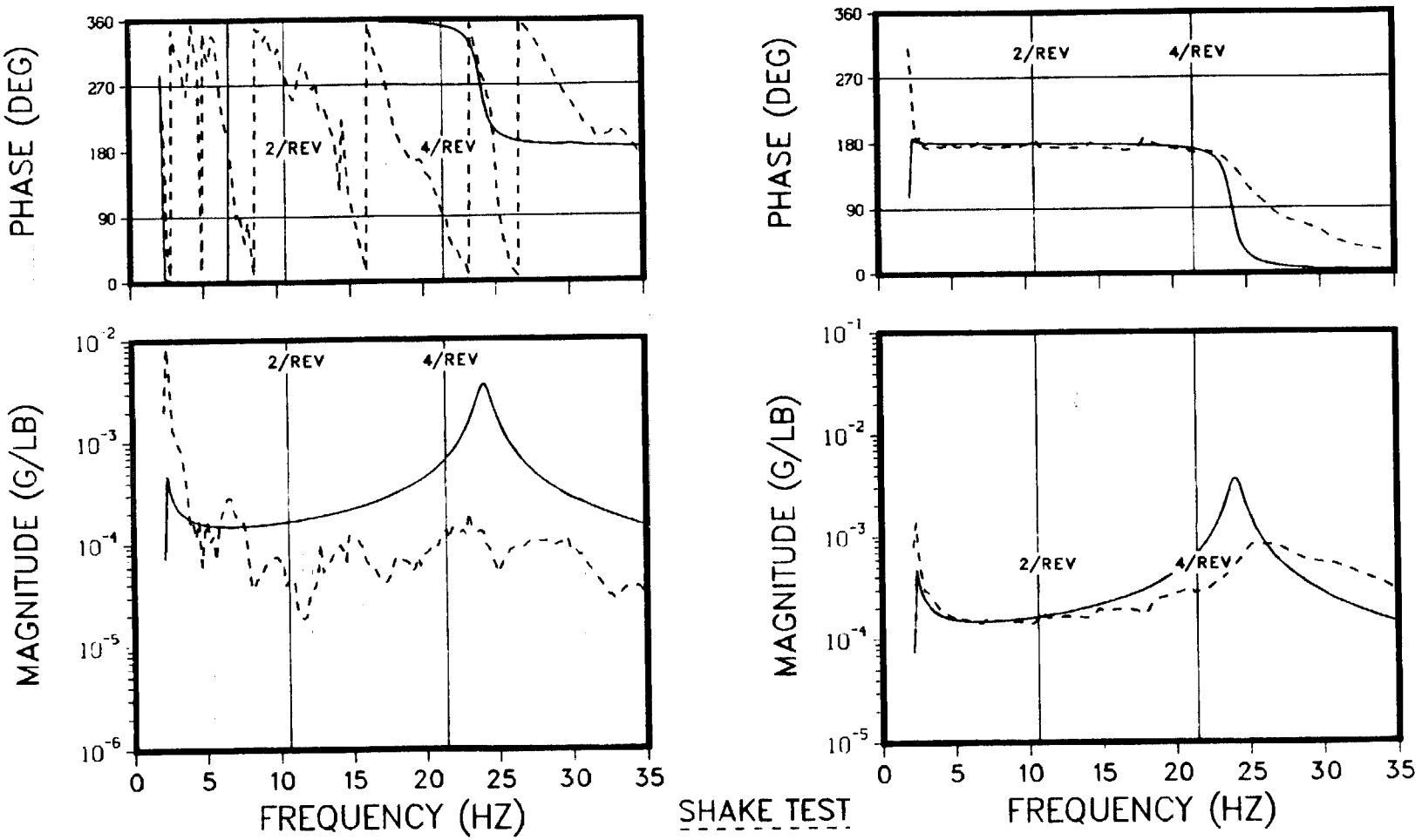

LEFT AFT MOUNT VERTICAL RESPONSE

RIGHT AFT MOUNT VERTICAL RESPONSE

LATERAL EXCITATION AT THE M/R HUB
THRUST = 1000 LB .NO DAMPERS INSTALLED
SHAKE TEST FORCE = 100 LB FROM 2 TO 6 HZ

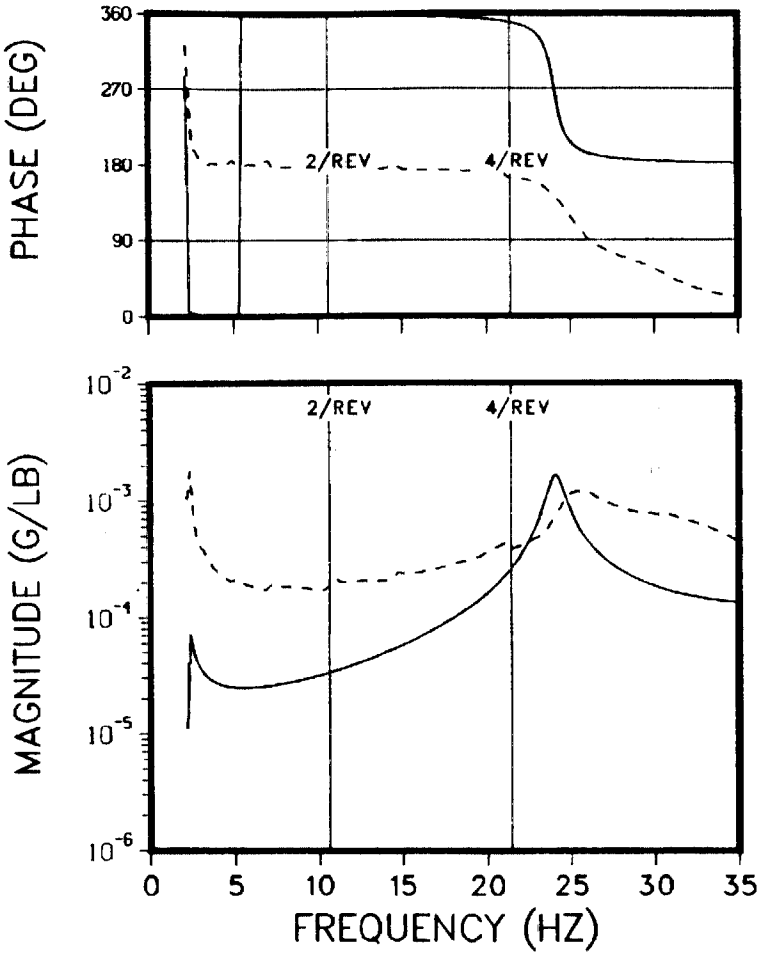

TRANSMISSION C.G. LATERAL RESPONSE

LATERAL EXCITATION AT THE M/R HUB
THRUST = 1000 LB . DAMPERS INSTALLED
SHAKE TEST FORCE = 100 LB FROM 2 TO 6 HZ

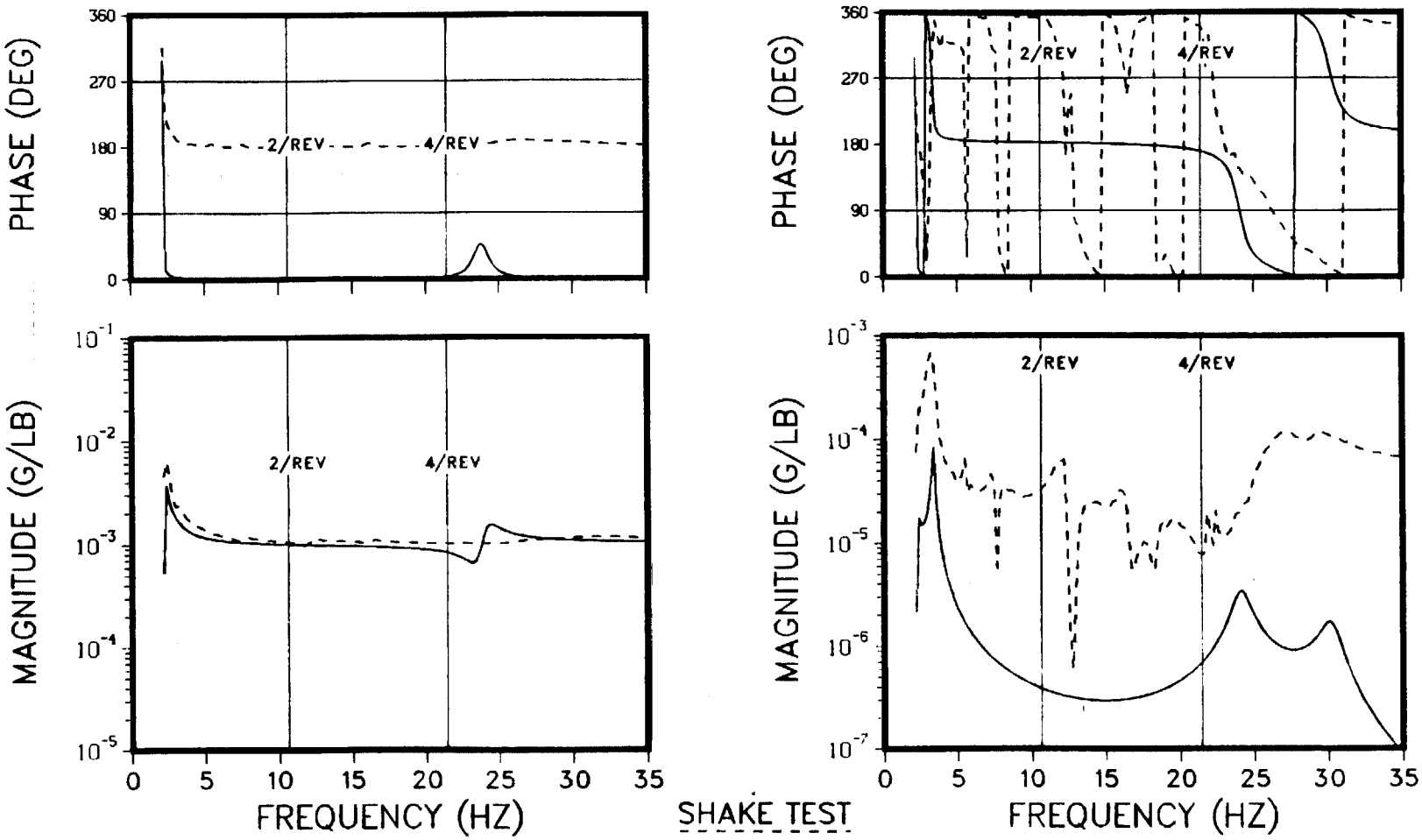

M/R HUB LATERAL RESPONSE

M/R HUB F/A RESPONSE

LATERAL EXCITATION AT THE M/R HUB
THRUST = 1000 LB . DAMPERS INSTALLED
SHAKE TEST FORCE = 100 LB FROM 2 TO 6 HZ

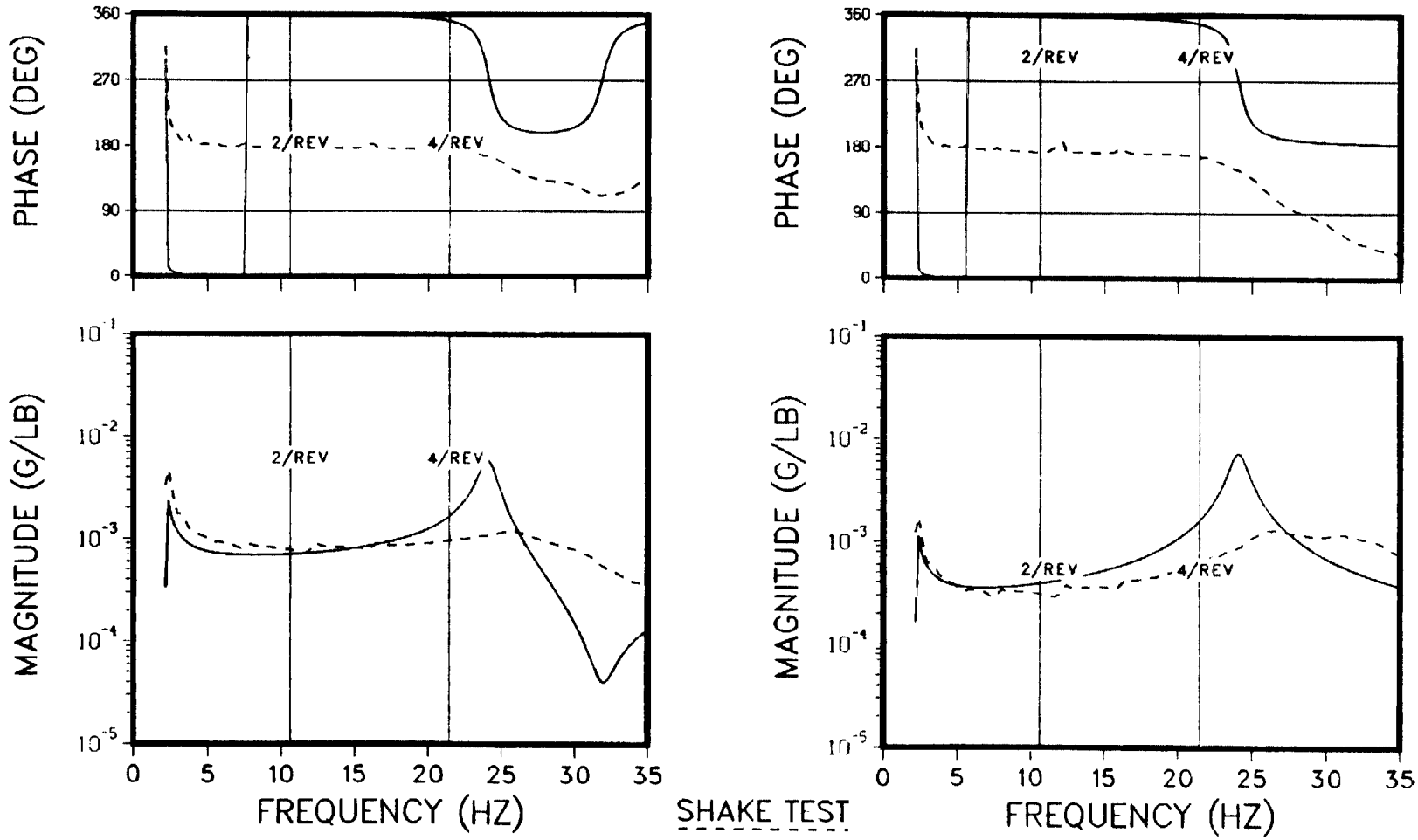

MID MAST (STA 22) LATERAL RESPONSE

TRANSMISSION UPPER BEARING LATERAL RESPONSE

LATERAL EXCITATION AT THE M/R HUB
THRUST = 1000 LB . DAMPERS INSTALLED
SHAKE TEST FORCE = 100 LB FROM 2 TO 6 HZ

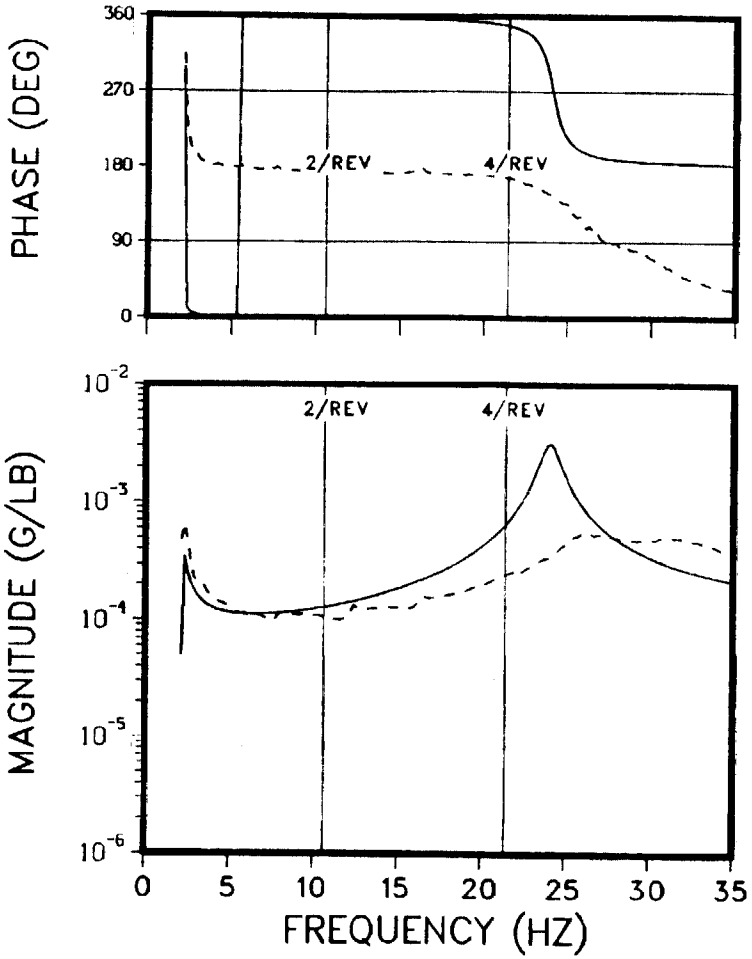

MID TRANSMISSION LATERAL RESPONSE

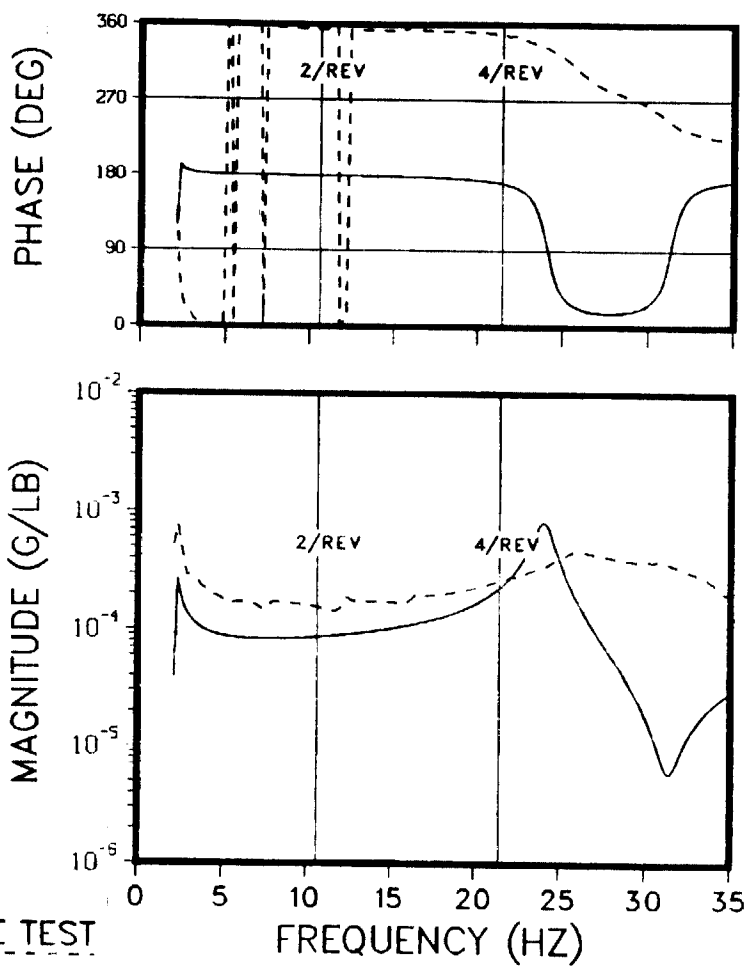

SHAKE TEST

NASTRAN

TRANSMISSION SUMP LATERAL RESPONSE

LATERAL EXCITATION AT THE M/R HUB
THRUST = 1000 LB . DAMPERS INSTALLED
SHAKE TEST FORCE = 100 LB FROM 2 TO 6 HZ

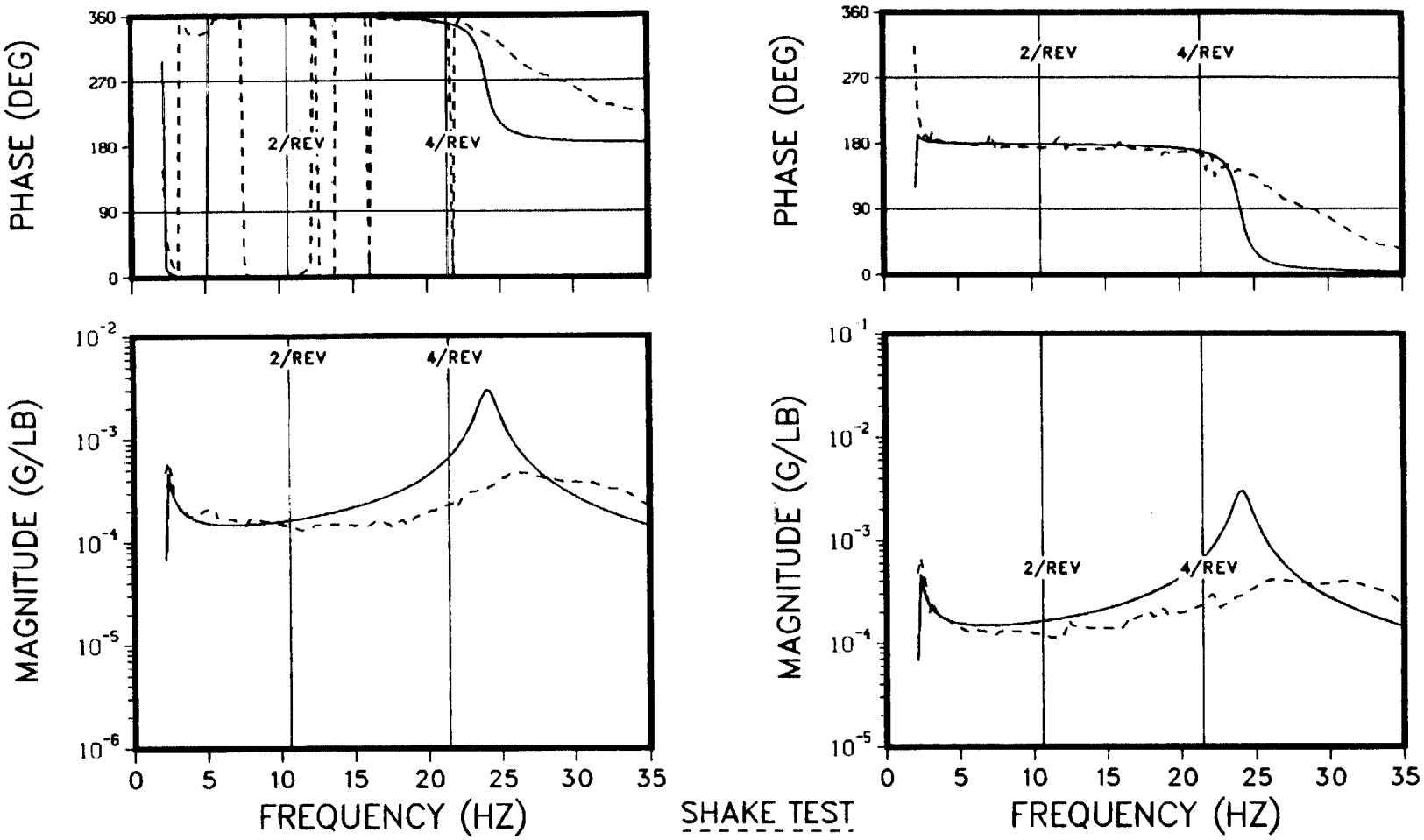

LEFT FORWARD MOUNT VERTICAL RESPONSE **RIGHT FORWARD MOUNT VERTICAL RESPONSE**

LATERAL EXCITATION AT THE M/R HUB
THRUST = 1000 LB . DAMPERS INSTALLED
SHAKE TEST FORCE = 100 LB FROM 2 TO 6 HZ

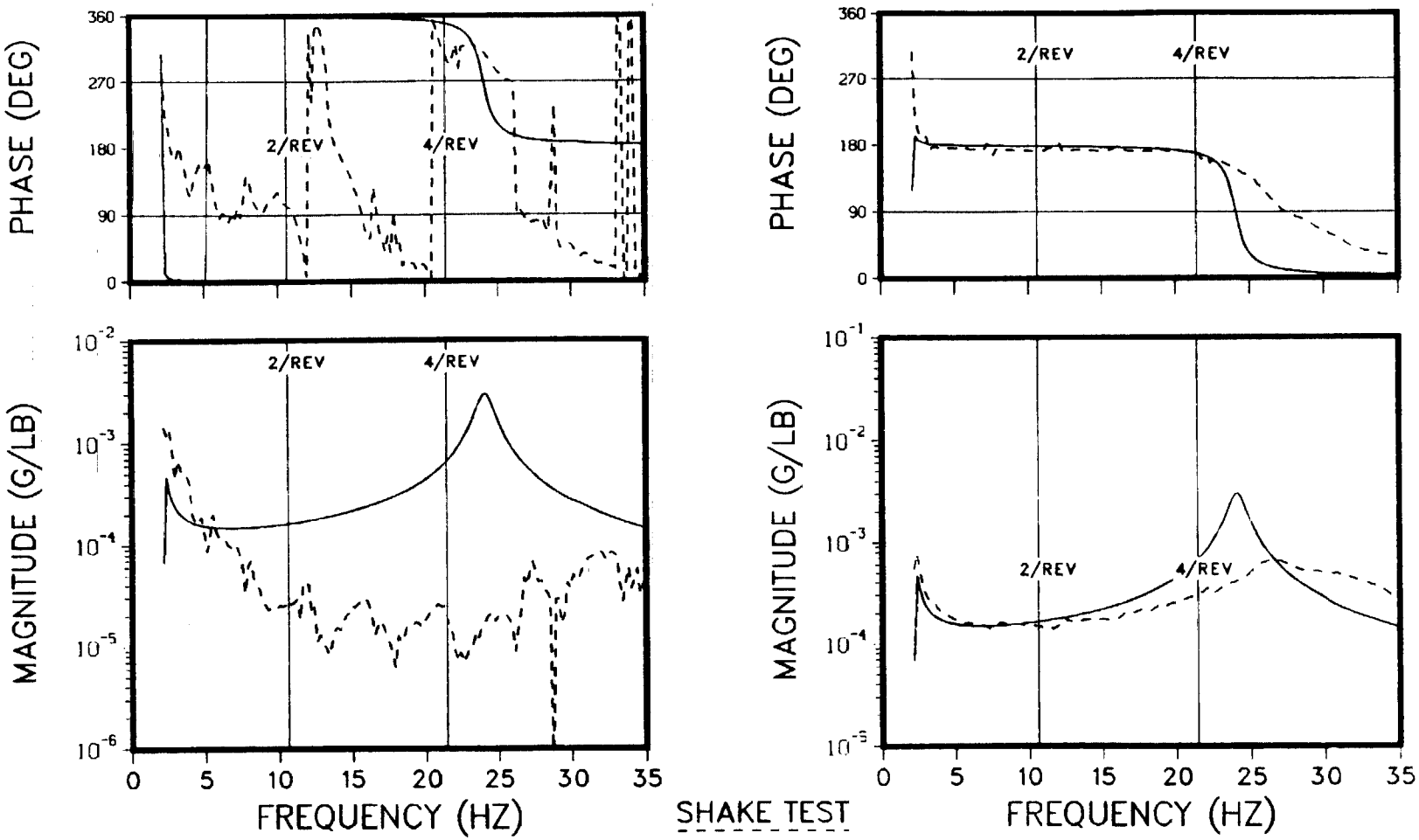

LEFT AFT MOUNT VERTICAL RESPONSE

RIGHT AFT MOUNT VERTICAL RESPONSE

LATERAL EXCITATION AT THE M/R HUB
THRUST = 1000 LB . DAMPERS INSTALLED
SHAKE TEST FORCE = 100 LB FROM 2 TO 6 HZ

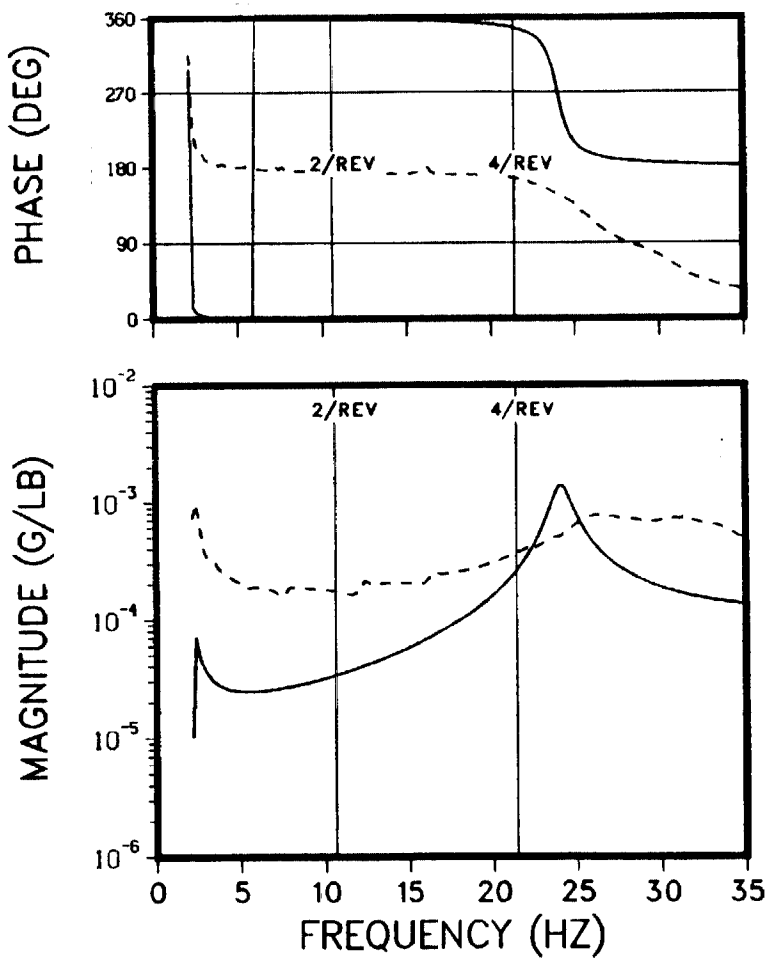

TRANSMISSION C.G. LATERAL RESPONSE

LATERAL EXCITATION AT THE M/R HUB
THRUST = 7000 LB . DAMPERS INSTALLED
SHAKE TEST FORCE = 100 LB FROM 2 TO 6 HZ

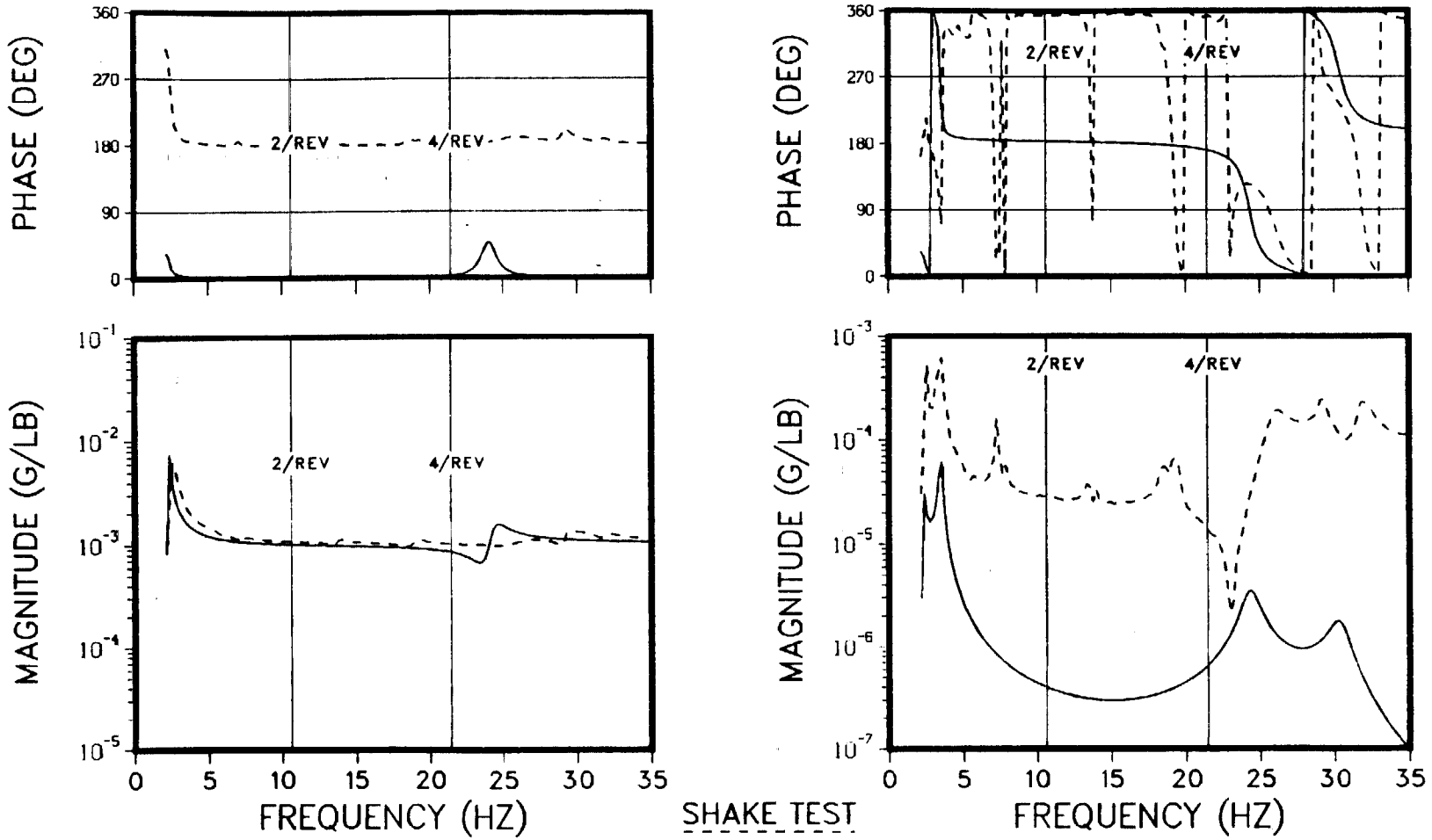

M/R HUB LATERAL RESPONSE

M/R HUB F/A RESPONSE

LATERAL EXCITATION AT THE M/R HUB
THRUST = 7000 LB . DAMPERS INSTALLED
SHAKE TEST FORCE = 100 LB FROM 2 TO 6 HZ

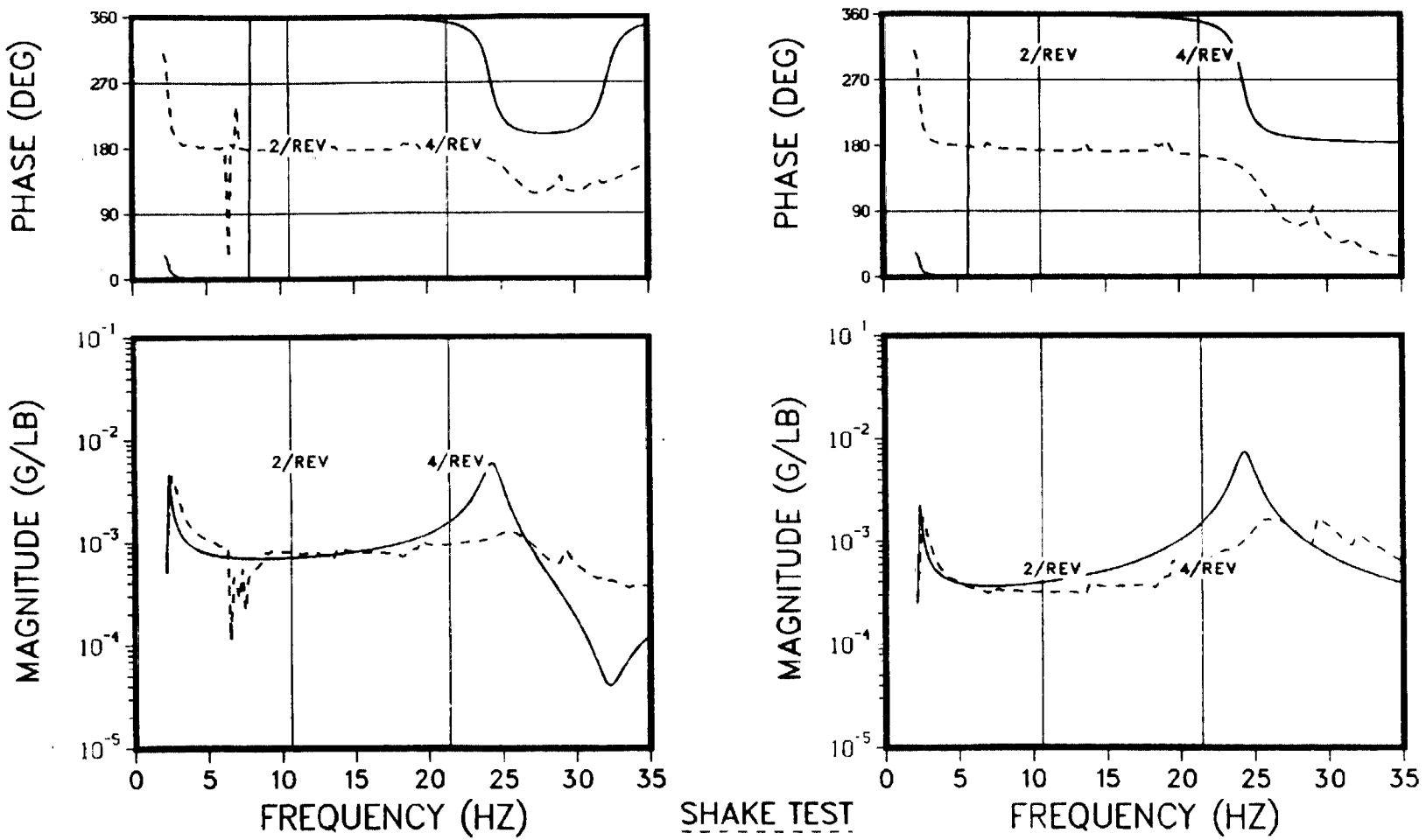

MID MAST (STA 22) LATERAL RESPONSE

TRANSMISSION UPPER BEARING LATERAL RESPONSE

LATERAL EXCITATION AT THE M/R HUB
THRUST = 7000 LB . DAMPERS INSTALLED
SHAKE TEST FORCE = 100 LB FROM 2 TO 6 HZ

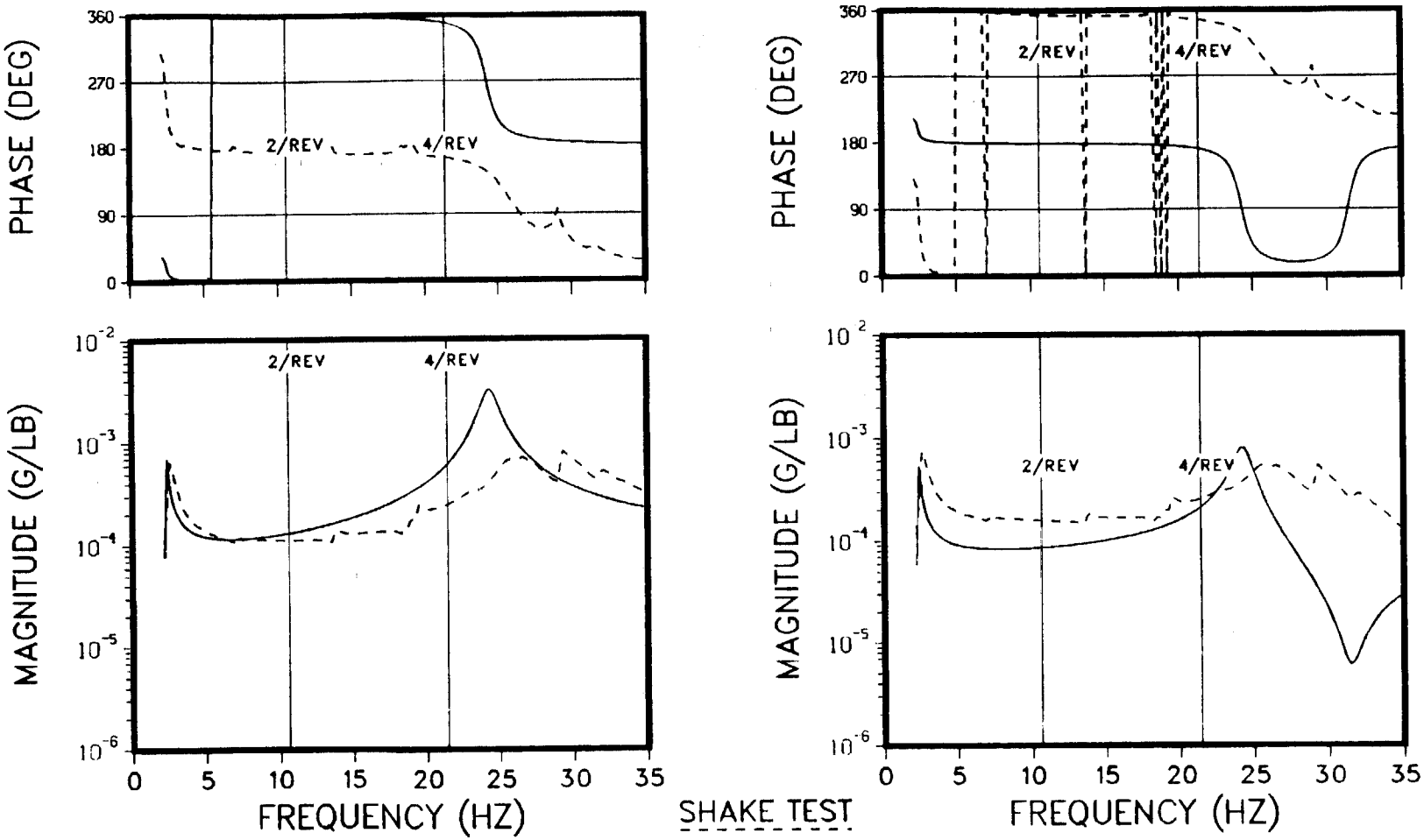

MID TRANSMISSION LATERAL RESPONSE

TRANSMISSION SUMP LATERAL RESPONSE

LATERAL EXCITATION AT THE M/R HUB
THRUST = 7000 LB . DAMPERS INSTALLED
SHAKE TEST FORCE = 100 LB FROM 2 TO 6 HZ

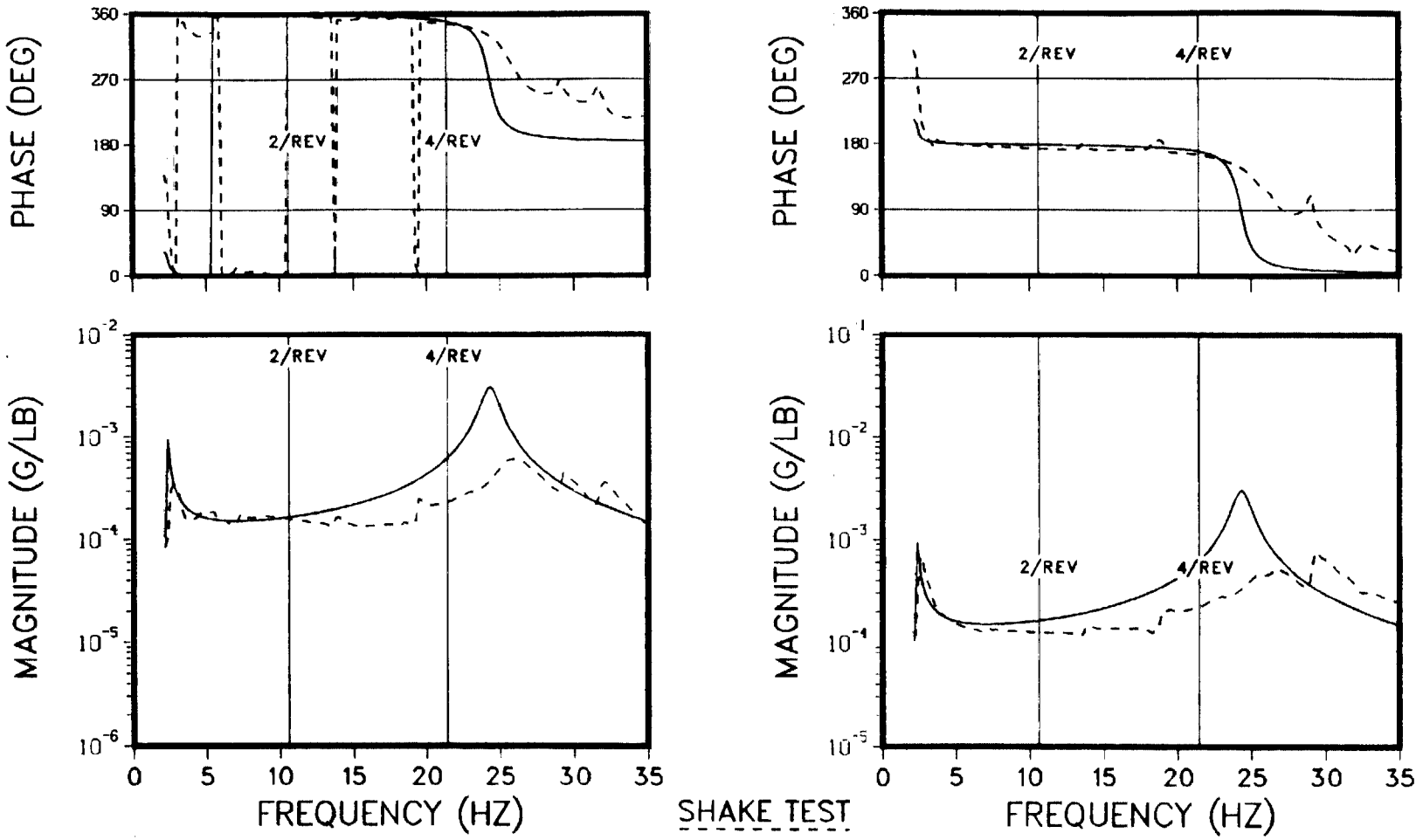

LEFT FORWARD MOUNT VERTICAL RESPONSE **RIGHT FORWARD MOUNT VERTICAL RESPONSE**

LATERAL EXCITATION AT THE M/R HUB
THRUST = 7000 LB . DAMPERS INSTALLED
SHAKE TEST FORCE = 100 LB FROM 2 TO 6 HZ

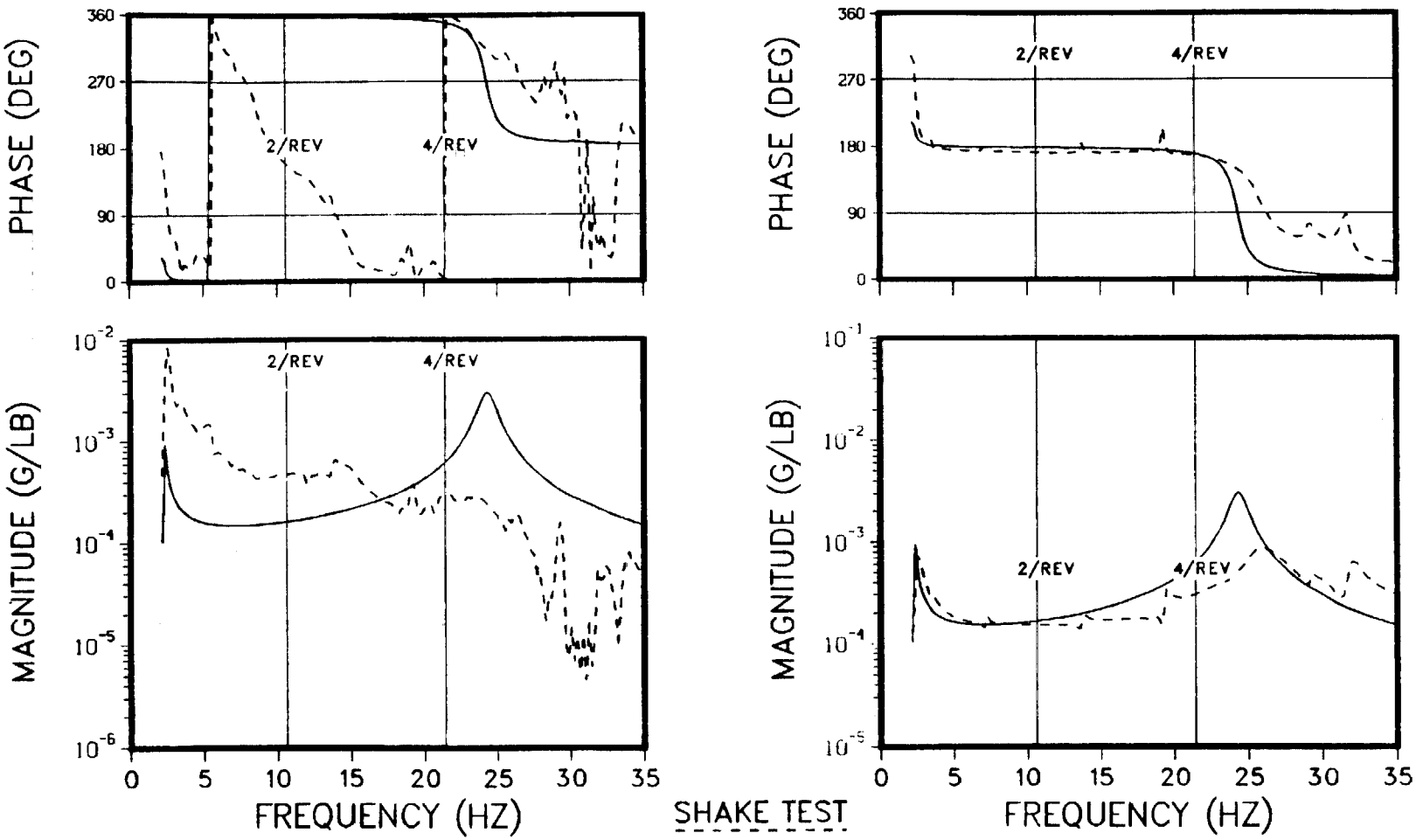

LEFT AFT MOUNT VERTICAL RESPONSE

RIGHT AFT MOUNT VERTICAL RESPONSE

LATERAL EXCITATION AT THE M/R HUB
THRUST = 7000 LB . DAMPERS INSTALLED
SHAKE TEST FORCE = 100 LB FROM 2 TO 6 HZ

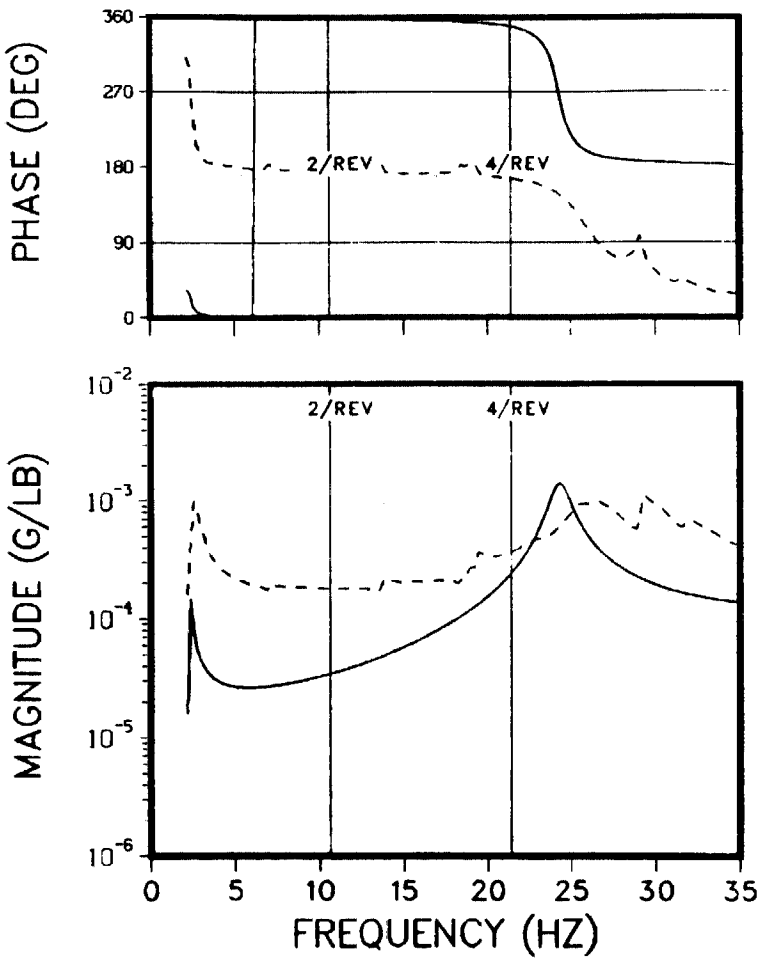

TRANSMISSION C.G. LATERAL RESPONSE

LATERAL EXCITATION AT THE M/R HUB
THRUST = 1000 LB . DAMPERS INSTALLED
SHAKE TEST FORCE = 200 LB

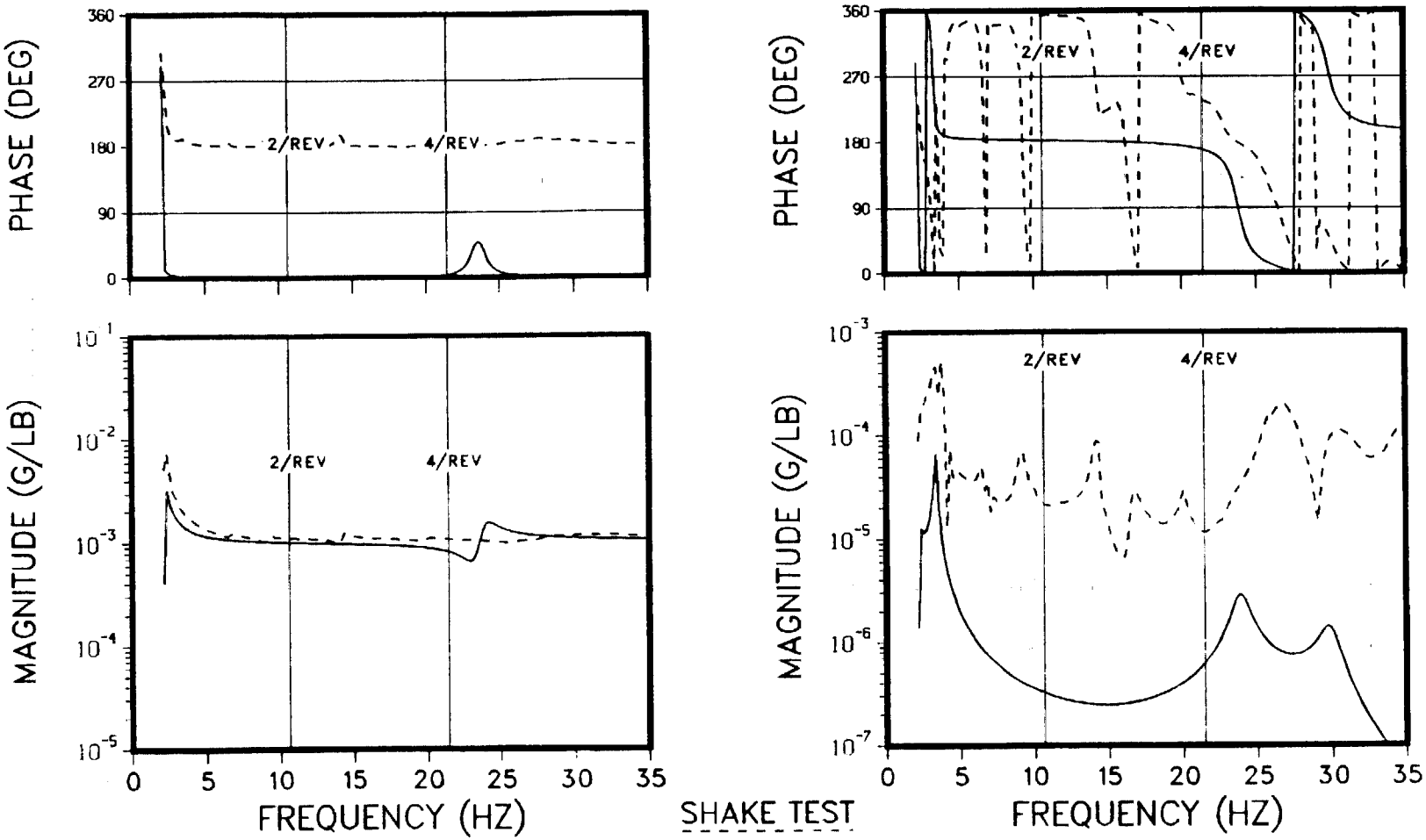

M/R HUB LATERAL RESPONSE

M/R HUB F/A RESPONSE

LATERAL EXCITATION AT THE M/R HUB
THRUST = 1000 LB . DAMPERS INSTALLED
SHAKE TEST FORCE = 200 LB

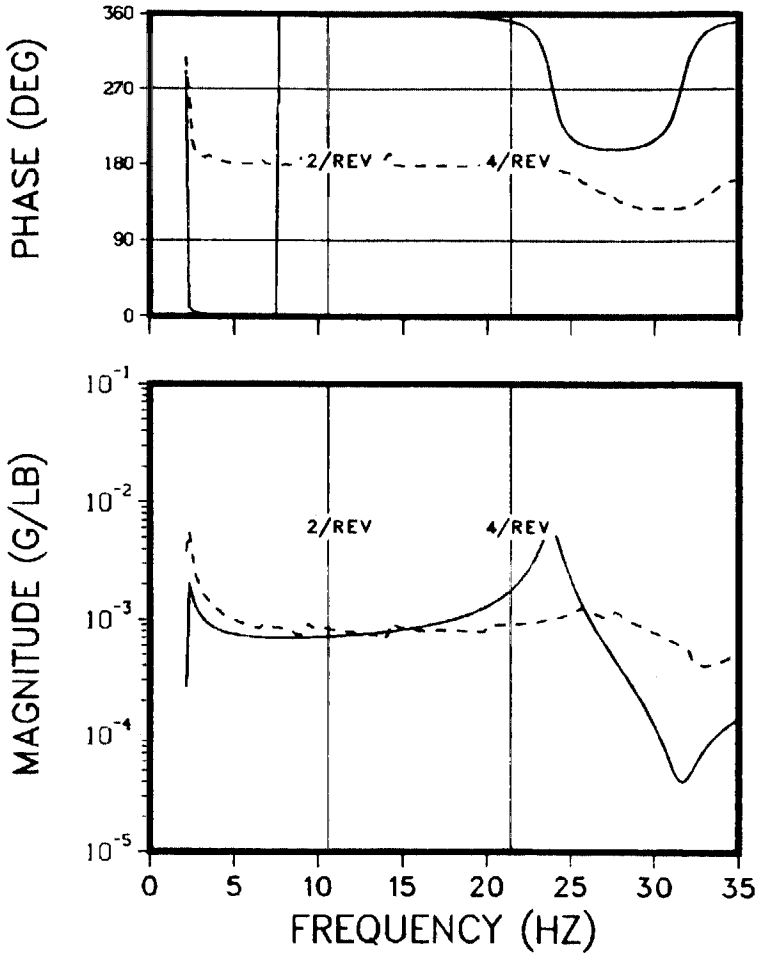

MID MAST (STA 22) LATERAL RESPONSE

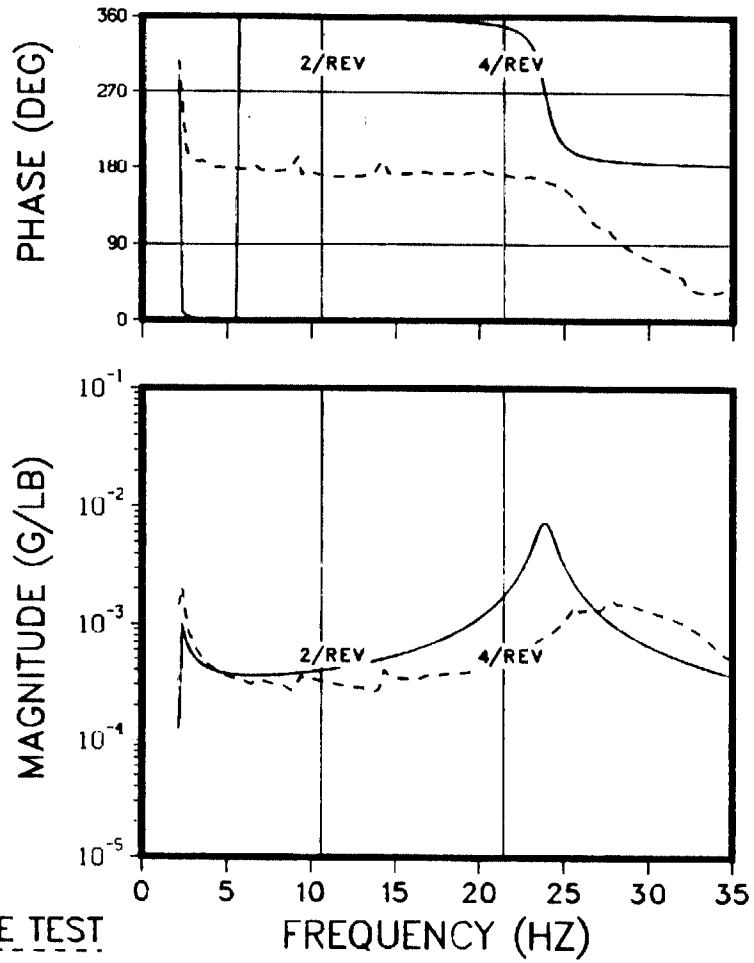

SHAKE TEST

NASTRAN

TRANSMISSION UPPER BEARING LATERAL RESPONSE

LATERAL EXCITATION AT THE M/R HUB
THRUST = 1000 LB . DAMPERS INSTALLED
SHAKE TEST FORCE = 200 LB

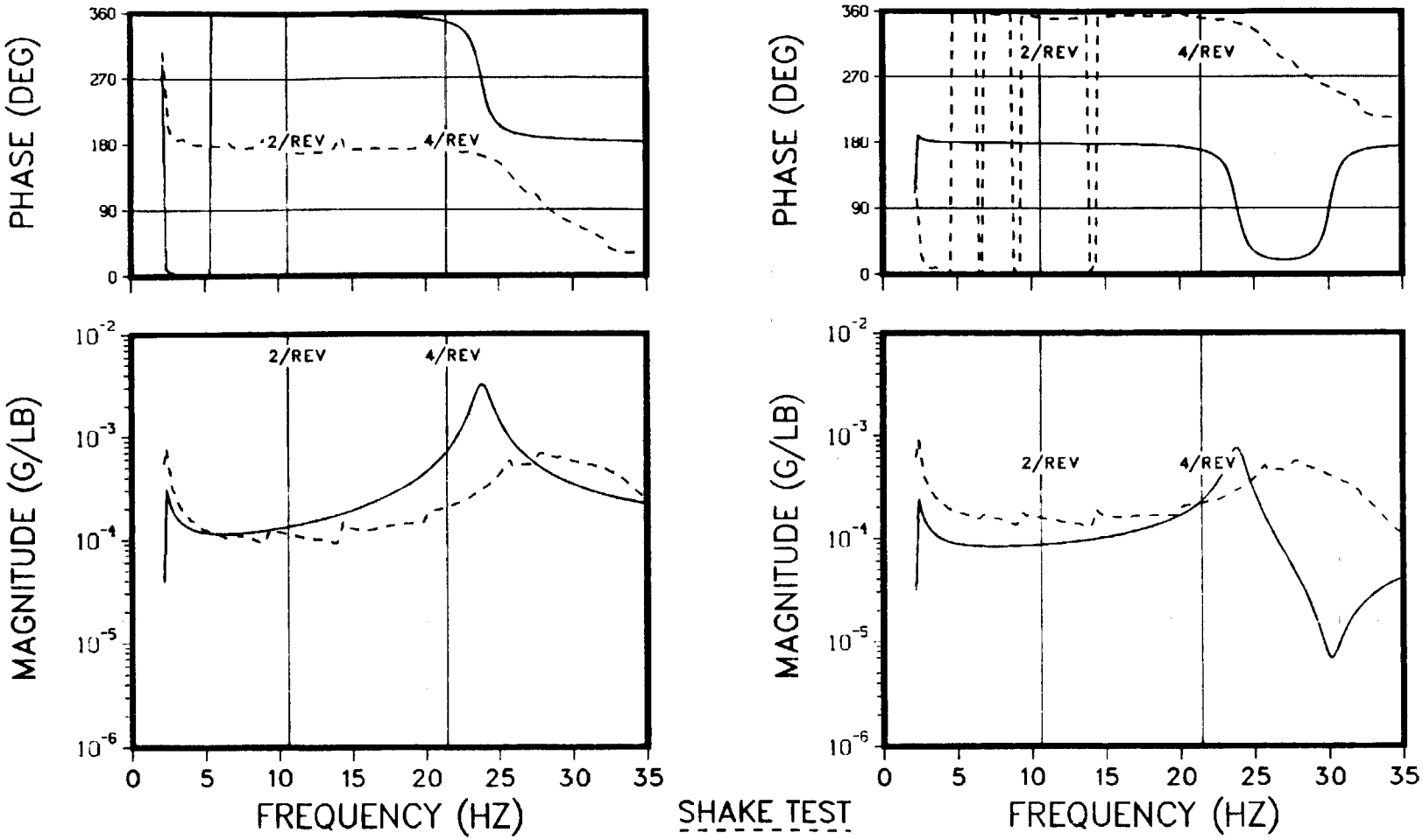

MID TRANSMISSION LATERAL RESPONSE

TRANSMISSION SUMP LATERAL RESPONSE

LATERAL EXCITATION AT THE M/R HUB
THRUST = 1000 LB . DAMPERS INSTALLED
SHAKE TEST FORCE = 200 LB

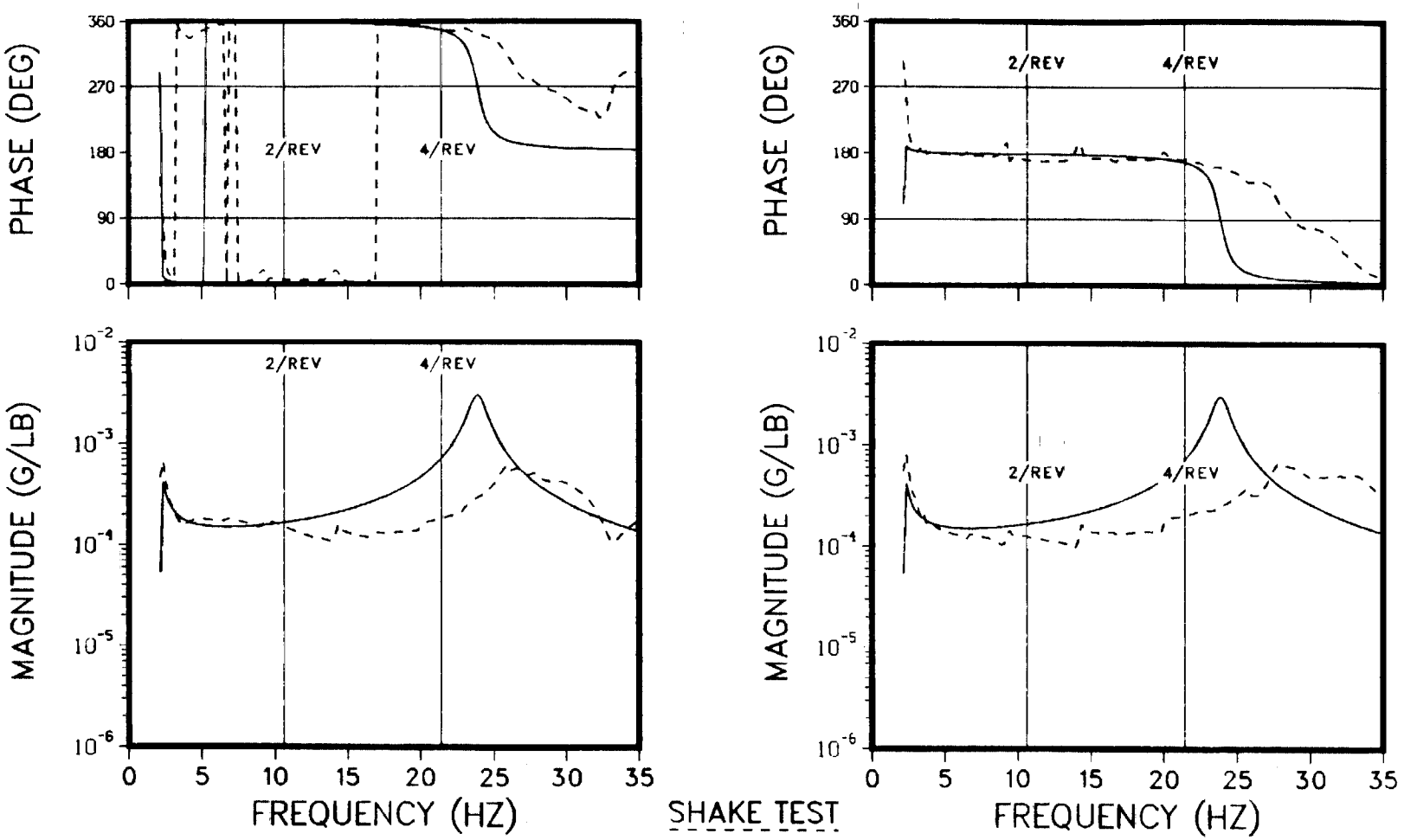

LEFT FORWARD MOUNT VERTICAL RESPONSE **RIGHT FORWARD MOUNT VERTICAL RESPONSE**

LATERAL EXCITATION AT THE M/R HUB
THRUST = 1000 LB . DAMPERS INSTALLED
SHAKE TEST FORCE = 200 LB

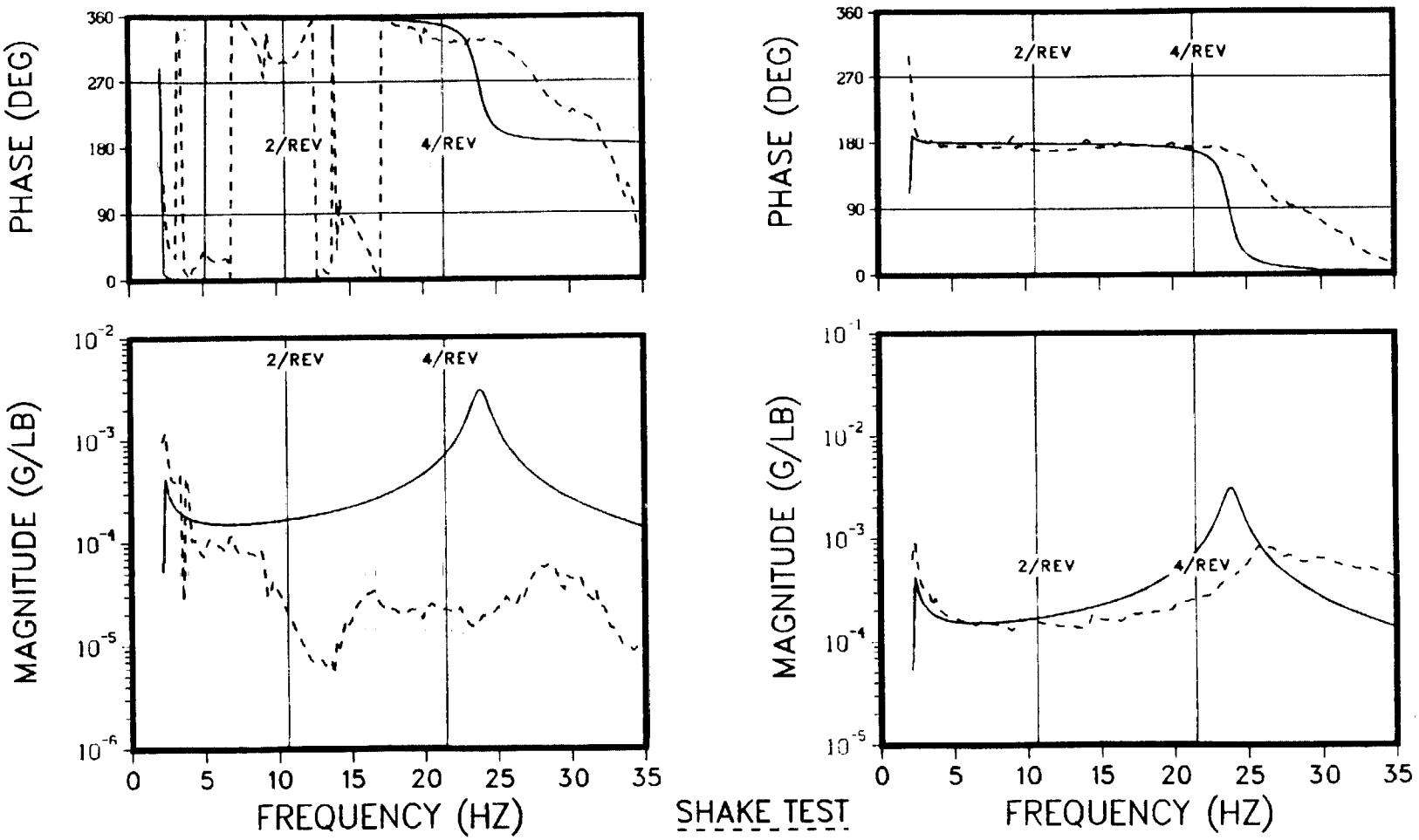

LEFT AFT MOUNT VERTICAL RESPONSE

RIGHT AFT MOUNT VERTICAL RESPONSE

LATERAL EXCITATION AT THE M/R HUB
THRUST = 1000 LB . DAMPERS INSTALLED
SHAKE TEST FORCE = 200 LB

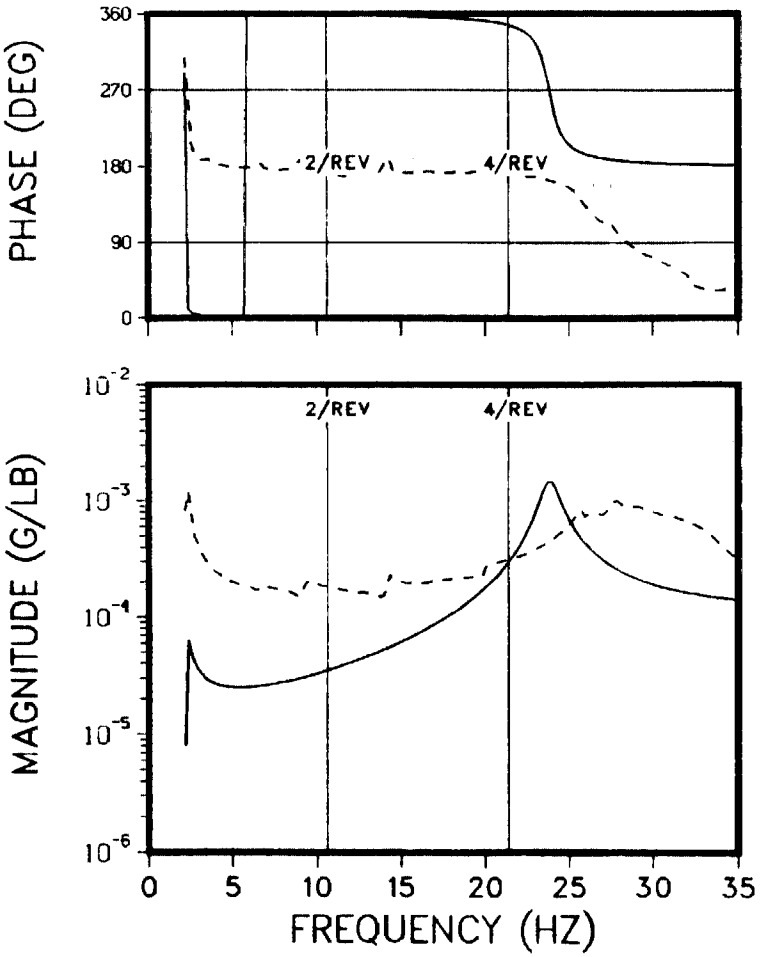

TRANSMISSION C.G. LATERAL RESPONSE

F/A EXCITATION AT THE M/R HUB
THRUST = 1000 LB . DAMPERS INSTALLED
SHAKE TEST FORCE = 200 LB . NO LIFT LINK

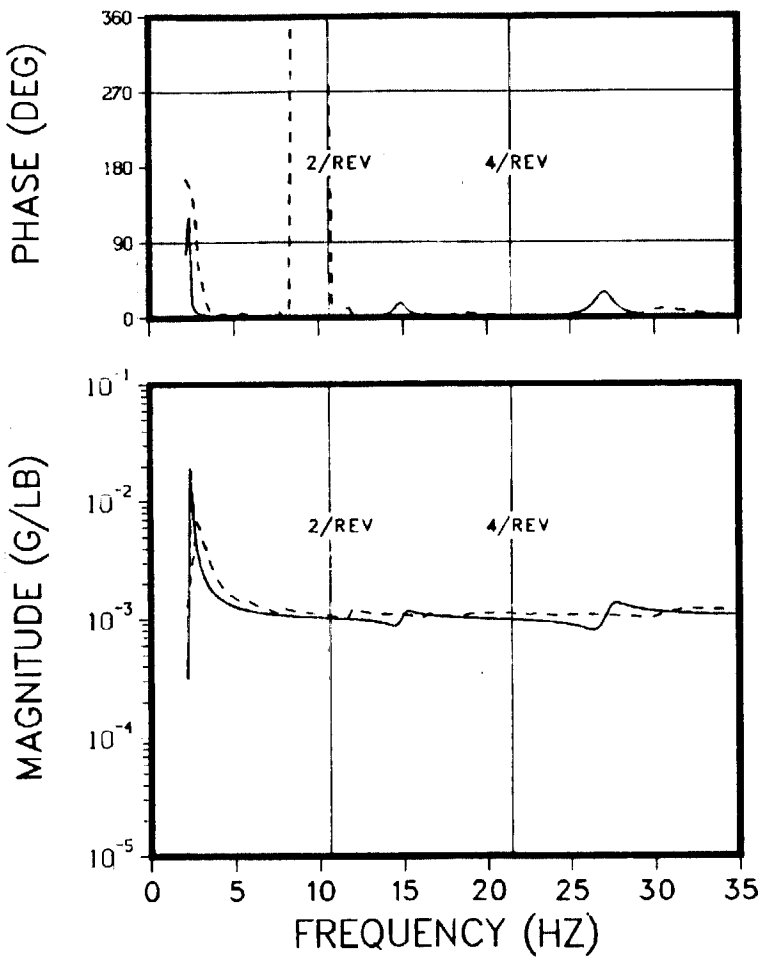

M/R HUB F/A RESPONSE

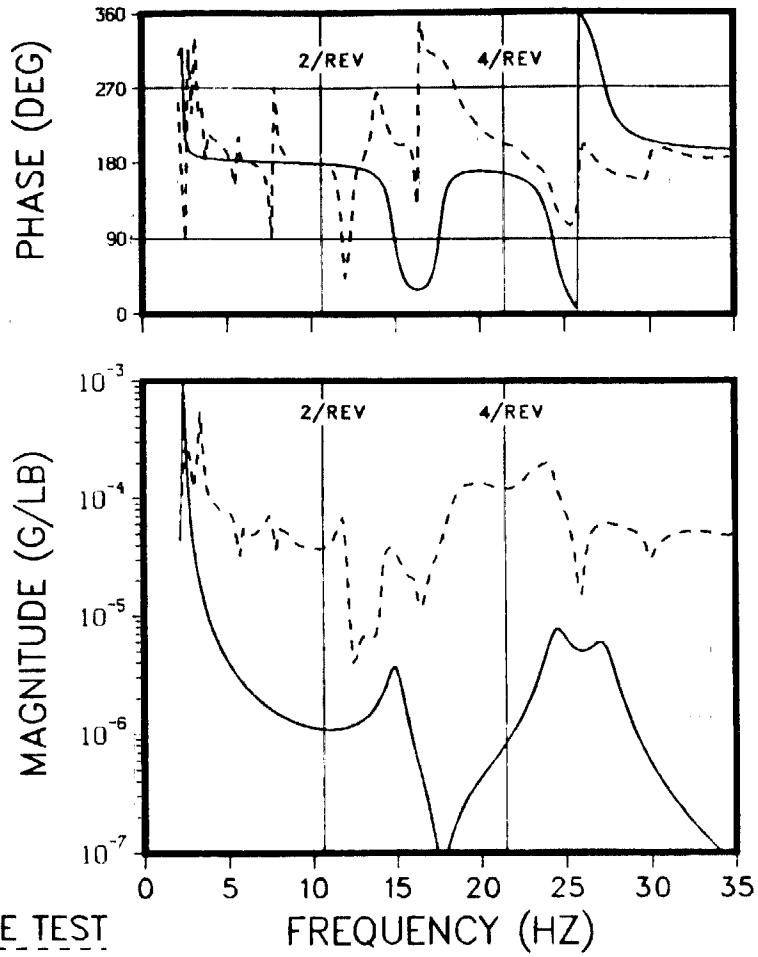

M/R HUB LATERAL RESPONSE

SHAKE TEST

NASTRAN

F/A EXCITATION AT THE M/R HUB
THRUST = 1000 LB . DAMPERS INSTALLED
SHAKE TEST FORCE = 200 LB. NO LIFT LINK

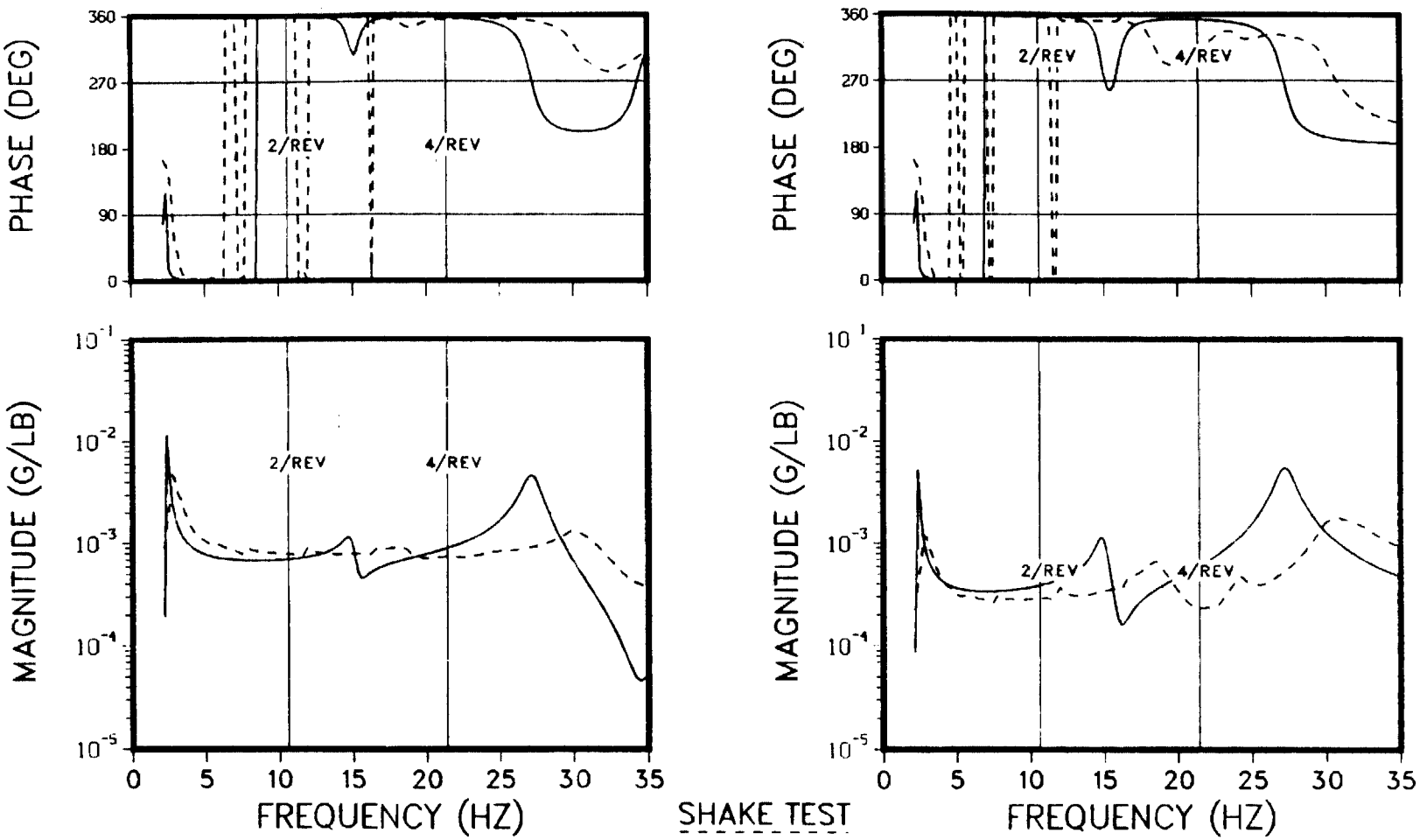

MID MAST (STA 22) F/A RESPONSE

TRANSMISSION UPPER BEARING F/A RESPONSE

F/A EXCITATION AT THE M/R HUB
THRUST = 1000 LB . DAMPERS INSTALLED
SHAKE TEST FORCE = 200 LB .NO LIFT LINK

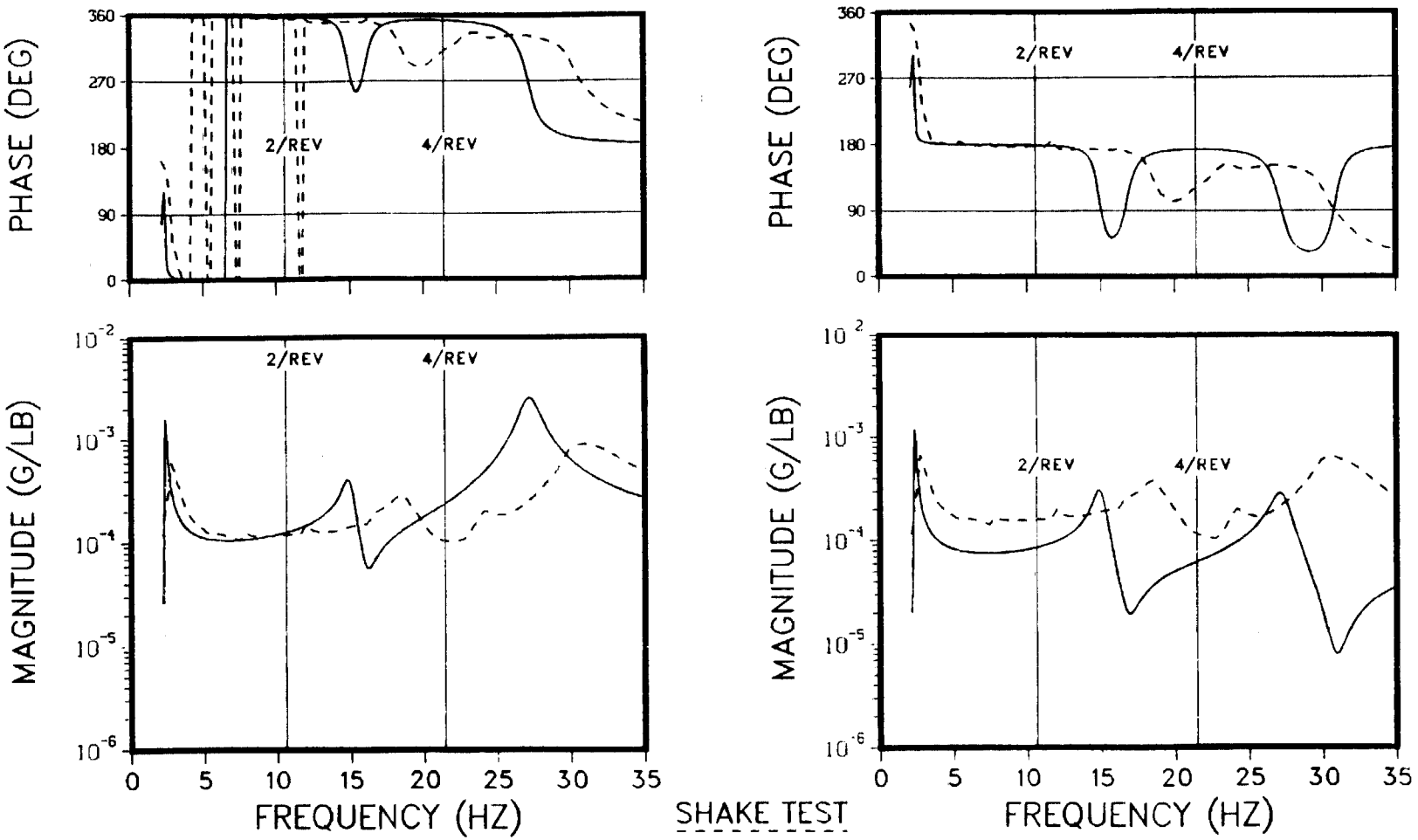

MID TRANSMISSION F/A RESPONSE

TRANSMISSION SUMP F/A RESPONSE

F/A EXCITATION AT THE M/R HUB
THRUST = 1000 LB . DAMPERS INSTALLED
SHAKE TEST FORCE = 200 LB. NO LIFT LINK

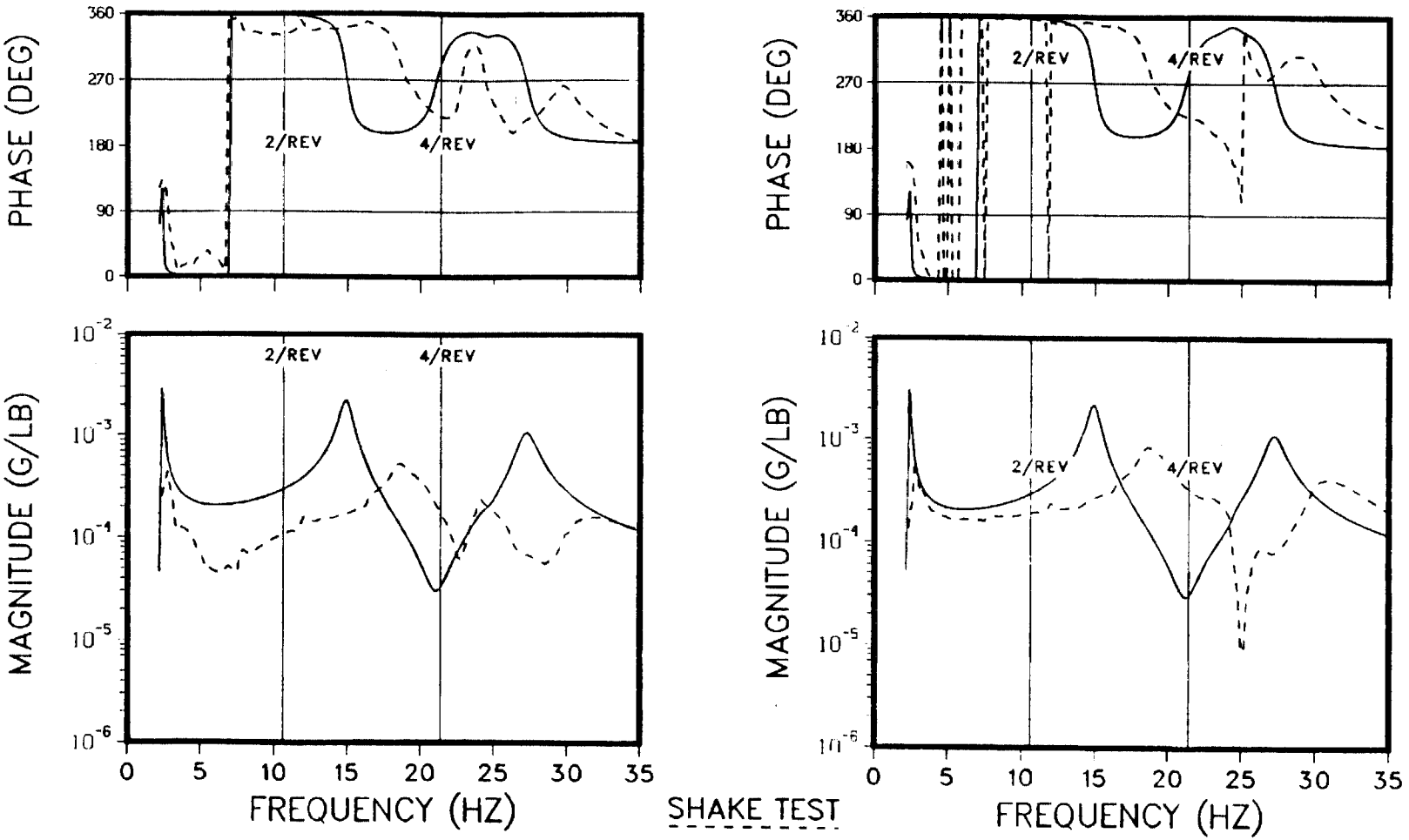

LEFT FORWARD MOUNT VERTICAL RESPONSE **RIGHT FORWARD MOUNT VERTICAL RESPONSE**

F/A EXCITATION AT THE M/R HUB
THRUST = 1000 LB . DAMPERS INSTALLED
SHAKE TEST FORCE = 200 LB. NO LIFT LINK

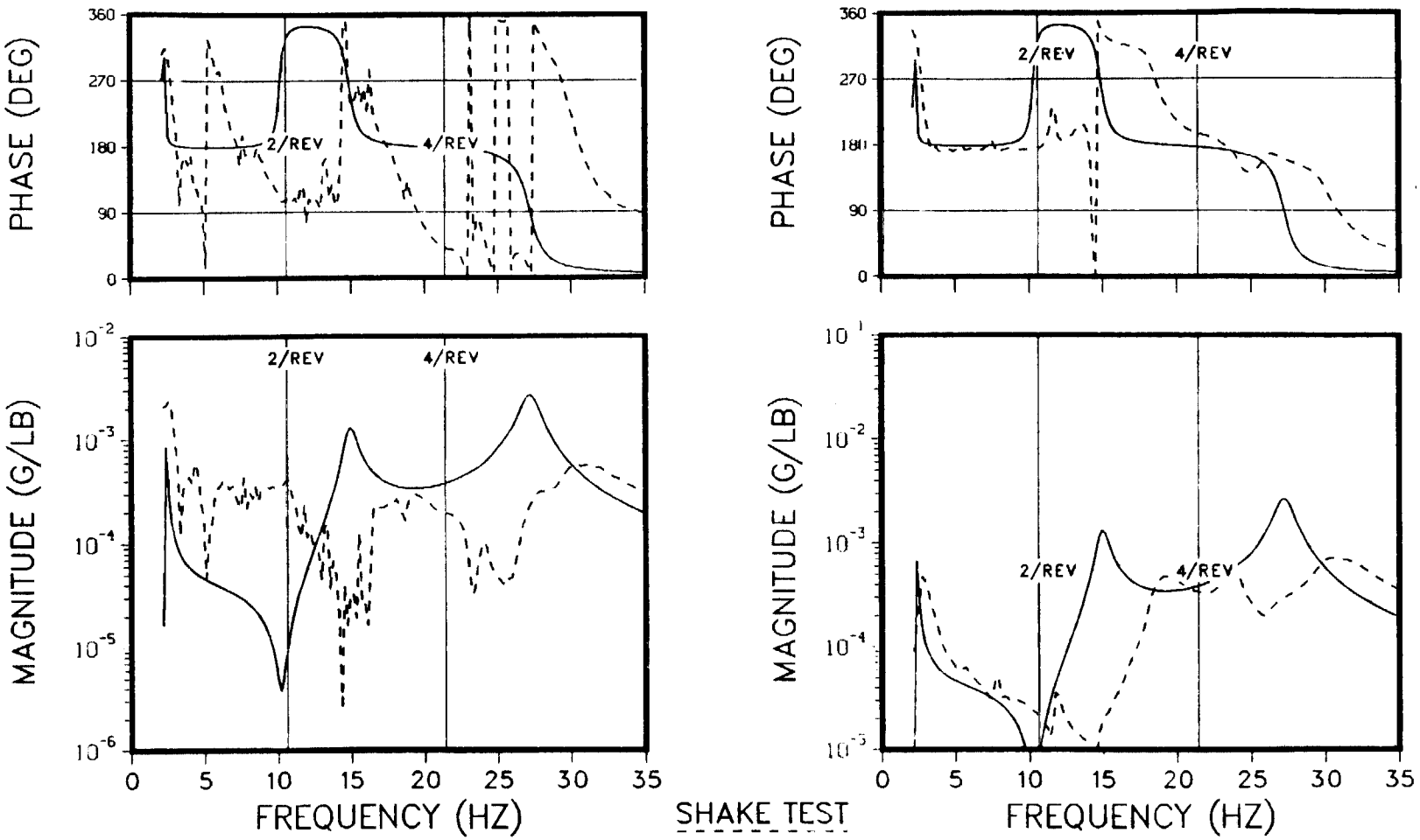

LEFT AFT MOUNT VERTICAL RESPONSE

RIGHT AFT MOUNT VERTICAL RESPONSE

NASA
National Aeronautics and Space Administration

Report Documentation Page

1. Report No.	2. Government Accession No.	3. Recipient's Catalog No.
NASA CR-181916, Volume II		

4. Title and Subtitle
Investigation of Difficult Component Effects on Finite Element Model Vibration Prediction for the Bell AH-1G Helicopter
Volume II - Correlation Results

5. Report Date
October 1989

6. Performing Organization Code

7. Author(s)
R.V. Dompka

8. Performing Organization Report No.
699-099-251, Volume II

10. Work Unit No.
505-63-51-01

9. Performing Organization Name and Address
Bell Helicopter Textron Inc.
P.O. Box 482
Fort Worth, Texas 76101

11. Contract or Grant No.
NAS1-17496

12. Sponsoring Agency Name and Address
National Aeronautics and Space Administration
Washington, D.C. 20546

13. Type of Report and Period Covered
Contractor Final Report

14. Sponsoring Agency Code

15. Supplementary Notes
Langley Technical Monitor: Raymond G. Kvaternik
Final Report (for Task #5 of the contract)

16. Abstract

Under the NASA-sponsored DAMVIBS (Design Analysis Methods for VIBrationS) program, a series of ground vibration tests and NASTRAN finite element model (FEM) correlations were conducted on the Bell AH-1G helicopter gunship to investigate the effects of difficult components on the vibration response of the airframe. Previous correlations of the AH-1G showed good agreement between NASTRAN and tests through 15-20 Hz, but poor agreement in the higher frequency range of 20-30 Hz. Thus, this effort emphasized the higher frequency airframe vibration response correlations and identified areas that need further R&T work. To conduct the investigations, selected difficult components (main rotor pylon, secondary structure, nonstructural doors/panels, landing gear, engine, fuel, etc.) were systematically removed to quantify their effects on overall vibratory response of the airframe. The entire effort was planned and documented, and the results reviewed by NASA and industry experts in order to ensure scientific control of the testing, analysis, and correlation exercise. In particular, secondary structure and damping had significant effects on the frequency response of the airframe above 15 Hz. Also, the nonlinear effects of thrust stiffening and elastomer mounts were significant on the low frequency pylon modes below main rotor 1p (5.4 Hz). This volume presents the results of the NASTRAN FEM correlations, including the findings and areas needing further work that were identified in the investigation.

17. Key Words (Suggested by Author(s))		18. Distribution Statement
Difficult Components	Helicopter	Unclassified - Unlimited
Airframe Vibrations	NASTRAN	
AH-1G Helicopter	Rotorcraft	Subject Category 39
Structural Analysis	Dynamic	
Finite Element		

19. Security Classif. (of this report)	20. Security Classif. (of this page)	21. No. of Pages	22. Price
Unclassified	Unclassified	231	A11

NASA FORM 1626 OCT 86